

***PROPAGATION PARAMETERS OF FIRST HIGHER MODE IN  
GRADED INDEX FIBER AND COUPLING OPTICS INVOLVING  
CYLINDRICAL MICROLENS ON THE TIP OF GRADED INDEX  
FIBER: ESTIMATION BY SIMPLE AND ACCURATE METHOD***

**THESIS SUBMITTED FOR THE DEGREE OF DOCTOR OF PHILOSOPHY  
(SCIENCE)**

**IN PHYSICS**

**BY**

**ANINDITA CHATTOPADHYAY**

**DEPARTMENT OF PHYSICS**

**JADAVPUR UNIVERSITY**

**KOLKATA 700032**

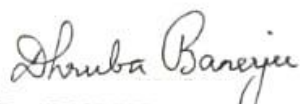
**2023**

## **CERTIFICATE FROM THE SUPERVISOR(S)**

This is to certify that the thesis entitled "Propagation Parameters of First Higher Mode in Graded Index Fiber and Coupling Optics Involving Cylindrical Microlens on the Tip of Graded Index Fiber: Estimation by Simple and Accurate Method" submitted by Smt. Anindita Chattopadhyay, who got her name registered on 09.08.16 as a research scholar for the award of Ph.D. (Science) degree in Physics of Jadavpur University, is absolutely based upon her own work under the supervision of Dr. Dhruba Banerjee and Dr. Sankar Gangopadhyay and that neither this thesis nor any part of it has been submitted for either any degree/diploma or any other academic award anywhere before.

### **Signature of the supervisors:**

1.

  
Dr. DHRUBA BANERJEE  
Assistant Professor  
Dept. of Physics  
JADAVPUR UNIVERSITY  
KOLKATA - 700 032

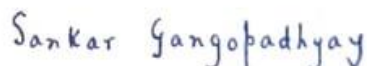
Dr. Dhruba Banerjee

Department of Physics

Jadavpur University, Kolkata: 700 032

18-12-2023

2.



DR. SANKAR GANGOPADHYAY  
Retired Associate Professor  
Dept. of Physics  
SURENDRANATH COLLEGE  
KOLKATA - 700009

18/12/2023

Dr. Sankar Gangopadhyay

Former Associate Professor in Physics

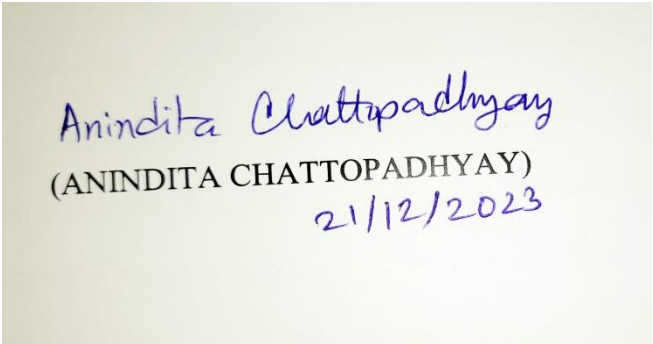
Surenranath College, Kolkata: 700009

**Dedicated**  
**To**  
**The supreme power of the**  
**universe**  
**And**  
**My parents, the reason of**  
**what I become today**

## ACKNOWLEDGEMENT

Foremost, I would like to convey my deepest gratitude to my two supervisors, **Dr. Dhruba Banerjee** and **Dr. Sankar Gangopadhyay**. Their patience, encouragement, valuable advice, immense knowledge, guidance, supervision were key motivations during different phases of my pre-doctoral work and without this, the present work would not have been possible indeed.

Further, I gratefully acknowledge the patience, understanding and amazing support of my parents **Dr. Arun Kumar Chattopadhyay** and **Mrs. Purabi Chattopadhyay** even during the most difficult period of doctoral pursuit. I am also thankful to my husband **Mr. Debasish Roy** and my son **Master Animikh Roy** whose constant adjustments have made my work easier. I am thankful to my departmental colleagues for their cooperation and support during the course of my Ph. D. work. Finally, it is my pleasure to state that I will remain indebted to the Swami Vivekananda Group of Institutes for providing me the necessary environment for research work. It also deserves mentioning that the academic enrichment, which I obtained through Course Work in Jadavpur University and interaction thereof with concerned faculty members, developed the mindset desirable for research work.



Anindita Chattopadhyay  
(ANINDITA CHATTOPADHYAY)  
21/12/2023



## Abstract

Communication through optical fiber has emerged as the potential area in present technology. This is because the doped silica made optical fiber has low attenuation loss (0.2 dB/km) and it has sufficient bandwidth (~1000 GHz) so as to meet the challenges of the huge growth of information traffic. Attenuation loss becomes minimum for the operating wavelength 1.55  $\mu\text{m}$  whereas for the operating window 1.3  $\mu\text{m}$ , zero material dispersion is obtained.

Broadening of a particular mode transmitted through a fiber happens due to dispersion. Total dispersion is the sum of waveguide dispersion, material dispersion and composite profile dispersion. Waveguide dispersion occurs due to the dependence of the propagation constant on the wavelength. Material dispersion is caused due to the propagation of different optical wavelengths with different velocities. Composite profile dispersion depends on the derivative with respect to wavelength of the relative core – cladding refractive index difference. It is less than 0.5ps/ (km nm) and hence practically negligible. During optical propagation, the refractive index profile and the radius of the core of the fiber are monitored in such a fashion that at the wavelength 1.55  $\mu\text{m}$ , the waveguide dispersion neutralizes the oppositely directed material dispersion. Hence the two main disturbing factors of optical communication such as dispersion and attenuation loss simultaneously are reduced to minimum at the wavelength of 1.55  $\mu\text{m}$ . Thus very long repeater less communication as well as very high bandwidth propagation can be possible within a fiber. The optical fiber having these properties is known as dispersion shifted fiber. Another kind of optical fiber, which practically possesses almost zero dispersion over a large range of wavelengths, is called dispersion flattened fiber. By using the later kind of fibers, the information carrying capacity can be enhanced by wavelength division multiplexing. Thus different kinds of novel modelling have been explored to study the propagation parameters of dispersion managed as well as other kind of optical fibers.

Recently, in optical communication system, the effect of nonlinearity in the doped material used in the optical fiber has emerged as the subject of interest in optical communication system. Different mathematical methods are available for the study of the effect of non-linearity. The non-linearity has huge impact on the data transferring capability and channel capacity of optical communication system. But the methods available in the literature for study of these nonlinear effects are very lengthy and complicated. So to predict different performance parameters of nonlinear optical fiber, there is a huge scope to find out a simple but accurate method. In addition, investigations relating to first higher mode in nonlinear optical fiber is also important in view of the performance of dual mode optical fiber.

Again, in order to optimize the optical beam launch involving the coupling of incident laser beam with the optical fiber, different types of micro lenses are designed. These lenses are fabricated at the tips of different kinds of fibers to get maximum efficiency. Hence, the design of different kinds of such coupling efficient couplers along with development of simple and accurate model for their study is of tremendous importance in present communication system. The structure of the thesis has been presented below in a nutshell.

Chapter 1 comprises introduction to basics of optical waveguides, electromagnetic theory associated with it and optical communication system. This chapter also describes the objective of the present research work together with its importance to contemporary interest and future researches as well. The relevant citations have also been made here.

Chapter 2 consists of the literature survey, highlighting its relevant research gaps and the needful address to the gaps thereof.

Chapter 3 involves study of some useful propagation parameters of graded index optical fibers for first higher order mode both in presence and absence of Kerr type nonlinearities. This chapter also contains prescription of a simple but accurate method based on Chabyshev technique for estimation of the concerned propagation parameters.

Chapter 4 presents the study of coupling optics relating to an optical coupler consisting of laser diode, graded index fiber and cylindrical microlens fabricated on the tip of the fiber. Here, ABCD formalism appropriate for the system has been developed to predict the coupling optics in a simple but accurate fashion.

Chapter 5 describes the conclusion arrived at on the basis of the research work described in the thesis. The conclusion basically aims at presenting the novelty of the present work and the enrichment of the literature in terms of its potential in present as well as future research.

Chapter 5 precedes the reference section which is followed by my publications and the reprints.



**CHAPTER**

<b>1. INTRODUCTION</b>	<b>1</b>
<b>1.1 FUNDAMENTALS OF FIBER OPTICS</b>	<b>2</b>
<b>1.2 STUDY OF OPTICAL FIBER COMMUNICATION IN THE FRAME         WORK OF ELECTROMAGNETIC THEORY</b>	<b>12</b>
<b>1.3 AIM OF THE THESIS AND FUTURE SCOPE</b>	<b>17</b>
<b>1.4 THE STRUCTURE OF THE THESIS</b>	<b>19</b>
 <b>2. LITERATURE SURVEY, RESEARCH GAPS AND ADDRESS</b>	<b>21</b>
<b>FIRST PART OF THE RESEARCH WORK</b>	
<b>2.1 LITERATURE SURVEY</b>	<b>22</b>
<b>2.2 RESEARCH GAPS</b>	<b>25</b>
<b>2.3 ADDRESS</b>	<b>25</b>
<b>SECOND PART OF THE RESEARCH WORK</b>	
<b>2.4 LITERATURE SURVEY</b>	<b>26</b>
<b>2.5 RESEARCH GAPS</b>	<b>28</b>
<b>2.6 ADDRESS</b>	<b>28</b>

<b>3. A SIMPLE BUT ACCURATE TECHNIQUE FOR PREDICTION OF CONFINEMENT, EXCITATION EFFICIENCY AND NORMALIZED GROUP DELAY PARAMETERS FOR PROPAGATION OF FIRST HIGHER ORDER MODE IN GRADED INDEX FIBER BOTH IN PRESENCE AND ABSENCE OF KERR TYPE NONLINEARITY</b>	<b>30</b>
<b>3.1 INTRODUCTION</b>	<b>31</b>
<b>3.2 THEORY</b>	<b>34</b>
<b>3.3 RESULTS AND DISCUSSION</b>	<b>39</b>
<b>3.4 SUMMARY</b>	<b>48</b>
<b>4. STUDY OF COUPLING OPTICS OF CYLINDRICAL MICROLENS FABRICATED ON TIPS OF GRADED INDEX FIBERS HAVING DIFFERENT PROFILE EXPONENTS</b>	<b>49</b>
<b>4.1 INTRODUCTION</b>	<b>50</b>
<b>4.2 THEORY</b>	<b>52</b>
<b>4.3 RESULTS AND DISCUSSION</b>	<b>57</b>
<b>4.4 SUMMARY</b>	<b>110</b>
<b>5. CONCLUSIONS</b>	<b>111</b>
<b>REFERENCES</b>	<b>116</b>
<b>LIST OF JOURNAL PUBLICATIONS</b>	<b>133</b>
<b>REPRINTS OF PUBLICATIONS</b>	<b>135</b>

# *CHAPTER 1*

## *INTRODUCTION*

## 1.1 FUNDAMENTALS OF FIBER OPTICS

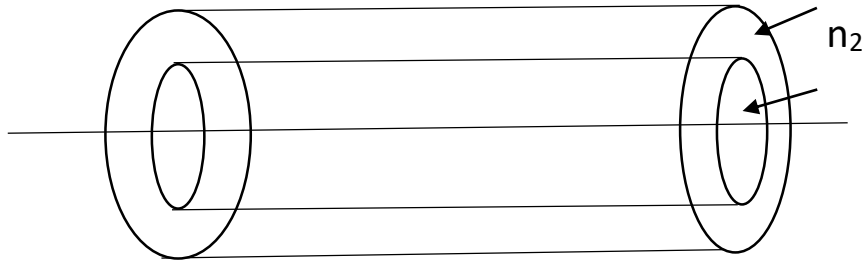


**Fig. 1.1: Schematic diagram of an optical fiber of core radius  $a$ , core refractive index  $n_1$  and cladding refractive index  $n_2$**

Figure 1.1 is the schematic diagram of an optical fiber. The use of optical fiber communication system has increased massively due to its low loss and high bandwidth signal transmission. A simple optical fiber has a thin cylindrical dielectric core and a coaxial dielectric cladding surrounding it. The cladding has a slightly less refractive index than that of the core. The material of the core and cladding is made of silica. To differentiate the refractive index of core from cladding, the silica is doped with elements like  $\text{GeO}_2$ . Further,  $1.3\text{ }\mu\text{m}$  to  $1.6\text{ }\mu\text{m}$  of wavelength range is the preferred wavelength range in optical communication system, because silica, the material of optical fiber, has low attenuation loss ( $\sim 0.15\text{ dB/km}$ ) at the wavelength  $1.55\text{ }\mu\text{m}$  and the material dispersion becomes zero around the wavelength  $1.3\text{ }\mu\text{m}$ . Hence, these two wavelengths are desirable windows for fiber optics communication. Incidentally, the attenuation loss of silica is nearly  $0.15\text{ dB/km}$  at the wavelength  $1.55\text{ }\mu\text{m}$  (Kanamori, Yokota, Tanaka, Watanabe, Ishiguro, Yoshida, Kakii, Itoh, Asano and Tanaka, 1986) and  $0.35\text{ dB/km}$  for the wavelength  $1.3\text{ }\mu\text{m}$  (Jablonowski, 1986). Researches on material science have been continuously conducted for further minimisation of attenuation loss and material dispersion as well (Borzycki, Osuch, 2023). The optical fiber which carries the fundamental mode only is called single mode optical fiber while the optical fiber which carries more than one mode is called multimode optical fiber. The diameter of the core of a single mode optical fiber is  $5 - 10\text{ }\mu\text{m}$  and that in case of the multimode one is  $50\text{ }\mu\text{m}$ , while the

diameter of the cladding is 125 $\mu$ m in both cases. Every fiber is characterised by a particular V number [

$V = k_0 a \sqrt{n_1^2 - n_2^2}$ , where,  $k_0 = \frac{2\pi}{\lambda}$ ] below which only the fundamental mode is allowed for transmission.

The concerned V number is called first higher order mode cut – off V number. For step, parabolic and triangular index fibers the first higher order cut – off V numbers are around 2.405, 3.518 and 4.381 respectively (Ghatak, Thyagarajan, 1998; Neuman 1988). Accordingly, single – mode guidance in step, parabolic and triangular index fibers can occur if V is less than 2.405, 3.518 and 4.381 respectively.

Fibers are characterized on the basis of the nature of refractive index profiles within the cores. If the core contains homogeneous refractive index profile distribution, then it is called step index fiber. If the refractive index distribution of the core is inhomogeneous then that may be graded index, W type or trapezoidal fiber etc. (Senior, 1994; Lundin, 1994; Matsui, Zhou and Nakajima, 2005). The first higher order mode cut off V numbers are different for the fibers having inhomogeneously distributed refractive index. The different refractive index distributions are shown below in Figs. 1.2 – 1.6, where  $R = r/a$ ,  $r$  = radial distance from the axis of the core and  $a$  = radius of the core of the fiber.

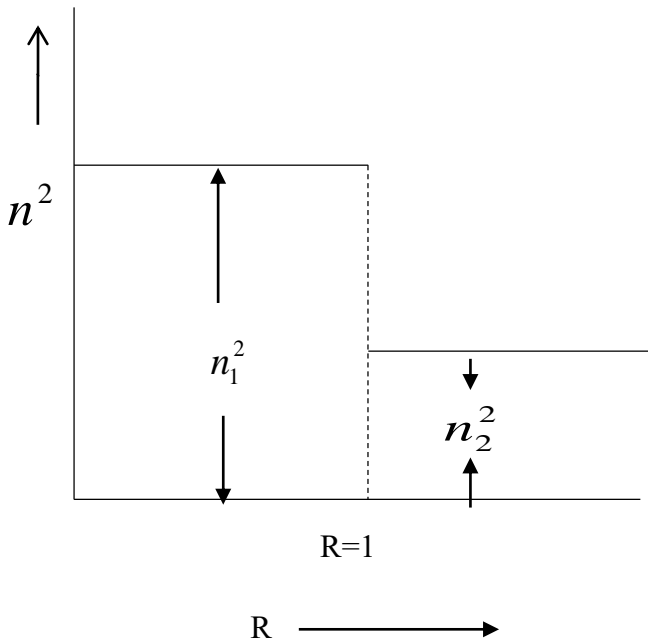


**Fig. 1.2: Refractive Index Distribution of Step Index Fiber**

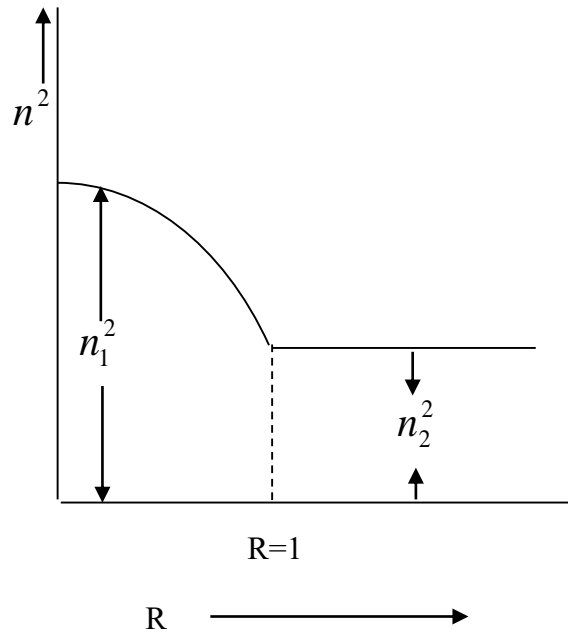


**Fig. 1.3: Refractive Index Distribution of Graded Index fiber**

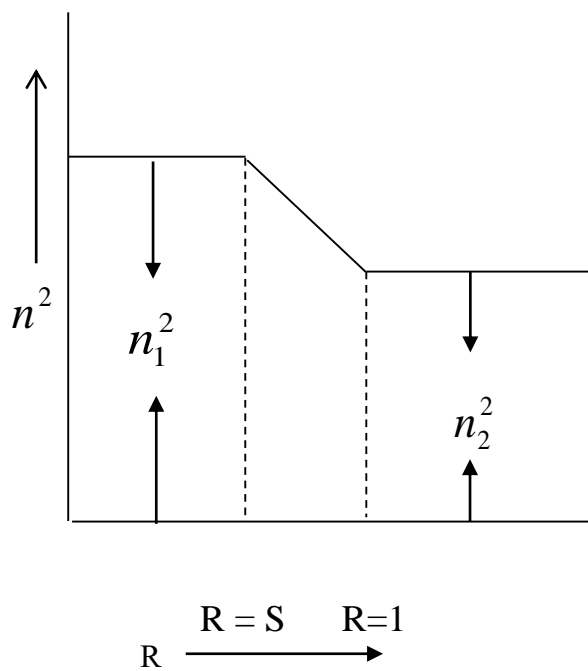


**Fig. 1.4: Refractive Index Distribution of Dispersion-shifted Trapezoidal Fiber**

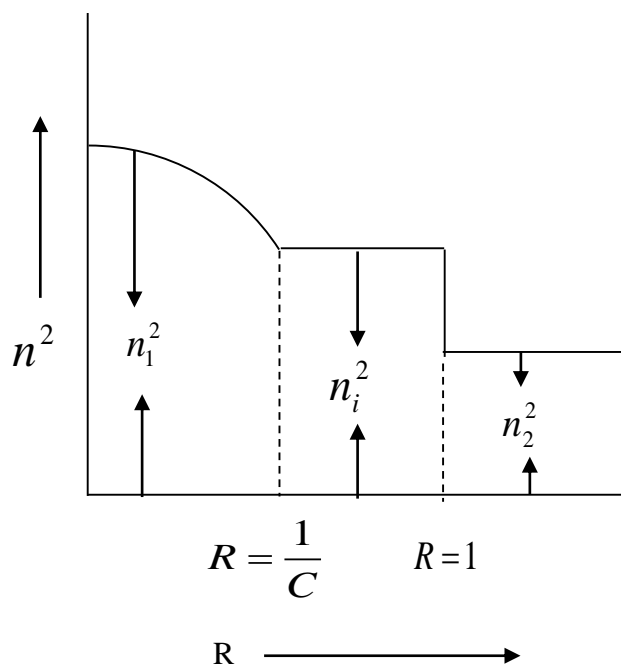


**Fig. 1.5: Refractive Index Distribution of Dispersion-flattened Graded W Fiber**

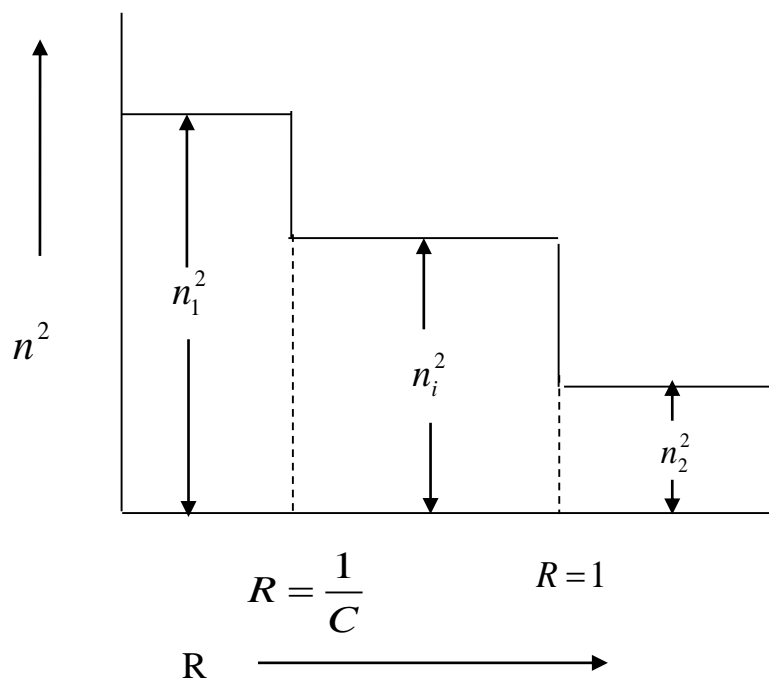


**Fig. 1.6: Refractive Index Distribution of Dispersion-flattened step W fiber**

In any communication system, attenuation and dispersion loss are to be minimised carefully. So, continuous development to minimise the attenuation loss and pulse broadening are being taken care of day by day. The problem of pulse broadening is termed as dispersion (Kapron and Keck, 1971; Payne and Gambling, 1975; Neumann, 1988). Due to this phenomenon, signals get overlapped. In step index multimode fiber, for the bandwidth 20 MHz-km, the dispersion becomes around 50 ns/km.nm. In graded core multimode fiber the dispersion drops down to 50 ps/km.nm. Clearly the improvement of bandwidth is 1000 times than that of the step index fiber. Due to the presence of intermodal and intramodal dispersion, the dispersion loss is unavoidable in multimode fiber (Olshansky and Keck, 1976). On the other hand, as only the fundamental mode propagates through single mode fiber, no intermodal dispersion takes place in this case. Hence, dispersion is minimised in single mode fiber and it consists of the waveguide, material and composite profile dispersion only. So for long distance communication, single mode fiber is preferable over the multimode one. Also, this permits use of less number of repeaters in optical communication system comprising single mode fiber. However, multimode fiber is more preferable over the coaxial copper cable. The dispersion, which occurs due to the dependence of the refractive index of core and cladding on the wavelength is called the material dispersion. The dependence of the propagation constant on the incident wavelength produces waveguide dispersion. Further, the monochromatic light source has some spectral width, however small it may be, influences material wave guide dispersions resulting in broadening of pulse as well, even in single mode optical fiber. The composite profile dispersion is proportional to the derivative of the difference of the relative core – cladding refractive indices with respect to the wavelength. It is very negligible ( $\sim <0.5\text{ps/km.nm}$ ) (Neumann, 1988) and as such it is not usually considered for evaluation of total dispersion. The waveguide dispersion shifts the zero total dispersion wavelength towards the larger wavelength side, in comparison to the zero material dispersion wavelength ( $\sim 1.274\text{ }\mu\text{m}$ ) (Cohen, Lin and French, 1979; Neumann, 1988; Ghatak and Thyagarjan, 1998; Tian, Markov, Wang and Skorobogatiy, 2015). Again, in case of silica made optical fiber, material dispersion and waveguide dispersion happen to be of opposite signs in the wavelength range between  $1.3\text{ }\mu\text{m}$  and  $1.8\text{ }\mu\text{m}$  (Neumann, 1988). Accordingly, the fiber parameters can be suitably monitored in order to ensure that

waveguide dispersion neutralises material dispersion at any wavelength, whatsoever. It deserves mentioning in this connection that zero material dispersion, however, occurs at the wavelength  $1.274\text{ }\mu\text{m}$  (Cohen et al., 1979; Neumann, 1988; Ghatak & Thyagarajan, 1998). The fibers modified in this fashion are known as dispersion shifted fiber (Paek, 1983). In another kind of fiber almost zero net dispersion can be obtained over a range of wavelengths. This type of fiber is known as dispersion flattened fiber (Mishra, Hosain, Goyal and Sharma, 1984). By wavelength division multiplexing, the information carrying capacity increases through this kind of fiber (Olsson, Hegartz, Logen, Johnson, Walker, Cohen, Kasper and Campbell, 1985). Further, system designers are continuously trying to design the refractive index profile in order to increase the first higher order mode cut – off frequency for the purpose of ensuring higher core radius and low splice loss.

Now a day in optical fiber communication, dual mode optical fiber has taken an important part (Spajer and Charquille, 1986; Eguchi, 2001; Eguchi, Koshiba and Tsuji, 2002; Amin, Ali, Chen and Shieh, 2011). Large negative waveguide dispersion is compensated by positive dispersion in the first higher mode of dual mode optical fiber. This happens around the wavelength  $1.55\text{ }\mu\text{m}$  and an erbium doped fiber operates around this wavelength (Pedersen, 1994). Lower transmission loss and bending loss is produced more efficiently by double – layer profile core dispersion shifted fiber in comparison to the single core – cladding dispersion shifted one (Monerie, 1982). Thus dual mode double – layer optical fiber is the preferred choice of for broadband transmission, working around the wavelength  $1.55\text{ }\mu\text{m}$ . The group delay between the fundamental and first higher order mode can be easily calculated with the time difference due to the spectral interface between two modes. Fundamental and leaky first higher mode can be generated due to the coupling of an ultra – short laser pulse and a dual mode optical fiber. With the help of this phenomenon, different parameters of  $\text{LP}_{11}$  mode are analysed using different approach (Ohashi, Kitayama, Kobayashi and Ishida, 1984). Also in dual mode propagation, method for calculations of  $\text{LP}_{01}$  and  $\text{LP}_{11}$  mode losses separately are reported (Ohashi, Kitayama, Kobayashi and Ishida, 1984). The group delay between the fundamental and first higher order mode is used in sensor technology as well. Thus, dual mode optical



fiber communication with linear, nonlinear and doped fiber happens to be an important research matter (Mayura, Mayura and Verma, 2023; Chen, Li, Zhang and Zhu, 2010; Ryu, Choi, Chang, Kim, Choi, Ahn, Kim, Yoon and Lee, 2012).

Many methods have been developed to predict the propagation parameters, both in fundamental and first higher order mode. To make the estimations user friendly, the relevant methods should be simple and accurate.

However, in case of graded index fiber employed for communication purpose, the relative core – cladding refractive index difference is kept small (less than 0.5%) in order to ensure low scattering loss and pulse dispersion as well. Such fibers are called weakly guiding fibers (Gloge, 1971) and in case of fibers of this kinds, the complicated vector wave equation can be approximated as a scalar wave equation, fibers of this kind are called weakly guiding fibers and the said approximation is called scalar wave approximation.

From the scalar wave equation, various propagation parameters can be estimated easily (Neumann, 1988; Ghatak & Thyagarjan, 1998). Though it is discovered that the parameters found by solving the scalar as well as vector wave equation are nearly equal (Gloge, 1971). The speciality of weakly guided approximation is, the modes are linearly polarized and have very small longitudinal component. The analytical scalar wave solutions are available for both types of fiber – the step index or the graded index one. For other kind of fibers, variational or numerical techniques are applied to find out the solutions from scalar wave equations (Pattojoshi and Hosain, 1998; Chaudhuri and Roy, 2007; Khijwania, Nair and Sarkar, 2009; Ghosh, Roy and Bhadra, 2010; Behera, Hosain and Pattojoshi, 2011; Mallick and Sarkar, 2014; Mukhopadhyay, 2016). From the analytical solutions, integrations, corresponding to Bessel function or modified Bessel function are to be executed in order to find out the propagation constants. This is very much tedious. On the other hand, the single parameter variational technique provides much simplicity in calculation (Marcuse, 1978). Though accuracy of this method is less. Again the two parameter variational technique provides more accurate result (Mishra, Hosain, Goyal and Sharma, 1984; Ankiewicz and Peng,

1992). But, this technique is complicated. Hence, the formulation of a simple and accurate expression for the fundamental or higher order modes of different kinds of fibers are always desirable, from which, different propagation parameters of different modes can be easily determined. Hence, the said formulation is on high demand in the optical communication technology.

Further, an accurate but simple power series expression of fundamental mode of graded index fiber has been formulated using Chebyshev method (Gangopadhyay, Sengupta, Mondal, Das and Sarkar, 1997).

This formalism employs application of linear least square fitting technique so as to develop a linear relation of  $\frac{K_1(W)}{K_0(W)}$  with  $\frac{1}{W}$  over the long and practical range of  $W$  values such as  $0.6 \leq W \leq 2.5$ . Using

the said linear relationship, Gangopadhyay, Sengupta, Mondal, Das and Sarkar, 1997 reported the simple but accurate power series expression for the fundamental modes of graded index fibers. Using, only the first four terms in the series expression, they confirmed that the developed series expressions for the fundamental modes are virtually indistinguishable with the simulated exact ones for both the core as well as the cladding. The execution of the developed formulation requires solution of a fourth order determinant with very less computations. This simple but accurate expression of fundamental mode of graded index fiber can be employed in order to estimate different propagation parameters of such fibers. In fact, the use of the said technique for estimating different propagation characteristics of single-mode graded index fibers has given excellent results (Gangopadhyay, Sengupta, Mondal, Das and Sarkar, 1997; Gangopadhyay and Sarkar, 1997a, 1998a, 1998b; Gangopadhyay, Choudhury and Sarkar, 1999) and accordingly, this formalism requires more application in the study of optical communication systems and optical sensors as well. Again, some modifications of the said method, in the form of linear least square fitting of  $\frac{K_1(W)}{K_0(W)}$  with  $\frac{1}{W}$  over a few small interval of  $W$ , has also accurately predicted graded index fiber characteristics in the low  $V$  region, such a  $V < 1.4$  for step index and  $V < 1.9$  for parabolic index fibers (Patra, Gangopadhyay and Sarkar, 2000).

Another important matter is the study of first higher order ( $LP_{11}$ ) modal field. Further, in case of step index fiber, the analytical expression for  $LP_{11}$  modal field is available in literature. Since, it contains modified Bessel functions, its applications in predicting the propagation characteristics involves complicated integrations. Accordingly, numerical techniques or approximate methods are usually applied for the concerned study. However, the existing numerical and approximate methods of the said kind for the prediction of  $LP_{11}$  modal field and associated propagation characteristics for graded index fibers involve cumbersome computations (Sharma, Goyal and Ghatak, 1981). Such techniques are, therefore, not user friendly for prediction of the fiber characteristics. Thus, prescription of a simple but accurate expression of the first higher modal field is still in demand in literature. The Chebyshev power series formalism for evaluating accurately  $LP_{11}$  mode cut-off frequency for graded index fibers, is available in literature (Chen, 1982; Shijun, 1987). This method takes care of solution of quadratic equation obtained from a determinant of third order and the concerned calculations can be done by using a pocket calculator only. This is, indeed convenient for the system designers. Again, power series expression for first higher order modal field for graded index fiber has been developed by using Chebyshev formalism (Patra, Gangopadhyay and Goswami, 2008). The developed simple but accurate power series form of first higher order modal field generates scopes for its application in estimating different propagation characteristics of graded index fibers. Side by side, the said method causes motivation for formulation of power series form of modal field of dispersion-shifted as well as dispersion-flattened fibers.

To get the optimal efficiency in optical communication, an excellent coupling between the laser source and the single mode fiber should be there. For this purpose, the microlenses of different types and shapes are inserted at the tip of the fiber. Also optical fibers of different refractive index profile are also used to make the gain maximum. These ideas are in high demand in the field of coupling optics. While inserting a microlense on a fiber tip, it should be kept in mind that its aperture should be large enough so that all incident radiation could enter into it and also the focal length of the micro lens should cause matching of laser and fiber modes. The lens should also be free of spherical aberration (Presby & Edwards, 1992a;

Edwards et al., 1993). Among different types of micro lenses, hyperbolic one is the most effective. Theoretically it can have 100% efficiency at a specific focal length (Presby & Edwards, 1992a). On the other hand, as hemispherical lens has small aperture, spherical aberration and modal mismatch, its efficiency is moderate (Edwards et al., 1993). But manufacturing hemispherical lens on a fiber tip is easier than that of the hyperbolic one. A hyperbolic lens can be fabricated by specialized laser micromachining techniques on the contrary, a hemispherical lens requires a simple photolithographic procedure. In this context, tapered lens is also used. Also the different refractive index profiles of different optical fibers, along with different types of micro lenses are studied to find out for which profile index and for what type of micro lens can provide the optimum output (Saruwatari & Nawata, 1979; Ghafouri-Shiraj & Asano, 1986; Sarkar et al., 1986; Ghafouri-Shiraj, 1988; Hillerich & Guttman, 1989; Modavis & Webb, 1995; An, 2000; Rahman et al., 2002; Tang et al., 2002; Thual et al., 2003; Hongzhan et al., 2005; Liu et al., 2005; Sambanthan & Rahman, 2005; Hu et al., 2008; Liu, 2008; Chao et al., 2010; Huang & Yang, 2010; Yang et al., 2010; Jie et al., 2010). To assume the coupling optics in simple but accurate fashion (Gangopadhyay and Sarkar, 1996, 1997b, 1998c, 1998d, 1998e; Mukhopadhyay, Gangopadhyay and Sarkar, 2007, 2010; Huang and Yang, 2010; Mukhopadhyay and Sarkar, 2011), ABCD matrix technique (Massey and Siegman, 1969; McMullin, 1986; Yariv, 1991) has been employed for various kinds of microlenses fabricated on the fiber tip of optical fibers.

It should be noted that small spot size of laser beam ( $\sim 1\mu\text{m}$ ) have to be increased by suitable lens to match it with the larger spot size ( $\sim 5\mu\text{m}$ ) of the fiber to get maximum coupling efficiency. Hence, to get maximum coupling efficiency, the idea of the spot size made by the lens transformed beam and that of the fiber itself, have to be very clear. Along with this, a concrete idea about the refractive index profile of the optical fiber should be present (Mukhopadhyay & Sarkar, 2011). Its theoretical prediction need phase matching technique, which require lengthy computation (John et al., 1994). A simple and accurate application of ABCD matrix formalism technique on the microlens – optical fiber couple can solve this

problem easily (Gangopadhyay & Sarkar, 1996; Gangopadhyay & Sarkar, 1997b; Gangopadhyay & Sarkar, 1998c).

In order to ensure all optical technology, the electronic amplifier is replaced by optical amplifier which requires doping the fiber with rare earth metal (Mears, Reekie, Jauncey and Payne, 1987). It is used mainly to amplify the weak signals optically, rather than following the conventional O/E or E/O technology. It is also necessary to study in a simple but accurate method, different types of optical devices inserted in the optical fibers for communication purpose like filters, sensors, fiber Bragg grating, directional couplers etc. (Lam and Garside, 1981; Gaylord and Moharam, 1985; Kersey, Berkoff and Morey, 1993; Jung, Nam, Lee, Byun and Kim, 1999; Sanyal, Gangopadhyay and Sarkar, 2000; Fang, Liao and Wang, 2010; Dai, Wang and Bowers, 2011).

Non - linear optics has huge effect on modern day optical communication system (Snyder et al., 1990; Agrawal & Boyd, 1992). Again, the third order Kerr nonlinearity has huge effect in fiber optics transmission. In this literature, the effect of Kerr nonlinearity on various propagation parameters on the commonly using modes  $LP_{01}$  and  $LP_{11}$  has been discussed. The modal field prediction in presence of Kerr nonlinearity for these two modes had already been cited (Chakraborty et al., 2018a; Chakraborty et al., 2018b). It helps to reduce the calculation complexities to find out the various parameters involving the propagation, by applying simple power series expansion on Chebyshev technique. Previously reported group delay (Mukherjee et al., 2020a), spot size (Aich et al., 2019; Aich et al., 2021), splicing loss (Maiti et al., 2019) and other parameters by different scholars, helps in determining dispersion loss and transmission speed in optical communication system. The changes in optical devices like directional couplers due to Kerr non linearity, using single mode fiber has also been elaborated (Mukherjee et al., 2020b). The same has been done for a triangular index fiber as well (Ray et al., 2021; Ray et al., 2022a). The splice loss in different types of fibers for  $LP_{01}$  and  $LP_{11}$  mode considering the Kerr type nonlinearity has also been studied by scholars (Rakshit et al., 2021; Rakshit et al., 2022a). By the combined effect of temporal and spatial solitons light pulse propagates simultaneously both temporally and spatially (Chen,

1991; Hasegawa & Kodama, 1991; Sammut et al., 1992; Triki et al., 2017). This increases the interest of the study on the application of the temporal – spatial soliton.

For long distance optical communication network, dispersion loss is a major concern as it deteriorates the transmitted optical signal and limits the performance. This problem in EDFA devices and directional couplers are cited in literature (Mukherjee et al., 2022; Rakshit et al., 2022b; Ray et al., 2022b).

## 1.2. STUDY OF OPTICAL FIBER COMMUNICATION IN THE FRAME WORK OF ELECTROMAGNETIC THEORY

The material of the fiber is assumed to be isotropic, non-conducting, non-magnetic and linear (Ghatak & Thyagarajan, 1998). Maxwell's equations for such kind of medium can be given by

$$\vec{\nabla} \times \vec{E} + \mu_0 \frac{\partial \vec{H}}{\partial t} = 0$$

$$\vec{\nabla} \times \vec{H} = \frac{\partial \vec{D}}{\partial t} \tag{1.1}$$

$$\vec{\nabla} \cdot \vec{B} = 0, \quad \vec{\nabla} \cdot \vec{D} = 0$$

Here,  $\vec{E}$ ,  $\vec{H}$ ,  $\vec{B}$  and  $\vec{D}$  represent the electric intensity, magnetic intensity, magnetic induction vector and electric displacement vector respectively.  $\vec{D}$  can be given as

$$\vec{D} = \epsilon_0 n^2 \vec{E} \tag{1.2}$$

where  $\mu_0$ ,  $\epsilon_0$  respectively denote the magnetic permeability and the permittivity of free space and while the refractive index of the corresponding medium is represented by  $n$ . Using Eq. (1.1) and (1.2) the following vector wave equations are obtained

$$\nabla^2 \vec{E} + \vec{\nabla} \left( \vec{E} \cdot \frac{\vec{\nabla} n^2}{n^2} \right) - \mu_0 \epsilon_0 n^2 \frac{\partial^2 \vec{E}}{\partial t^2} = 0 \quad (1.3)$$

$$\nabla^2 \vec{H} + \frac{1}{n^2} (\vec{\nabla} n^2) \times (\vec{\nabla} \times \vec{H}) - \mu_0 \epsilon_0 n^2 \frac{\partial^2 \vec{H}}{\partial t^2} = 0 \quad (1.4)$$

For an inhomogeneous medium, Eq. (1.3) shows that  $E_x$ ,  $E_y$  and  $E_z$  are coupled while  $H_x$ ,  $H_y$  and  $H_z$  are also coupled as shown by Eq. (1.4).

Considering optical waveguide for which the refractive index profile does not vary along the direction of propagation ( $z$  axis), we can write,

$$n^2 = n^2(x, y) \quad (1.5)$$

In case of refractive index profile given by Eq. (1.5), the solutions of Eqs. (1.3) and (1.4) can be given as

$$\vec{E}(x, y, z, t) = \vec{E}(x, y) e^{j(\beta z - \omega t)} = [\vec{E}_t(x, y) + \vec{E}_z(x, y)] e^{j(\beta z - \omega t)} \quad (1.6)$$

$$\vec{H}(x, y, z, t) = \vec{H}(x, y) e^{j(\beta z - \omega t)} = [\vec{H}_t(x, y) + \vec{H}_z(x, y)] e^{j(\beta z - \omega t)} \quad (1.7)$$

Here,  $\vec{E}_t$  (or  $\vec{H}_t$ ) and  $\vec{E}_z$  (or  $\vec{H}_z$ ) are respectively the transverse and longitudinal components of electric or magnetic field vectors in the Cartesian system of coordinates respectively and  $\beta$  represents the propagation constant.

Using Eqs. (1.6) and (1.3), one can obtain the vector wave equation for  $\vec{E}_t$  as follows

$$\nabla_t^2 \vec{E}_t + [k_0^2 n^2(x, y) - \beta^2] \vec{E}_t = -\vec{\nabla}_t [\vec{E}_t \cdot \vec{\nabla}_t (\ln n^2)] \quad (1.8)$$

$$\text{where, } \vec{\nabla}_t = \vec{\nabla} - \hat{z} \frac{\partial}{\partial z}; \quad k_0 = \omega / c = 2\pi / \lambda_0 \quad (1.9)$$

and,  $k_0$  is the free space wave number.

Practically, in case of most of the optical waveguides and optical fibers, the relative core cladding refractive index difference is kept very small in order to achieve minimum pulse dispersion and scattering loss (Neumann, 1988). This is called the weakly guiding condition (Gloge, 1971). Under this condition, the term on the right hand side of Eq. (1.8) becomes so small that we can neglect it for all practical purposes. Accordingly, Eq. (1.8) under this condition, known as scalar wave approximation (Gloge, 1971), reduces to a scalar wave equation given below,

$$\nabla_t^2 f + [k_0^2 n^2(x, y) - \beta^2] f = 0 \quad (1.10)$$

Where,  $f$  is either the x or y component of  $\vec{E}(x, y)$  and  $\nabla_t^2$  is the scalar Laplacian operator.

Since,  $n^2$  for practical fibers depends on the radial distance from the core axis, it is convenient to use the cylindrical coordinates in eq. (1.10) and accordingly it can be written as

$$\frac{\partial^2 f}{\partial r^2} + \frac{1}{r} \frac{\partial f}{\partial r} + \frac{1}{r^2} \frac{\partial^2 f}{\partial \phi^2} + [k_0^2 n^2(r) - \beta^2] f = 0 \quad (1.11)$$

Eq. (1.11) can be solved by using separation of variables method since the medium has cylindrical symmetry. Hence, one can use

$$f(r, \phi) = \psi(r) F(\phi) \quad (1.12)$$

Applying Eq. (1.12) in Eq. (1.11), we get,



$$\frac{r^2}{\psi} \left( \frac{d^2 \psi}{dr^2} + \frac{1}{r} \frac{d\psi}{dr} \right) + r^2 [k_0^2 n^2(r) - \beta^2] = -\frac{1}{F} \frac{d^2 F}{d\phi^2} = l^2 \quad (1.13)$$

Here,  $l$  is a constant. Thus from the above Eq. (1.13) we get,

$$\frac{d^2 F}{d\phi^2} + l^2 F = 0 \quad (1.14)$$

The solution of the eq. (1.14) is

$$F(\phi) = \sin l\phi \text{ or } \cos l\phi \quad (1.15)$$

The boundary condition  $F(\phi + 2\pi) = F(\phi)$  leads to  $l = 0, 1, 2, \dots$  etc. The negative values of  $l$  correspond to the same field distribution. Here,  $m$  is known as azimuthal mode number.

Also, we get the following equation from Eq. (1.13)

$$\frac{d^2 \psi}{dr^2} + \frac{1}{r} \frac{d\psi}{dr} + \left[ k_0^2 n^2(r) - \beta^2 - \frac{l^2}{r^2} \right] \psi = 0 \quad (1.16)$$

For a given value of  $l$  and a particular set of values of the fiber parameters, eq. (1.16) provides a finite number of allowed solutions for  $\beta^2$  which can be presented as  $\beta_{l1}^2, \beta_{l2}^2, \beta_{l3}^2, \dots$  etc. These can be represented generally in the form of  $\beta_{lm}^2$  with  $m$  being 1, 2, 3, .... etc. The corresponding modes are known as  $LP_{lm}$  (linearly polarized) modes while 'm' is known as the radial mode number. Thus, for example  $LP_{11}$  stands for the linearly polarized mode, obtained from the solution of the eq. (1.16) corresponding to the propagation constant  $\beta_{11}$ .

For a weakly guiding fiber, the refractive index profile  $n(R)$  becomes

$$n^2(R) = n_1^2 (1 - 2\delta f(R)), \quad R \leq 1$$

$$n^2(R) = n_2^2, \quad R > 1 \quad (1.17)$$

where,  $R = \frac{r}{a}$ ,  $a$  = radius of the core and  $r$  = radius from the core axis.

Further,  $\delta = \frac{(n_1^2 - n_2^2)}{2n_1^2}$ ,  $n_1$  and  $n_2$  are the refractive indices along the core axis and the cladding respectively.

and  $f(R)$  denotes the shape of the refractive index profile.

Combining Eqs. (1.16) and (1.17) we get the following equations

$$\frac{d^2\psi}{dR^2} + \frac{1}{R} \frac{d\psi}{dR} + [V^2(1 - f(R)) - W^2]\psi - \frac{l^2}{R^2}\psi = 0, \quad R \leq 1 \quad (1.18)$$

$$\text{and } \frac{d^2\psi}{dR^2} + \frac{1}{R} \frac{d\psi}{dR} - W^2\psi - \frac{l^2}{R^2}\psi = 0, \quad R > 1 \quad (1.19)$$

where,  $V(= k_0 a(n_1^2 - n_2^2)^{1/2})$  is the normalized frequency and  $W(= a(\beta^2 - k_0^2 n_2^2)^{1/2})$  is the cladding decay parameter.

For fundamental mode ( $l=0$ ), Eq. (1.18) and Eq. (1.19) are given by

$$\frac{d^2\psi}{dR^2} + \frac{1}{R} \frac{d\psi}{dR} + [V^2(1 - f(R)) - W^2]\psi = 0, \quad R \leq 1 \quad (1.20)$$

$$\frac{d^2\psi}{dR^2} + \frac{1}{R} \frac{d\psi}{dR} - W^2\psi = 0, \quad R > 1 \quad (1.21)$$

For the large value of  $WR$ , the approximate solution of Eq. (1.21) will be as follows

$$\psi(R) \sim \left( \frac{\pi}{2WR} \right)^{1/2} \exp(-WR) \quad (1.22)$$

From Eq. (1.22), it is observed that the electric field inside the cladding decays almost exponentially as a function of  $WR$ , since the square root term decays less rapidly than the exponential term. That is why,  $W$  is termed as the cladding decay parameter.

For a particular refractive index profile, the number of allowed  $\beta$  values, which give the number of linearly polarized modes propagating through the fiber, depends on 'a', ' $n_1$ ', ' $n_2$ ', ' $\lambda$ ' and as a whole on the normalized frequency 'V'.

In optical fiber communication, the propagation constant for guided mode which decays in an exponential manner inside the cladding, should also satisfy the following condition (Ghatak & Thyagarajan, 1998).

$$k_0^2 n_1^2 > \beta^2 > k_0^2 n_2^2 \quad (1.23)$$

### 1.3 AIM OF THE THESIS AND FUTURE SCOPE

In the first stage of research work, simple but analytical expressions for fractional modal power, the excitation efficiency and the normalized group delay parameter for first higher order mode in graded index fibers are considered. Next, those expressions are first used to evaluate the said parameters in absence of Kerr type nonlinearity, then the method of interaction is applied in order to predict the said parameters for some typical graded index fibers in presence of some suitable Kerr non linearity in case of first higher order mode. The same predictions were made by rigorous finite element method. The interesting outcome is that our results found on the basis of Chebyshev formalism match excellently with the results found by quite complicated finite element technique.

Then the formalism developed generates enough scope for its application in other kinds of fiber like photonic crystal fiber, holey fiber in the context of estimation of various propagation parameters in presence of Kerr type nonlinearities. Scopes are also there to use its applicability in other kinds of

nonlinearity like fifth order etc, including saturable nonlinearity. Conclusively, this simple formalism, if extended as such, will benefit the system users immensely in the field of nonlinear photonics.

The prediction of coupling optics involving different kinds of microlenses fabricated on the tips of different kinds of optical fibers is a potential area in the field of optical communication and sensor technology. Accordingly, in the next phase of research work, we concentrated on prediction of coupling optics in case of cylindrical microlense fabricated on the tips of graded index fiber having different profile exponents. This theoretical investigation involved application of ABCD matrix formalism appropriate for cylindrical microlens. In our study, we estimate the coupling efficiency for two commonly used wavelengths such as  $1.3\text{ }\mu\text{m}$  and  $1.5\text{ }\mu\text{m}$ . It has been found that the wavelength  $1.3\text{ }\mu\text{m}$  provides more efficient coupling. The objective is to find out the most coupling efficient graded index fiber. It has been found that the graded index fiber having the profile exponent 4 gives maximum coupling efficiency of the wavelength  $1.3\text{ }\mu\text{m}$ .

Incidentally, the same coupling optics could have been predicted by applying complex numerical interpretation based on phase matching technique. ABCD matrix formalism provides a simple but accurate method for prediction of coupling optics. This is why the prediction of coupling optics is now a days made by the relevant ABCD matrix formalism in place of complex numerical interpretation.

The previous analysis generates scope for future researchers in the context of application of ABCD matrix formalism in prediction of coupling optics related to different types of microlenses as well as tapered lenses on the tips of various kinds of fibers. The problem is to formulate the relevant matrix appropriate for the coupling device in order to predict the concerned coupling optics.

## **1.4 THE STRUCTURE OF THE THESIS**

Chapter 1 of the thesis contains brief introduction to the basics of optical waveguides along with concerned electromagnetic theory. It also contains different available methods for evaluation of propagation parameters both for fundamental and first higher order mode. Also, the technology of launch optics involving different kind of microlenses fabricated on various types of fibers have been presented in this chapter. The merits of different kinds of such optical couplers in respect of coupling efficiency have also been discussed here. This chapter also comprises brief introduction to dual mode optical fiber, rare earth metal doped optical fiber and nonlinear optics with special emphasis on Kerr type nonlinearity. Further, this chapter describes the objective of the present research work together with its importance to contemporary interest and future researches as well. The relevant citations have also been made here.

Chapter 2 consists of the literature survey, highlighting the relevant research gaps and the needful address to the gaps thereof.

Chapter 3 comprises prescription of a simple but accurate method for prediction of confinement and normalized group delay parameters for first higher order mode in graded index fiber. The said parameters have been estimated both in presence and absence of Kerr type nonlinearities. This said prescription involves use of Chebyshev technique for estimation of the concerned propagation parameters. In case of nonlinearity, method of iteration has been applied for necessary prediction,

Chapter 4 presents the study of coupling optics relating to an optical coupler consisting of laser diode, graded index fiber and cylindrical microlens fabricated on the tip of the fiber. Here, ABCD formalism appropriate for the system has been developed in order to predict the coupling optics in a simple but accurate fashion. The investigation has been carried on for graded index fibers having different profile exponents. The profile exponent which is most coupling efficient in this context has been predicted.

Chapter 5 describes the conclusion found on the basis of the research work described in the thesis. The conclusion basically aims at presenting the novelty of the present work and the enrichment of the literature in terms of its potential in present as well as future research. Chapter 5 precedes references which have been cited in the thesis.

The said research work has led to two publications in international journals of repute. The said two publications have been taken care of in drafting chapters 3 and 4.

# *CHAPTER 2*

## *LITERATURE SURVEY, RESEARCH GAPS AND ADDRESS*

## **FIRST PART OF THE RESEARCH WORK**

### **2.1 LITERATURE SURVEY**

Single-mode optical communication system is always preferable owing to its large bandwidth. The operating wavelength for silica made optical fiber is usually kept between  $1.3\mu\text{m}$  and  $1.6\mu\text{m}$  in order to minimize attenuation and dispersion simultaneously. By properly designing the refractive index profile together with the core radius of optical fiber, one can cancel material dispersion by the wave guide dispersion at a particular wavelength  $1.55\mu\text{m}$  (Neumann, 1988; Ghatak & Thyagarajan, 2002). This gives negligible attenuation and dispersion simultaneously at the wavelength  $1.55\mu\text{m}$  and silica – made optical fiber of such kind is called dispersion shifted fiber (Paek, 1983; Ainslie & Day, 1986; Tewari et al., 1992). In another kind of optical fiber known as dispersion flattened fiber, very small dispersion is provided over a wavelength range (Garth, 1989) and fiber of this kind is effective in increasing the information capacity by wavelength division multiplexing (Olsson et al., 1985). Further, nonlinearity induced distortion has effect on the effective core area of the optical fiber (Streckert & Wilezewski, 1996; Namihara, 1997a; Namihara, 1997b; Ghatak & Thyagarajan, 2002). Less effective core area causes more nonlinear effect on the optical signal. Therefore, evaluation of effective core area both in presence and absence of nonlinearity in case of optical fibers is very important in the study of present optical communication systems. The index of refraction controls the net delay of optical light beam in a specific mode. The estimation of the interaction between  $\text{LP}_{01}$  and  $\text{LP}_{11}$  mode in case of a dual mode optical fiber requires the knowledge of the effective index of refraction (Savolinen et al., 2012). Again, the said knowledge is also essential for system modeling and fiber Bragg grating sensors (Patrick et al., 1996). Further, the knowledge of accurate value of cladding decay parameter ( $W$ ) is also necessary for accurate estimation of effective index of refraction. Two parameters such as intensity of optical beam and nature of transmitting medium are responsible for generation of various types of nonlinearity like third order, fifth order, saturable, etc.



(Agrawal, 2013). Kerr nonlinearity is also known as third order nonlinearity. Further, nonlinearity being responsible for production of noise in optical signal (Antonelli et al., 2017), the study of the effect of Kerr nonlinearity on different propagation parameters like effective core area and effective index of refraction of single-mode dispersion managed fibers etc. are subjects of contemporary interest in the field of nonlinear photonics. Recently, investigations related to effect of Cross-Kerr nonlinearity on parity and time symmetry in optical lattices in case of nonlinear atoms have enriched the literature (Din et al., 2021). Further, the effect of optical Kerr nonlinearity on various propagation characteristics of fibers having various types of refractive index profiles has already been added to the literature (Hayata et al., 1987; Okamoto et al., 1994; Saitoh et al., 2006; Khijwania et al., 2009). Influence of optical Kerr nonlinearity on the first higher order mode cutoff frequency of single-mode dispersion shifted and dispersion flattened fibers is also a significant contribution in the domain of nonlinear photonics (Mondal & Sarkar, 1996). However, the estimation using the formulations in Refs (Hayata et al., 1987; Mondal & Sarkar, 1996; Okamoto & Marcatelli, 1994; Khijwania et al. 2009) requires complicated computations involving a lot of time. Side by side, literature has been enriched by formulation of the simple but accurate Chebyshev formalism in the context of prediction of different propagation characteristics of single-mode graded index fibers both in the linear (Gangopadhyay & Sarkar, 1997a; Gangopadhyay et al., 1997; Gangopadhyay et al. 1998b; Patra et al., 2001a; Patra et al. 2001b) and Kerr type nonlinear domain as well (Sadhu et al., 2013; Chakraborty et al., 2017a; Maiti et al, 2019; Roy et al., 2020; Mukherjee et al., 2020b). The said Chebyshev formalism has also been found to provide excellent accuracy in predicting effective core area, effective index of refraction and fractional modal power through the fiber core for Kerr type nonlinear single-mode graded index fiber (Maiti et al., 2020). Further, the same formalism has been used for estimation of effective core area and effective index of refraction for mono-mode nonlinear dispersion shifted and dispersion flattened fibers (Gangopadhyay & Sarkar, 1997a; Gangopadhyay et al., 1997b; Gangopadhyay & Sarkar, 1998b; Patra et al., 2001a; Patra et al. 2001b; Sadhu et al., 2013; Chakraborty et al., 2017a; Maiti et al, 2019; Roy et al., 2020; Mukherjee et al., 2020b).

If the electromagnetic field of the incident light is of high intensity, it generates nonlinearity in silica made optical fiber. This causes nonlinear variation of total induced polarization  $P$  with the electric field  $E$ . Further, the centrosymmetric  $\text{SiO}_2$  being the material of the fiber, the refractive index of the material does not depend on terms like  $E$ ,  $E^3$ ,  $E^5$  etc. Accordingly, the refractive index comprises terms containing intensity of light and its higher powers. Kerr nonlinearity is concerned with the dependence of the refractive index on the intensity of light ( $E^2$ ) only. Further, it is also known as third order nonlinearity as the concerned scalar wave equation contains cubic term in  $E$ . This change of refractive index causes change in the modal field inside the fiber and consequently the different propagation parameters associated with the fiber undergo change. It is relevant to mention in this connection that other higher orders of nonlinearity are generated due to dependence on terms like  $E^4$ ,  $E^6$  etc. Recently, polarized light manipulation utilizing Kerr nonlinearity has been contributed to the literature [Wen, Hu, Rui, Lv, He, Gu and Cui, 2014]. Again, it has already been investigated how Kerr nonlinearity affects the propagation-related concerns of graded index (GI) and PCFs [Hayata, Koshihara and Suzuki, 1987; Okamoto and Marcaty, 1994; Saitoh, Fujisawa, Kirihaara and Koshihara, 2006; Khijwania, Nair and Sarkar, 2009]. Additionally, there is literature that discusses how Kerr nonlinearity affects the  $\text{LP}_{11}$  mode cutoff  $V$  number for both dispersion-shifted and dispersion-flattened fibers [Mondal and Sarkar, 1996]. As described earlier, the approaches in Refs. [Hayata, Koshihara and Suzuki, 1987; Okamoto and Marcaty, 1994; Mondal and Sarkar, 1996; Saitoh, Fujisawa, Kirihaara and Koshihara, 2006; Khijwania, Nair and Sarkar, 2009] require time-consuming calculations to be performed. Accordingly, the literature demands the development of a realistic yet straightforward methodology for estimating of optical fiber propagation parameters in the nonlinear domain in the context of both communication systems and sensor technology. In this aspect, it is pertinent to note that the Chebyshev technique-based simple series formulation of the fundamental ( $\text{LP}_{01}$ ) mode of graded index fiber has been reported to be outstanding at projecting its propagation properties in the linear realm [Gangopadhyay and Sarkar, 1997a; Gangopadhyay, Sengupta, Mondal, Das and Sarkar, 1997; Patra, Gangopadhyay and Sarkar, 2000; Patra, Gangopadhyay and Sarkar,

2001a]. Additionally, by using the iterative method, the aforementioned formulations have been used to project the propagation-related concerns and the performance of directional couplers of GI and dispersion-managed fibers in the Kerr category nonlinear area [Sadhu, Karak and Sarkar, 2013; Aich, Maiti, Majumdar and Gangopadhyay, 2019; Roy, Majumdar, and Gangopadhyay, 2020; Mukherjee, Maiti, Majumdar and Gangopadhyay, 2020; Rakshit, Majumdar and Gangopadhyay, 2021; Aich, Majumdar and Gangopadhyay, 2021; Ray, Majumdar and Gangopadhyay, 2021; Rakshit, Majumdar, Maiti and Gangopadhyay, 2022a; Mukherjee, Majumdar and Gangopadhyay, 2022b]. Recent literature reports on the far field pattern of the  $LP_{11}$  mode dispersion-controlled fibers utilizing the same formalism [Roy, Majumdar and Gangopadhyay, 2022]. Moreover, using the same technique, the effect of Kerr nonlinearity on signal and pump intensities in an EDFA built of  $LP_{11}$  mode SI fiber has also been introduced to the literature [Ray, Majumdar and Gangopadhyay, 2022b].

## 2.2 RESEARCH GAPS

Actually, the study of Kerr nonlinearity has come to light as a possible issue of current interest. Technologists and researchers are working to develop fresh concepts in this field. In this regard, the study such as the impact of nonlinearity regarding characteristics such as FMP directed via the fiber core, excitation efficiency, and normalized group delay for  $LP_{11}$  mode GI fibers is significant for the domain of optical engineering. The FEM can be used to estimate how Kerr nonlinearity will affect the above-mentioned parameters [Hayata, Koshihara and Suzuki, 1987]. However, this method is stringent and requires time-consuming computation.

## 2.3 ADDRESS

We chose to use the Chebyshev formalism to estimate the aforementioned propagation characteristics of Kerr type nonlinear GI fibers because of the accuracy and simplicity of the formalism. To get the constants in the series expression of the  $LP_{11}$  modal field for GI fiber in this setting, we employ the

approach of iteration while taking care of the relevant nonlinearity. Step and parabolic profile fibers are used in our investigation as typical instances of GI fibers, along with one common type of Kerr nonlinearity, with each being taken into account for both +Ve and -Ve nonlinearity. Moreover, we compare our results with the exact results produced by employing a strict FEM in order to confirm the accuracy of our formalism. In this regard, it is noteworthy to mention that, to the best of our knowledge, no such easy method based on the Chebyshev formalism for the evaluation of these key parameters of Kerr-type nonlinear fibers have been reported till date, making our approach innovative.

## **SECOND PART OF THE RESEARCH WORK**

### **2.4 LITERATURE SURVEY**

The intermodal dispersion being absent in single-mode optical fiber, it possesses large bandwidth and as such single-mode optical fiber emerges as the most effective medium in the field of communication. As regards laser diode to fiber coupling, microlenses fabricated on the single-mode fiber tips are most coupling efficient (Presby et al., 1992a; Edwards et al., 1993; John et al., 1994). Thus, various types of microlenses are being fabricated on fiber tips and the concerned coupling efficiencies are being investigated and reported. (Presby et al., 1992a; Presby et al., 1992b, Edwards et al., 1993; John et al., 1994; Gangopadhyay & Sarkar, 1996). These microlenses have self-centering characteristics (John et al., 1994). Again, as discussed earlier, the operating wavelength is kept between  $1.3\mu\text{m}$  and  $1.6\mu\text{m}$  in order to get minimum attenuation loss and minimum material dispersion simultaneously. Although, slightly less efficient but easily fabricable hemispherical microlens on the fiber tip is used widely (John et al., 1994), the hyperbolic microlens on the tip of step index fiber produces almost 100% coupling efficiency theoretically (Kurokawa et al., 1975; Presby et al., 1992a; Edwards et al., 1993; John et al., 1994, Gangopadhyay & Sarkar, 1996; Gangopadhyay & Sarkar, 1998d). But the fabrication of hyperbolic lensed fiber needs application of sophisticated laser micromachining technique (Edwards et al., 1993). Further, the hemispherical microlens on the fiber tip is less efficient on account of its limited aperture; spherical

aberration and mode mismatch (Presby et al., 1992a; Edwards et al., 1993). But, it is used most as its fabrication needs use of simple photographic technique (Edwards et al., 1993). Again, fabrication of different types of upside down tapered lenses on fibers having various kinds of refractive index profiles in optical fiber are being continuously reported to the literature of optimum coupling optics (Yuan & Shou, 1990; Yuan & Qui, 1992; Mondal et al., 1998; Mondal & Sarkar, 1999; Lie et al., 2010; Mukhopadhyay et al., 2010; Mujumdar et al., 2017; Maiti et al., 2017; Mandal et al., 2018; Maiti et al., 2019). The big aperture of the tapered lens allows good acceptance of laser light and this is the reason why coupler of this kind is being used in the domain of micro optical systems and large span sensors (Yuan & Shou, 1990; Yuan & Qui, 1992). Again, the easily fabricable cylindrical lensed fiber is also employed in the field of coupling optics because of its reasonably good coupling efficiency (Zhang, 2002; Zhang, 2003). ABCD matrix formalism permits simple but accurate prediction of coupling optics in couplers having different kinds of microlenses and upside down tapered lenses on fiber tips as well (Gangopadhyay & Sarkar, 1996; Gangopadhyay & Sarkar, 1997b; Gangopadhyay & Sarkar, 1998c; Gangopadhyay & Sarkar, 1998d; Mondal & Sarkar, 1999, Mukhopadhyay et al., 2007; Mukhopadhyay et al., 2010; Mukhopadhyay & Sarkar 2011; Bose et al., 2012; Majumdar et al., 2017; Maiti et al., 2017; Mandal et al., 2018; Maiti et al., 2019). It is also relevant to mention in this context that graded index fibers like parabolic and triangular index fibers are important components in the field of optical communication as those have large bandwidth and negligible sensitivity to micro and macro bending. Accordingly, reports of the investigations of launch optics involving graded index fiber are continuously enriching the literature (Mukhopadhyay & Sarkar, 2011; Bose et al., 2012; Maiti et al., 2017; Mandal et al., 2018; Maiti et al., 2019). Very recently study on the coupling optics of hyperbolic microlens on graded index fiber tip of different profile exponents have been made (Mukhopadhyay and Sarkar, 2011).

As discussed above, for the purpose of maximising the coupling, multiple forms of tapered lenses are put on the tip of optical fibers having different kind of refractive index profiles [Mondal, Gangopadhyay and Sarkar, 1998; Yuan, Qui, 1992; Mondal and Sarkar, 1999; Yuan and Shou 1990; Lie, 2010; Mukhopadhyay,

Gangopadhyay and Sarkar, 2010; Majumdar, Mandal and, Gangopadhyay, 2017; Maiti, Maiti and Gangopadhyay, 2017; Mandal, Maiti, Chiu and Gangopadhyay, 2018; Maiti, Biswas, Gangopadhyay, 2019]. In this case, more laser light enters in an optical fiber and increases the coupling efficiency. Due to this advantage, tapered lens is used widely in micro optical studies, light amplification techniques and sensors of large span.

## **2.5 RESEARCH GAPS**

Cylindrical microlens is also a very good coupler and also it is very easy to fabricate, thus it is widely used in the field of coupling optics [Zhang, 2002; Zhang, 2003]. ABCD matrix formalism is a very useful and simple theoretical technique in optical coupling system when multiple forms of micro lenses and the tapered lenses are used on the tips of optical fibers [Gangopadhyay and Sarkar, 1996; Gangopadhyay and Sarkar, 1997; Bose, Gangopadhyay and Saha, 2012; Mondal and Sarkar, 1999; Mukhopadhyay, Gangopadhyay and Sarkar, 2010; Majumdar, Mandal and Gangopadhyay, 2017; Maiti, Maiti and Gangopadhyay, 2017; Mandal, Maiti, Chiu and Gangopadhyay, 2018; Maiti, Biswas and Gangopadhyay, 2019; Mukhopadhyay and Sarkar, 2011; Gangopadhyay and Sarkar, 1998; Gangopadhyay and Sarkar, 1998; Mukhopadhyay, Gangopadhyay and Sarkar, 2007]. The study of the coupling efficiencies of the cylindrical microlens on the graded index fibers were investigated earlier [Roy, Majumdar, Maity S and Gangopadhyay, 2020] but for not for different profile exponents to be done by us.

## **2.6 ADDRESS**

Thus we apply this formalism to compute the coupling efficiency of the cylindrical microlens on the graded index optical fiber for different refractive index profile exponents ( $g$ ) having values  $g = 4.0, 8.0, 10.0$  and  $20.0$ . Here, the coupling is studied for two laser diodes having different wavelengths of  $1.3 \mu\text{m}$  and  $1.5 \mu\text{m}$  [John, Maclean, Ghafouri-Shiraz and Niblett, 1994]. In this study we have applied the limited aperture

technique and the field distribution associated with the source and the fiber are considered to be Gaussian [Sarkar, Thyagrajan and Kumar, 1984; Marcuse, 1978; Sarkar, Pal and Thyagrajan, 1986]. Using the ABCD matrix concept, a simple analytical expression of the coupling efficiency has been found by which one can easily find out the most effective coupler for a particular wavelength of light. The most efficient coupler thus studied should be not only be cost effective but also simple to use. Thus, the simple approach developed will benefit the system users in the process of predicting the coupling optics accurately in a very short time.

Further, as far as our knowledge is concerned, no such investigation on cylindrical microlensed graded index fiber employing ABCD matrix formalism has been reported till date. Thus the concerned method is a novel one.

# *CHAPTER 3*

*A SIMPLE BUT ACCURATE TECHNIQUE FOR  
PREDICTION OF CONFINEMENT, EXCITATION  
EFFICIENCY AND NORMALIZED GROUP DELAY  
PARAMETERS FOR PROPAGATION OF FIRST  
HIGHER ORDER MODE IN GRADED INDEX FIBER  
BOTH IN PRESENCE AND ABSENCE OF KERR TYPE  
NONLINEARITY*



### 3.1 INTRODUCTION

The rapid expansion of information has put immense strain on the backbone as society moves into the information era. As time goes on, optical fiber technology emerges and advances toward high speed and high carrying capacity in order to relieve the transmission pressure brought on by a huge volume of data and to meet the need for information in present-day society [Agarwal, 2007; Li, Zhang, Tang, Gao, Zhang and Huang, 2018; Lei, Zheng, Qian, Xie, Bai, Gao and Huang 2019; Gao, Zhao, Xie, Lei, Song, Bi, Zheng and Huang 2019; Zou, Zhang, Whang, Zhang, Zhang and Liu 2020]. Again, nonlinear effects and dispersion are unavoidable during the transmission process, which makes it challenging to boost the optical fiber's transmission rate. Transmitted optical pulses can successfully generate solitons when the dispersion and nonlinear effects achieve equilibrium. As a result, several theoretical and experimental studies on solitons have been conducted [Biswas, Kara, Ullah, Zhou, Triki and Belic, 2017; Zhou, Ullah, Triki, Moshokoa and Belic, 2017; Gou, Zhang, Wang, Chen and Yang, 2018; Lu, Fu and Wang, 2018; Biswas; Aouadi, Bouzida, Daoui, Triki, Zhou and Liu, 2019]. How to manage the equilibrium between dispersion and nonlinear effects in the use of solitons becomes a significant issue in ultrafast optics [Zhu, Liu, Jiang, Xu, Su, Jiang, Qian and Xu 2015; Zhang, Liu, Fan, Peng, Gou, Jiang, Qian and Su 2018; Zhang, Wu, Liu, Pang, Ma, Jiang, Wu and Su, 2018; Liu, Liu, Liu, Quhe, Lei, Fang, Teng and Wei 2019]. Nonlinear optics is the study of phenomena that result from changes in a material system's optical properties as a result of interaction with intense light. If the electromagnetic field of the incident light is of high intensity, it generates nonlinearity in silica made optical fiber. This causes nonlinear variation of total induced polarization  $P$  with the electric field  $E$ . Further, the centrosymmetric  $\text{SiO}_2$  being the material of the fiber, the refractive index (RI) of the material does not depend on terms like  $E$ ,  $E^3$ ,  $E^5$  etc. Accordingly, in case of nonlinearity, the RI comprises terms containing intensity of light and its higher powers. Kerr nonlinearity is concerned with the dependence of the RI on the intensity of light ( $E^2$ ) only. Further, it is

also known as third order nonlinearity since the concerned scalar wave equation contains cubic term in  $E$ . This intensity dependent change of RI causes changes in the modal field inside the fiber and consequently the different propagation parameters associated with the fiber undergo change. It is relevant to mention in this connection that other higher orders of nonlinearity are generated due to dependence of RI on terms like  $E^4$ ,  $E^6$  etc. Recently, polarized light manipulation utilizing Kerr nonlinearity has been contributed to the literature [Wen, Hu, Rui, Lv, He, Gu and Cui, 2014]. Again, it has already been investigated how Kerr nonlinearity affects the propagation-related parameters of graded index (GI) and Photonic – crystal fibers (PCF) [Hayata, Koshiba and Suzuki, 1987; Okamoto and Marcayile, 1994; Saitoh, Fujisawa, Kirihaara and Koshiba, 2006; Khijwania, Nair and Sarkar, 2009]. Additionally, there is literature that discusses how Kerr nonlinearity affects the  $LP_{11}$  mode cutoff V number for both dispersion-shifted and dispersion-flattened fibers [Mondal and Sarkar, 1996]. However, the approaches in Refs. [Hayata, Koshiba and Suzuki, 1987; Okamoto and Marcayile, 1994; Mondal and Sarkar, 1996; Saitoh, Fujisawa, Kirihaara and Koshiba, 2006; Khijwania, Nair and Sarkar, 2009] require time-consuming calculations to be performed. Accordingly, the literature demands the development of a realistic yet straightforward methodology for estimating of optical fiber propagation parameters in the nonlinear domain in the context of both communication systems and sensor technology. In this aspect, it is pertinent to note that the Chebyshev technique-based simple series formulation of the fundamental ( $LP_{01}$ ) mode of GI fiber has been reported to be outstanding at estimation of its propagation properties in the linear domain [Gangopadhyay and Sarkar, 1997; Gangopadhyay, Sengupta, Mondal, Das and Sarkar, 1997; Patra, Gangopadhyay and Sarkar, 2000; Patra, Gangopadhyay and Sarkar, 2001]. Additionally, by using the iterative method, the aforementioned formulations have been used to evaluate the propagation parameters and analyze the performance of directional couplers of GI and dispersion-managed fibers in the Kerr category nonlinear area [Sadhu, Karak and Sarkar, 2013; Aich, Maiti, Majumdar and Gangopadhyay, 2019; Sarkar, Majumdar, and Gangopadhyay, 2020; Mukherjee, Maiti, Majumdar and Gangopadhyay, 2020; Rakshit, Majumdar and Gangopadhyay, 2021; Aich, Majumdar and Gangopadhyay, 2021; Ray, Majumdar and Gangopadhyay, 2021; Rakshit, Majumdar, Maiti and Gangopadhyay, 2022; Mukherjee, Majumdar and Gangopadhyay, 2022]. Recent literature

reports on the far field pattern of the first higher order mode ( $LP_{11}$ ) mode dispersion-controlled fibers utilizing the same formalism [Roy, Majumdar and Gangopadhyay, 2022]. Moreover, using the same technique, the effect of Kerr nonlinearity on signal and pump intensities in an erbium doped fiber amplifier (EDFA) built of  $LP_{11}$  mode step index (SI) fiber has also been added to the literature [Ray, Majumdar and Gangopadhyay, 2022]. Actually, the study of Kerr nonlinearity has emerged as a possible issue of current interest. Technologists and researchers are working to develop fresh concepts in this field. In this regard, the study of the the impact of nonlinearity regarding characteristics such as finite element method (FEM) transmitted through the fiber core, excitation efficiency, and normalized group delay for  $LP_{11}$  mode in GI fibers is significant in the domain of optical engineering. The FEM can be used to estimate how Kerr nonlinearity will affect the above-mentioned parameters [Hayata, Koshiba and Suzuki, 1987]. However, this method is stringent and requires time-consuming computation.

In this chapter, we use the Chebyshev formalism in order to estimate the aforementioned propagation characteristics of Kerr type nonlinear GI fibers because of the accuracy and simplicity of the formalism. To get the constants in the series expression of the  $LP_{11}$  modal field for GI fiber in this formalism, we employ the approach of iteration while taking care of the relevant nonlinearity. Step and parabolic profile fibers are used in our investigation as typical examples of GI fibers, along with a commonly used value of Kerr type nonlinearity, having same value both positively and negatively. Moreover, we compare our results with the exact results found by rigorous FEM in order to confirm the accuracy of our formalism.

In this regard, it is noteworthy to mention that, to the best of our knowledge, no such simple but accurate method based on the Chebyshev formalism for the evaluation of these key parameters of Kerr-type nonlinear fibers have been reported to date. Thus our method can be considered as a novel one.

## 3.2 THEORY

The RI profile  $n(R)$  for a GI fiber can be presented as

$$n^2(R) = n_1^2(1 - 2\delta f(R)), \quad R \leq 1 \quad (3.1)$$

$$n^2(R) = n_2^2, \quad R > 1$$

where  $R = \frac{r}{a}$ ,  $a$  = core radius,

Here,  $\delta = (n_1^2 - n_2^2)/2n_1^2$ ,  $n_1$  and  $n_2$  are the refractive indices of the core and cladding respectively.  $f(R)$  denotes the shape of RI profile and

$$f(R) = 0, \quad 0 < R \leq 1 \text{ for SI fiber} \quad (3.2)$$

$$f(R) = R^2, \quad 0 < R \leq 1 \text{ for parabolic index (PI) fiber}$$

In presence of Kerr-type nonlinearity, the RI is written as [Mondal and Sarkar, 1996]

$$n^2(R) = n_L^2(R) + \frac{n_2^2 n_{NL}(R)}{\eta_0} \psi^2(R) \quad (3.3)$$

where  $\eta_0$  is equal to  $\sqrt{\frac{\mu_0}{\epsilon_0}}$  with  $\mu_0$ ,  $\epsilon_0$  and  $n_{NL}(R)$  being the free space permeability, free space permittivity and nonlinear Kerr coefficient respectively. Here,  $\psi(R)$  is the field of  $LP_{11}$  mode which satisfies the equation given below [Mondal and Sarkar, 1996]

$$\frac{d^2\psi(R)}{dR^2} + \frac{1}{R} \frac{d\psi(R)}{dR} + [V^2(1 - f(R)) - W^2]\psi(R) - \frac{\psi(R)}{R^2} + V^2 g(R) \psi^3(R) = 0 \quad (3.4)$$

where, 
$$g(R) = \frac{n_2 n_{NL} P}{\pi a^2 (n_1^2 - n_2^2)} \quad (3.5)$$

Here, P is the power. Again, at the interface of core-clad of the fiber the boundary condition is as under

$$\left[ \frac{1}{\psi} \frac{d\psi}{dR} \right]_{R=1} = - \left[ 1 + \frac{WK_0(W)}{K_1(W)} \right] \quad (3.6)$$

Here,  $K_1$  and  $K_0$  are the modified Bessel functions of first and zero order respectively [Watson, 1995; Gradshteyn and Ryzhik, 2014, Abramowitz and Stegun, 2012]. Again,  $V(= k_0 a \sqrt{n_1^2 - n_2^2})$  is the normalized frequency,  $W(= a \sqrt{\beta^2 - n_2^2 k_0^2})$  is the cladding decay parameter,  $k_0$  is the free space wave number and  $\beta$  is the propagation constant.

In case of  $LP_{11}$  mode the field,  $\psi(R)$  is expressed as [Bose, Gangopadhyay and Saha, 2013]

$$\begin{aligned} \psi(R) &= a_1 R + a_3 R^3 + a_5 R^5, \quad R \leq 1 \\ &= (a_1 R + a_3 R^3 + a_5 R^5) \frac{K_1(WR)}{K_1(R)}, \quad R > 1 \end{aligned} \quad (3.7)$$

Using Eqs. (3.7) and (3.4) we get,

$$\begin{aligned} &a_1 \{V^2(1 - f(R)) - W^2 + V^2 g \psi^2(R)\} + a_3 \{8 + R^2 [V^2(1 - f(R)) - W^2 + V^2 g \psi^2(R)]\} + \\ &a_5 \{24R^2 + R^4 [V^2(1 - f(R)) - W^2 + V^2 g \psi^2(R)]\} = 0 \end{aligned} \quad (3.8)$$

The Chebyshev points are given as [Chen, 1982; Shijun, 1987]

$$R_m = \cos\left(\frac{2m-1}{2M-1} \frac{\pi}{2}\right), \quad m = 1, 2, \dots, (M-1) \quad (3.9)$$

Eqs. (3.10) and (3.11) can be obtained if we consider Eq. (3.8) and take  $M = 3$  in Eq. (3.9) to get two Chebyshev values  $R_1$  and  $R_2$  [Patra, Gangopadhyay and Goswami, 2008]

$$a_1\{V^2(1-f(R_1)) - W^2 + V^2g\psi^2(R_1)\} + a_3\{8 + R_1^2[V^2(1-f(R_1)) - W^2 + V^2g\psi^2(R_1)]\} + a_5\{24R_1^2 + R_1^4[V^2(1-f(R_1)) - W^2 + V^2g\psi^2(R_1)]\} = 0 \quad (3.10)$$

and

$$a_1\{V^2(1-f(R_2)) - W^2 + V^2g\psi^2(R_2)\} + a_3\{8 + R_2^2[V^2(1-f(R_2)) - W^2 + V^2g\psi^2(R_2)]\} + a_5\{24R_2^2 + R_2^4[V^2(1-f(R_2)) - W^2 + V^2g\psi^2(R_2)]\} = 0 \quad (3.11)$$

The following relation of  $\frac{K_1(W)}{K_0(W)}$  with  $\frac{1}{W}$  in the range  $0.6 \leq W \leq 2.5$  is obtained by least square fitting technique. [Gangopadhyay, Sengupta, Mondal, Das and Sarkar, 1997]

$$\frac{K_1(W)}{K_0(W)} = \alpha + \frac{\beta}{W} \quad (3.12)$$

where  $\alpha = 1.034623$  and  $\beta = 0.3890323$  [Gangopadhyay, Sengupta, Mondal, Das and Sarkar, 1997]

Using Eqs. (3.6), (3.7) and (3.12) we get

$$a_1[2(\alpha W + \beta) + W^2] + a_3[4(\alpha W + \beta) + W^2] + a_5[6(\alpha W + \beta) + W^2] = 0 \quad (3.13)$$

Eqs. (3.10), (3.11) and (3.13) will give non-trivial solution, if the following condition is satisfied.

$$\begin{vmatrix} A_1 & B_1 & C_1 \\ A_2 & B_2 & C_2 \\ A_3 & B_3 & C_3 \end{vmatrix} = 0 \quad (3.14)$$

where,  $A_1 = V^2(1-f(R_1)) - W^2 + V^2g\psi^2(R_1)$

$A_2 = V^2(1-f(R_1)) - W^2 + V^2g\psi^2(R_1)$

$A_3 = 2(\alpha W + \beta) + W^2$

$$B_1 = 8 + R_1^2[V^2(1 - f(R_1)) - W^2 + V^2 g \psi^2(R_1)]$$

$$B_2 = 8 + R_2^2[V^2(1 - f(R_2)) - W^2 + V^2 g \psi^2(R_2)]$$

$$B_3 = 4(\alpha W + \beta) + W^2$$

$$C_1 = 24R_1^2 + R_1^4[V^2(1 - f(R_1)) - W^2 + V^2 g \psi^2(R_1)]$$

$$C_2 = 24R_2^2 + R_2^4[V^2(1 - f(R_2)) - W^2 + V^2 g \psi^2(R_2)]$$

$$C_3 = 6(\alpha W + \beta) + W^2 \quad (3.15)$$

Solution of Eq. (3.14) is essential to find the W value for a certain V value in linear region where g value is equal to zero. Then, by substituting this W value for that V value in any two of Eqs. (3.10), (3.11) and (3.13), one may determine the values of normalized coefficients of Eq. (3.7) with respect to  $a_1$  in the linear domain. Now, we first select a certain g value for a specific fiber with the stated V number and then continue the iteration process till converging values of W in the nonlinear domain are obtained. For a single g value corresponding to a specific fiber with the given V number, one may calculate the values of normalized coefficients in respect of  $a_1$  by substituting this convergent value of W in any two of Eqs. (3.10), (3.11) and (3.13). For each and every value of g, this method of evaluation is used for various fibers.

The fractional power  $f_{CO}$  of the LP<sub>11</sub> mode is as follows [Bose, Gangopadhyay and Saha, 2011]

$$f_{CO} = \frac{\int_0^1 |\psi(R)|^2 R dR}{\int_0^1 |\psi(R)|^2 R dR} \quad (3.16)$$

Using Eqs. (3.7) and (3.16), we obtain

$$f_{CO} = \frac{S_2}{S_2 - S_1(1 - (K_0(W)K_2(W)/K_1^2(W))} \quad (3.17)$$

here,  $S_1 = \frac{(a_1+a_3+a_5)^2}{2}$  and  $S_2 = \frac{a_1^2}{4} + \frac{a_1a_3}{3} + \frac{a_3^2+2a_1a_5}{8} + \frac{a_3a_5}{5} + \frac{a_5^2}{12}$

We consider a light source which is expressed below [Gangopadhyay and Sarkar, 1997]

$$E_s = 1, \quad 0 < r < a_s \quad (3.18a)$$

$$E_s = 0, \quad a_s < r < \infty \quad (3.18b)$$

The excitation efficiency ( $\eta$ ) associated with LP<sub>11</sub> mode of the fiber in case of a light source, having intensity  $E_s$ , is given as [Gangopadhyay and Sarkar, 1997]

$$\eta = \frac{|\int_0^\infty E_s \psi^* r dr|^2}{\int_0^\infty |E_s|^2 r dr \int_0^\infty |\psi|^2 r dr} \quad (3.19)$$

Using  $\psi(R)$  from Eq. (3.7),  $E_s$  from Eqs. (3.18a) and (3.18b), we have [Bose, Gangopadhyay, Saha, 2011]

$$\eta = \frac{\left(\frac{2}{R_s^2}\right)[S_3 + S_4 \left(\frac{R_s^2 K_1(W R_s)}{K_1(W)}\right) - 1]^2}{S_2 - (S_4^2/2) \left(1 - \left(\frac{K_0(W) K_2(W)}{K_1^2(W)}\right)\right)} \quad (3.20)$$

where,  $S_3 = \frac{a_1}{3} + \frac{a_3}{5} + \frac{a_5}{7}, \quad S_4 = a_1 + a_3 + a_5$

Now, the normalized Petermann II ( $W_d$ ) spot size is related to normalized group delay ( $b_1$ ) and normalized propagation constant ( $b$ ) as follows

$$b_1 = b + \frac{4}{V^2 W_d^2} \quad (3.20)$$

where  $b = \frac{W^2}{V^2}$  [Tewari, Hosain and Thyagarajan, 1983; Mishra, Hosain, Goyal and Sharma, 1984]



$$\text{and } W_d^2 = \frac{2 \left[ S_2 - S_1 \left( 1 - \frac{K_0(W)K_2(W)}{K_1^2(W)} \right) \right]}{S_5 - S_4^2 \left[ - \left( \frac{W^6}{6} \right) \left( \frac{10K_0^2(W) - 4K_2^2(W) - K_3^2(W)}{10K_1^2(W)} - \frac{1}{2} \right) - \left( \frac{K_0^2(W)}{2K_1^2(W)} \right) - 1 - \left( \frac{W^3}{3} \right) \left( \frac{K_0(W) - K_2(W)}{K_1(W)} \right) \right]}$$

[Bose, Gangopadhyay and Saha, 2011]

$$\text{here, } S_5 = \frac{a_1^2}{2} + \frac{3}{2}a_3^2 + \frac{5}{2}a_5^2 + \frac{3}{2}a_1a_3 + \frac{5}{3}a_1a_5 + \frac{15}{4}a_3a_5$$

### 3.3 RESULTS AND DISCUSSIONS

In our investigation, we have used V values larger than first higher order mode (LP<sub>11</sub>) cut-off V number for the respective fibers so that in addition to the fundamental mode, the first higher order mode also propagates through the fiber. It deserves mentioning in this connection that LP<sub>11</sub> cut- off V values for step and parabolic index fibers are 2.4048 and 3.51802 respectively (Shijun, 987; Neumann, 1988).

In Table 3.1a, we present the obtained values of  $f_{co}$  for the first higher order mode in absence of nonlinearity as well as in presence of positive and negative nonlinearities in case of step index fibers of different V numbers.

**Table 3.1a**

**LP<sub>11</sub> mode fractional power  $f_{co}$  for step index fiber**

V	$n_{NL}P = +1.5 \times 10^{-14}$	$n_{NL}P = 0$	$n_{NL}P = -1.5 \times 10^{-14}$
2.6	0.477889096	0.44961939	0.4222013758
2.8	0.59097979	0.57387879	0.5553249715
3.0	0.668779884	0.6561005	0.6426416216
3.2	0.725988028	0.716006005	0.7055417962
3.4	0.760071487	0.76164498	0.7531325033

In Fig. 3.1a, we use the results given in Table 3.1a, in order to show the variation of  $f_{co}$  with V number for step index fiber. Here, we present our observation as well as the simulated exact results obtained by applying finite element method. Our results are seen to match exceedingly well with the exact results.

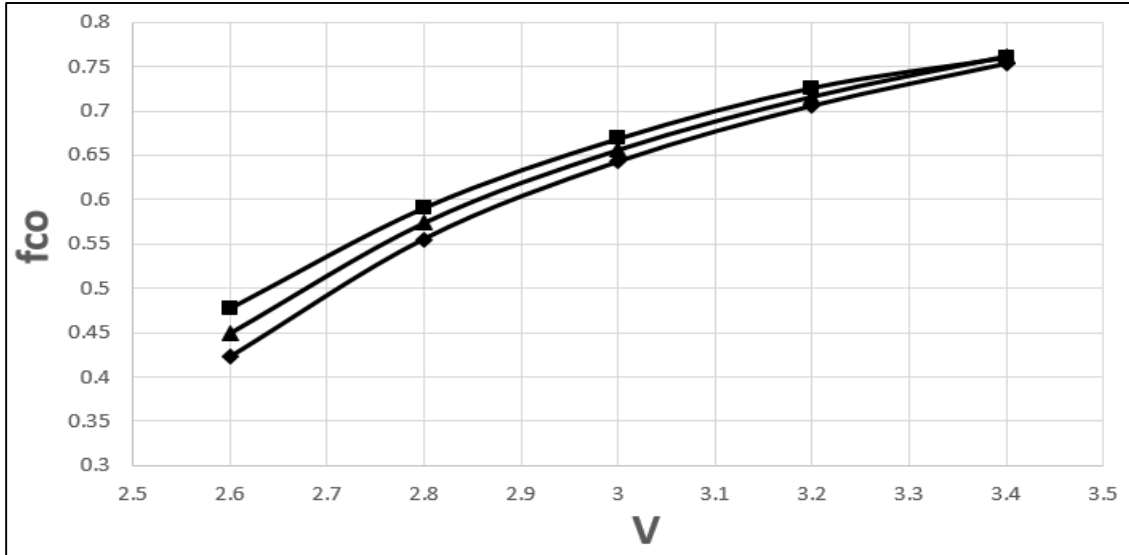


**Fig. 3.1a: Variation of fractional power  $f_{co}$  for different V values in absence as well as in presence of positive and negative of nonlinearities in case of step index fiber.  $\blacktriangle$  for  $n_{NL}P = 0$ ,  $\blacksquare$  for  $n_{NL}P = +1.5 \times 10^{-14}$  and  $\blacklozenge$  for  $n_{NL}P = -1.5 \times 10^{-14}$ . Solid lines are simulated exact results.**

In Table 3.1b, we present the obtained values of  $f_{co}$  for the first higher order mode in absence of nonlinearity and in presence of positive and negative nonlinearities in case of parabolic index fibers of different V numbers.

**Table 3.1b**

**LP<sub>11</sub> mode fractional power  $f_{co}$  for parabolic index fiber**

V	$n_{LP} = +1.5 \times 10^{-14}$	$n_{LP} = 0$	$n_{LP} = -1.5 \times 10^{-14}$
3.7	0.565607088	0.521512793	0.466637995
3.9	0.66343525	0.635746006	0.60335142
4.1	0.731776563	0.712353639	0.6902515
4.3	0.782212484	0.76775564	0.75159888
4.5	0.82070013	0.809488537	0.797157685

As before, we use the results given in Table 3.1b in order to present the variation of  $f_{co}$  versus V number for parabolic index fiber. Here also, the match between our prediction and the exact one is excellent.

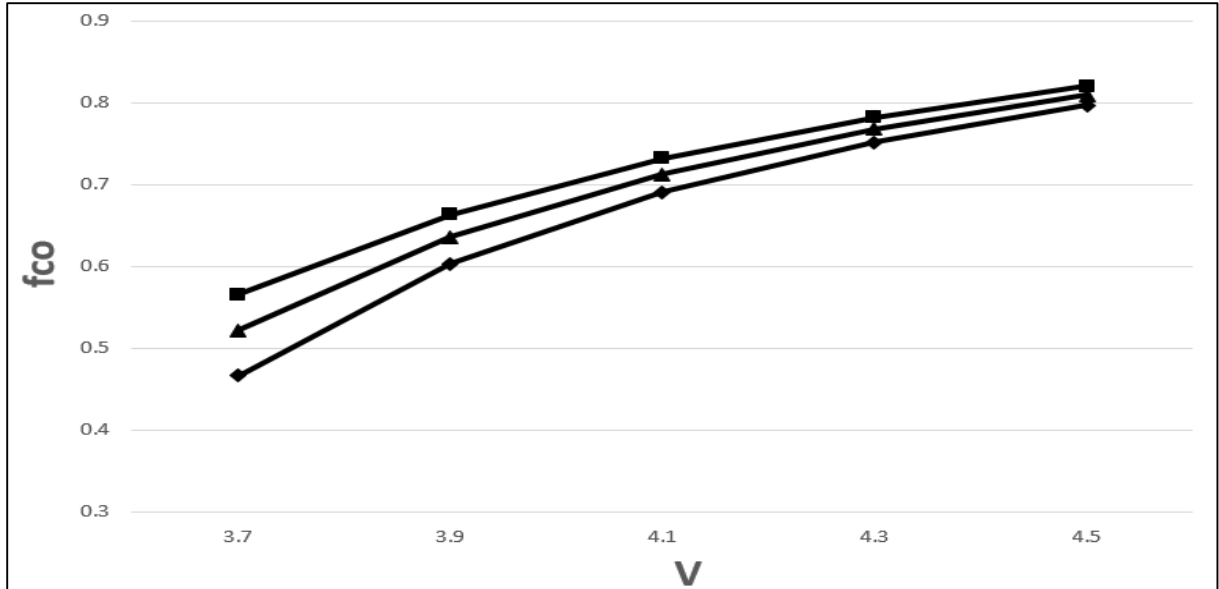


**Fig. 3.1b: Variation of fractional power  $f_{co}$  for different V values in absence as well as in presence of positive and negative of nonlinearities in case of parabolic index fiber.  $\blacktriangle$  for  $n_{NLP} = 0$ ,  $\blacksquare$  for  $n_{NLP} = +1.5 \times 10^{-14}$  and  $\blacklozenge$  for  $n_{NLP} = -1.5 \times 10^{-14}$ . Solid lines are simulated exact results.**

In Table 3.2a, we present the obtained values of excitation efficiency  $\eta$ , for the first higher order mode in absence as well as in presence of positive and negative nonlinearities in case of step index fibers, for  $R_s$  being equal to 2, of different  $V$  numbers.

**Table 3.2a**

**LP<sub>11</sub> mode excitation efficiency  $\eta$  for step index fiber for  $R_s = 2$**

$V$	$n_{NL}P = +1.5 \times 10^{-14}$	$n_{NL}P = 0$	$n_{NL}P = -1.5 \times 10^{-14}$
2.6	0.027869029	0.012193293	0.002574913
2.8	0.187417482	0.153540148	0.120896641
3.0	0.388250429	0.352688569	0.316247077
3.2	0.571614297	0.541042625	0.508831917
3.4	0.718989562	0.695212547	0.669923583

In Fig. 3.2a, we use results given in Table 3.2a in order to show the variation of  $\eta$  with  $V$  number for step index fiber having  $R_s$  value equal to 2. Here, we also show that our results are virtually indistinguishable from the exact ones.

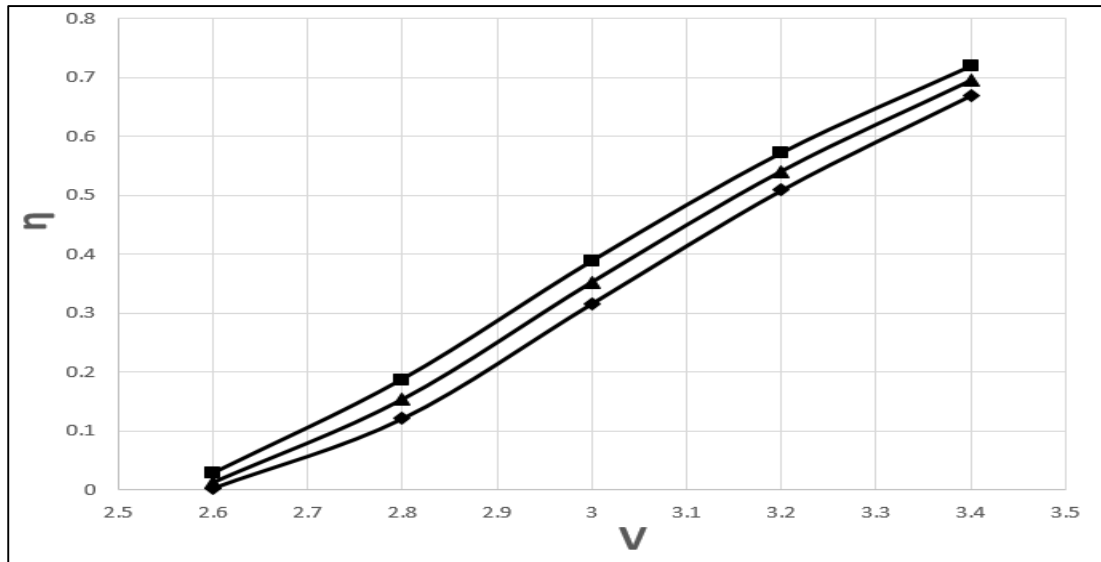


**Fig. 3.2a: Variation of excitation efficiency  $\eta$  for different  $V$  values and for  $R_s = 2$  in absence as well as in presence of positive and negative of nonlinearities in case of step index fiber.  $\blacktriangle$  for  $n_{NL}P = 0$ ,  $\blacksquare$  for  $n_{NL}P = +1.5 \times 10^{-14}$  and  $\blacklozenge$  for  $n_{NL}P = -1.5 \times 10^{-14}$ . Solid lines are simulated exact results.**

In Table 3.2b, we show the obtained values of the excitation efficiency,  $\eta$ , for the first higher order mode in absence as well as in presence of positive and negative nonlinearities, for  $R_S$  being equal to 5, in case of step index fibers of different  $V$  numbers.

**Table 3.2b**

**LP<sub>11</sub> mode excitation efficiency  $\eta$  for step index fiber for  $R_S = 5$**

V	$n_{NL}P = +1.5 \times 10^{-14}$	$n_{NL}P = 0$	$n_{NL}P = -1.5 \times 10^{-14}$
2.6	0.055224076	0.03347864	0.013439998
2.8	0.144545561	0.133676601	0.120673722
3.0	0.180343374	0.176434494	0.171624908
3.2	0.192982441	0.191829652	0.190284028
3.4	0.196605068	0.196620453	0.196476845

In Fig. 3.2b, the results given in Table 3.2b are used to show the variation of  $\eta$  with  $V$  number for step index fiber having  $R_S$  value equal to 5. Here, we also show that our predictions have excellent match with the exact results.

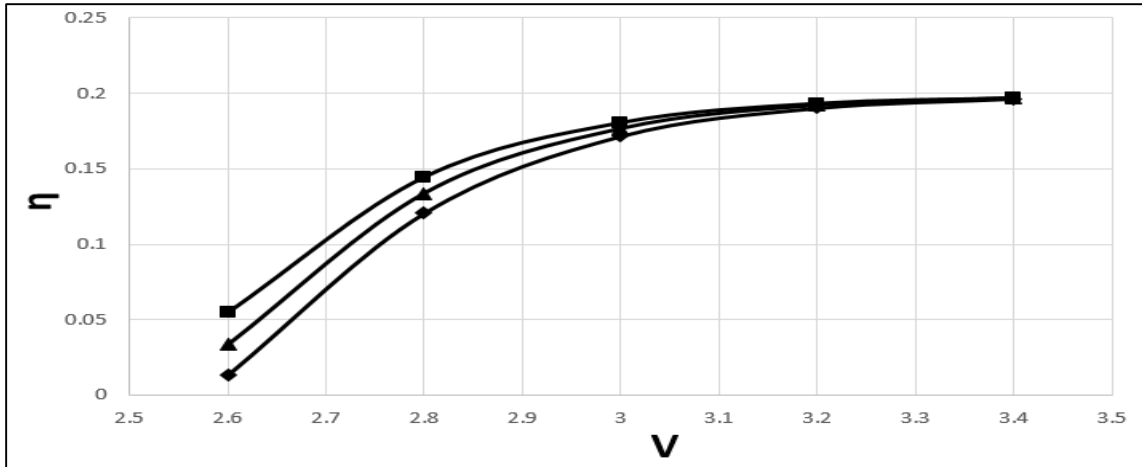


**Fig. 3.2b: Variation of excitation efficiency  $\eta$  for different  $V$  values and for  $R_S = 5$  in absence as well as in presence of positive and negative of nonlinearities in case of step index fiber.  $\blacktriangle$  for  $n_{NL}P = 0$ ,  $\blacksquare$  for  $n_{NL}P = +1.5 \times 10^{-14}$  and  $\blacklozenge$  for  $n_{NL}P = -1.5 \times 10^{-14}$ . Solid lines are simulated exact results.**

In Table 3.2c, we present the values of  $\eta$  for the first higher order mode in absence of nonlinearity and also in presence of positive and negative nonlinearities in case of parabolic index fibers, for  $R_s$  having value is equal to 1.5, of different  $V$  numbers.

**Table 3.2c**

**LP<sub>11</sub> mode excitation efficiency  $\eta$  for parabolic index fiber for  $R_s = 1.5$**

$V$	$n_{NL}P = +1.5 \times 10^{-14}$	$n_{NL}P = 0$	$n_{NL}P = -1.5 \times 10^{-14}$
3.7	0.119114004	0.07923979	0.044411175
3.9	0.255082506	0.207395177	0.160411528
4.1	0.39912551	0.351618859	0.302454499
4.3	0.534631602	0.491158553	0.445326882
4.5	0.65384785	0.616081522	0.57563983

In Fig. 3.2c, the results of Table 3.2c are used to show the variation of  $\eta$  with  $V$  number for parabolic index fiber having  $R_s$  value equal to 1.5. Here, also our predictions have excellent agreement with the exact results.

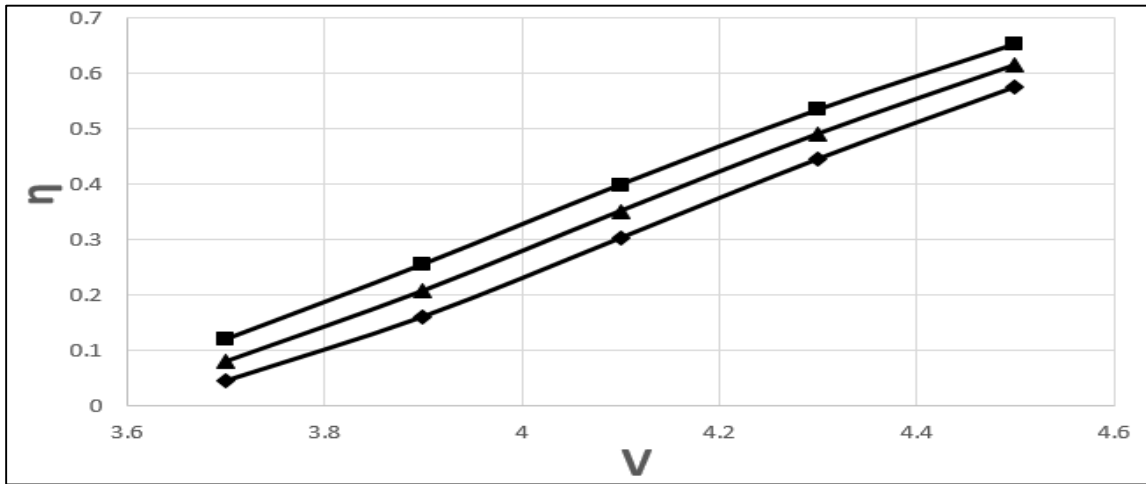


**Fig. 3.2c: Variation of excitation efficiency  $\eta$  for different  $V$  values and for  $R_s = 1.5$  in absence as well as in presence of positive and negative of nonlinearities in case of parabolic index fiber.  $\blacktriangle$  for  $n_{NL}P = 0$ ,  $\blacksquare$  for  $n_{NL}P = +1.5 \times 10^{-14}$  and  $\blacklozenge$  for  $n_{NL}P = -1.5 \times 10^{-14}$ . Solid lines are simulated exact results.**

In Table 3.2d, the obtained values of  $\eta$  are shown for the first higher order mode in absence as well as in presence of positive and negative nonlinearities in case of parabolic index fibers for  $R_s = 3$  in case of different  $V$  numbers.

**Table 3.2d**

**LP<sub>11</sub> mode excitation efficiency  $\eta$  for parabolic index fiber for  $R_s = 3$**

$V$	$n_{NL}P = +1.5 \times 10^{-14}$	$n_{NL}P = 0$	$n_{NL}P = -1.5 \times 10^{-14}$
3.7	0.052202397	0.015058212	0.000145865
3.9	0.187708385	0.142326698	0.094024725
4.1	0.295697583	0.264112416	0.226868202
4.3	0.362491593	0.343906398	0.321051694
4.5	0.397968641	0.388474178	0.376132746

In Fig. 3.2d, we have used the results in Table 3.2d to show how the excitation efficiency  $\eta$  varies with  $V$  number for parabolic index fiber having  $R_s$  value equal to 3. Here, also the obtained results have excellent match with the exact ones.

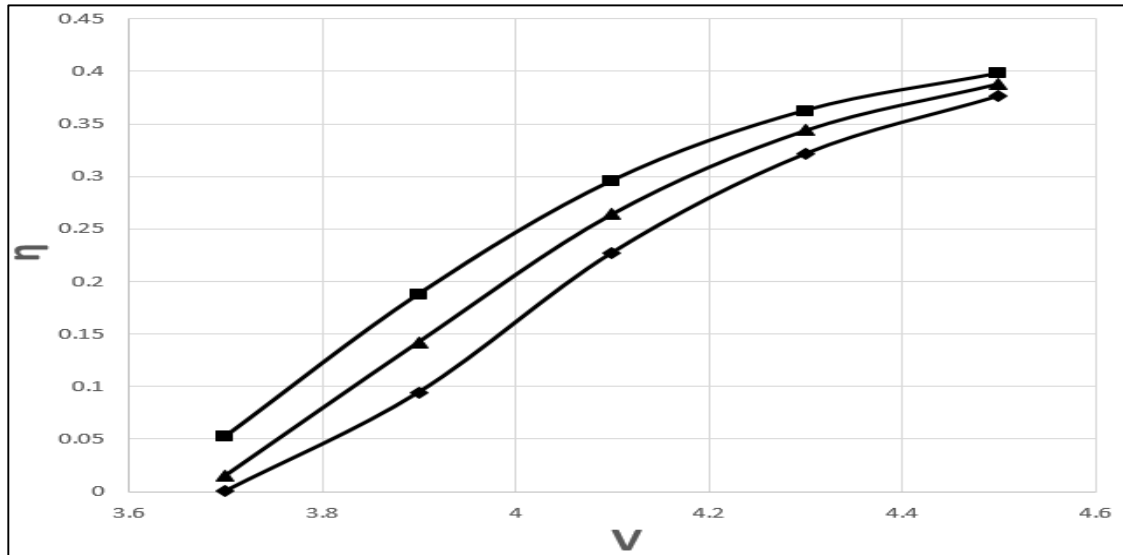


**Fig. 3.2d: Variation of excitation efficiency  $\eta$  for different  $V$  values and for  $R_s = 3$  in absence as well as in presence of positive and negative of nonlinearities in case of parabolic index fiber. ▲ for  $n_{NL}P = 0$ , — for  $n_{NL}P = +1.5 \times 10^{-14}$  and ◆ for  $n_{NL}P = -1.5 \times 10^{-14}$ . Solid lines are simulated exact results.**

In Table 3.3a, we have shown the obtained values of group delay parameter  $b_1$  for the first higher order mode in absence and also in presence of positive and negative nonlinearities in case of step index fibers of different  $V$  numbers.

**Table 3.3a**

**LP<sub>11</sub> mode normalized group delay parameter  $b_1$  for step index fiber**

$V$	$n_{NLP} = +1.5 \times 10^{-14}$	$n_{NLP} = 0$	$n_{NLP} = -1.5 \times 10^{-14}$
2.6	0.2665696554	0.261227167	0.090815047
2.8	0.726923589	0.455608744	0.3890241693
3.0	4.7563457	2.803363663	1.887725928
3.2	3.0147425264	2.6570162179	1.522944475

The variation of the normalized group delay parameter  $b_1$  with  $V$  number for step index fiber is shown in Fig. 3.3a, which is obtained by using the results given in Table 3.3a. Again, the obtained results agree excellently with the exact ones.

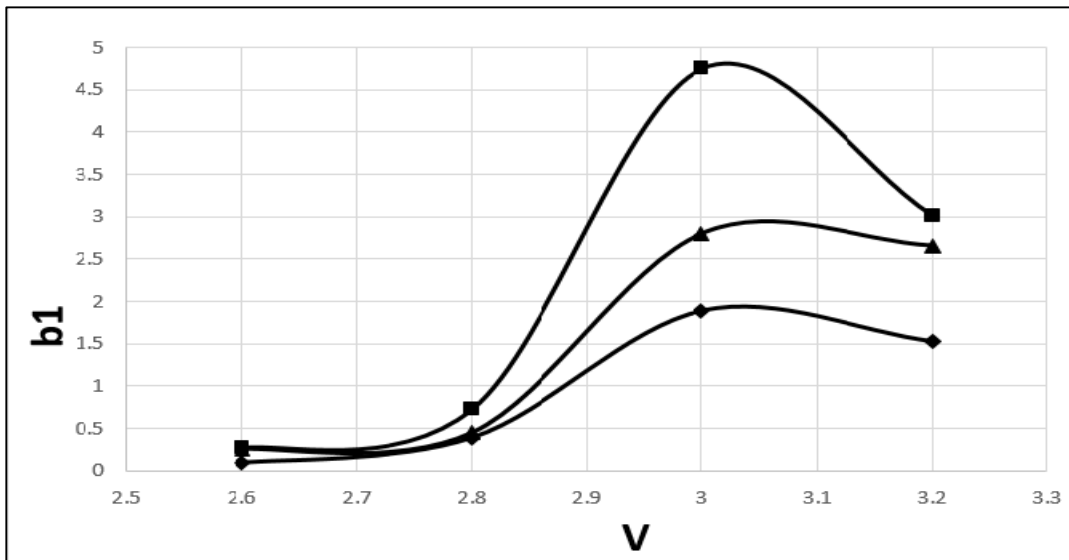


**Fig. 3.3a: Variation of normalized group delay parameter  $b_1$  for different  $V$  values in absence as well as in presence of positive and negative of nonlinearities in case of step index fiber.  $\blacktriangle$  for  $n_{NLP} = 0$ ,  $\text{—}$  for  $n_{NLP} = +1.5 \times 10^{-14}$  and  $\blacklozenge$  for  $n_{NLP} = -1.5 \times 10^{-14}$ . Solid lines are simulated exact results.**



In Table 3.3b, the obtained values of  $b_1$  for the first higher order mode in absence of nonlinearity and also in presence of positive and negative nonlinearities in case of parabolic index fibers of different  $V$  numbers, are shown.

**Table 3.3b**

**LP<sub>11</sub> mode normalized group delay parameter  $b_1$  for parabolic index fiber**

$V$	$n_{NL}P = +1.5 \times 10^{-14}$	$n_{NL}P = 0$	$n_{NL}P = -1.5 \times 10^{-14}$
3.7	0.1627375817	0.1098405228	0.0517396928
3.9	0.2736966587	0.187880704	0.1209294298
4.1	0.5910951828	0.432049784	0.3249002357
4.3	0.9149238242	0.7262457731	0.5675927609

In Fig. 3.3b, the variation of the normalized group delay parameter  $b_1$  with the  $V$  number for parabolic index fiber is presented. It is obtained by using the results shown in Table 3.3b. Here, again the obtained results agree excellently with the exact ones.

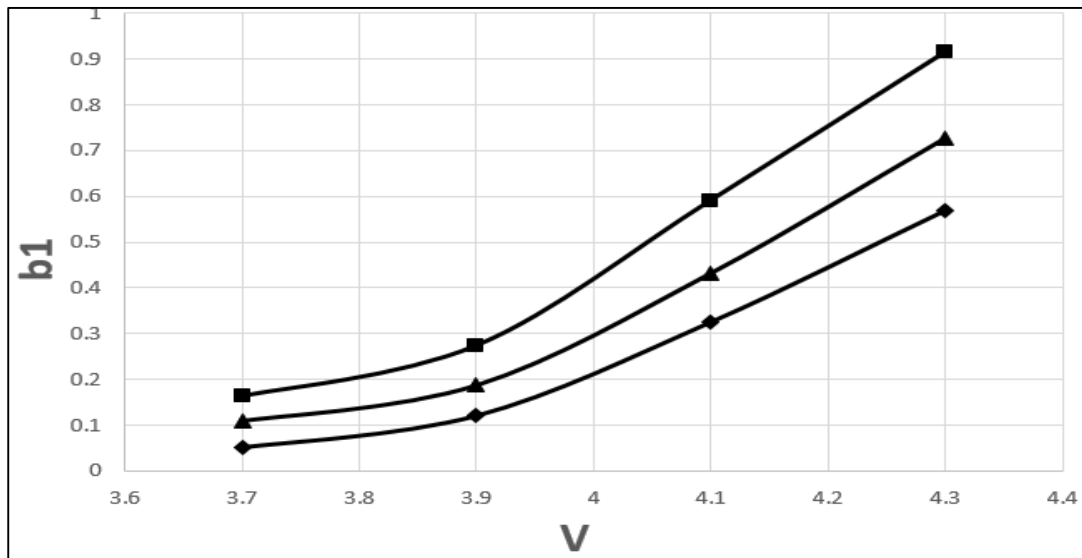


**Fig. 3.3b: Variation of normalized group delay parameter  $b_1$  for different  $V$  values in absence as well as in presence of positive and negative of nonlinearities in case of parabolic index fiber.  $\blacktriangle$  for  $n_{NL}P = 0$ ,  $\blacksquare$  for  $n_{NL}P = +1.5 \times 10^{-14}$  and  $\blacklozenge$  for  $n_{NL}P = -1.5 \times 10^{-14}$ . Solid lines are simulated exact results.**

### 3.4 SUMMARY

This chapter involves simple but accurate estimation of fractional modal power inside the core and the excitation efficiency and normalized group delay in case of graded index fibers both in presence and absence of Kerr type non linearity. The study has been made for first higher order mode in step and parabolic index fibers having some typical V numbers. We have employed Chebyshev power series expression for first higher mode in graded index fiber in order to prescribe analytical expression for the said propagation parameters in absence of Kerr type nonlinearity. Thereafter, making use of those analytical expressions, method of iteration is applied for the evaluation of the concerned parameters in presence of Kerr type nonlinearity. In this context, two common nonlinearity parameters namely,  $n_{NL}P = +1.5 \times 10^{-14} \text{m}^2$  and  $n_{NL}P = -1.5 \times 10^{-14} \text{m}^2$  has been used for the estimation of the said parameters. It is relevant to mention that the method of iteration is continued till the convergent values are arrived at. Our results are found to be in excellent agreement with the exact results, which have been obtained by applying rigorous finite element method. Thus this user friendly but accurate formalism for the evaluation of these propagation parameters both in presence and absence of nonlinearity will prove beneficial in the fields of optical sensors and communication engineering.

# *CHAPTER 4*

*STUDY OF COUPLING OPTICS OF  
CYLINDRICAL MICROLENS FABRICATED  
ON TIPS OF GRADED INDEX FIBERS  
HAVING DIFFERENT PROFILE EXPONENTS*

## 4.1 INTRODUCTION

An optical fiber having single mode is the most favorite one in case of optical communication as it provides maximum bandwidth. Micro lenses are put on the tip of a single mode graded index fiber (GIF), as it enhances the laser to optical fiber coupling efficiency [Presby and Edwards, 1992; Presby and Edwards, 1992; Edwards, Presby and Dragone, 1993; John, Maclean, Ghafouri-Shiraz, Niblett, 1994; Gangopadhyay and Sarkar, 1996]. When a hyperbolic micro lens is put on the tip of a single mode step index fiber, it has been observed that it produces nearly one hundred percent coupling efficiency [Edwards, Presby and Dragone, 1993; Presby and Edwards, 1992; John, Maclean, Ghafouri-Shiraz, Niblett, 1994; Gangopadhyay and Sarkar, 1996; Edwards and Presby, 1993; Kurokawa and Becker 1975; Gangopadhyay and Sarkar, 1997]. But its fabrication needs sophisticated laser micromachining technique [Edwards, Presby and Dragone, 1993]. The refractive index (RI) profiles of some particular step index, parabolic index and triangular index fibers have been studied for coupling via cylindrical micro lenses (CMLs) on the end faces of the fibers [Roy, Majumdar, Maity and Gangopadhyay, 2020]. For the purpose of finding out the maximum coupling efficiency involving the source of light and the fiber, different profile exponents of graded index fibers have been studied [Bose, Gangopadhyay and Saha, 2012]. Though hemispherical micro lens is popular due to its simple photographic technique, it is not an efficient coupler owing to its limited aperture, spherical aberration and modal mismatch [Edwards, Presby and Dragone, 1993; Presby and Edwards, 1992]. In order to optimize the coupling, multiple forms of tapered lenses are put on the tips of optical fibers having different kind of RI profiles [Mondal, Gangopadhyay and Sarkar, 1998; Yuan, Qui, 1992; Mondal and Sarkar, 1999; Yuan and Shou 1990; Lie, 2010; Mukhopadhyay, Gangopadhyay and Sarkar, 2010; Majumdar, Mandal and, Gangopadhyay, 2017; Maiti, Maiti and Gangopadhyay, 2017; Mandal, Maiti, Chiu and Gangopadhyay, 2018; Maiti, Biswas, Gangopadhyay, 2019]. More laser light enters an optical fiber and increases the coupling efficiency, if a

tapered lens of large aperture is used. Due to this advantage, tapered lens is used widely in micro optical studies, light amplification techniques and sensors of large span. Further, CML provides good coupling and also it is very easy to fabricate, thus it is widely used in the field of coupling optics [Zhang, 2002; Zhang, 2003]

ABCD matrix formalism is a very useful and simple theoretical technique in optical coupling system when multiple forms of micro lenses and the tapered lenses are used on the tips of optical fibers [Gangopadhyay and Sarkar, 1996; Gangopadhyay and Sarkar, 1997; Bose, Gangopadhyay and Saha, 2012; Mondal and Sarkar, 1999; Mukhopadhyay, Gangopadhyay and Sarkar, 2010; Majumdar, Mandal and Gangopadhyay, 2017; Maiti, Maiti and Gangopadhyay, 2017; Mandal, Maiti, Chiu and Gangopadhyay, 2018; Maiti, Biswas and Gangopadhyay, 2019; Mukhopadhyay and Sarkar, 2011; Gangopadhyay and Sarkar, 1998; Gangopadhyay and Sarkar, 1998; Mukhopadhyay, Gangopadhyay and Sarkar, 2007]. Thus we apply this formalism to compute the coupling efficiency of the CML on the graded index optical fiber for different RI profile exponents ( $g$ ) having values  $g = 4.0, 8.0, 10.0$  and  $20.0$ . The study of the coupling efficiencies of the CMLs on the tips of step, parabolic and triangular index fibers were investigated earlier [Roy, Majumdar, Maity S and Gangopadhyay, 2020]. In this chapter the coupling is studied for graded index fibers having different profile exponents at two different wavelengths  $1.3 \mu\text{m}$  and  $1.5 \mu\text{m}$  [John, Maclean, Ghafouri-Shiraz and Niblett, 1994].

In this chapter, we have taken care of the limited aperture of CML and the field distribution associated with the source and the fiber are considered to be Gaussian [Sarkar, Thyagrajan and Kumar, 1984; Marcuse, 1978; Sarkar, Pal and Thyagrajan, 1986]. Using the ABCD matrix concept, a simple analytical expression of the coupling efficiency has been found by which one can easily find out the most coupling efficient profile exponent appropriate for a cylindrical micro lensed graded index fiber at a particular wave-length of light. Thus, the simple formalism

developed for this coupler will benefit the system users in the process of predicting the coupling optics accurately within a small period of time.

Further, as far our knowledge is concerned, no such ABCD matrix based coupling optics prediction involving CML on graded index fibers of different profile exponents have been reported till date. Accordingly, our present work can be considered as a novel contribution to the literature.

## 4.2 THEORY

In Fig. 4.1, the coupling scheme is shown. The intensity profile of the laser light is elliptical and it is described by Gaussian distribution of spot sizes along  $x$  and  $y$  directions. Let the spot sizes along  $x$  and  $y$  axes, respectively, be  $w_{1x}$  and  $w_{1y}$ .

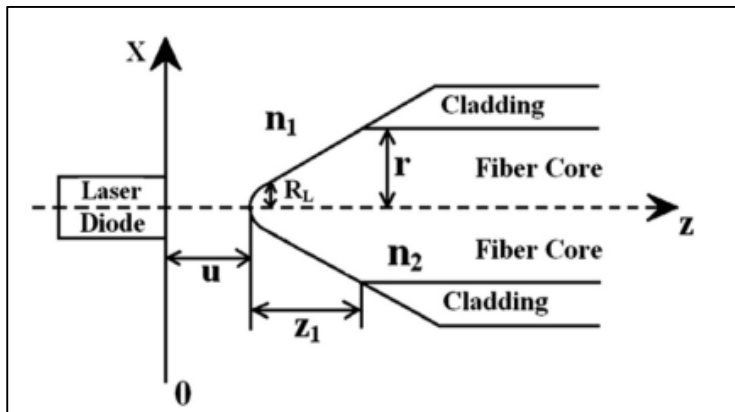


**Fig. 4.1: Schematic diagram of laser source to cylindrical micro lens coupling of a graded index fiber**

Here the light is considered to be travelling along the  $z$  axis and the junction plane is along the  $x$  axis. At a distance  $u$  from the laser source to the lens, the laser field is given by [Sarkar, Thyagrajan and Kumar, 1984]

$$\psi_u = \exp \left[ - \left( \frac{x^2}{w_{1x}^2} + \frac{y^2}{w_{1y}^2} \right) \right] \exp \left[ - \frac{jk_1(x^2+y^2)}{2R_1} \right] \quad (4.1)$$

where the radius of curvature of the incident wave front is denoted by  $R_1$  and the incident wave number is represented as  $k_1$ . The circular core single mode fiber has been found to predict accurately the coupling optics, even when we assume simple Gaussian approximation for its fundamental modal field as given below [Marcuse, 1978; Sarkar, Pal and Thyagrajan, 1986; John, Maclean, Ghafouri-Shiraz and Niblett, 1994; Gangopadhyaya and Sarkar, 1996; Gangopadhyay and Sarkar, 1997; Bose, Gangopadhyay and Saha, 2012; Mondal and Sarkar, 1999; Mukhopadhyay, Gangopadhyay and Sarkar, 2010; Majumdar, Mandal and Gangopadhyay, 2017; Maiti, Maiti and Gangopadhyay, 2017; Mandal, Maiti, Chiu and Gangopadhyay, 2018; Maiti, Biswas and Gangopadhyay, 2019; Mukhopadhyay and Sarkar, 2011; Gangopadhyay and Sarkar, 1998; Gangopadhyay and Sarkar, 1998; Mukhopadhyay, Gangopadhyay and Sarkar, 2007]

$$\psi_f = \exp \left[ - \frac{x^2+y^2}{w_f^2} \right] \quad (4.2)$$

Again, the RI profile of the material of the fiber can be taken as [Marcuse, 1978]

$$\begin{aligned} n(r) &= n_{co} \sqrt{1 - 2 \left( \frac{r}{a_0} \right)^g \Delta} && \text{for } r < a_0 \\ &= n_{cl} = n_{co} \sqrt{1 - 2\Delta} && \text{for } r > a_0 \end{aligned} \quad (4.3)$$

Here,  $n_{co}$  and  $n_{cl}$  are the RIs of the core and cladding of the fiber respectively,  $a_0$  is the radius of the core,  $\Delta$  is the grading parameter ( $\Delta = \frac{n_{co}^2 - n_{cl}^2}{2n_{co}^2}$ ) and  $g$  is the profile exponent which in this chapter has been taken as 4, 8, 10 and 20 respectively. The spot size  $w_f$  of a graded index fiber is taken as [Marcuse, 1978]

$$w_f = a_0 \left[ \frac{A'}{V^{\frac{2}{g+2}}} + \frac{B'}{V^{\frac{3}{2}}} + \frac{C'}{V^6} \right] \quad (4.4)$$

here, V is the normalized frequency which is given as  $V = k_0 a_0 \sqrt{n_{co}^2 - n_{cl}^2}$  and  $k_0$  is the free space wave number. Here A', B' and C' are the optimizable parameters which can be expressed as (validity,  $1.5 < V < \infty$ )

$$A' = \sqrt{\frac{2}{5} \left\{ 1 + 4 \sqrt{\frac{2}{g}} \right\}}$$

$$B' = \exp\left(\frac{0.298}{g}\right) - 1 + 1.478 [1 - \exp(-0.077g)] \quad (4.5)$$

$$C' = 3.76 + \exp\left(\frac{4.19}{g^{0.418}}\right)$$

The laser field after passing through the cylindrical lens on the fibre tip can be expressed as [Sarkar, Thyagrajan and Kumar, 1984; Sarkar, Pal and Thyagrajan, 1986]

$$\psi_v = \exp\left[-\left(\frac{x^2}{w_{2x}^2} + \frac{y^2}{w_{2y}^2}\right)\right] \exp\left[-\frac{jk_2}{2}\left(\frac{x^2}{R_{2x}} + \frac{y^2}{R_{2y}}\right)\right] \quad (4.6)$$

where  $k_2$  is the wave number inside the lens medium and  $w_{2x}$ ,  $w_{2y}$  and  $R_{2x}$ ,  $R_{2y}$  are the spot sizes and the radii of curvatures of the wave front after passing through the lens. Now the coupling efficiency of the laser to the single mode fiber coupling via CML is given by [Gangopadhyay and Sarkar, 1996]

$$\eta_0 = \frac{\left| \iint \psi_v \psi_f^* dx dy \right|^2}{\left| \iint |\psi_v|^2 dx dy \iint |\psi_f|^2 dx dy \right|} \quad (4.7)$$

Using Eqs. (4.2), (4.6) and (4.7) we get



$$\eta_0 = \frac{4w_{2x}w_{2y}w_f^2}{\sqrt{\left[\left(w_f^2+w_{2x}^2\right)+\frac{k_2^2w_f^4w_{2x}^4}{4R_{2x}^2}\right]\left[\left(w_f^2+w_{2y}^2\right)+\frac{k_2^2w_f^4w_{2y}^4}{4R_{2y}^2}\right]}} \quad (4.8)$$

In case of CML, the aperture is limited, which lowers the coupling of the beam and the fiber. Let  $\rho_c$  be the limited radius within which transmission is allowed, then we have [Edwards, Presby and Dragone, 1993]

$$\rho_c = \frac{n_1 R_L}{n_2} \quad (4.9)$$

here,  $n_1$  and  $n_2$  are the RIs of the incident medium and the lens medium, respectively, and  $R_L$  is the radius of curvature along the XY plane of the cylindrical micro lens. The transitivity factor of the lens is given by [Edwards, Presby and Dragone, 1993]

$$T = \frac{\int_0^{\rho_c} |\psi_f t|^2 r dr}{\int_0^{\infty} |\psi_f|^2 r dr} \quad (4.10)$$

where  $t$  is the transmission coefficient taken as [Edwards, Presby and Dragone, 1993]

$$t = \frac{2\sqrt{n_1 n_2}}{n_1 + n_2} \quad (4.11)$$

Using Eqs. (4.2) and (4.10) we get,

$$T = t^2 \left[ 1 - \exp\left(-\frac{2\rho_c^2}{w_f^2}\right) \right] \quad (4.12)$$

The effective efficiency  $\eta$  becomes

$$\eta = \eta_0 T \quad (4.13)$$

The output and input parameters  $q_1$  and  $q_2$  for this coupling device are related as,

$$q_2 = \frac{Aq_1+B}{Cq_1+D} \quad (4.14)$$

$$\text{and } \frac{1}{q_{1,2}} = \frac{1}{R_{1,2}} - \frac{j\lambda_0}{\pi w_{1,2}^2 n_{1,2}} \quad (4.15)$$

here,  $\lambda_0$  is the free space wavelength.

For a radius of  $R_L$ , the ray matrix for the CML on the fiber tip along the plane vertical to the propagation of light i.e. XZ plane is given by [Roy, Majumder, Maity and Gangopadhyay, 2020]

$$M_x = \begin{pmatrix} A_x & B_x \\ C_x & D_x \end{pmatrix} = \begin{pmatrix} 1 & z_1 \\ 0 & 1 \end{pmatrix} \begin{pmatrix} 1 & 0 \\ \frac{1-n}{nR_L} & \frac{1}{n} \end{pmatrix} \begin{pmatrix} 1 & u \\ 0 & 1 \end{pmatrix} \quad (4.16)$$

$$\text{i.e., } A_x = 1 + \frac{z_1(1-n)}{nR_L}$$

$$B_x = u + \frac{uz_1(1-n)}{nR_L} + \frac{z_1}{n}$$

$$C = \frac{(1-n)}{nR_L} \quad (4.17)$$

$$D = \frac{1}{n} + \frac{(1-n)u}{nR_L}$$

Here,  $u$  is the distance of the source from the cylindrical micro lens,  $R_L$  is the radius of curvature of the lens and  $n$  is the RI of the lens material and  $z_1$  is the distance of the core of the fiber from the tip of the micro lens.

As from the previous studies, it is seen that the coupling efficiency along the horizontal plane is very less [Roy, Majumdar, Maity and Gangopadhyay, 2020], hence it is not considered here.

Eqs. (4.14) and (4.15) can be used to calculate the lens transformed spot sizes  $w_{2x,2y}$  and the radii of curvatures of the wave fronts  $R_{2x,2y}$ .

$$w_{2x,2y}^2 = \frac{A_1^2 w_{1x,1y}^2 + \frac{\lambda_1^2 B^2}{w_{1x,1y}^2}}{n(A_1 D - B C_1)} \quad (4.18)$$

$$\frac{1}{R_{2x,2y}} = \frac{A_1 C_1 w_{1x,1y}^2 + \frac{\lambda_1^2 B D}{w_{1x,1y}^2}}{A_1^2 w_{1x,1y}^2 + \frac{\lambda_1^2 B^2}{w_{1x,1y}^2}} \quad (4.19)$$

Where,  $\lambda_1 = \frac{\lambda}{n}$ ,  $\lambda = \frac{\lambda_0}{n_1}$ ,  $A_1 = A + \frac{B}{R_1}$  and  $C_1 = C + \frac{D}{R_1}$

But for the sake of simplicity and accuracy, planer wave front model has been used [John, Maclean, Ghafouri – Shiraz and Niblett; Maiti, Maiti and Gangopadhyay, 2017; Mandal, Maiti, Chiu and Gangopadhyay, 2018; Maiti, Biswas and Gangopadhyay, 2019, Mukhopadhyay and Sarkar, 2011; Gangopadhyay and Sarkar, 1998; Gangopadhyay and Sarkar, 1998; Mukhopadhyay, Gangopadhyay and Sarkar, 2007]. Hence,  $R_1 = \infty$  here and from the above relations,  $A_1 = A$  and  $C_1 = C$ .

### 4.3. RESULTS AND DISCUSSIONS

For the purpose of evaluation of the maximum coupling efficiency by using a cylindrical micro lens, two laser diodes of wavelengths 1.5  $\mu\text{m}$  and 1.3  $\mu\text{m}$  are used. The study is done for the RI distribution of the profile exponents such as  $g = 4$  having V values 1.924, 2.806, 3.500,  $g = 8$  having V values 1.924, 2.164, 2.700,  $g = 10$  having V values 1.924, 2.124, 2.650 and finally  $g = 20$  having V values 1.924, 2.004, 2.500. The spot size ( $w_f$ ) of the fibers are found by using Eqs. (4.4) and (4.5) [Bose, Gangopadhyay and Saha,

2012; Mukhopadhyay and Sarkar, 2011]. Again, the RIs of the lens, core and cladding are taken as 1.55, 1.46 and 1.45 respectively [John, Maclean, Ghafouri – Shiraz and Niblett, 1994; Maiti, Maiti and Gangopadhyay, 2017; Mandal, Maiti, Chiu and Gangopadhyay, 2018]. At first, we varied the value of  $z_1$  starting from  $z_1 = 1$  and then the optimized values of  $R_L$  and  $u$  are found for which we get the maximum coupling efficiency. The coupling efficiency for  $z_1 = 1$  is found to be more than those for higher  $z_1$  values. Hence we search the maximum efficiency by optimizing  $R_L$  and  $u$  values, keeping the value of  $z_1$  as 1. Tables 4.1.1, 4.1.2 and 4.1.3 present the variations of  $u$  and  $R_L$  for the RI profile exponent  $g = 4$  corresponding to three different  $V$  values respectively. Tables 4.2.1, 4.2.2 and 4.2.3 present the variations of  $u$  and  $R_L$  for the RI profile exponent  $g = 8$  corresponding to three different  $V$  values respectively. Tables 4.3.1, 4.3.2 and 4.3.3 present the variations of  $u$  and  $R_L$  for the RI profile exponent  $g = 10$  corresponding to three different  $V$  values respectively. Finally, Tables 4.4.1, 4.4.2 and 4.4.3 present the variations of  $u$  and  $R_L$  for the RI profile exponent  $g = 20$  corresponding to three different  $V$  values respectively. All these are evaluated for the source wavelength  $1.5 \mu\text{m}$ . The same has been done for the source wavelength  $1.3 \mu\text{m}$  as well. Tables 4.5.1, 4.5.2, 4.5.3, 4.6.1, 4.6.2, 4.6.3, 4.7.1, 4.7.2, 4.7.3, 4.8.1, 4.8.2 and 4.8.3 represent those correspondingly. Figs. 4.1.1a, 4.1.2a and 4.1.3a present the variations of coupling efficiency versus  $R_L$  for the fixed value of  $u$  for which the efficiency is maximum. It is done for the said three different  $V$  values respectively and for the same RI profile exponent  $g = 4$  when  $1.5 \mu\text{m}$  light source is used, whereas 4.1.1b, 4.1.2b, 4.1.3b show the variations of coupling efficiency with the  $u$  values for the fixed value of  $R_L$  which produced maximum coupling efficiency as obtained from the previous graphs. Similar graphical representation is given in Figs. 4.2.1a, 4.2.2a, 4.2.3a and 4.2.1b, 4.2.2b, 4.2.3b respectively for the RI profile exponent  $g = 8$ . Likewise, graphical representations are

shown in Figs. 4.3.1a, 4.3.2a, 4.3.3a and 4.3.1b, 4.3.2b, 4.3.3b respectively for the RI profile exponent  $g = 10$  and finally, similar graphical representations in Figs. 4.4.1a, 4.4.2a, 4.4.3a and 4.4.1b, 4.4.2b, 4.4.3b respectively are shown for the RI profile exponent  $g = 20$ . All these graphs are drawn from the results obtained from the source of light of wavelength  $1.5 \mu\text{m}$ . For the source of light of wavelength  $1.3 \mu\text{m}$ , graphical representations are shown in Figs. 4.5.1a, 4.5.2a, 4.5.3a and 4.5.1b, 4.5.2b, 4.5.3b respectively for the RI of profile exponent  $g = 4$ , in Figs. 4.6.1a, 4.6.2a, 4.6.3a and 4.6.1b, 4.6.2b, 4.6.3b respectively graphical representations are shown for the RI of profile exponent  $g = 8$ , in Figs. 4.7.1a, 4.7.2a, 4.7.3a and 4.7.1b, 4.7.2b, 4.7.3b respectively graphical representations are presented for the RI profile of exponent  $g = 10$  and finally, in Figs. 4.8.1a, 4.8.2a, 4.8.3a and 4.8.1b, 4.8.2b, 4.8.3b respectively graphical representations are shown for the RI of profile exponent  $g = 20$ .

Tables 4.9 and 4.10 show that the maximum coupling efficiencies for the optimized values of  $R_L$  and  $u$  in case of laser wavelengths  $1.5 \mu\text{m}$  and  $1.3 \mu\text{m}$  respectively for the four kinds of optical fibers, having RI distribution profile indices 4, 8 10 and 20 respectively together with different  $V$  values. From the analysis, it is clear that wavelength  $1.3 \mu\text{m}$  produces more efficient coupler in comparison to the wavelength  $1.5 \mu\text{m}$ .

Further analyzing Tables 4.9 and 4.10, it is observed that the maximum coupling efficiency is obtained for the RI profile exponent  $g = 4$ , excited by the wavelength  $1.3 \mu\text{m}$ .

The optical designers will be benefited from the results presented here. Further, as the coupling efficiency along the horizontal plane of the source is negligibly small, the coupling efficiency is studied along the vertical plane only.

**Table 4.1.1**

**Values of coupling efficiencies  $\eta$ , for the RI of profile exponent  $g = 4$ ,  $V$  value 1.924, excited by wavelength  $1.5 \mu\text{m}$  with  $w_f = 5.008 \mu\text{m}$ ,  $w_{1x} = 0.843 \mu\text{m}$  and  $w_{1y} = 0.857 \mu\text{m}$**

u	$R_L = 1$	$R_L = 6$	$R_L = 6.5$	$R_L = 7$	$R_L = 7.5$	$R_L = 11$	$R_L = 16$	$R_L = 21$
1	0.375	8.464	9.034	9.563	9.962	11.127	11.025	10.883
6	0.059	25.889	24.562	24.244	23.072	18.821	15.471	14.003
8	0.029	44.030	39.761	37.929	34.436	23.765	17.813	15.488
10	0.017	62.992	59.951	57.313	51.031	30.207	20.516	17.101
11	0.013	63.048	66.209	65.673	59.893	34.017	21.999	17.948
12	0.011	55.199	65.363	68.979	66.613	38.155	23.559	18.816
13	0.009	44.167	57.918	65.536	68.764	42.481	25.181	19.697
16	0.005	20.068	29.596	37.747	48.964	53.614	30.159	22.335
21	0.003	7.115	10.340	13.326	18.341	47.856	36.053	25.918
31	0.001	2.032	2.816	3.521	4.676	15.539	26.645	24.709

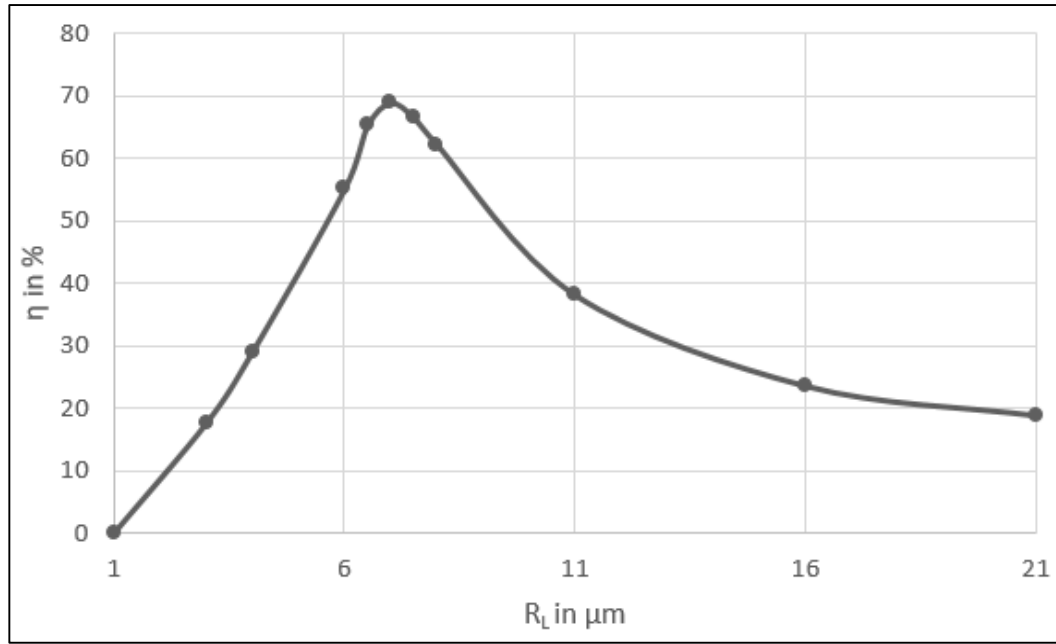


**Fig. 4.1.1a: Maximum coupling efficiency ( $\eta$ ) vs radius of the fiber ( $r$ ) for RI profile exponent  $g=4$  having  $V$  value 1.924 ( $w_f = 5.008 \mu\text{m}$ ) and excitation wavelength  $1.5 \mu\text{m}$**

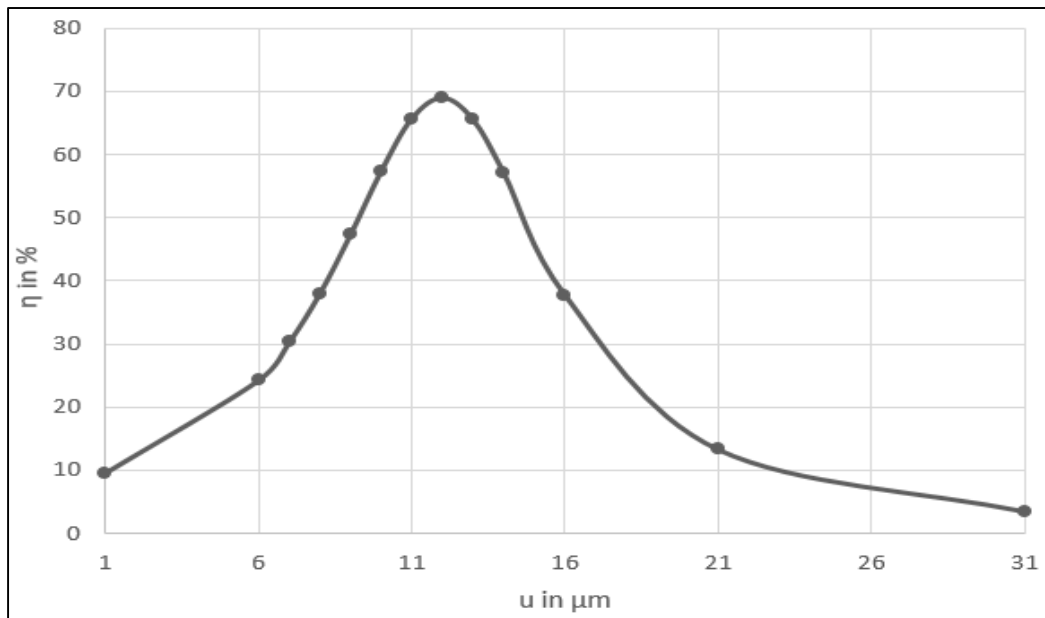


**Fig. 4.1.1b: Maximum coupling efficiency ( $\eta$ ) vs distance of the laser from the tip of cylindrical lens ( $u$ ) of the fiber for RI profile exponent  $g=4$  having  $V$  value 1.924 ( $w_f = 5.008 \mu\text{m}$ ) and excitation wavelength  $1.5 \mu\text{m}$**

**Table 4.1.2**

**Values of coupling efficiencies for the RI profile exponent  $g = 4$ ,  $V$  value 2.405, excited by wavelength  $1.5 \mu\text{m}$  with  $w_f = 3.831 \mu\text{m}$ ,  $w_{1x} = 0.843 \mu\text{m}$  and  $w_{1y} = 0.857 \mu\text{m}$**

U	$R_L = 1$	$R_L = 5.5$	$R_L = 6$	$R_L = 6.5$	$R_L = 7$	$R_L = 11$	$R_L = 16$	$R_L = 21$
1	1.046	16.395	17.262	17.767	18.206	18.516	18.058	17.818
6	0.170	46.807	44.793	41.908	40.532	29.120	24.030	21.912
8	0.084	65.237	62.341	57.363	54.630	34.418	26.501	23.405
9	0.063	69.386	68.477	64.027	61.162	37.087	27.669	24.071
10	0.049	67.133	69.917	67.856	65.728	39.618	28.752	24.663
11	0.039	59.597	66.058	67.621	67.126	41.865	29.717	25.170
12	0.032	49.844	58.444	63.403	64.938	43.668	30.531	25.577
16	0.016	21.196	27.500	34.45	39.067	44.177	31.764	26.044
21	0.009	8.888	11.628	15.026	17.615	32.689	28.485	24.017
31	0.004	2.875	3.696	4.732	5.593	13.493	16.740	16.171



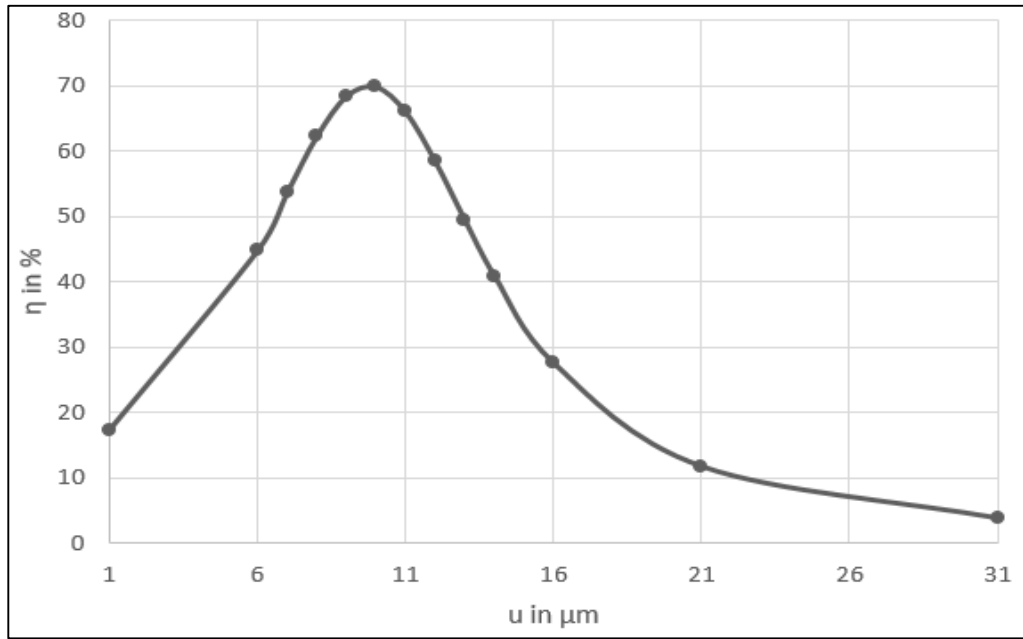


**Fig. 4.1.2a: Maximum coupling efficiency ( $\eta$ ) vs radius of the fiber ( $r$ ) for RI profile exponent  $g=4$  having  $V$  value 2.405 ( $w_f = 3.831 \mu\text{m}$ ) and excitation wavelength  $1.5 \mu\text{m}$**

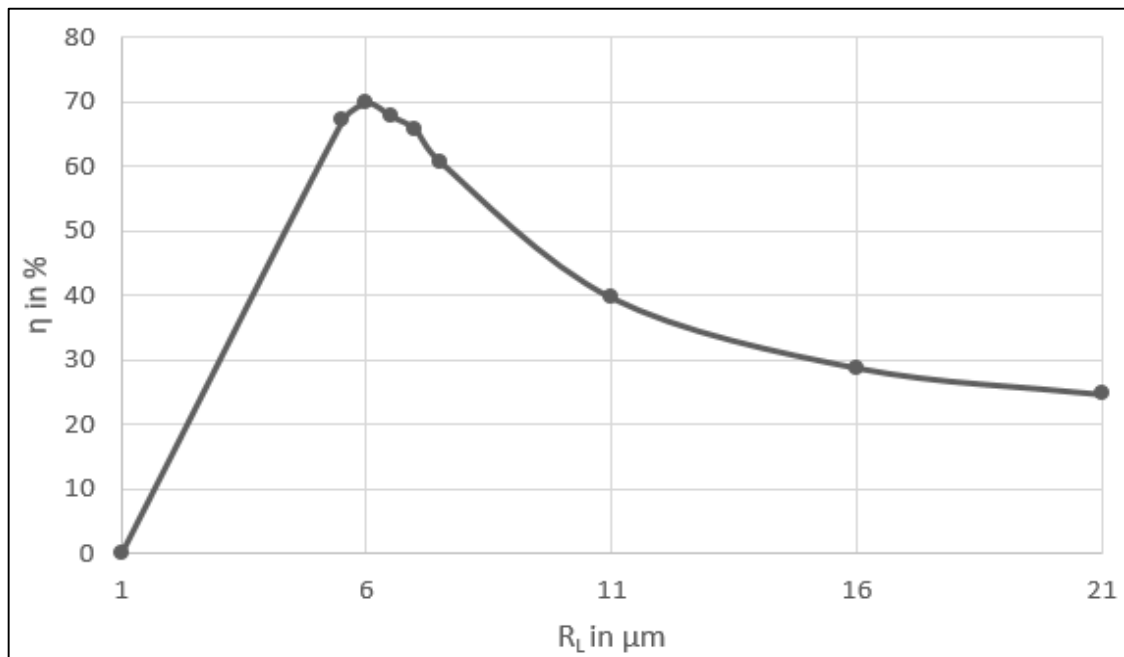


**Fig. 4.1.2b: Maximum coupling efficiency ( $\eta$ ) vs distance of the laser from the tip of cylindrical lens ( $u$ ) of the fiber for RI profile exponent  $g=4$  having  $V$  value 2.405 ( $w_f = 3.831 \mu\text{m}$ ) and excitation wavelength  $1.5 \mu\text{m}$**

**Table 4.1.3**

**Values of coupling efficiencies for the RI profile exponent  $g = 4$ ,  $V$  value 3.000, excited by wavelength  $1.5 \mu\text{m}$  with  $w_f = 3.284 \mu\text{m}$ ,  $w_{1x} = 0.843 \mu\text{m}$  and  $w_{1y} = 0.857 \mu\text{m}$**

u	$R_L = 1$	$R_L = 5.5$	$R_L = 6$	$R_L = 6.5$	$R_L = 7$	$R_L = 11$	$R_L = 16$	$R_L = 21$
1	2.175	24.504	24.909	25.014	25.103	24.244	23.640	23.361
6	0.364	59.702	56.116	52.050	49.743	35.491	29.778	27.384
7	0.249	67.401	63.218	58.258	55.364	37.633	30.719	27.880
8	0.180	72.000	68.319	63.216	60.038	39.516	31.483	28.231
9	0.316	71.911	70.041	65.904	62.953	41.023	32.040	28.426
10	0.106	67.168	67.851	65.663	63.499	42.045	32.367	28.459
11	0.084	59.402	62.423	62.556	61.551	42.502	32.447	28.329
16	0.036	24.377	28.784	33.035	35.385	36.630	29.404	25.544
21	0.019	11.201	13.516	16.117	17.811	25.322	23.175	20.806
31	0.008	3.878	4.672	5.619	6.268	11.219	12.612	12.332

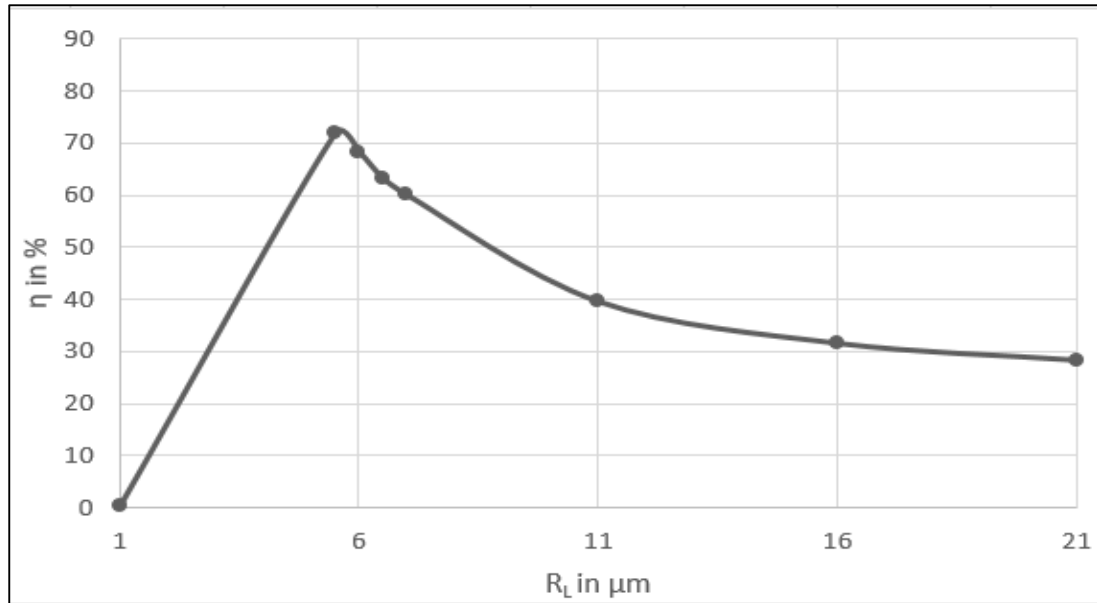


**Fig. 4.1.3a: Maximum coupling efficiency ( $\eta$ ) vs radius of the fiber ( $r$ ) for RI profile exponent  $g=4$  having  $V$  value 3.000 ( $w_f = 3.284 \mu\text{m}$ ) and excitation wavelength  $1.5 \mu\text{m}$**

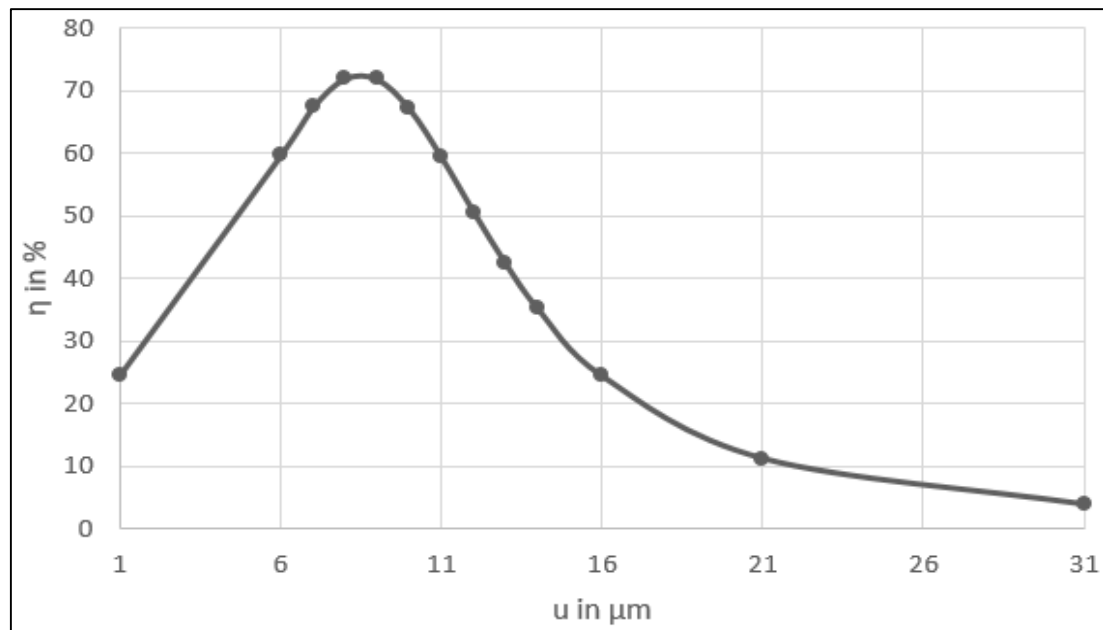


**Fig. 4.1.3b: Maximum coupling efficiency ( $\eta$ ) vs distance of the laser from the tip of cylindrical lens ( $u$ ) of the fiber for RI profile exponent  $g = 4$  having  $V$  value 3.000 ( $w_f = 3.284 \mu\text{m}$ ) and excitation wavelength  $1.5 \mu\text{m}$**

**Table 4.2.1**

**Values of coupling efficiencies for the RI profile exponent  $g = 8$ ,  $V$  value 1.924, excited by wavelength  $1.5 \mu\text{m}$  with  $w_f = 4.714 \mu\text{m}$ ,  $w_{1x} = 0.843 \mu\text{m}$  and  $w_{1y} = 0.857 \mu\text{m}$**

u	$R_L = 1$	$R_L = 6$	$R_L = 6.5$	$R_L = 7$	$R_L = 7.5$	$R_L = 11$	$R_L = 16$	$R_L = 21$
1	0.473	10.055	10.658	11.204	11.592	12.549	12.344	12.187
6	0.075	29.856	28.254	27.761	26.311	20.968	17.173	15.566
10	0.021	65.910	63.208	60.699	54.517	32.678	22.382	18.758
11	0.017	65.041	68.040	67.629	62.278	36.350	23.845	19.590
12	0.014	57.174	66.308	69.552	67.464	40.176	25.344	20.429
13	0.011	46.469	58.922	65.581	68.303	43.970	26.856	21.257
14	0.009	36.414	49.096	57.477	64.472	47.466	28.351	22.060
16	0.007	22.180	31.566	39.160	49.005	52.264	31.129	23.560
21	0.004	8.155	11.589	14.648	19.587	44.323	32.736	26.020
31	0.001	2.374	3.244	4.005	5.229	15.425	24.067	22.610

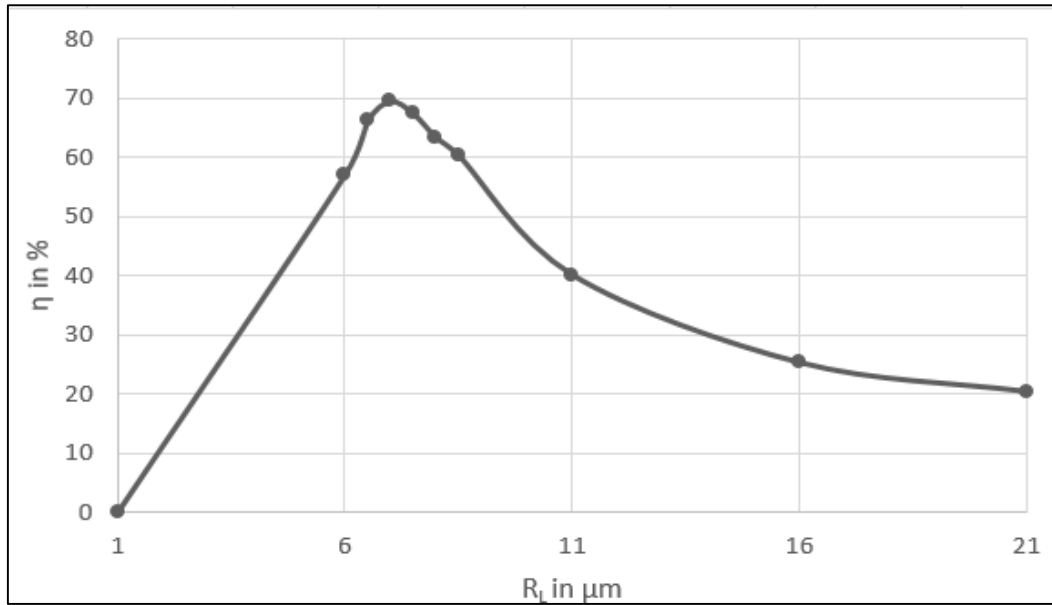


**Fig. 4.2.1a: Maximum coupling efficiency ( $\eta$ ) vs radius of the fiber ( $r$ ) for RI profile exponent  $g = 8$  having  $V$  value 1.924 ( $w_f = 4.714 \mu\text{m}$ ) and excitation wavelength  $1.5 \mu\text{m}$**

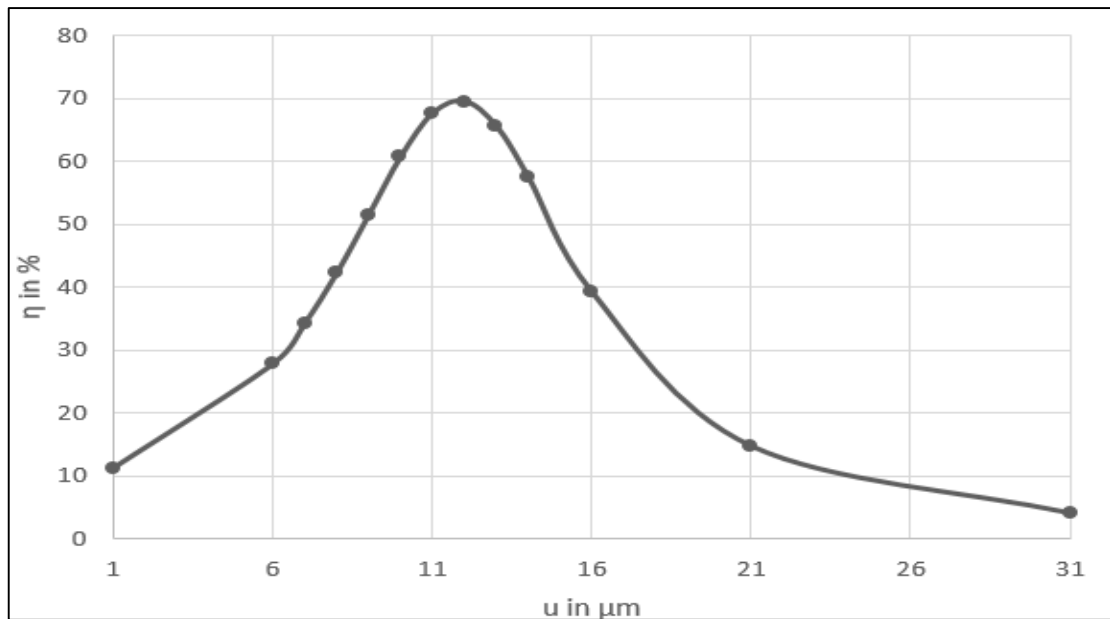


**Fig. 4.2.1b: Maximum coupling efficiency ( $\eta$ ) vs distance of the laser from the tip of cylindrical lens ( $u$ ) of the fiber for RI profile exponent  $g = 8$  having  $V$  value 1.924 ( $w_f = 4.714 \mu\text{m}$ ) and excitation wavelength  $1.5 \mu\text{m}$**

**Table 4.2.2**

**Values of coupling efficiencies for the RI profile exponent  $g = 8$ ,  $V$  value 2.164, excited by wavelength  $1.5 \mu\text{m}$  with  $w_f = 4.136 \mu\text{m}$ ,  $w_{1x} = 0.843 \mu\text{m}$  and  $w_{1y} = 0.857 \mu\text{m}$**

u	$R_L = 1$	$R_L = 5.5$	$R_L = 6$	$R_L = 6.5$	$R_L = 7$	$R_L = 11$	$R_L = 16$	$R_L = 21$
1	0.773	13.437	14.254	14.862	15.372	16.078	15.707	15.511
6	0.124	40.912	39.134	36.826	35.810	25.959	21.315	19.399
8	0.061	61.162	57.983	53.197	50.671	31.408	23.879	20.990
9	0.046	67.337	66.069	61.474	58.593	34.370	25.179	21.760
10	0.036	66.451	69.509	67.413	65.148	37.385	26.462	22.496
11	0.028	59.020	66.671	68.973	68.571	40.322	27.700	23.187
12	0.023	48.698	58.917	65.531	67.712	43.011	28.859	23.819
16	0.012	19.286	25.984	34.161	39.969	47.558	32.032	25.510
21	0.006	7.745	10.416	13.997	16.883	36.764	30.992	25.146
31	0.002	2.436	3.193	4.204	5.025	14.411	19.170	18.389

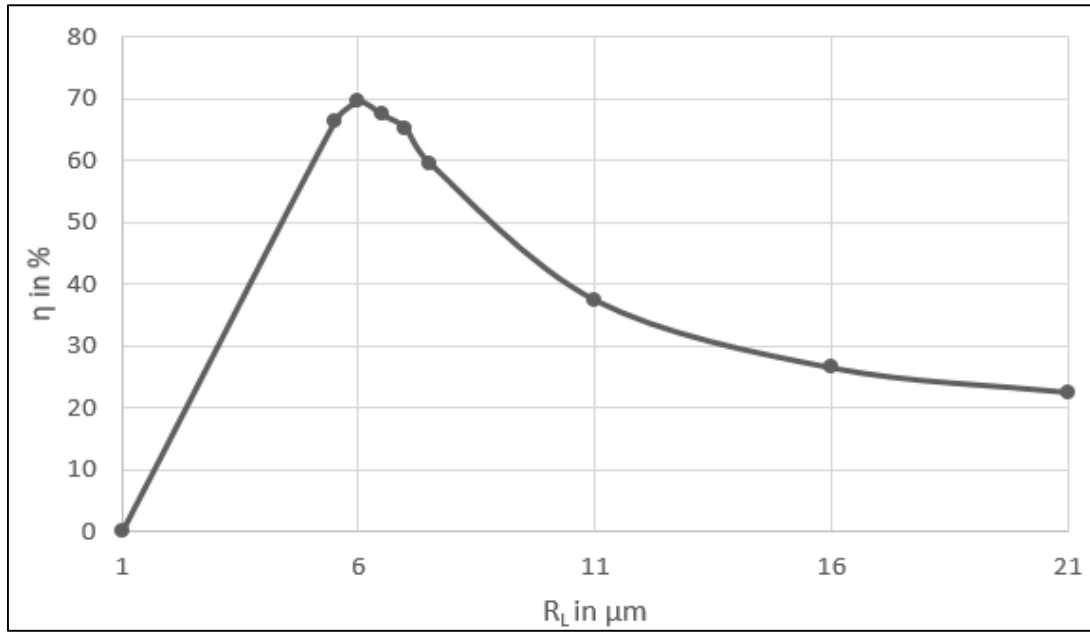


**Fig. 4.2.2a: Maximum coupling efficiency ( $\eta$ ) vs radius of the fiber ( $r$ ) for RI profile exponent  $g = 8$  having  $V$  value 2.164 ( $w_f = 4.136 \mu\text{m}$ ) and excitation wavelength  $1.5 \mu\text{m}$**

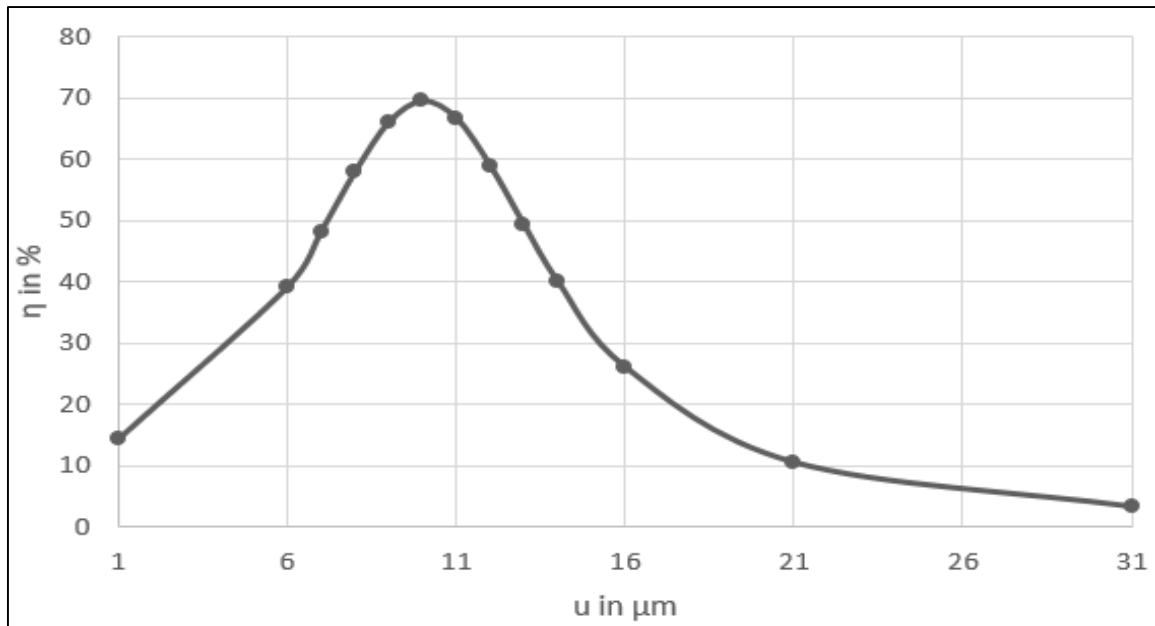


**Fig. 4.2.2b: Maximum coupling efficiency ( $\eta$ ) vs distance of the laser from the tip of cylindrical lens ( $u$ ) of the fiber for RI profile exponent  $g = 8$  having  $V$  value 2.164 ( $w_f = 4.136 \mu\text{m}$ ) and excitation wavelength  $1.5 \mu\text{m}$**

**Table 4.2.3**

**Values of coupling efficiencies for the RI profile exponent  $g = 8$ ,  $V$  value 2.700, excited by wavelength  $1.5 \mu\text{m}$  with  $w_r = 3.526 \mu\text{m}$ ,  $w_{1x} = 0.843 \mu\text{m}$  and  $w_{1y} = 0.857 \mu\text{m}$**

u	$R_L = 1$	$R_L = 5$	$R_L = 5.5$	$R_L = 6$	$R_L = 6.5$	$R_L = 11$	$R_L = 16$	$R_L = 21$
1	1.418	19.060	20.072	20.827	21.263	21.439	20.895	20.644
6	0.234	56.266	52.882	50.328	47.099	32.552	27.075	24.807
7	0.160	65.342	61.697	58.412	54.128	34.993	28.210	25.471
8	0.115	69.807	68.190	65.235	60.541	37.339	29.244	26.041
9	0.087	67.405	70.026	68.974	65.102	39.473	30.144	26.502
10	0.068	59.397	66.428	68.0369	66.653	41.266	30.878	26.842
11	0.054	49.199	58.875	63.636	64.746	42.591	31.418	27.049
16	0.023	16.635	22.729	28.134	33.730	40.132	30.733	26.034
21	0.012	7.292	10.010	12.601	15.676	28.542	25.602	22.404
31	0.005	2.482	3.353	4.185	5.212	12.298	14.379	13.999



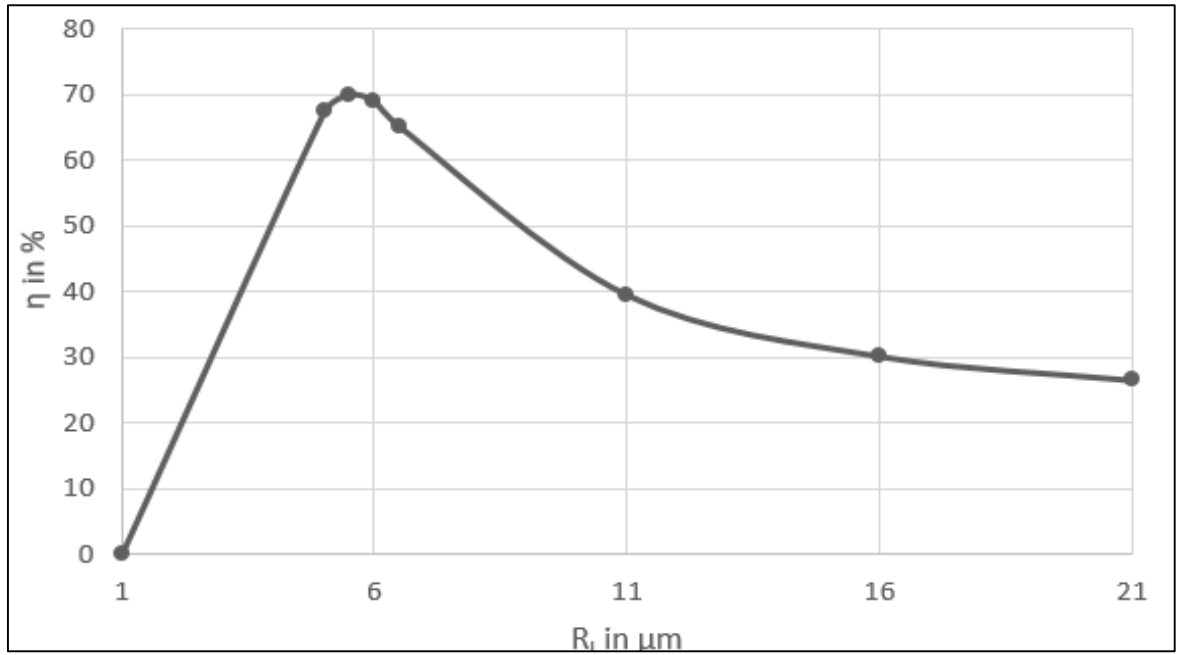


**Fig. 4.2.3a: Maximum coupling efficiency ( $\eta$ ) vs radius of the fiber ( $r$ ) for RI profile exponent  $g = 8$  having  $V$  value 2.700 ( $w_f = 3.526 \mu\text{m}$ ) and excitation wavelength  $1.5 \mu\text{m}$**

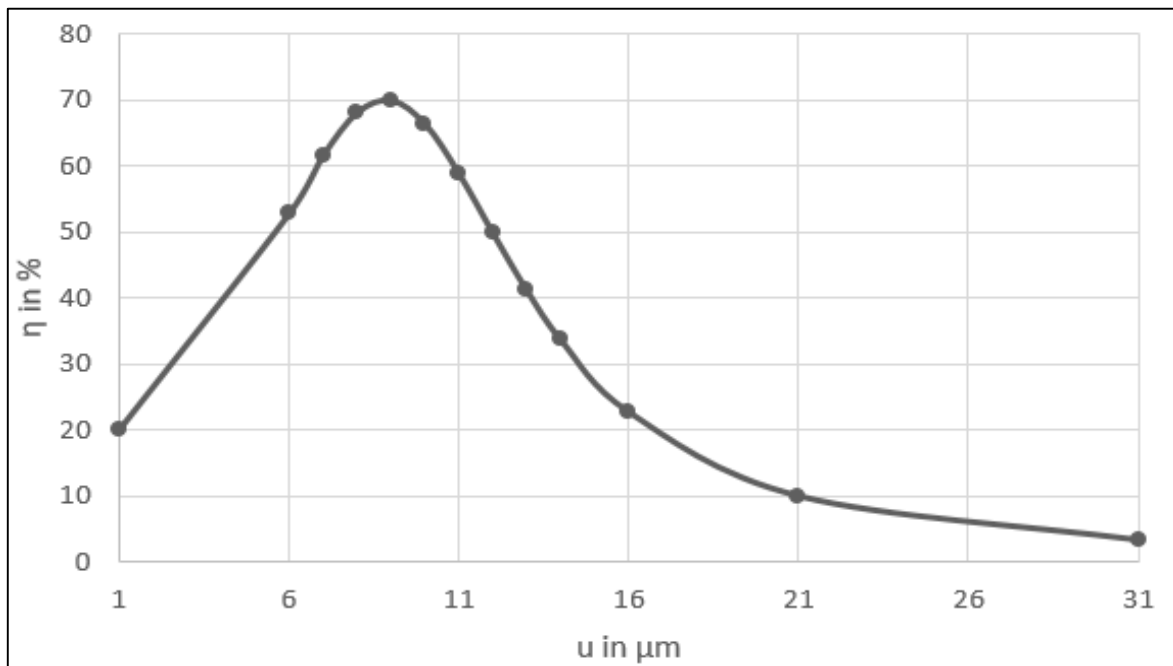


**Fig. 4.2.3b: Maximum coupling efficiency ( $\eta$ ) vs distance of the laser from the tip of cylindrical lens ( $u$ ) of the fiber for RI profile exponent  $g = 8$  having  $V$  value 2.700 ( $w_f = 3.526 \mu\text{m}$ ) and excitation wavelength  $1.5 \mu\text{m}$**

**Table 4.3.1**

**Values of coupling efficiencies for the RI profile exponent  $g = 10$ ,  $V$  value 2.700, excited by wavelength  $1.5 \mu\text{m}$  with  $w_r = 4.715 \mu\text{m}$ ,  $w_{1x} = 0.843 \mu\text{m}$  and  $w_{1y} = 0.857 \mu\text{m}$**

u	$R_L = 1$	$R_L = 6$	$R_L = 6.5$	$R_L = 7$	$R_L = 7.5$	$R_L = 11$	$R_L = 16$	$R_L = 21$
1	0.472	10.051	10.654	11.200	11.587	12.544	12.339	12.182
6	0.074	29.848	28.246	27.753	26.303	20.961	17.197	15.561
10	0.021	65.915	63.210	60.699	57.513	32.670	22.376	18.752
11	0.017	65.050	68.047	67.635	62.280	36.344	23.838	19.588
12	0.014	57.180	66.319	69.563	67.472	40.171	25.338	20.424
13	0.011	46.470	58.931	65.593	68.315	43.967	26.851	21.251
14	0.009	39.414	49.101	57.486	64.486	47.466	28.346	22.059
16	0.007	22.178	31.566	39.162	49.013	52.271	31.126	23.562
21	0.004	8.153	11.587	14.645	19.586	44.337	34.742	26.021
31	0.001	2.373	3.243	4.004	5.227	15.426	24.076	22.619

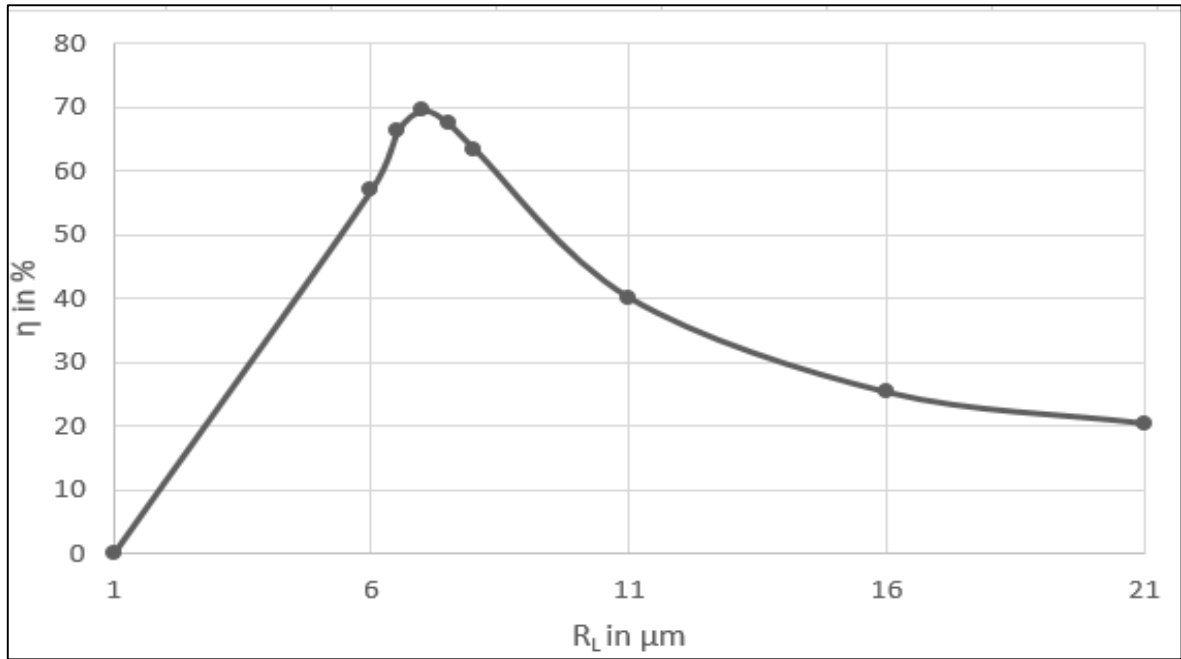


**Fig. 4.3.1a: Maximum coupling efficiency ( $\eta$ ) vs radius of the fiber ( $r$ ) for RI profile exponent  $g = 10$  having value 1.924 ( $w_f = 4.715 \mu\text{m}$ ) and excitation wavelength  $1.5 \mu\text{m}$**

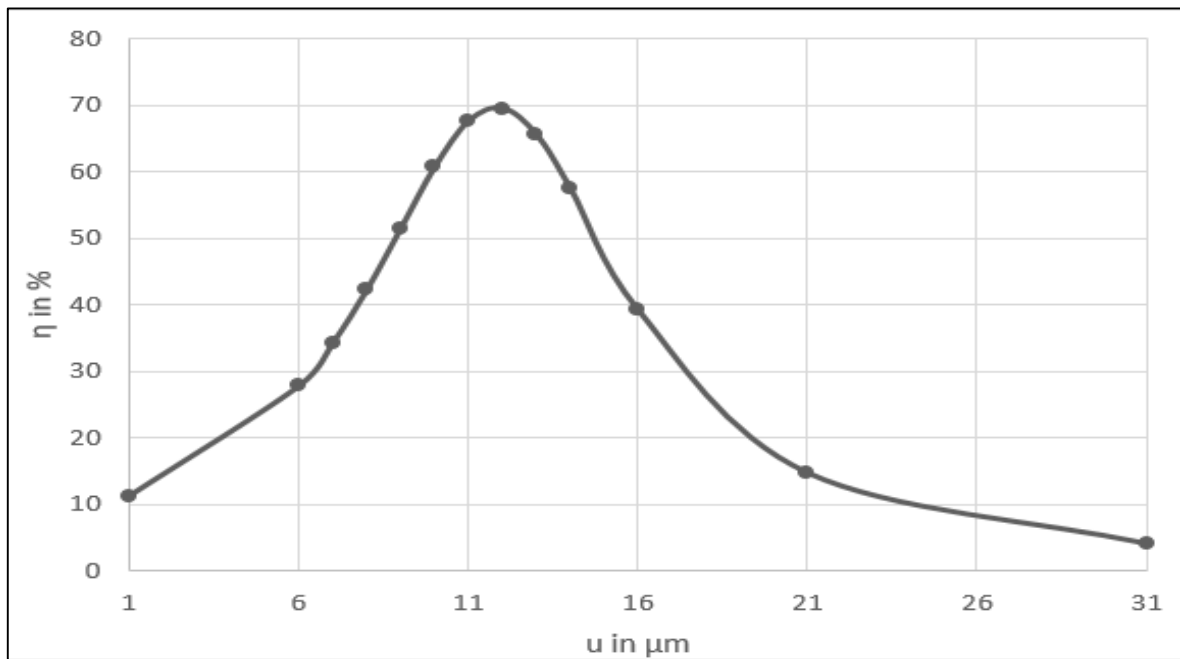


**Fig. 4.3.1b: Maximum coupling efficiency ( $\eta$ ) vs distance of the laser from the tip of cylindrical lens ( $u$ ) of the fiber for RI profile exponent  $g = 10$  having  $V$  value 1.924 ( $w_f = 4.715 \mu\text{m}$ ) and excitation wavelength  $1.5 \mu\text{m}$**

**Table 4.3.2**

**Values of coupling efficiencies for the RI profile exponent  $g = 10$ ,  $V$  value 2.124, excited by wavelength  $1.5 \mu\text{m}$  with  $w_r = 4.230 \mu\text{m}$ ,  $w_{1x} = 0.843 \mu\text{m}$  and  $w_{1y} = 0.857 \mu\text{m}$**

u	$R_L = 1$	$R_L = 5.5$	$R_L = 6$	$R_L = 6.5$	$R_L = 7$	$R_L = 11$	$R_L = 16$	$R_L = 21$
1	0.709	12.631	13.452	14.055	14.579	15.424	15.066	14.878
6	0.114	39.126	37.490	35.282	34.370	25.073	20.548	18.687
8	0.056	59.680	56.536	51.734	49.288	30.521	23.112	20.286
9	0.042	66.396	65.128	60.311	57.527	33.538	24.434	21.286
10	0.032	65.920	69.155	66.914	64.617	36.659	25.755	21.836
11	0.026	58.543	66.640	69.028	68.649	39.765	27.051	22.565
12	0.021	48.088	58.855	65.853	68.230	42.689	28.291	23.247
16	0.011	18.635	25.428	33.858	40.004	48.502	31.983	25.246
21	0.006	7.394	10.037	13.615	16.560	38.031	31.681	25.382
31	0.002	2.309	3.046	4.036	4.853	14.649	19.938	19.066

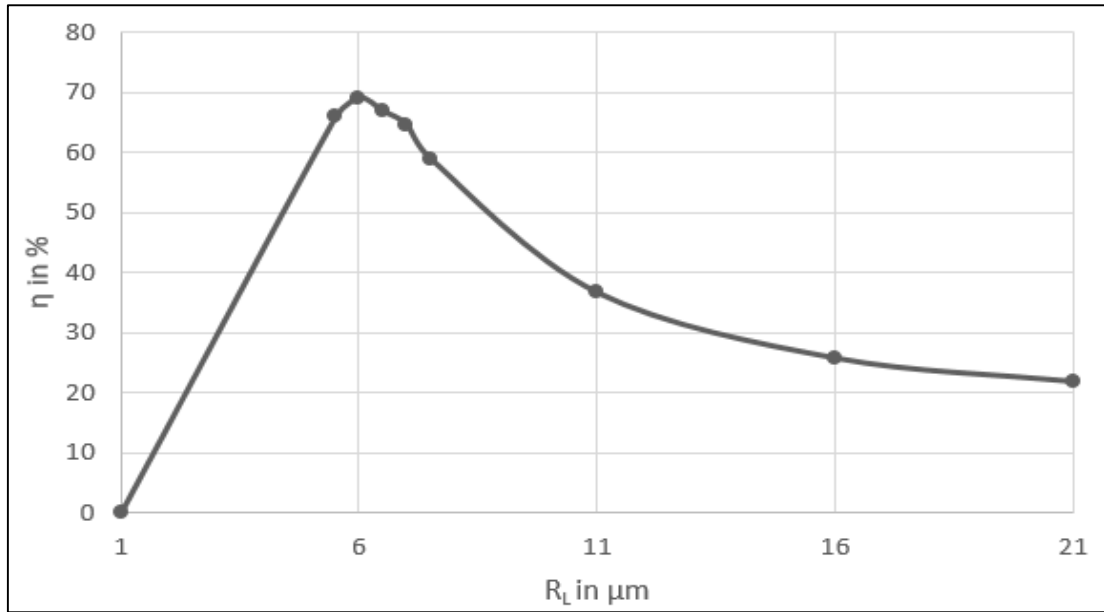


**Fig. 4.3.2a: Maximum coupling efficiency ( $\eta$ ) vs radius of the fiber ( $r$ ) for RI profile exponent  $g = 10$  having  $V$  value 2.124 ( $w_f = 4.230 \mu\text{m}$ ) and excitation wavelength  $1.5 \mu\text{m}$**

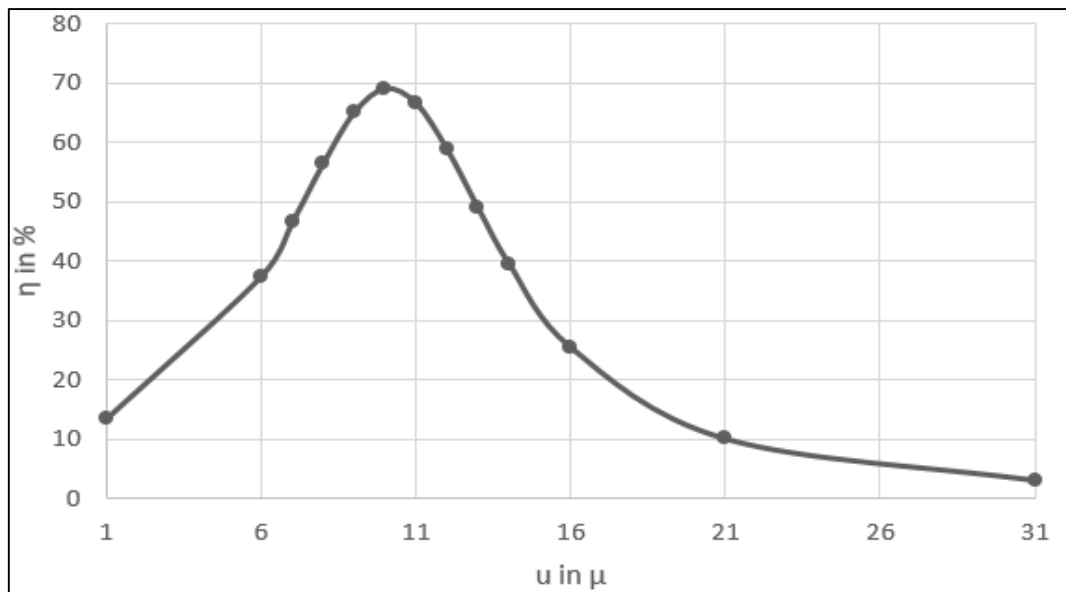


**Fig. 4.3.2b: Maximum coupling efficiency ( $\eta$ ) vs distance of the laser from the tip of cylindrical lens ( $u$ ) of the fiber for RI profile exponent  $g = 10$  having  $V$  value 2.124 ( $w_f = 4.230 \mu\text{m}$ ) and excitation wavelength  $1.5 \mu\text{m}$**

**Table 4.3.3**

**Values of coupling efficiencies for the RI profile exponent  $g = 10$ ,  $V$  value 2.650, excited by wavelength  $1.5 \mu\text{m}$  with  $w_r = 3.596 \mu\text{m}$ ,  $w_{1x} = 0.843 \mu\text{m}$  and  $w_{1y} = 0.857 \mu\text{m}$**

u	$R_L = 1$	$R_L = 5.5$	$R_L = 6$	$R_L = 6.5$	$R_L = 7$	$R_L = 11$	$R_L = 16$	$R_L = 21$
1	1.304	19.165	19.943	20.411	20.786	20.714	20.186	19.940
6	0.215	51.517	49.060	45.935	44.308	31.737	26.338	24.109
7	.0146	60.643	57.398	53.160	50.857	34.234	27.510	24.806
8	0.106	67.669	64.688	59.951	57.174	36.679	28.600	25.420
9	0.079	70.054	69.002	65.033	62.299	38.960	29.576	25.941
10	0.062	66.755	68.859	67.112	65.163	40.945	30.405	26.638
11	0.498	59.193	64.312	65.568	65.045	42.500	31.056	26.638
16	0.021	22.436	28.062	34.010	37.714	41.100	31.029	26.093
21	0.011	9.766	12.401	15.576	17.859	29.486	26.280	22.815
31	0.005	3.243	4.075	5.112	5.884	12.591	14.906	14.492

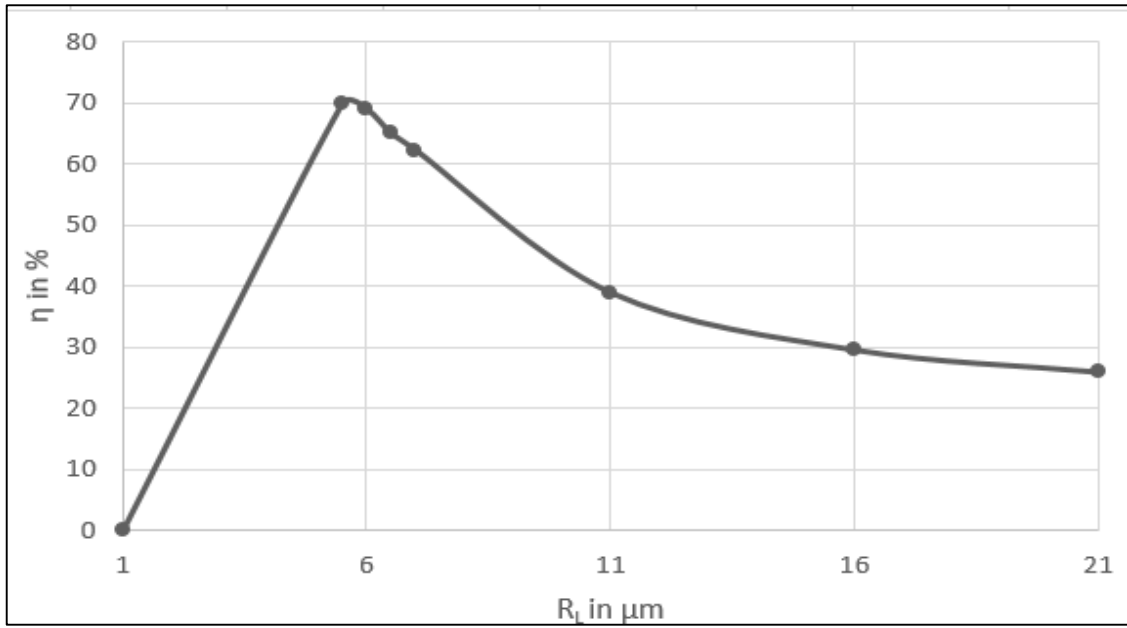


**Fig. 4.3.3a: Maximum coupling efficiency ( $\eta$ ) vs radius of the fiber ( $r$ ) for RI profile exponent  $g = 10$  having  $V$  value 2.650 ( $w_f = 3.596 \mu\text{m}$ ) and excitation wavelength  $1.5 \mu\text{m}$**

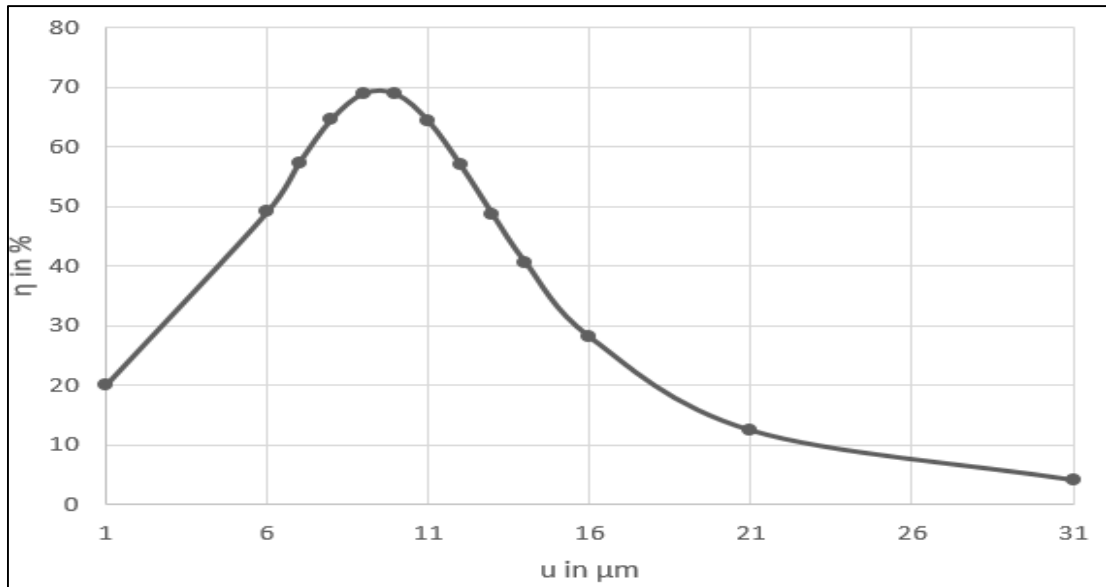


**Fig. 4.3.3b: Maximum coupling efficiency ( $\eta$ ) vs distance of the laser from the tip of cylindrical lens ( $u$ ) of the fiber for RI profile exponent  $g = 10$  having  $V$  value 2.650 ( $w_f = 3.596 \mu\text{m}$ ) and excitation wavelength  $1.5 \mu\text{m}$**

**Table 4.4.1**

**Values of coupling efficiencies for the RI profile exponent  $g = 20$ ,  $V$  value 1.924, excited by wavelength  $1.5 \mu\text{m}$  with  $w_r = 4.858 \mu\text{m}$ ,  $w_{1x} = 0.843 \mu\text{m}$  and  $w_{1y} = 0.857 \mu\text{m}$**

u	$R_L = 1$	$R_L = 6$	$R_L = 6.5$	$R_L = 7$	$R_L = 7.5$	$R_L = 11$	$R_L = 16$	$R_L = 21$
1	0.409	9.240	9.826	10.358	10.752	11.828	11.670	11.521
6	0.064	27.856	26.390	25.968	24.660	19.888	16.309	14.771
10	0.018	64.568	61.686	59.065	52.818.	31.468	21.447	17.924
11	0.014	64.163	67.244	66.726	61.155	35.225	22.925	18.769
12	0.012	56.296	65.949	69.335	67.112	39.224	24.461	19.625
13	0.010	45.410	58.527	65.621	68.593	43.301	26.036	20.484
14	0.008	35.261	48.451	57.354	64.992	47.195	27.623	21.336
16	0.006	21.152	30.640	38.508	49.042	53.020	30.685	22.973
21	0.003	7.635	10.972	13.995	18.987	46.093	35.431	26.009
31	0.001	2.200	3.029	3.760	4.952	15.515	25.324	23.646



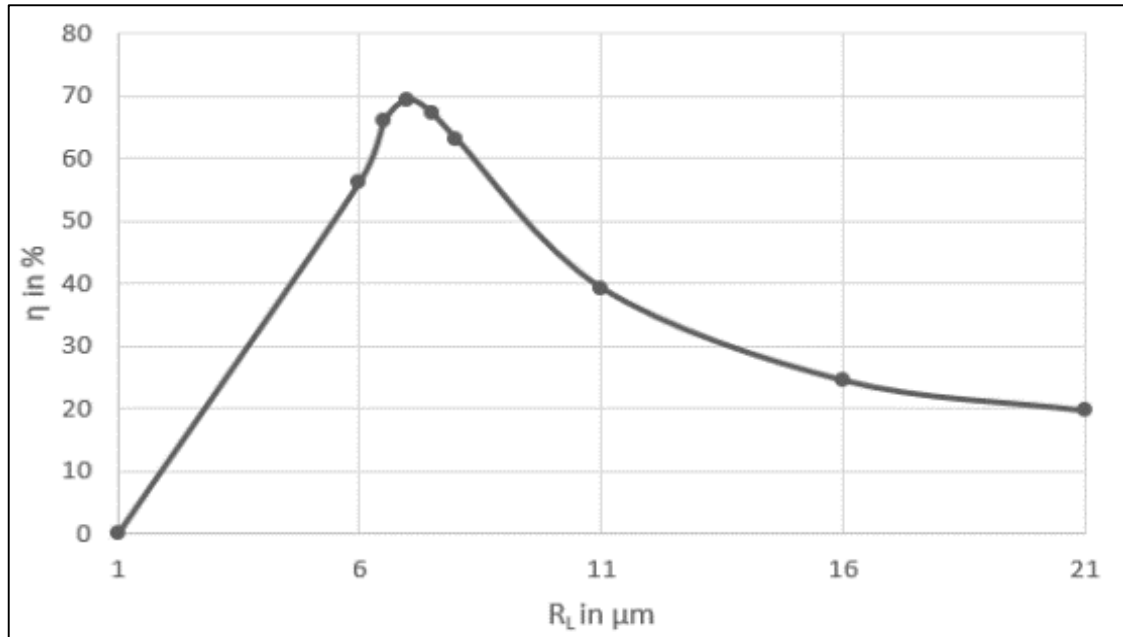


**Fig. 4.4.1a: Maximum coupling efficiency ( $\eta$ ) vs radius of the fiber ( $r$ ) for RI profile exponent  $g = 10$  having  $V$  value 1.924 ( $w_f = 4.858 \mu\text{m}$ ) and excitation wavelength  $1.5 \mu\text{m}$**

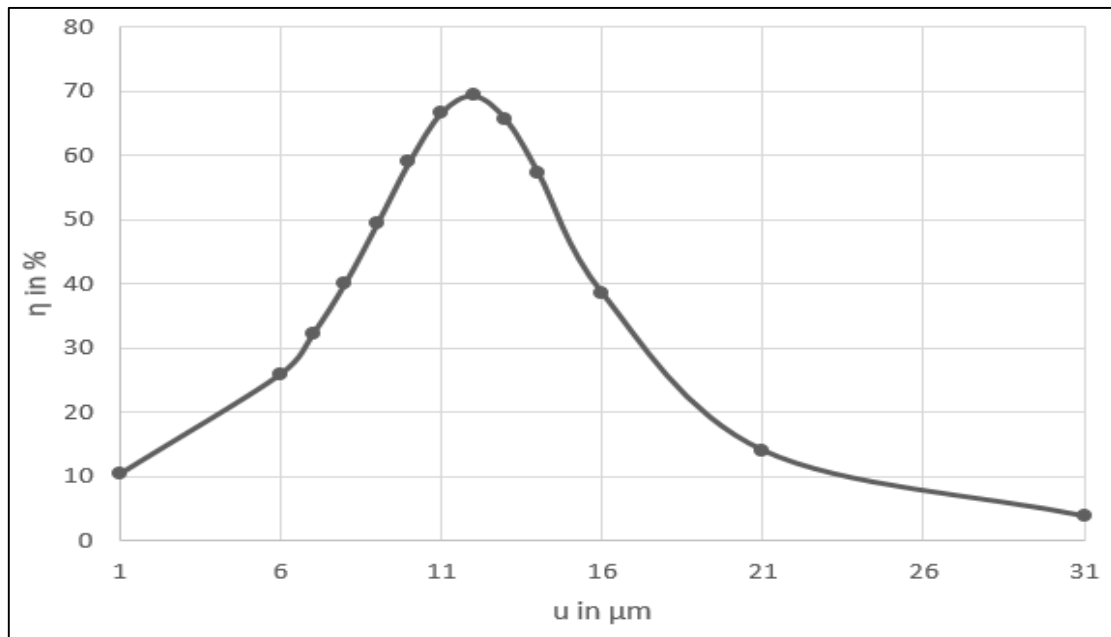


**Fig. 4.4.1b: Maximum coupling efficiency ( $\eta$ ) vs distance of the laser from the tip of cylindrical lens ( $u$ ) of the fiber for RI profile exponent  $g = 10$  having  $V$  value 1.924 ( $w_f = 4.858 \mu\text{m}$ ) and excitation wavelength  $1.5 \mu\text{m}$**

**Table 4.4.2**

**Values of coupling efficiencies for the RI profile exponent  $g = 20$ ,  $V$  value 2.124, excited by wavelength  $1.5 \mu\text{m}$  with  $w_r = 4.642 \mu\text{m}$ ,  $w_{1x} = 0.843 \mu\text{m}$  and  $w_{1y} = 0.857 \mu\text{m}$**

u	$R_L = 1$	$R_L = 6$	$R_L = 6.5$	$R_L = 7$	$R_L = 7.5$	$R_L = 11$	$R_L = 16$	$R_L = 21$
1	0.501	10.491	11.096	11.643	12.026	12.940	12.702	12.542
6	0.079	30.899	29.210	28.665	27.145	21.547	17.628	15.986
10	0.023	66.517	63.873	61.396	55.272	33.307	22.863	19.190
11	0.018	65.411	68.322	67.929	62.709	36.927	24.313	20.018
12	0.014	57.548	66.373	69.502	67.490	40.653	25.788	20.841
13	0.012	46.947	59.014	65.410	68.009	44.292	27.263	21.647
14	0.010	36.957	49.327	57.401	64.073	47.578	28.704	22.427
16	0.007	22.687	31.978	39.390	48.870	51.861	31.325	23.851
21	0.004	8.422	11.892	14.952	19.847	43.450	32.353	25.995
31	0.001	2.465	3.354	4.126	5.363	15.367	23.444	22.090

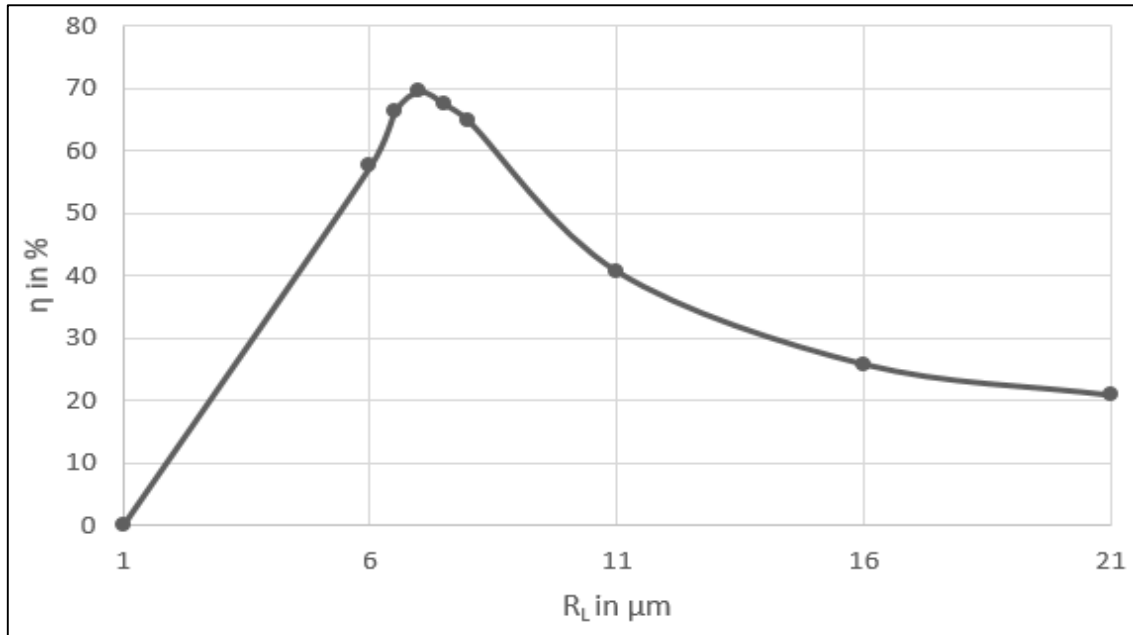


**Fig. 4.4.2a: Maximum coupling efficiency ( $\eta$ ) vs radius of the fiber ( $r$ ) for RI profile exponent  $g = 10$  having  $V$  value 2.004 ( $w_f = 4.642 \mu\text{m}$ ) and excitation wavelength  $1.5 \mu\text{m}$**

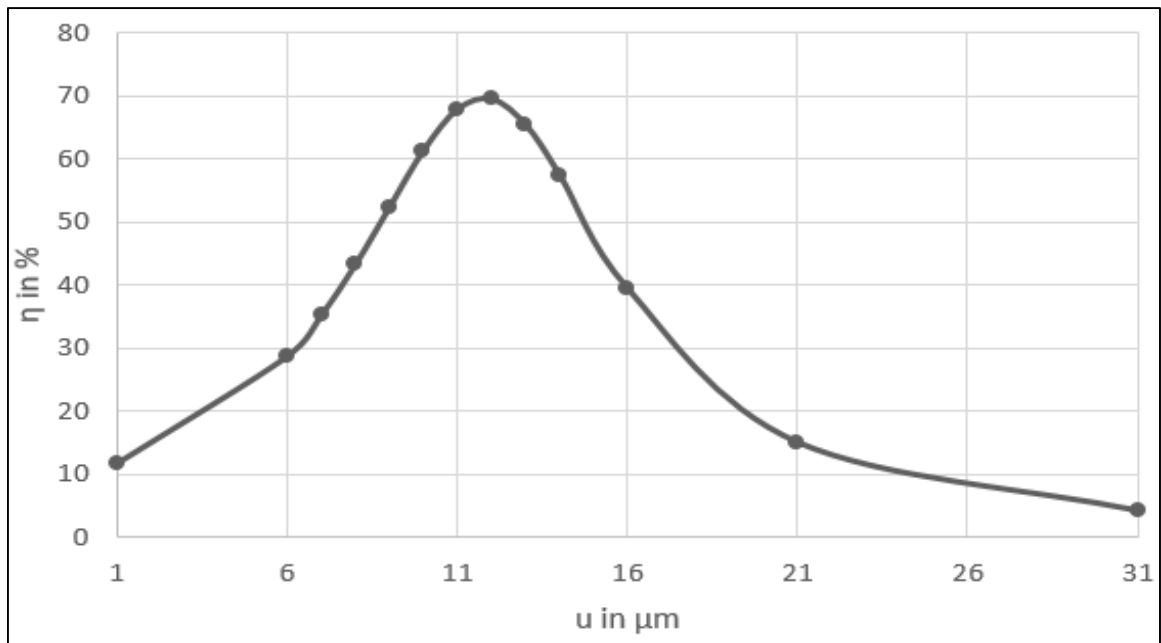


**Fig. 4.4.2b: Maximum coupling efficiency ( $\eta$ ) vs distance of the laser from the tip of cylindrical lens ( $u$ ) of the fiber for RI profile exponent  $g = 10$  having  $V$  value 2.004 ( $w_f = 4.642 \mu\text{m}$ ) and excitation wavelength  $1.5 \mu\text{m}$**

**Table 4.4.3**

**Values of coupling efficiencies for the RI profile exponent  $g = 20$ ,  $V$  value 2.500, excited by wavelength  $1.5 \mu\text{m}$  with  $w_f = 3.868 \mu\text{m}$ ,  $w_{1x} = 0.843 \mu\text{m}$  and  $w_{1y} = 0.857 \mu\text{m}$**

u	$R_L = 1$	$R_L = 5.5$	$R_L = 6$	$R_L = 6.5$	$R_L = 7$	$R_L = 11$	$R_L = 16$	$R_L = 21$
1	1.009	15.436	16.826	17.384	17.536	18.180	17.729	17.512
6	0.164	44.447	43.991	41.277	34.390	28.694	23.657	21.586
8	0.080	62.502	61.719	56.895	44.548	34.022	26.146	23.098
9	0.061	66.759	68.102	63.782	49.737	36.736	27.334	23.780
10	0.047	64.746	69.787	67.879	54.307	39.337	28.447	24.396
11	0.038	57.485	66.056	67.858	57.568	41.677	29.452	24.929
12	0.031	48.005	58.438	63.726	58.903	43.596	360.314	25.370
16	0.016	20.238	27.288	34.463	45.672	44.583	31.800	26.003
21	0.008	8.439	11.461	14.917	23.446	33.159	28.779	24.178
31	0.003	2.720	3.626	4.669	7.526	13.607	17.013	16.437

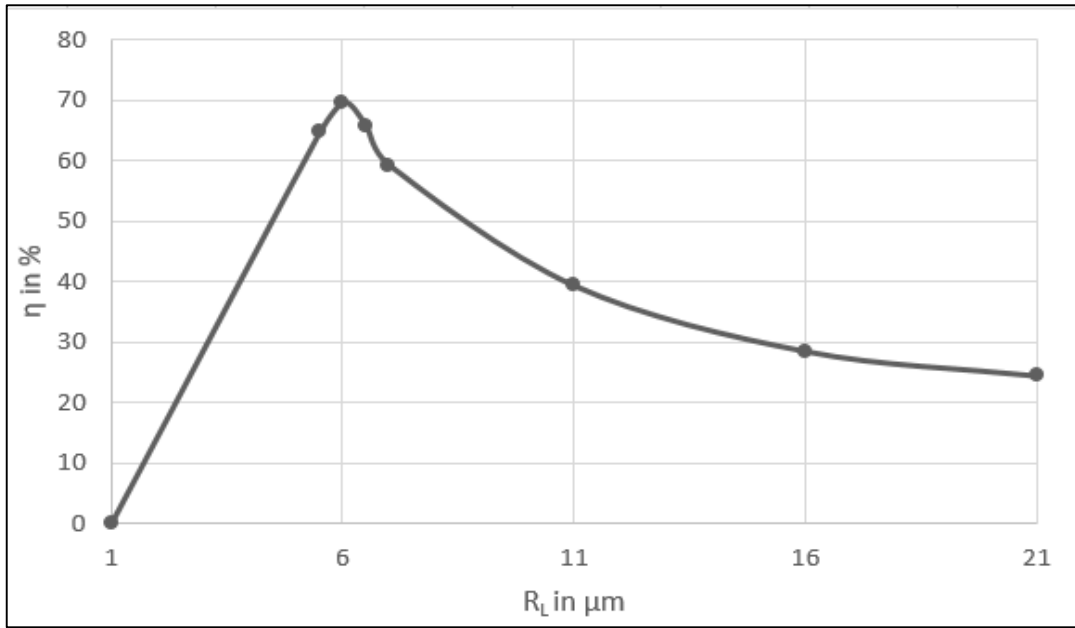


**Fig. 4.4.3a: Maximum coupling efficiency ( $\eta$ ) vs radius of the fiber ( $r$ ) for RI profile exponent  $g = 20$  having  $V$  value 2.500 ( $w_f = 3.868 \mu\text{m}$ ) and excitation wavelength  $1.5 \mu\text{m}$**

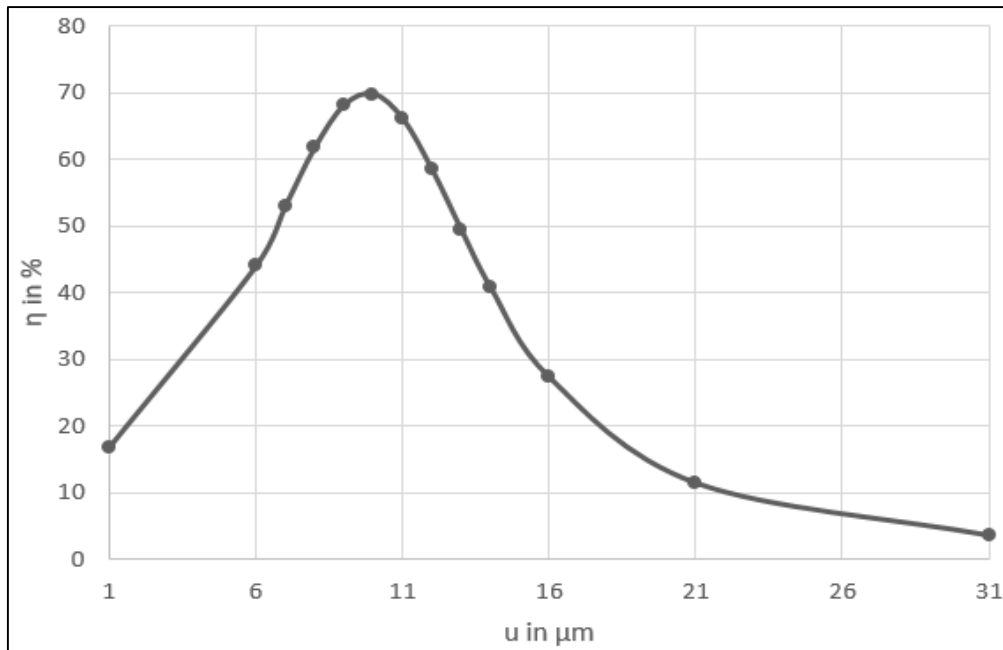


**Fig. 4.4.3b: Maximum coupling efficiency ( $\eta$ ) vs distance of the laser from the tip of cylindrical lens ( $u$ ) of the fiber for RI profile exponent  $g = 20$  having  $V$  value 2.500 ( $w_f = 3.868 \mu\text{m}$ ) and excitation wavelength  $1.5 \mu\text{m}$**

**Table 4.5.1**

**Values of coupling efficiencies for the RI profile exponent  $g = 4$ ,  $V$  value 1.924, excited by wavelength  $1.3 \mu\text{m}$  with  $w_f = 5.008 \mu\text{m}$ ,  $w_{1x} = 1.081 \mu\text{m}$  and  $w_{1y} = 1.161 \mu\text{m}$**

u	$R_L = 1$	$R_L = 6$	$R_L = 9$	$R_L = 9.5$	$R_L = 10$	$R_L = 11$	$R_L = 16$	$R_L = 21$
1	0.201	13.209	17.430	17.722	17.915	18.185	18.204	18.735
6	0.076	33.714	32.123	31.559	30.837	29.731	25.181	27.435
11	0.021	62.545	62.872	59.694	56.228	51.099	35.376	35.466
13	0.015	51.051	77.596	74.011	69.626	62.606	40.427	38.706
14	0.013	42.865	83.080	80.148	75.913	68.451	43.115	40.307
15	0.011	35.260	86.019	84.510	81.096	73.884	45.870	41.876
16	0.009	28.831	85.813	86.357	84.482	78.430	48.646	43.396
17	0.008	23.641	82.504	85.343	85.540	81.595	51.382	44.846
21	0.005	11.673	54.410	61.827	68.584	75.897	60.335	49.514
31	0.002	3.514	15.452	18.306	21.697	27.971	50.522	47.911

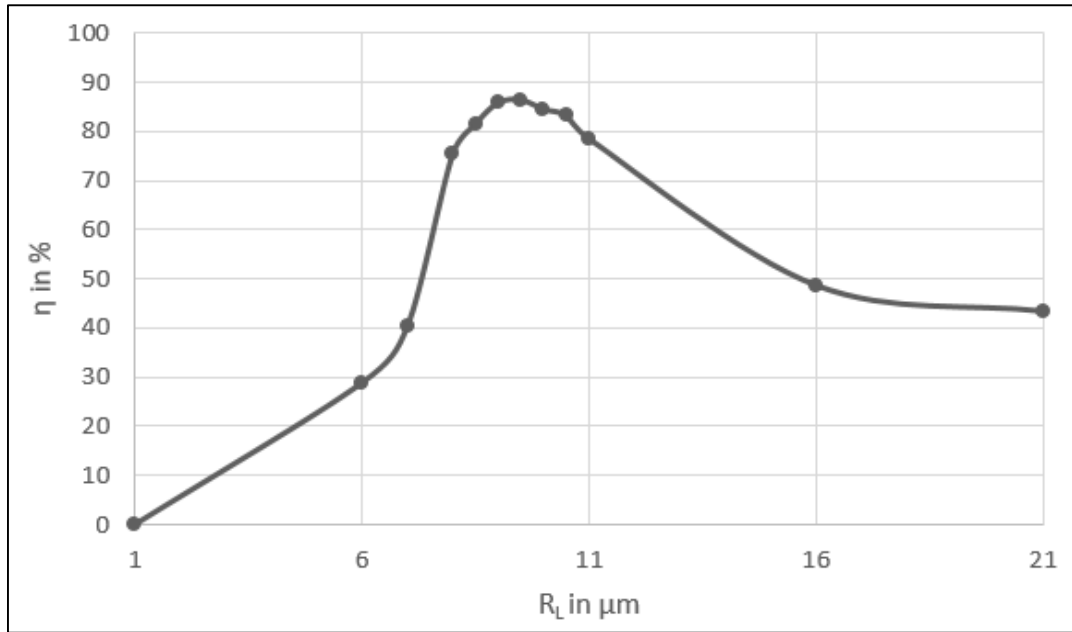


**Fig. 4.5.1a: Maximum coupling efficiency ( $\eta$ ) vs radius of the fiber ( $r$ ) for RI profile exponent  $g = 4$  having  $V$  value 1.924 ( $w_f = 5.008 \mu\text{m}$ ) and excitation wavelength  $1.3 \mu\text{m}$**

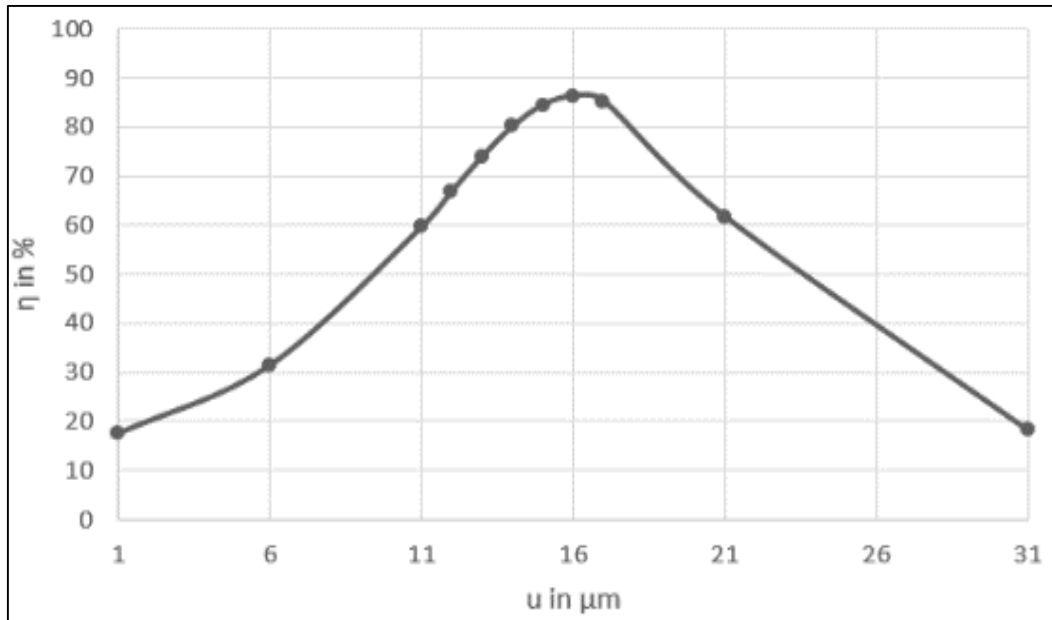


**Fig. 4.5.1b: Maximum coupling efficiency ( $\eta$ ) vs distance of the laser from the tip of cylindrical lens ( $u$ ) of the fiber for RI profile exponent  $g = 4$  having  $V$  value 1.924 ( $w_f = 5.008 \mu\text{m}$ ) and excitation wavelength  $1.3 \mu\text{m}$**

**Table 4.5.2**

**Values of coupling efficiencies for the RI profile exponent  $g = 4$ ,  $V$  value 2.405, excited by wavelength  $1.3 \mu\text{m}$  with  $w_f = 3.831 \mu\text{m}$ ,  $w_{1x} = 1.081 \mu\text{m}$  and  $w_{1y} = 1.161 \mu\text{m}$**

u	$R_L = 1$	$R_L = 6$	$R_L = 6.5$	$R_L = 7$	$R_L = 7.5$	$R_L = 11$	$R_L = 16$	$R_L = 21$
1	0.638	26.250	27.623	28.505	29.130	30.169	29.934	29.763
6	0.284	60.124	60.213	60.133	58.729	50.549	44.078	41.089
11	0.084	80.549	85.701	87.527	86.749	69.545	54.416	47.794
12	0.069	75.843	83.276	86.510	87.400	72.055	55.815	48.597
13	0.058	69.111	78.320	82.889	85.668	73.793	56.915	49.200
14	0.050	61.491	71.720	77.307	81.849	74.657	57.668	49.597
16	0.037	46.808	57.053	63.431	70.254	73.627	58.180	49.757
21	0.021	23.323	29.754	34.352	40.598	59.131	53.622	46.742
31	0.009	8.117	10.415	12.129	14.679	28.075	34.245	33.296



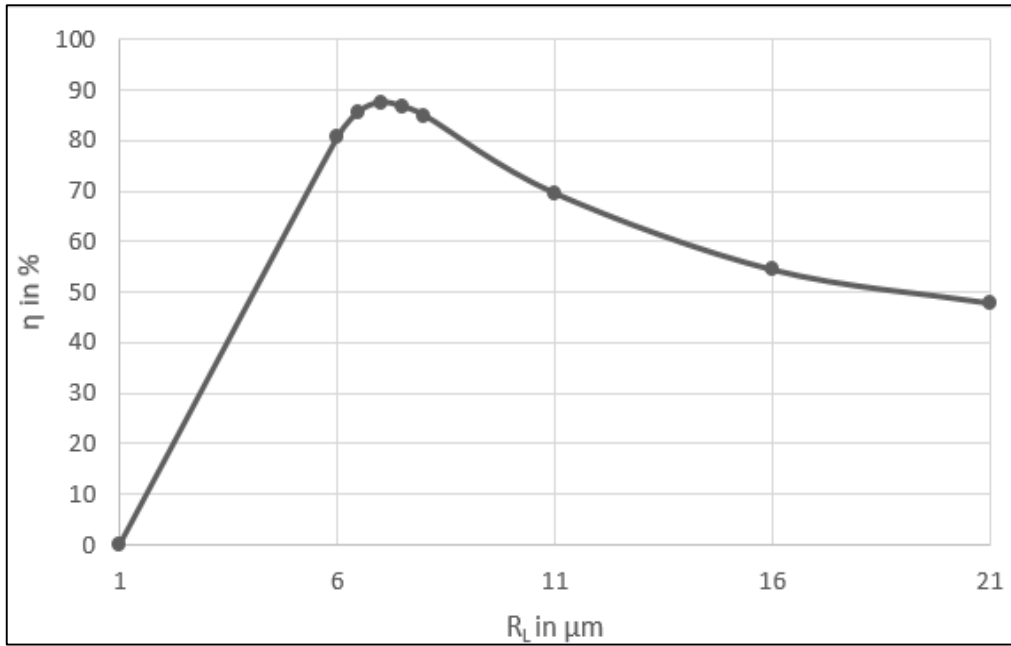


**Fig. 4.5.2a: Maximum coupling efficiency ( $\eta$ ) vs radius of the fiber ( $r$ ) for RI profile exponent  $g = 4$  having  $V$  value 2.405 ( $w_f = 3.831 \mu\text{m}$ ) and excitation wavelength  $1.3 \mu\text{m}$**

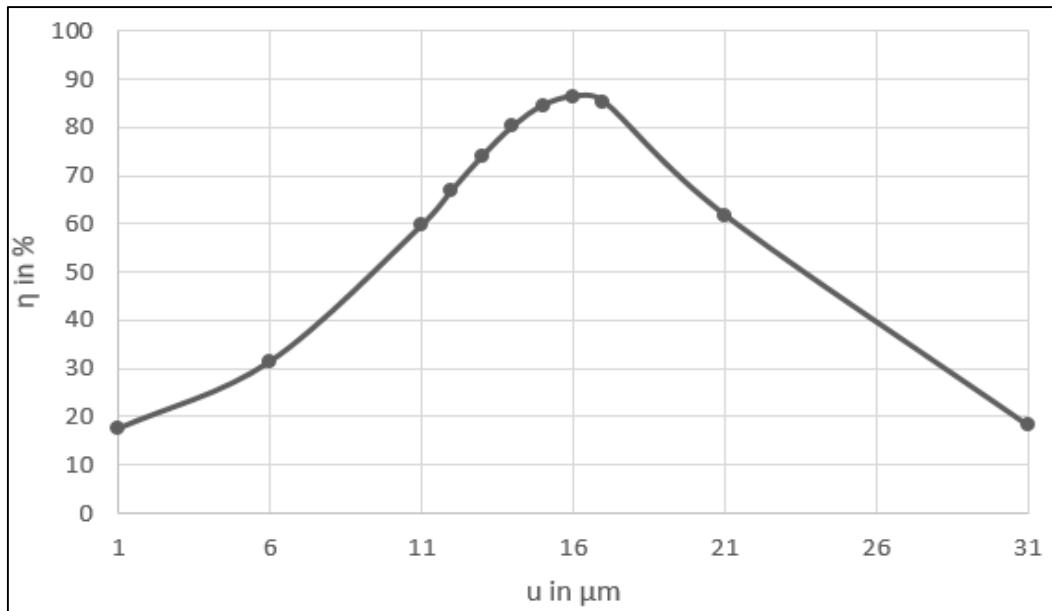


**Fig. 4.5.2b: Maximum coupling efficiency ( $\eta$ ) vs distance of the laser from the tip of cylindrical lens ( $u$ ) of the fiber for RI profile exponent  $g = 4$  having  $V$  value 2.405 ( $w_f = 3.831 \mu\text{m}$ ) and excitation wavelength  $1.3 \mu\text{m}$**

**Table 4.5.3**

**Values of coupling efficiencies for the RI profile exponent  $g = 4$ ,  $V$  value 3.000, excited by wavelength  $1.3 \mu\text{m}$  with  $w_f = 3.284 \mu\text{m}$ ,  $w_{1x} = 1.081 \mu\text{m}$  and  $w_{1y} = 1.161 \mu\text{m}$**

u	$R_L = 1$	$R_L = 5$	$R_L = 5.5$	$R_L = 6$	$R_L = 6.5$	$R_L = 11$	$R_L = 16$	$R_L = 21$
1	1.137	33.030	36.337	36.415	37.352	38.573	38.248	38.080
6	0.512	72.660	76.621	73.926	72.718	59.883	53.006	49.835
7	0.385	78.562	83.496	80.688	79.273	63.335	54.922	51.087
8	0.296	81.186	87.817	85.533	84.382	66.296	56.462	52.008
9	0.233	79.973	88.797	87.723	87.417	68.659	57.614	52.608
10	0.186	75.338	86.315	86.926	87.974	70.327	58.366	52.900
11	0.152	68.423	80.976	83.362	86.023	71.229	58.713	52.893
16	0.068	33.656	44.255	49.754	56.478	64.603	54.873	49.058
21	0.038	17.066	23.060	26.717	31.650	48.389	45.260	41.95
31	0.016	6.351	8.610	10.049	12.121	23.790	26.570	26.071

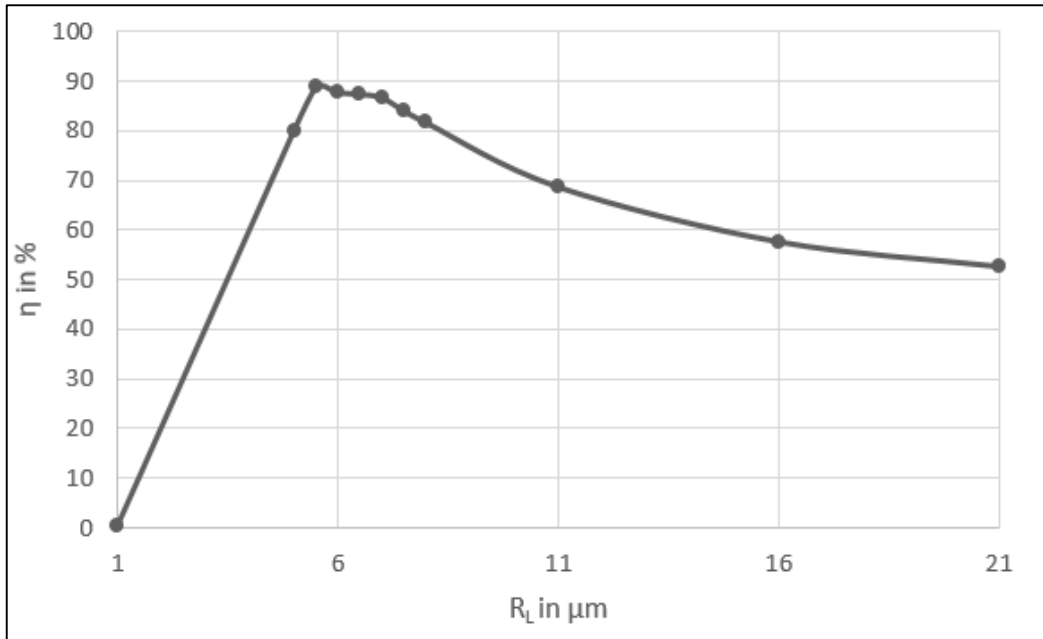


**Fig. 4.5.3a: Maximum coupling efficiency ( $\eta$ ) vs radius of the fiber ( $r$ ) for RI profile exponent  $g = 4$  having  $V$  value 3.000 ( $w_f = 3.284 \mu\text{m}$ ) and excitation wavelength  $1.3 \mu\text{m}$**

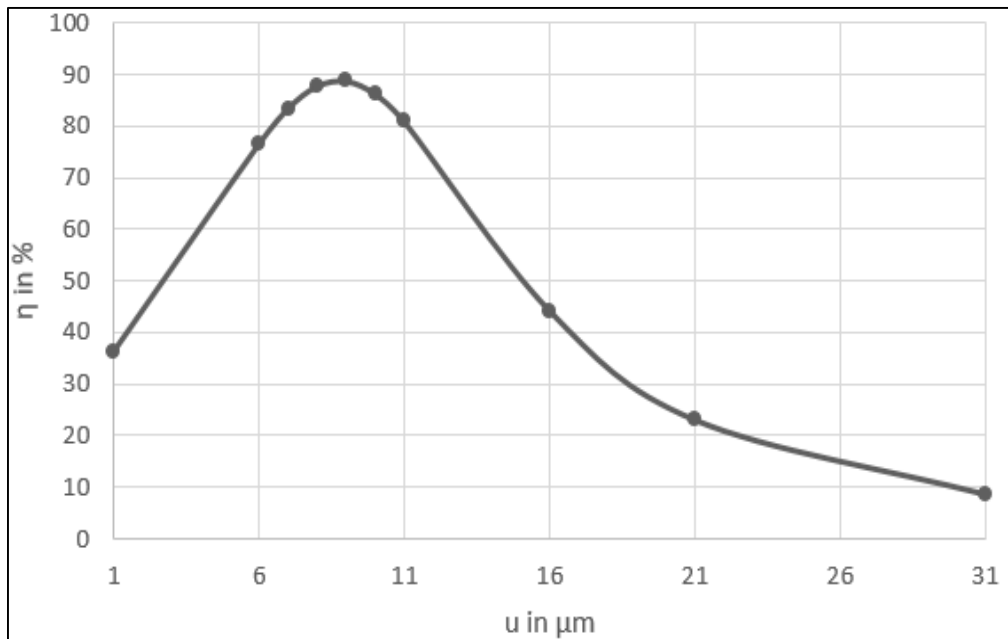


**Fig. 4.5.3b: Maximum coupling efficiency ( $\eta$ ) vs distance of the laser from the tip of cylindrical lens ( $u$ ) of the fiber for RI profile exponent  $g = 4$  having  $V$  value 3.000 ( $w_f = 3.284 \mu\text{m}$ ) and excitation wavelength  $1.3 \mu\text{m}$**

**Table 4.6.1**

**Values of coupling efficiencies for the RI profile exponent  $g = 8$ ,  $V$  value 1.924, excited by wavelength  $1.3 \mu\text{m}$  with  $w_f = 4.714 \mu\text{m}$ ,  $w_{1x} = 1.081 \mu\text{m}$  and  $w_{1y} = 1.161 \mu\text{m}$**

u	$R_L = 1$	$R_L = 6$	$R_L = 8$	$R_L = 8.5$	$R_L = 9$	$R_L = 11$	$R_L = 16$	$R_L = 21$
1	0.284	15.775	19.373	19.874	20.250	20.941	20.988	20.863
6	0.125	40.965	41.515	41.408	40.424	37.758	32.693	30.233
11	0.036	68.187	76.549	75.363	71.548	60.940	44.963	38.361
12	0.030	64.847	81.960	81.250	77.602	65.946	47.4849	39.910
13	0.025	58.701	85.084	85.332	82.519	70.699	49.970	41.415
14	0.021	51.282	85.370	86.977	85.708	74.929	52.375	42.861
16	0.016	37.095	77.858	82.377	85.460	80.661	56.736	45.506
21	0.009	16.608	44.229	50.079	58.335	72.904	62.385	49.773
31	0.004	5.293	13.984	16.146	19.754	31.407	46.707	44.505

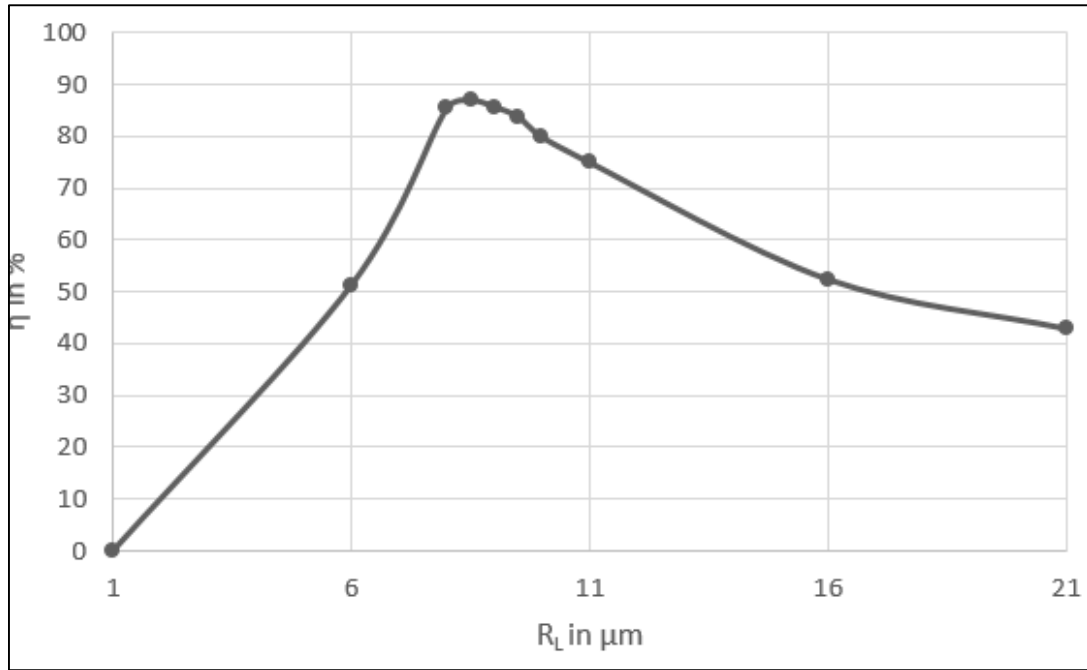


**Fig. 4.6.1a: Maximum coupling efficiency ( $\eta$ ) vs radius of the fiber ( $r$ ) for RI profile exponent  $g = 8$  having  $V$  value 1.924 ( $w_f = 4.714 \mu\text{m}$ ) and excitation wavelength  $1.3 \mu\text{m}$**

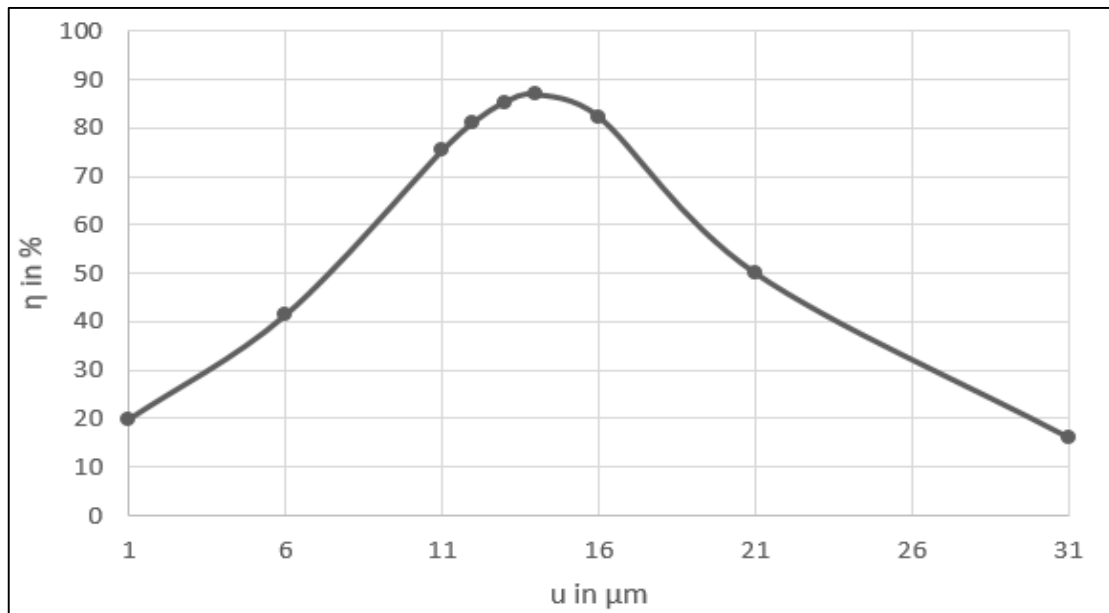


**Fig. 4.6.1b: Maximum coupling efficiency ( $\eta$ ) vs distance of the laser from the tip of cylindrical lens ( $u$ ) of the fiber for RI profile exponent  $g = 8$  having  $V$  value 1.924 ( $w_f = 4.714 \mu\text{m}$ ) and excitation wavelength  $1.3 \mu\text{m}$**

**Table 4.6.2**

**Values of coupling efficiencies for the RI profile exponent  $g = 8$ ,  $V$  value 2.164, excited by wavelength  $1.3 \mu\text{m}$  with  $w_f = 2.164 \mu\text{m}$ ,  $w_{1x} = 1.081 \mu\text{m}$  and  $w_{1y} = 1.161 \mu\text{m}$**

u	$R_L = 1$	$R_L = 7$	$R_L = 7.5$	$R_L = 8$	$R_L = 8.5$	$R_L = 11$	$R_L = 16$	$R_L = 21$
1	0.469	24.290	25.009	25.523	25.506	26.482	26.326	26.173
6	0.208	53.606	52.584	51.680	50.334	45.749	39.695	36.884
11	0.061	85.412	84.892	83.181	80.416	67.108	51.251	44.504
12	0.051	85.553	86.958	86.291	83.952	70.697	53.190	45.681
13	0.043	82.642	86.325	87.142	85.582	73.651	54.920	46.715
14	0.036	77.292	83.137	85.633	85.106	75.787	56.397	47.592
16	0.027	62.984	71.516	76.826	78.457	77.086	58.441	48.821
21	0.015	32.774	39.991	46.016	49.503	64.463	57.332	48.526
31	0.006	11.021	13.685	16.153	17.818	29.752	38.575	37.284

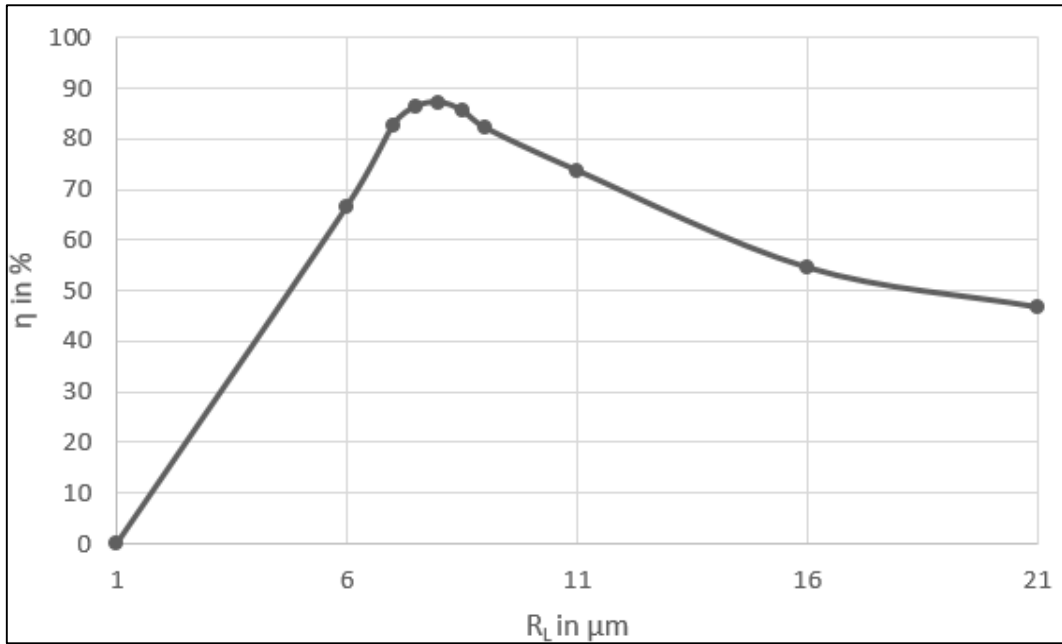


**Fig. 4.6.2a: Maximum coupling efficiency ( $\eta$ ) vs radius of the fiber ( $r$ ) for RI profile exponent  $g = 8$  having  $V$  value 2.164 ( $w_f = 4.136 \mu\text{m}$ ) and excitation wavelength  $1.3 \mu\text{m}$**

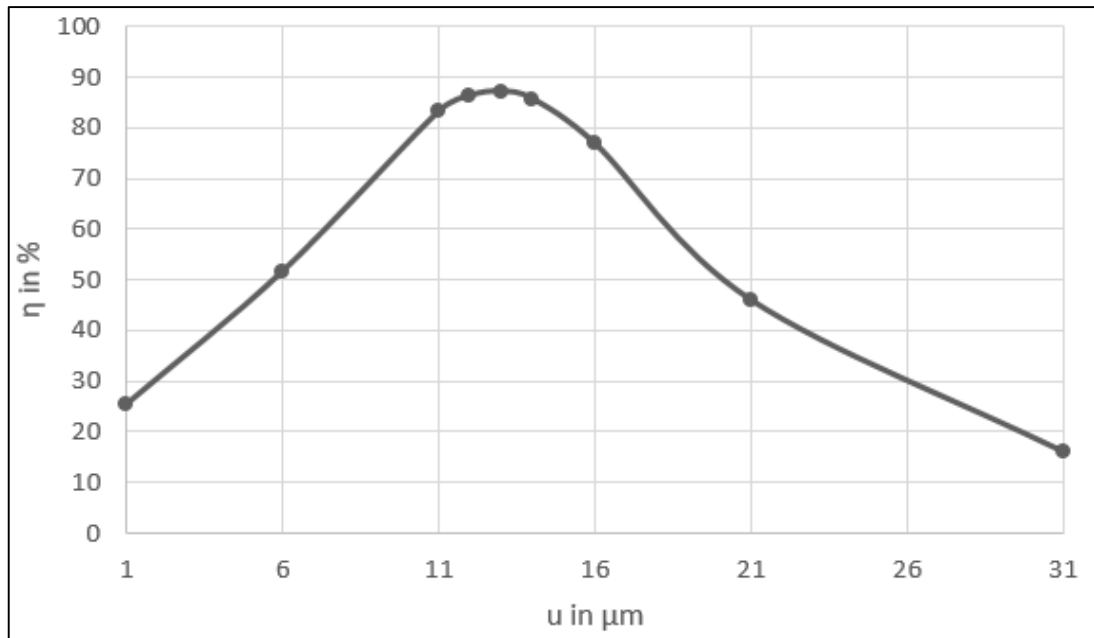


**Fig. 4.6.2b: Maximum coupling efficiency ( $\eta$ ) vs distance of the laser from the tip of cylindrical lens ( $u$ ) of the fiber for RI profile exponent  $g = 8$  having  $V$  value 2.164 ( $w_f = 4.136 \mu\text{m}$ ) and excitation wavelength  $1.3 \mu\text{m}$**

**Table 4.6.3**

**Values of coupling efficiencies for the RI profile exponent  $g = 8$ ,  $V$  value 2.700, excited by wavelength  $1.3 \mu\text{m}$  with  $w_f = 5.008 \mu\text{m}$ ,  $w_{1x} = 1.081 \mu\text{m}$  and  $w_{1y} = 1.161 \mu\text{m}$**

u	$R_L = 1$	$R_L = 6$	$R_L = 6.5$	$R_L = 7$	$R_L = 7.5$	$R_L = 11$	$R_L = 16$	$R_L = 21$
1	0.871	31.632	32.691	33.480	33.938	34.511	34.213	34.058
6	0.391	68.102	67.254	66.831	64.974	55.642	48.874	45.785
10	0.142	85.901	87.470	87.747	85.607	68.975	56.066	50.332
11	0.116	83.199	86.693	87.971	86.877	70.961	57.086	50.846
12	0.096	77.934	83.323	85.736	86.034	72.184	57.752	51.112
13	0.081	71.061	77.960	81.430	83.230	72.151	58.050	51.132
16	0.051	49.174	57.382	62.402	67.412	68.985	56.788	49.806
21	0.029	25.543	31.178	35.098	40.115	53.261	49.171	44.096
31	0.012	9.263	11.457	13.064	15.354	25.852	29.915	29.259



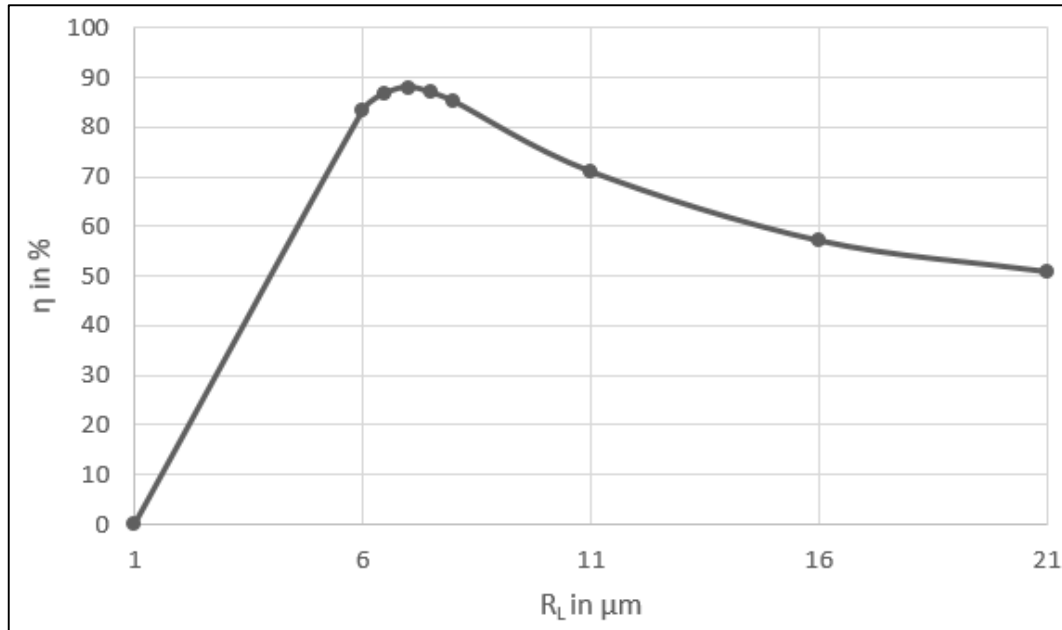


**Fig. 4.6.3a: Maximum coupling efficiency ( $\eta$ ) vs radius of the fiber ( $r$ ) for RI profile exponent  $g = 8$  having  $V$  value 2.700 ( $w_f = 3.526 \mu\text{m}$ ) and excitation wavelength  $1.3 \mu\text{m}$**

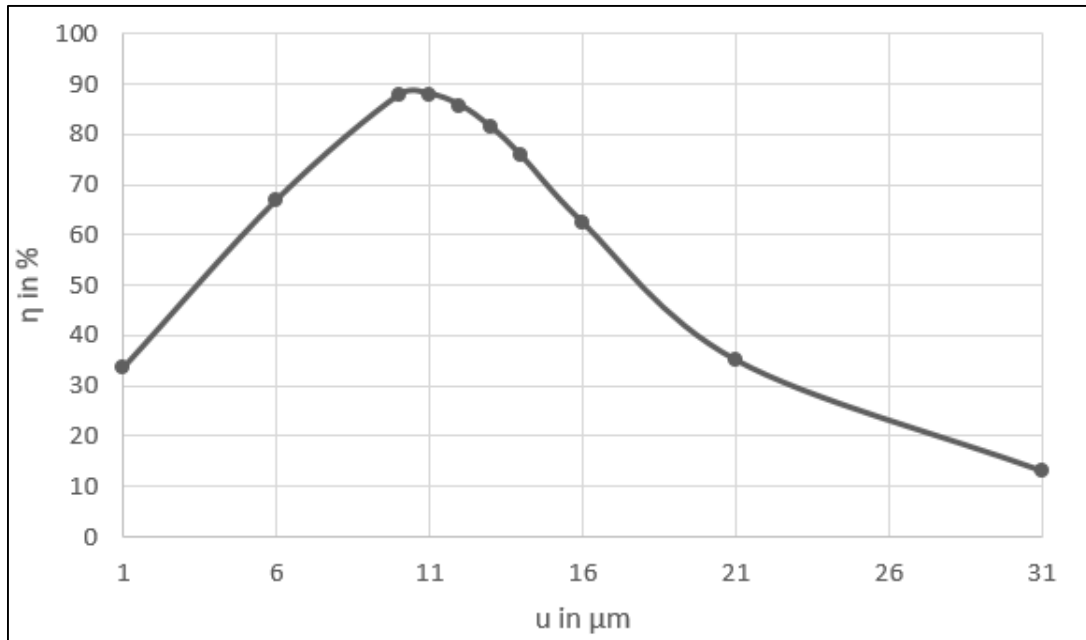


**Fig. 4.6.3b: Maximum coupling efficiency ( $\eta$ ) vs distance of the laser from the tip of cylindrical lens ( $u$ ) of the fiber for RI profile exponent  $g = 8$  having  $V$  value 2.7000 ( $w_f = 3.526 \mu\text{m}$ ) and excitation wavelength  $1.3 \mu\text{m}$**

**Table 4.7.1**

**Values of coupling efficiencies for the RI profile exponent  $g = 10$ ,  $V$  value 1.924, excited by wavelength  $1.3 \mu\text{m}$  with  $w_f = 4.715 \mu\text{m}$ ,  $w_{1x} = 1.081 \mu\text{m}$  and  $w_{1y} = 1.161 \mu\text{m}$**

u	$R_L = 1$	$R_L = 6$	$R_L = 8$	$R_L = 8.5$	$R_L = 9$	$R_L = 11$	$R_L = 16$	$R_L = 21$
1	0.284	15.770	19.366	19.867	20.242	20.933	20.980	20.855
6	0.125	40.954	41.503	41.396	40.412	37.746	32.682	30.223
11	0.036	68.184	76.543	75.356	71.540	60.930	44.952	38.351
12	0.030	64.845	81.958	81.248	77.598	65.938	47.475	39.901
13	0.025	58.699	85.086	85.333	82.519	70.694	49.961	41.406
14	0.021	51.278	85.375	86.982	85.712	74.927	52.368	42.853
15	0.018	43.838	82.799	85.930	86.741	78.343	54.644	44.224
16	0.016	37.090	77.865	82.386	85.470	80.667	56.732	45.500
21	0.009	16.604	44.228	50.081	58.340	72.919	62.393	49.774
31	0.004	5.291	13.981	16.144	19.752	31.409	46.721	44.517

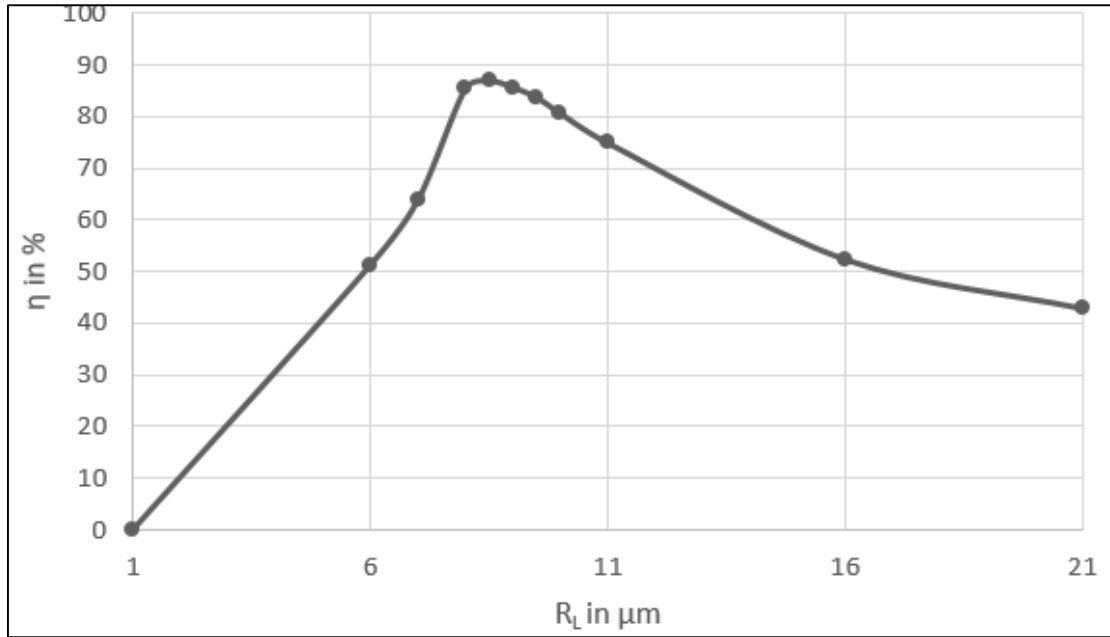


**Fig. 4.7.1a: Maximum coupling efficiency ( $\eta$ ) vs radius of the fiber ( $r$ ) for RI profile exponent  $g = 10$  having  $V$  value 1.924 ( $w_f = 4.715 \mu\text{m}$ ) and excitation wavelength  $1.3 \mu\text{m}$**

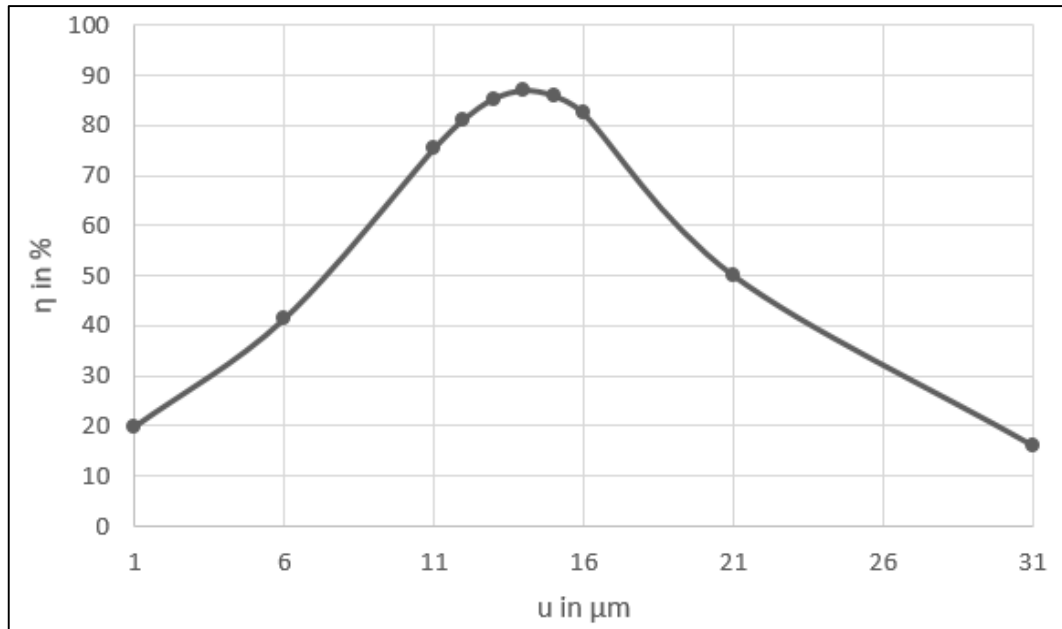


**Fig. 4.7.1b: Maximum coupling efficiency ( $\eta$ ) vs distance of the laser from the tip of cylindrical lens ( $u$ ) of the fiber for RI profile exponent  $g = 10$  having  $V$  value 1.924 ( $w_f = 4.715 \mu\text{m}$ ) and excitation wavelength  $1.3 \mu\text{m}$**

**Table 4.7.2**

**Values of coupling efficiencies for the RI profile exponent  $g = 10$ ,  $V$  value 2.124, excited by wavelength  $1.3 \mu\text{m}$  with  $w_f = 4.230 \mu\text{m}$ ,  $w_{1x} = 1.081 \mu\text{m}$  and  $w_{1y} = 1.161 \mu\text{m}$ .**

u	$R_L = 1$	$R_L = 7$	$R_L = 7.5$	$R_L = 8$	$R_L = 8.5$	$R_L = 11$	$R_L = 16$	$R_L = 21$
1	0.429	23.109	23.855	24.404	24.793	25.461	25.337	25.189
6	0.190	51.626	50.731	49.945	49.431	44.346	38.444	35.689
11	0.068	80.833	79.163	77.041	75.385	61.963	48.028	42.108
12	0.056	84.421	84.005	82.372	80.847	66.211	50.235	43.482
13	0.046	84.897	86.478	85.912	84.868	70.085	52.305	44.747
14	0.039	82.203	86.175	87.162	86.950	73.380	54.194	45.885
16	0.033	76.936	83.189	85.952	86.821	75.890	55.859	46.883
21	0.014	31.139	39.605	45.956	50.464	65.988	58.332	48.910
31	0.006	10.657	13.333	15.851	17.836	30.155	39.910	38.495

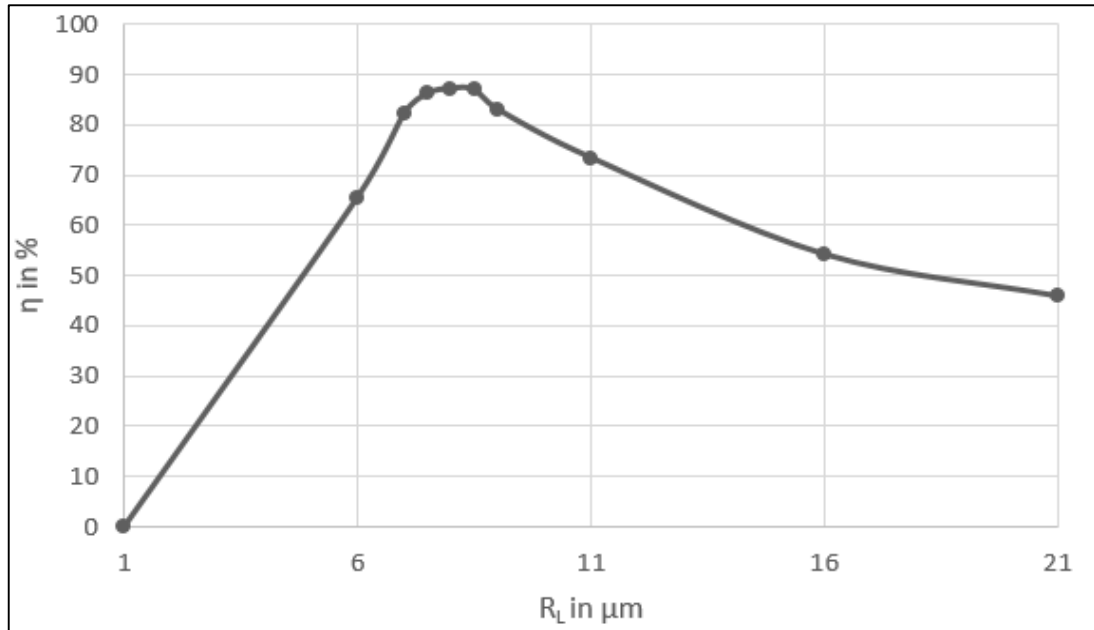


**Fig. 4.7.2a: Maximum coupling efficiency ( $\eta$ ) vs radius of the fiber ( $r$ ) for RI profile exponent  $g = 10$  having  $V$  value 2.124 ( $w_f = 4.230 \mu\text{m}$ ) and excitation wavelength  $1.3 \mu\text{m}$**

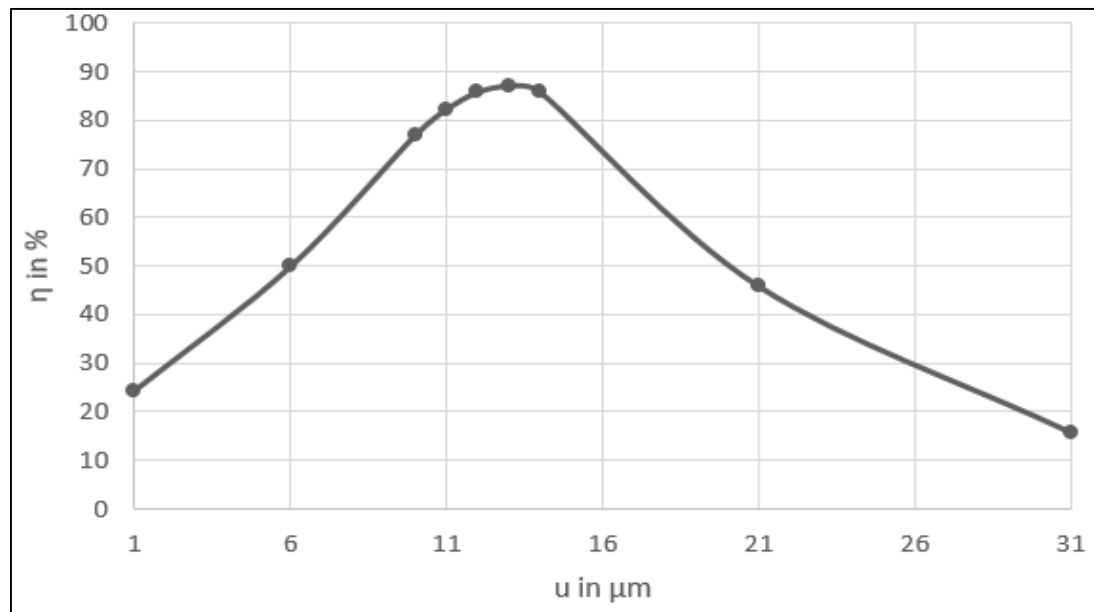


**Fig. 4.7.2b: Maximum coupling efficiency ( $\eta$ ) vs distance of the laser from the tip of cylindrical lens ( $u$ ) of the fiber for RI profile exponent  $g = 10$  having  $V$  value 2.124 ( $w_f = 4.230 \mu\text{m}$ ) and excitation wavelength  $1.3 \mu\text{m}$**

**Table 4.7.3**

**Values of coupling efficiencies for the RI profile exponent  $g = 10$ ,  $V$  value 2.650, excited by wavelength  $1.3 \mu\text{m}$  with  $w_f = 3.596 \mu\text{m}$ ,  $w_{1x} = 1.081 \mu\text{m}$  and  $w_{1y} = 1.161 \mu\text{m}$**

u	$R_L = 1$	$R_L = 6$	$R_L = 6.5$	$R_L = 7$	$R_L = 7.5$	$R_L = 11$	$R_L = 16$	$R_L = 21$
1	0.799	30.370	31.431	32.267	32.783	33.443	33.152	33.002
6	0.358	66.395	65.599	65.301	63.576	47.726	47.726	44.666
9	0.162	84.567	84.623	84.339	81.727	54.434	53.830	48.667
10	.0130	85.375	87.023	87.444	85.381	68.459	55.329	49.542
11	0.106	82.918	86.580	88.044	87.055	70.731	56.517	50.183
12	0.088	77.771	83.429	86.089	86.556	72.265	57.368	50.588
16	0.047	48.840	57.409	62.785	68.233	70.138	57.197	49.887
21	0.026	25.127	30.906	35.019	40.350	54.637	50.235	44.779
31	0.011	9.022	11.227	12.874	15.243	26.401	30.894	30.185

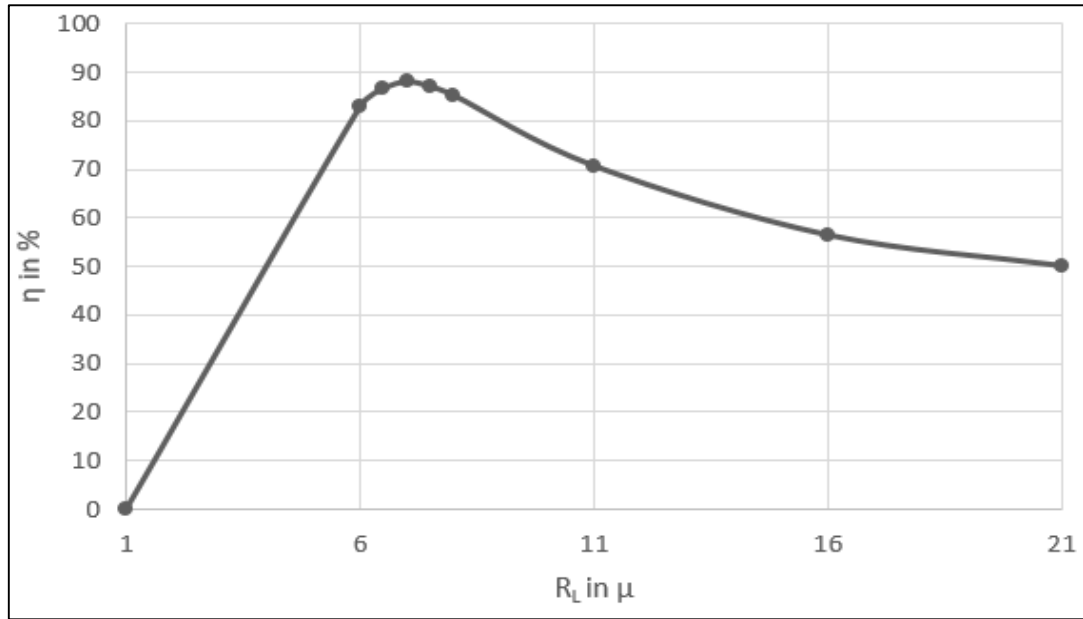


**Fig. 4.7.3a: Maximum coupling efficiency ( $\eta$ ) vs radius of the fiber ( $r$ ) for RI profile exponent  $g = 10$  having  $V$  value 2.650 ( $w_f = 3.596 \mu\text{m}$ ) and excitation wavelength  $1.3 \mu\text{m}$**

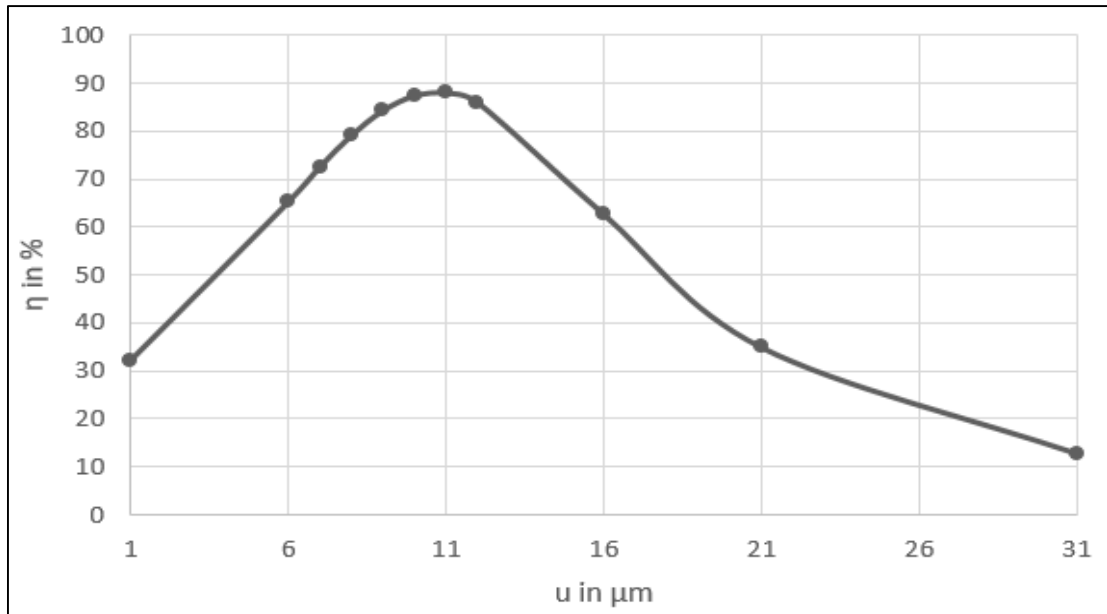


**Fig. 4.7.3b: Maximum coupling efficiency ( $\eta$ ) vs distance of the laser from the tip of cylindrical lens ( $u$ ) of the fiber for RI profile exponent  $g = 20$  having  $V$  value 2.650 ( $w_f = 3.596 \mu\text{m}$ ) and excitation wavelength  $1.3 \mu\text{m}$**

**Table 4.8.1**

**Values of coupling efficiencies for the RI profile exponent  $g = 20$ ,  $V$  value 1.924, excited by wavelength  $1.3 \mu\text{m}$  with  $w_f = 4.858 \mu\text{m}$ ,  $w_{1x} = 1.081 \mu\text{m}$  and  $w_{1y} = 1.161 \mu\text{m}$**

u	$R_L = 1$	$R_L = 6$	$R_L = 9$	$R_L = 9.5$	$R_L = 10$	$R_L = 11$	$R_L = 16$	$R_L = 21$
1	0.253	14.534	19.010	19.307	19.480	19.792	19.878	19.779
6	0.111	38.313	38.332	37.805	37.046	35.987	31.159	28.817
11	0.032	65.667	69.586	66.948	63.825	59.224	43.385	36.917
12	0.027	62.516	76.019	73.216	69.750	64.463	45.979	38.510
13	0.022	56.504	81.427	78.816	75.274	69.550	48.576	40.078
14	0.019	49.202	85.154	83.197	79.965	74.210	51.133	41.609
16	0.014	35.303	85.759	86.395	85.112	80.977	55.927	44.492
21	0.008	15.572	58.366	64.279	69.265	74.618	63.178	49.710
31	0.003	4.911	19.218	22.232	25.608	31.517	48.637	46.200



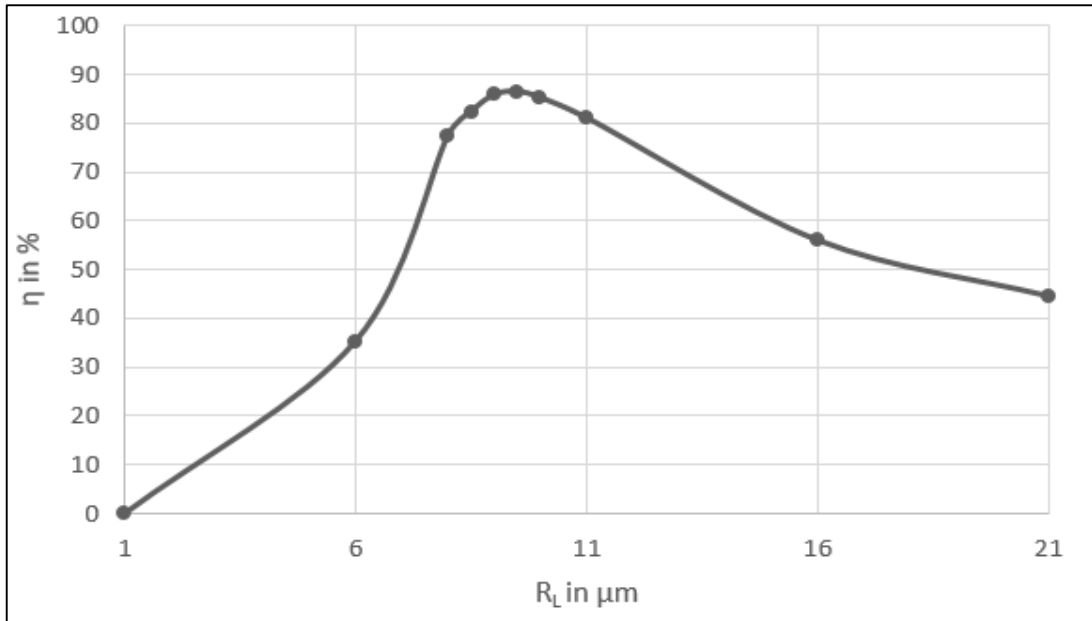


**Fig. 4.8.1a: Maximum coupling efficiency ( $\eta$ ) vs radius of the fiber ( $r$ ) for RI profile exponent  $g = 20$  having  $V$  value 1.924 ( $w_f = 4.858 \mu\text{m}$ ) and excitation wavelength  $1.3 \mu\text{m}$**

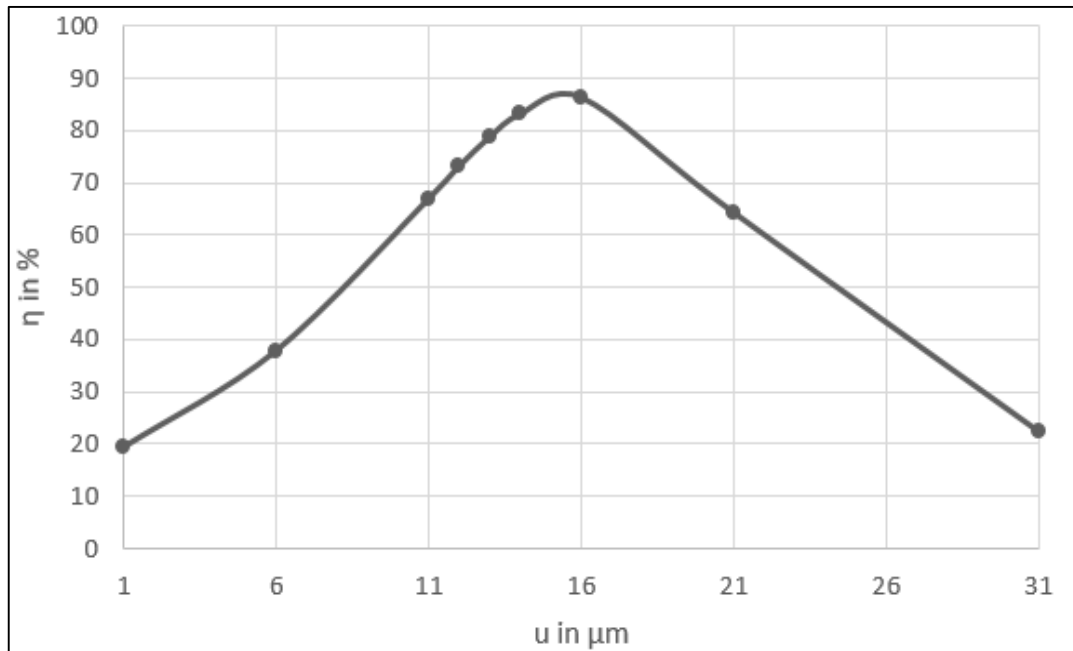


**Fig. 4.8.1b: Maximum coupling efficiency ( $\eta$ ) vs distance of the laser from the tip of cylindrical lens ( $u$ ) of the fiber for RI profile exponent  $g = 20$  having  $V$  value 1.924 ( $w_f = 4.858 \mu\text{m}$ ) and excitation wavelength  $1.3 \mu\text{m}$**

**Table 4.8.2**

**Values of coupling efficiencies for the RI profile exponent  $g = 20$ ,  $V$  value 2.004, excited by wavelength  $1.3 \mu\text{m}$  with  $w_f = 4.642 \mu\text{m}$ ,  $w_{1x} = 1.081 \mu\text{m}$  and  $w_{1y} = 1.161 \mu\text{m}$**

u	$R_L = 1$	$R_L = 7$	$R_L = 8$	$R_L = 8.5$	$R_L = 9$	$R_L = 11$	$R_L = 16$	$R_L = 21$
1	0.301	18.616	20.042	20.534	20.897	21.560	21.565	21.436
6	0.133	43.547	42.691	42.538	41.493	38.702	33.478	30.975
11	0.039	79.002	77.529	76.303	72.468	61.822	45.739	39.099
12	0.032	80.775	82.700	81.953	78.310	66.699	48.214	40.621
13	0.027	78.975	85.568	85.763	82.962	71.271	50.633	42.087
14	0.023	74.087	85.641	87.155	85.870	75.274	52.950	43.483
15	0.020	67.198	82.933	85.916	86.645	78.427	55.115	44.792
16	0.017	59.490	77.960	82.281	85.192	80.477	57.071	45.993
21	0.009	28.950	44.600	50.280	58.226	72.036	61.897	49.754
31	0.004	9.079	14.277	16.428	19.997	31.330	45.707	43.639

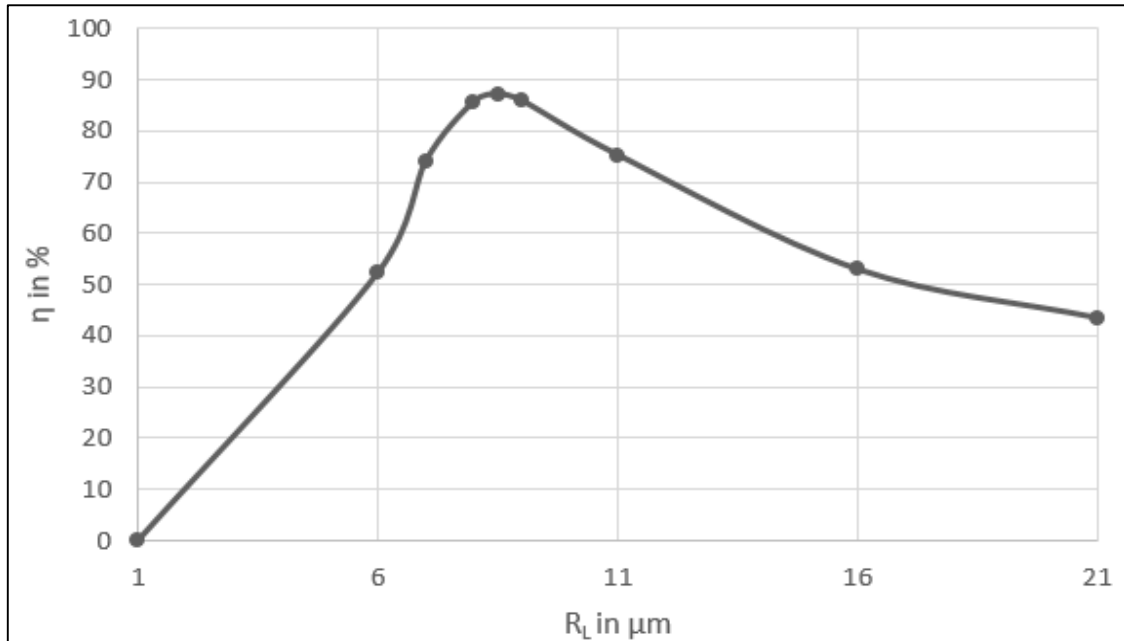


**Fig. 4.8.2a: Maximum coupling efficiency ( $\eta$ ) vs radius of the fiber ( $r$ ) for RI profile exponent  $g = 20$  having  $V$  value 2.004 ( $w_f = 4.645 \mu\text{m}$ ) and excitation wavelength  $1.3 \mu\text{m}$**

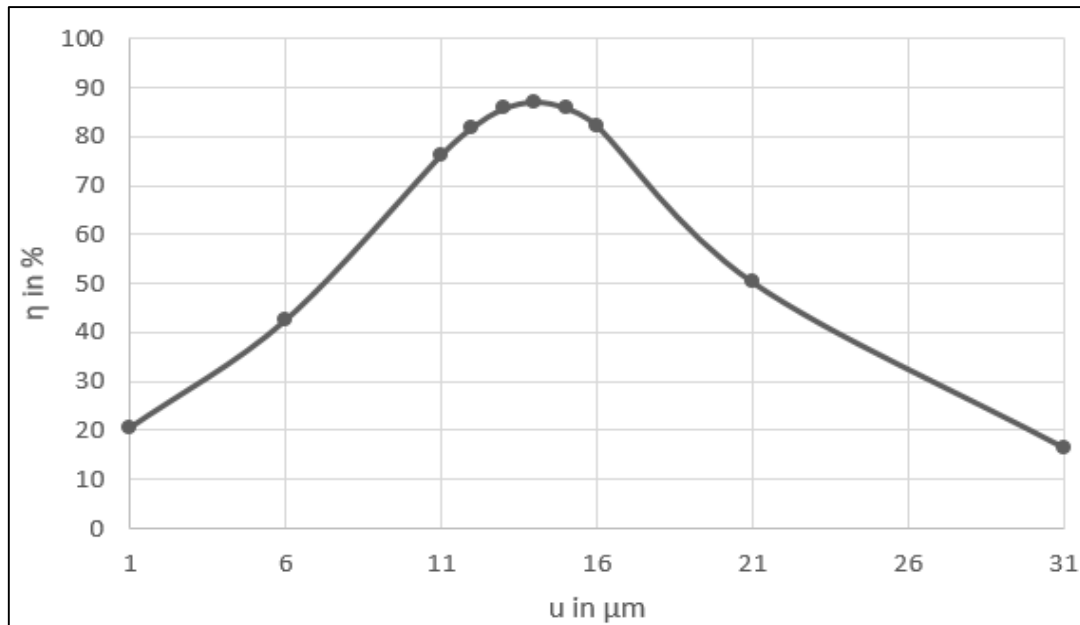


**Fig. 4.8.2b: Maximum coupling efficiency ( $\eta$ ) vs distance of the laser from the tip of cylindrical lens ( $u$ ) of the fiber for RI profile exponent  $g = 20$  having  $V$  value 2.004 ( $w_f = 4.645 \mu\text{m}$ ) and excitation wavelength  $1.3 \mu\text{m}$**

**Table 4.8.3**

**Values of coupling efficiencies for the RI profile exponent  $g = 20$ ,  $V$  value 2.500, excited by wavelength  $1.3 \mu\text{m}$  with  $w_f = 3.868 \mu\text{m}$ ,  $w_{1x} = 1.081 \mu\text{m}$  and  $w_{1y} = 1.161 \mu\text{m}$**

u	$R_L = 1$	$R_L = 6$	$R_L = 7$	$R_L = 7.5$	$R_L = 8$	$R_L = 11$	$R_L = 16$	$R_L = 21$
1	0.603	25.866	27.959	28.606	29.056	29.691	29.428	29.291
6	0.269	59.642	59.334	57.994	56.841	49.952	43.472	40.549
10	0.097	82.298	85.371	83.477	81.210	66.039	52.260	46.359
11	0.079	80.749	87.364	86.639	84.895	69.300	53.987	47.398
12	0.065	76.074	86.489	87.468	86.687	71.952	55.461	48.254
13	0.055	69.312	82.954	85.868	86.373	73.846	56.645	48.918
14	0.047	61.629	77.398	82.122	84.025	74.868	57.510	49.380
16	0.035	46.816	63.459	70.506	74.722	74.113	58.199	49.681
21	0.019	23.212	34.204	40.594	45.692	59.812	54.048	47.000
31	0.008	8.041	12.003	14.578	16.884	28.311	34.731	33.781

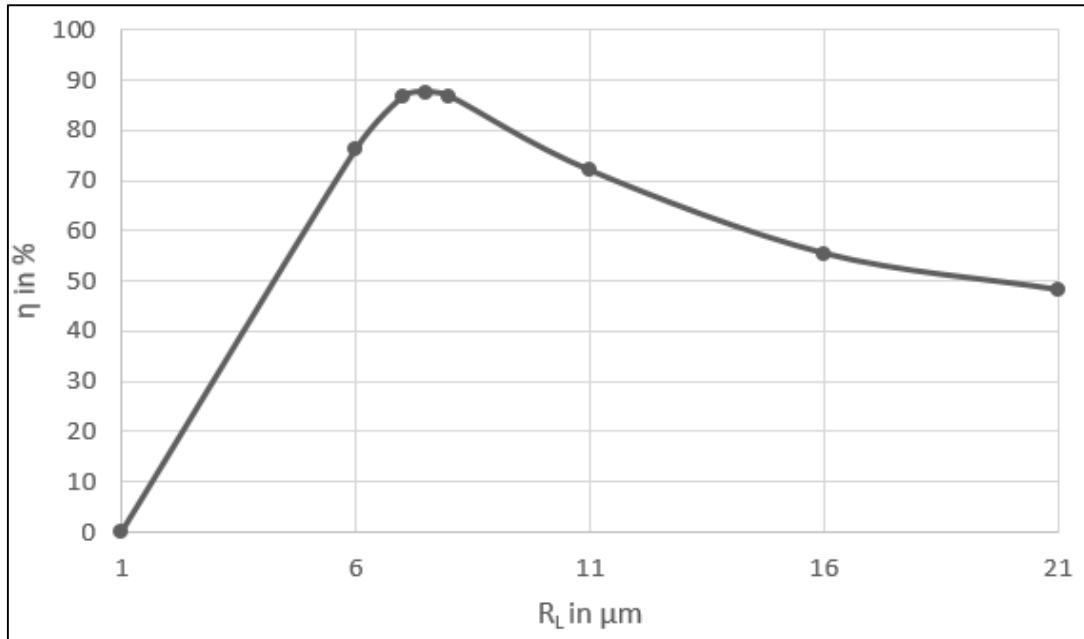


**Fig. 4.8.3a: Maximum coupling efficiency ( $\eta$ ) vs radius of the fiber ( $r$ ) for RI profile exponent  $g = 20$  having  $V$  value 2.500 ( $w_f = 3.868 \mu\text{m}$ ) and excitation wavelength  $1.3 \mu\text{m}$**

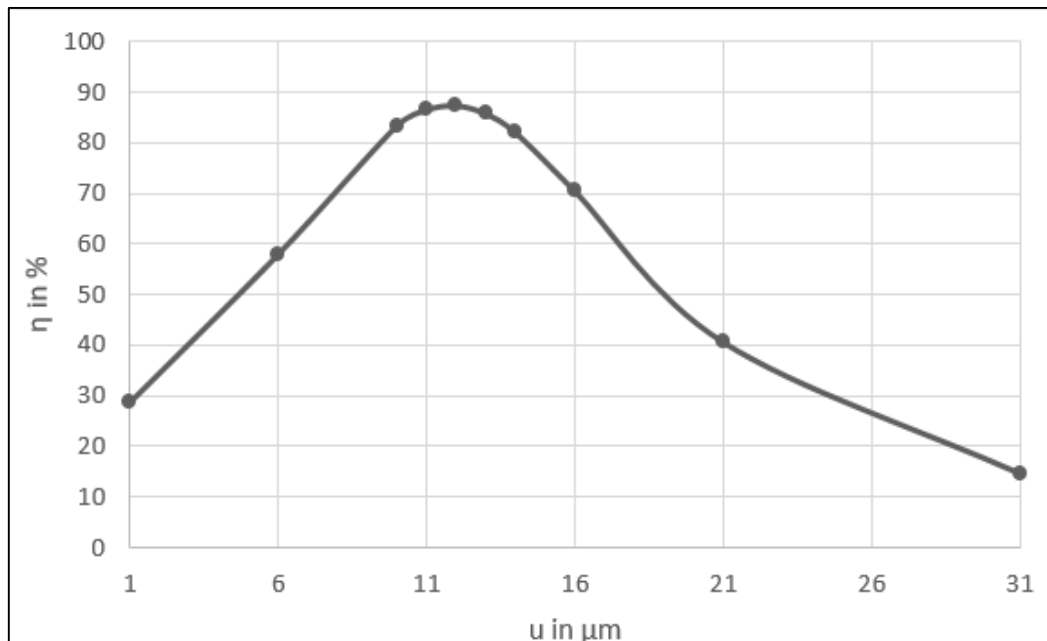


**Fig. 4.8.3b: Maximum coupling efficiency ( $\eta$ ) vs distance of the laser from the tip of cylindrical lens ( $u$ ) of the fiber for RI profile exponent  $g = 20$  having  $V$  value 2.500 ( $w_f = 3.868 \mu\text{m}$ ) and excitation wavelength  $1.3 \mu\text{m}$**

**Table 4.9**

**Values of maximum coupling efficiencies for the RI profile exponents  $g=4, 8, 10$  and  $20$ , excitation wavelength  $1.5\text{ }\mu\text{m}$ ,  $w_{1x} = 0.843\text{ }\mu\text{m}$  and  $w_{1y} = 0.857\text{ }\mu\text{m}$**

Profile index	V	$w_f$ in $\mu\text{m}$	$R_L$ in $\mu\text{m}$	u in $\mu\text{m}$	$\eta_{\text{max}}$ in %
4	1.924	5.008	7.0	12.0	68.979
	2.405	3.831	6.0	10.0	69.917
	3.000	3.284	5.5	8.0	72.000
8	1.924	4.714	7.0	12.0	69.552
	2.164	4.136	6.0	10.0	69.509
	2.700	3.526	5.5	9.0	70.026
10	1.924	4.715	7.0	12.0	69.563
	2.124	4.230	6.0	10.0	69.155
	2.650	3.596	5.5	9.0	70.054
20	1.924	4.858	7.0	12.0	69.335
	2.004	4.642	7.0	12.0	69.502
	2.500	3.868	6.0	10.0	69.787

**Table 4.10**

**Values of maximum coupling efficiencies for the RI profile exponents  $g=4, 8, 10$  and  $20$ , excitation wavelength  $1.3\text{ }\mu\text{m}$ ,  $w_{1x} = 1.081\text{ }\mu\text{m}$ , and  $w_{1y} = 1.161\text{ }\mu\text{m}$**

Profile index	V	$w_f$ in $\mu\text{m}$	$R_L$ in $\mu\text{m}$	u in $\mu\text{m}$	$\eta_{\max}$ in %
4	1.924	5.008	9.5	16.0	86.357
	2.405	3.831	7.0	11.0	87.529
	3.000	3.284	5.5	9.0	88.797
8	1.924	4.714	8.5	14.0	86.977
	2.164	4.136	8.0	13.0	87.142
	2.700	3.526	7.0	11.0	87.971
10	1.924	4.715	8.5	14.0	86.982
	2.124	4.230	8.0	14.0	87.162
	2.650	3.596	7.0	11.0	88.045
20	1.924	4.858	9.5	16.0	86.395
	2.004	4.642	8.5	14.0	87.155
	2.500	3.868	7.5	12.0	87.468

## 4.4 SUMMARY

This chapter comprises application of ABCD matrix formalism in order to predict the coupling efficiency of a single mode circular core GIF excited by laser diode via cylindrical micro lens on the fiber tip. We investigate the efficiencies for RI distribution of some specific profile exponents such as  $g = 4.0, 8.0, 10.0$  and  $20.0$ . The efficiency is calculated along the vertical plane, as the efficiency is very poor along the horizontal plane. Two commonly used wavelengths namely  $1.3\ \mu\text{m}$  and  $1.5\ \mu\text{m}$  are used in our study. The graded index fiber having profile exponent ( $g$ ) equal to 4 is found to be most coupling efficient at the wavelength  $1.3\ \mu\text{m}$ . Thus the results will be beneficial to the optical designers and packagers in the context of use of such coupler.



# *CHAPTER 5*

## *CONCLUSIONS*

## CONCLUSIONS:

Chapter 1 of the thesis contains brief introduction to the basics of optical waveguides along with concerned electromagnetic theory. It also contains different available methods for evaluation of propagation parameters both for fundamental and first higher order mode. Also, the technology of launch optics involving different kind of microlenses fabricated on various types of fibers have been presented in this chapter. The merits of different kinds of such optical couplers in respect of coupling efficiency have also been discussed here. This chapter also comprises brief introduction to dual mode optical fiber, rare earth metal doped optical fiber and nonlinear optics with special emphasis on Kerr type nonlinearity. Further, this chapter describes the objective of the present research work together with its importance to contemporary interest and future researches as well. The relevant citations have also been made here.

Chapter 2 consists of the literature survey, highlighting the relevant research gaps and the needful address to the gaps thereof.

Chapter 3 comprises prescription of a simple but accurate method for prediction of confinement and normalized group delay parameters for first higher order mode in graded index fiber. The said parameters have been estimated both in presence and absence of Kerr type nonlinearities. The necessary prescription involves use of Chebyshev technique for estimation of the concerned propagation parameters. In case of nonlinearity, method of iteration has been applied for the prediction. The finite element method can be used to estimate how Kerr nonlinearity will affect the above-mentioned parameters [Hayata, Koshiha and Suzuki, 1987]. However, this method is stringent and requires time-consuming computation. We choose to use the Chebyshev formalism to estimate the aforementioned propagation characteristics of Kerr type nonlinear graded index fibers because of the accuracy and simplicity of the formalism. To get

the constants in the series expression of the  $LP_{11}$  modal field for GI fiber in this setting, we employ the approach of iteration while taking care of the relevant nonlinearity. Step and parabolic profile fibers are used in our investigation as typical instances of graded index fibers, along with one common type of Kerr nonlinearity, with each being taken into account for both +Ve and -Ve nonlinearity. Moreover, we compare our results with the exact results produced by employing a strict FEM in order to confirm the accuracy of our formalism. It is relevant to mention in this connection that our results show excellent match with the results found by rigorous FEM. In this regard, it is noteworthy to note that, to the best of our knowledge, no easy method based on the Chebyshev formalism for the evaluation of these key parameters of Kerr-type nonlinear fibers have been described to date, making our approach innovative. Further, different kinds of fibers important in different areas of operation are being fabricated in different laboratories and enriching the literature thereby. We have shown here in Chapter 3 how the series formulation of modal field based on Chebyshev technique can predict the various propagation parameters associated with Kerr type graded index fibers both in the linear region and nonlinear region. Such formulation has made it possible to avoid complicated mathematical operation involving Bessel functions. Thus it opens up for the research workers that the present formalism may be extended for analysis of propagation characteristics both in the linear and nonlinear region.

Chapter 4 presents the study of coupling optics relating to an optical coupler consisting of laser diode, graded index fiber and cylindrical microlens fabricated on the tip of the fiber. Here, ABCD matrix formalism appropriate for the system has been developed in order to predict the coupling optics in a simple but accurate fashion. The investigation has been carried on for graded index fibers having different profile exponents. The profile exponent which is most coupling efficient in this context has been predicted. Thus we apply this formalism to compute the coupling efficiency of the cylindrical microlens on the graded index optical fiber for

different refractive index profile exponents ( $g$ ) having values  $g = 4.0, 8.0, 10.0$  and  $20.0$ . The study of the coupling efficiencies of the cylindrical microlens on the graded index fibers were investigated earlier but for not for different profile exponents as done by us [Roy, Majumdar, Maity S and Gangopadhyay, 2020]. In this thesis the coupling is studied for two laser diodes having different wavelengths of  $1.3 \mu\text{m}$  and  $1.5 \mu\text{m}$  [John, Maclean, Ghafouri-Shiraz and Niblett, 1994]. In this study we have applied the limited aperture technique and the field distribution associated with the source and the fiber are considered to be Gaussian [Sarkar, Thyagrajan and Kumar, 1984; Marcuse, 1978; Sarkar, Pal and Thyagrajan, 1986]. Using the ABCD matrix concept, a simple analytical expression of the coupling efficiency has been found by which one can easily find out the most effective coupler for a particular wavelength of light. The most efficient coupler thus studied should be not only be cost effective but also simple to use. Thus, the simple approach developed will benefit the system users in the process of predicting the coupling optics accurately in a very short time

Moreover, light of wavelength  $\lambda=1.5\mu\text{m}$  provides the lowest loss window and is also used in optical amplification involving rare earth doped material. Accordingly, this investigation of coupling optics will prove extremely beneficial for the designers and packagers in the domain of all optical technology. The present study will be also useful for the design of optimum launch optics in polarisation-maintained fiber optic sensors and also in coherent fiber optic communication systems (Zhang and Lit, 1993). The fabrication process very often cannot ensure full circularity for the core of the fiber and the present analysis can take care of such deviation from circularity in the context of estimation of relevant coupling optics in case of elliptical-core single-mode fibers (Sarkar, Pal and Thyagarajan, 1986; Mukhopadhyay, Gangopadhyay and Sarkar, 2007a, 2007b, 2010; Yang, Chen, Ro and Liang, 2010). Again, the aspect ratio of the elliptic core fiber requires consideration in the field of optimum coupling optics.

In fact, the present work generates motivation for going ahead with the prescribed formalism in various functions of microlens. Again, literature is being continuously enriched as different microlenses like, ellipsoidal, tapered hyperbolic lens, parabolic microlenses are being fabricated in various laboratories. The present method of coupling optics may further be extended for analysis of coupler involving the photonic crystal fibers as well as multi core fibers (Villatoro, Finazzi, Minkovich, Pruneri and Badenes, 2007; Zhao, Yang, Lu, Jin and Demonkan, 2004). Again, one needs to keep track with relevant publications from places where necessary infrastructural facilities for such intricate experiments are available. This will enable one to formulate relevant ABCD matrix in order to review the lensing schemes in respect of optimum launch optics taking care of all possible mismatches in fabrication.

Thus, such motivation for research work may lead to prescription of proposal of simple but accurate theoretical model for estimation of the coupling optics relating to microlenses of novel designs and fibers with novel refractive index profiles as well.

# *REFERENCES*

Abramowitz, M. and Stegun, I.A. (2012), “Handbook of mathematical functions: with formulas, graphs, and mathematical tables”, New York, USA: Dover Books on Mathematics.

Agrawal G.P. (2013). Nonlinear fiber optics, Cambridge, Massachusetts: Academic Press.

Agrawal GP, Boyd R.W. (1992). Contemporary Nonlinear Optics. Boston: Academic Press.

Agrawal, G.P. (2007), “Nonlinear fiber optics”, 4th ed, San Diego, Academic Press.

Aich, J., Maiti, A.K., Majumdar, A. and Gangopadhyay, S. (2019), “A novel and simple formalism for study of effect of Kerr nonlinearity on Petermann I and II spot sizes of single-mode-graded index fiber”, J Opt Commun. <https://doi.org/10.1515/joc-2019-0167>

Aich, J., Majumdar, A. and Gangopadhyay, S. (2021), “Analysis of optical Kerr effect on effective core area and index of refraction in single- mode dispersion shifted and dispersion flattened fibers” J Opt Commun. <https://doi.org/10.1515/joc-2021-0211>

Ainslie, B. J. and Day, C. R. (1986), “A review of single mode fibers with modified dispersion characteristics”, IEEE J. Lightwave Tech., **LT-4**: 967.

Amin, A. A., Ali. A., Chen, X. and Shieh, W. (2011), “LP<sub>01</sub>/ LP<sub>11</sub> dual-mode and dual polarization CO-OFDM transmission on two-mode fiber”, Electron. Lett., **47**: 606.

An, H. L (2000), “Theoretical investigation on the effective coupling from laser diode to tapered lensed single-mode optical fiber”, Opt. Commun., **181**: 89.

Ankiewicz, A. and Peng, G.D. (1992), “Generalised Gaussian Approximation for Single Mode Fibers”, IEEE J. Lightwave Tech., **10**: 22.

Antonelli C., Golani O., Shtaif M., Mecozzi A. (2017). Nonlinear interference noise in space-division multiplexed transmission through optical fibers, Opt Express., **25**:13055–78.

Aouadi, S., Bouzida, A., Daoui, A.K., Triki, H., Zhou, Q. and Liu, S. (2019), “W-shaped, bright and dark solitons of Biswas–Arshed equation”, *Optik*, **182**:227 - 32.

Behera, S., Hosain, S. I. and Patojoshi, P. (2011), “Effect of On-Axis Dip in Refractive-Index Profile on the Cutoff Frequency of Modes of Few Mode Fibers: A Numerical Approach”, *Eiber and Integrated Optics*, **30**:112.

Biswas, A., Kara, A.H., Ullah, M.Z., Zhou, Q., Triki, H. and Belic, M. (2017), “Conservation laws for cubic–quartic optical solitons in Kerr and power law media”. *Optik*, **145**:650–4.

Biswas, A., Zhou, Q., Ullah, M.Z., Triki, H., Moshokoa, S.P. and Belic, M. (2017), “Optical soliton perturbation with anti-cubic nonlinearity by semi- inverse variational principle”, *Optik*, **143**:131–4.

Borzycki, K. and Osuch, T. (2023), “Hollow core optical fibers for telecommunications and data transmission”, *Appl. Sci.*, **13**: 19.

Bose, A., Gangopadhyay, S. and Saha, S.C. (2011), “A simple method of prediction of fractional modal power guided inside the core, excitation efficiency of the mode by uniform light source and Petermann I and II spot sizes: All for first higher order mode in graded index fibers”, *Optik*, **122**:215–9.

Bose, A., Gangopadhyay, S. and Saha, S.C. (2012), “Laser diode to single mode circular core graded index fiber excitation via hemispherical microlens on the fiber tip: identification of suitable refractive index profile for maximum efficiency with consideration for allowable aperture”, *J Opt Commun*, **33**:15–9.

Bose, A., Gangopadhyay, S. and Saha, S.C. (2013), “A simple technique of prediction of far-field pattern for first order (LP<sub>11</sub>) mode in graded index fibers”, *Optik*, **124**:189–91.

Chakraborty S., Mandal C.K., Gangopadhyay S. (2017a). Prediction of fundamental modal field for graded index fiber in the presence of Kerr nonlinearity, *J. Opt. Commun.*, <https://doi.org/10.1515/joc-2017-0126>

Chakraborty S., Mandal C.K., Gangopadhyay S. (2017b). Prediction of first higher order modal field for graded index fiber in presence of Kerr nonlinearity, *J. Opt. Commun.*, <https://doi.org/10.1515/joc-2017-0206>



- Chao, C. K., Hu, J. Y., Hung, S. Y. and Yang, H. H. (2010), “Theoretical prediction of fiber coupling for ellipsoidal microlens”, *Journal of Mechanics*, **26**: 29.
- Chaudhuri, P. R. and Roy, S. (2007), “Analysis of arbitrary index profile planar optical waveguides and multilayer nonlinear structures: A simple finite difference algorithm”, *Optical and Quantum Electronics*, **39**:221.
- Chen, M. Y., Li, Y. R., Zhang, Y. and Zhu, Y. F. (2010), “Design of dual – mode optical fibers for the FTTH applications”, *Journal of Optics*, **13**(1): 015402.
- Chen, P.Y.P. (1982), “Fast method for calculating cut-off frequencies in single-mode fibers with arbitrary index profile”. *Electron Lett*; **18**:1048–9.
- Chen, Y. (1991), “Self trapped light in saturable non-linear media”, *Opt. Lett.*, **16**: 4.
- Cohen, L. G., Lin, C. and French, W. G. (1979), “Tailoring zero chromatic dispersion into the 1.5-1.6 $\mu$ m low-loss spectral region of single mode fibers”, *Electron Lett.*, **15**: 334.
- Dai, D., Wang, Z. and Bowers, J. E. (2011), “Ultrashort broadband polarization beam splitter based on an asymmetrical directional coupler” *Opt. Lett.*, **36**: 2590.
- Din R.U., Zeng X., Ahmad I., Yang X.F., Khan A.A., Ge G.Q. (2021). Enhanced crossKerr nonlinearity induced PT – symmetry in optical lattices, *J. Opt.*, **23**:0254.
- Edwards, C.A. and Presby, H.M. (1993), “Coupling-sensitivity comparison of hemispheric and hyperbolic microlens”, *Appl Opt*, **32**:1573–7.
- Edwards, C.A., Presby, H.M. and Dragone, C. (1993), “Ideal microlenses for laser to fiber coupling. *IEEE J Lightwave Technol*, **11**:252–7.
- Eguchi, M. (2001), “Dispersion-Compensating Dual-Mode optical fibers desirable for erbium-doped-fiber-amplified systems”, *J. Opt. Soc. Am. B.*, **18**: 737.
- Eguchi, M., Koshiha, M. and Tsuji, Y. (2002), “Dispersion compensation based on dual-mode optical fiber with inhomogeneous profile core”, *J. Lightwave Technol.*, **14**: 2387.
- Fang, X., Liao, C. R. and Wang, D. N. (2010), “Femtosecond laser fabricated fiber Bragg grating in microfiber for refractive index sensing”, *Opt. Lett.*, **35**: 1007.

Gangopadhyay, S. and Sarkar, S. N. (1996), “Laser diode to single-mode fibre excited via hyperbolic lens on the fibre tip: formulation of ABCD matrix and efficiency computation”, *Opt. Commun.*, **132**: 55-60.

Gangopadhyay, S. and Sarkar, S. N. (1997a), “Confinement and excitation of the fundamental mode in single-mode graded index fibers: computation by a simple technique”, *Int J Optoelectron*, **11**: 285–9.

Gangopadhyay, S. and Sarkar, S. N. (1997b), “ABCD matrix for reflection and refraction of Gaussian light beams at surfaces of hyperboloid of revolution and efficiency computation for laser diode to singlemode fiber coupling by way of a hyperbolic lens on the fiber tip”. *Appl Opt*, **36**: 8582–6.

Gangopadhyay, S. and Sarkar, S. N. (1998a), “Prediction of modal dispersion in single-mode graded index fibers by Chebyshev technique”, *J. Opt. Commun.*, **19**: 145.

Gangopadhyay, S. and Sarkar, S. N. (1998b), “Evaluation of modal spot size in single-mode graded index fibers by a simple technique”, *J. Opt. Commun.*, **19**: 173.

Gangopadhyay, S. and Sarkar, S. N. (1998c), “Laser diode to single-mode fiber excitation via hemispherical lens on the fiber tip: efficiency computation by ABCD matrix with consideration for allowableaperture”, *J Opt Commun*, **19**: 42–4.

Gangopadhyay, S. and Sarkar, S. N. (1998d), “Misalignment considerations in laser diode to single-mode fibre excitation via hyperbolic lens on the fibretip”, *Opt Commun*, **146**: 104–8.

Gangopadhyay, S. and Sarkar, S. N. (1998e), “Misalignment Considerations in Laser Diode to Single-Mode Fibre Excitation Via Hyperbolic Lens on the Fibre Tip”, *Opt. Commun.*, **146**: 104.

Gangopadhyay, S., Choudhury, S. and Sarkar, S. N. (1999), “Evaluation of splice loss in single-mode graded index fibers by a simple technique”, *Opt. and Quant. Electron.*, **31**: 1247.

Gangopadhyay, S., Sengupta, M., Mondal, S.K., Das, G. and Sarkar, S.N. (1997), “Novel method for studying single-mode fibers involving Chebyshev technique”, *J Opt Commun.*; **18**: 75–8.

Gao, X.L., Zhao, M.Y., Xie, M.T., Lei, M.Z., Song, X.Y., Bi, K., Zheng, Z. and Huang, S. (2019), “2D opticallycontrolled radio frequency orbital angular momentum beamsteering system based on a dual-parallel Mach–Zehnder modulator”, *Opt Lett*, **44**: 255–8.

- Garth, S. J. (1989), “Characterisation of modal noise, splice and bending loss in single mode depressed cladding fibers”, *J. Mod. Opt.*, **36**: 611.
- Gaylord, T. K. and Moharam, M. G. (1985), “Analysis and applications of optical diffraction gratings”, *Proc. IEEE*, **73**: 894.
- Ghafouri-Shiraj H. (1988), Experimental investigations on coupling efficiency between semiconductor laser diodes and single mode fibers by an etching technique, *Opt. quantum. Electron.*, **20**: 493.
- Ghafouri-Shiraj H., Asano T. (1986), Microlens for coupling a semiconductor laser to a single mode fiber, *Opt. Lett.*, **11**, 537.
- Ghatak, A.K. and Thyagarajan, K. (1998), “Optical Electronics”, Cambridge University Press.
- Ghatak, A.K., Thyagarajan, K. (2002). Introduction to fiber optics, 2<sup>nd</sup> edn. Cambridge University Press, UK.
- Ghosh, D., Roy, S. and Bhadra, S. K. (2010), “Determination of modal effective indices and dispersion of microstructured fibers with different configurations: a variational approach”, *J. Mod. Opt.*, **57**: 607.
- Gloge. D. (1971), Weakly Guiding Fibers”, *Appl. Opt.*, **10**: 2252.
- Gradshteyn, I.S. and Ryzhik, I.M. (2014), “Table of integrals, series and products”, London: Academic Press.
- Guo, M., Zhang, Y., Wang, M., Chen, Y.D. and Yang, H.W. (2018), “A new ZK-ILW equation for algebraic gravity solitary waves in finite depth stratified atmosphere and the research of squall lines formation mechanism”, *Comput Math Appl.*, **75**: 3589–603.
- Hasegawa, A. and Kodama, Y. (1991), “Guiding-center soliton”, *Phys. Rev. Lett.*, **66**: 161.
- Hayata, K., Koshiba, M. and Suzuki, M. (1987) “Finite-element solution of arbitrarily nonlinear, graded-index slab waveguides”. *ElectronLett.*, **23**: 429–31.
- Hillerich, B. and Guttman, J. (1989), “Deterioration of taper lens performance due to taper asymmetry,” *J. Light Tech.*, **7**: 99.

Hongzhan, L., Liren, L., Rongwei, X, Zhu, L. (2005), “Simple ABCD matrix method for evaluating optical coupling system of laser diode to single-mode fiber with a lensed-tip, *Optik*, **116**: 415 – 18.

Hu, J. Y., Lin, C. P., Hung, S. Y., Yang, H. and chao, C. K. (2008), “Semi-ellipsoid microlens simulation and fabrication for enhancing optical fiber coupling efficiency,” *Sensors and Actuators A: Physics*, **147**: 93.

Huang, J. and Yang, H. J. (2010), “ABCD matrix model of quadric interface-lensed fiber and its application in coupling efficiency calculation”, *Optik.*, **121**: 531.

Jablonski, D. P. (1986), “Fiber manufacture at AT & with the MCVD process”, *IEEE J. Light., Tech.*, **LT-4**: 1016.

Jie Y. (2010). Theoretical analysis of tapered fiber microlens parameter and its new fabricating technique. In 2010 International Conference on Computer Application and System Modeling, *IEEE, ICCASM*, **13**: 13-448.

John, J., Maclean, T.S.M., Ghafouri-Shiraz, H. and Niblett, J. (1994), “Matching of single-mode fiber to laser diode by microlenses at 1.5–1.3  $\mu\text{m}$  wavelength”, *IEEE Proc J Optoelectron*, **141**: 178–84.

Jung, J., Nam, H., Lee, B., Byun, J. O. and Kim, N. S. (1999), “Fiber Bragg grating temperature sensor with controllable sensitivity”, *Appl. Opt.*, **38**: 2752.

Kanamori, H., Yokota, H., Tanaka, G., Watanabe, M., Ishiguro, Y., Yoshida, I., Kakii, T., Itoh, S., Asano, Y. and Tanaka, S. (1986), “Transmission characteristics and reliability of pure-silica-core single-mode fibers”, *IEEE J. Light. Tech.*, **LT-4**: 1144.

Kapron, F.P. and Keck, D. B. (1971), “Pulse transmission through a dielectric optical waveguide”, *Appl. Opt.* **10**: 1519-23.

Kersey, A. D., Berkoff, T. A. and Morey, W. W. (1993), “Multiplexed fiber Bragg grating strain-sensor system with a fiber Fabry–Perot wavelength filter”, *Opt. Lett.*, **18**: 1370.

Khijwania, S.K., Nair, V.M. and Sarkar, S.N. (2009), “Propagation characteristics of single-mode graded-index elliptical core linear and nonlinear fiber using super-Gaussian approximation”. *Appl Opt*, **48**: G156—62.

- Kurokawa, K. and Becker, E.E. (1975), “Laser fiber coupling with a hyperbolic lens”, *IEEE Trans Microw Theor Tech*, **23**: 309–11.
- Lam, D. K. W. and Garside, B. K. (1981), “Characterization of single-mode optical fiber filters”, *Appl. Opt.*, **20**: 440.
- Lei, M.Z., Zheng, Z.N., Qian, J.W., Xie, M.T., Bai, Y.P., Gao, X.L. and Huang, S. (2019), “Broadband chromatic-dispersion-induced power-fading compensation for radio-over-fiber links based on Hilbert transform”, *Opt Lett*, **44**: 155–8.
- Li, X., Zhang, L., Tang, Y., Gao, T., Zhang, Y.J. and Huang, S.G., (2018), “On-demand routing, modulation level and spectrum allocation (OD-RMSA) for multicast service aggregation in elastic optical networks”, *Opt Express*, **26**: 24506–30.
- Lie, Y. (2010), “Theoretical analysis of tapered fiber microlens parameter and its new fabricating technique”, *IEEE Int Con on Comp App and Sys Mod.*, **13**: 448–51.
- Liu, H., (2008), “The approximate ABCD matrix for a parabolic lens of revolution and its application in calculating the coupling efficiency”, *Optik*, **119**: 666.
- Liu, W.J., Liu, M.L., Liu, B., Quhe, R.G., Lei, M., Fang, S.B., Teng, H. and Wei, Z.W. (2019), “Nonlinear optical properties of MoS<sub>2</sub>-WS<sub>2</sub> heterostructure in fiber lasers”, *Opt Express*, **27**: 6689–99.
- Lu, C., Fu, C. and Yang, H.W. (2018), “Time-fractional generalized Boussinesq equation for Rossby solitary waves with dissipation effect in stratified fluid and conservation laws as well as exact solutions”, *Appl Math Comput*, **327**: 104–16.
- Lundin, R. (1994), “Dispersion Flattening in a W fiber”, *Appl. Opt.*, **33**: 1011.
- Maiti S., Majumdar A., Biswas S.K., Gangopadhyay S. (2020). Evaluation of splice loss of single-mode graded index fiber in presence of Kerr nonlinearity, *Optik*, **203**:1–7.
- Maiti, S., Biswas, S.K. and Gangopadhyay, S. (2019), “Study of coupling optics involving graded index fiber excitation via upside down tapered parabolic microlens on the fiber tip”, *Optik*, **199**:1–8.

Maiti, S., Maiti, A.K. and Gangopadhyay, S. (2017), “Laser diode to single-mode triangular-index fiber excitation via upside down hemispherical microlens on the fiber tip: prescription of ABCD matrix of transmission and estimation of coupling efficiency”, *Optik*, **144**:481–9.

Maity M., Maiti A.K., Mandal H., Gangopadhyay S. (2020). “A simple method for study of effect of Kerr nonlinearity on effective core area, index of refraction and fractional modal power through the core of monomode graded index fibre”, *Int. J Nanoparticles (IJNP)* **12**:136–51.

Majumdar, A., Mandal, C.K. and Gangopadhyay, S. (2017), “Laser diode to single-mode circular core parabolic index fiber coupling via upside down tapered hyperbolic micro lens on the tip of the fiber: prediction of coupling optics by ABCD matrix formalism”, *J Opt Commun.* **40**:171–80.

Mallick, A. K. and Sarkar, S. (2014), “Empirical relations to determine the normalized spot size of a single-mode trapezoidal index fiber and computation of its propagation characteristics”, *Opt. Eng.*, **53**: 076103.

Mandal, H., Maiti, S., Chiu, T.L. and Gangopadhyay, S. (2018), “Mismatch considerations in laser diode to single-mode circular core triangular index fiber excitation via upside down tapered hemispherical microlens on the fiber tip”, *Optik*, **168**: 533–40.

Marcuse, D. (1978), “Gaussian approximation of the fundamental modes of graded index fibers”, *J Opt Soc Am*, **68**: 103–9.

Massey, G. A. and Siegman, A. E. (1969), “Reflection and refraction of Gaussian light beams at tilted ellipsoidal surfaces”, *Appl. Opt.*, **8**: 975.

Matsui, T., Zhou, J. and Nakajima, K. (2005), “Dispersion flattened photonic crystal fiber with large effective area and low confinement loss”, *J. Light. Tech.*, **23**: 4178.

Mayura, S., Mayura, P. and Verma, R. (2023), “Dual mode fiber optic high – performance sensor designs for ultra – low concentrations in NIR region”. *Opt. and Quant. Electr.*, **55**: 405.

McMullin, J. N. (1986), “The ABCD matrix in arbitrary tapered quadratic-index waveguides”, *Appl. Opt.*, **25**:2184.

Mears, R. J., Reekie, L., Jauncey, I. M. and Payne, D. N. (1987), “Low noise erbium-doped fiber amplifier at 1.54 $\mu\text{m}$ ”, *Electron. Lett.*, **23**: 1026.

Mishra, P. K., Hosain, S.I., Goyal, I.C. and Sharma, A. (1984), “Scalar variational analysis of single mode graded core W – type fibers”, *Opt. Quantum. Electron.*, **16**: 287.

Modavis, R. A. and Webb, T. W. (1995), “Anamorphic microlens for laser diode to single-mode fiber coupling”, *IEEE Photonics Tech. Lett.*, **7**: 798.

Mondal, S.K. and Sarkar, S.N. (1996), “Effect of optical Kerr effect nonlinearity on  $LP_{11}$  mode cutoff frequency of single-mode dispersion shifted and dispersion flattened fibers”. *Opt Commun*, **127**: 25–30.

Mondal, S.K. and Sarkar, S.N. (1999), “Coupling of a laser diode to single-mode fiber with an upside-down tapered lens end”, *Appl Opt*, **38**: 6272–7.

Mondal, S.K., Gangopadhyay, S. and Sarkar, S.N. (1998), “Analysis of an upsidedown taper lens end from a single-mode step-index fiber”, *Appl Opt*, **37**: 1006–9.

Monerie, M. (1982), “Propagation in doubly clad single mode fibers”, *IEEE J. Quant. Electron.*, **QE 18**: 534.

Mukherjee T., Maiti S., Majumdar A., Gangopadhyay S. (2020). A simple but accurate formalism for study of single-mode graded index fiber directional coupler in presence of Kerr nonlinearity, *Optik*, **213**: 164772.

Mukherjee T., Majumdar A., Gangopadhyay S. (2020a). Influence of Kerr nonlinearity on group delay and modal dispersion parameters of single-mode graded index fibers: evaluation by a simple but accurate method. *J. Optical Commun.* <https://doi.org/10.1515/joc-2020-0192>

Mukherjee T., Majumdar A., Gangopadhyay S. (2020b). A simple but accurate formalism for study of single-mode graded index fiber directional coupler in presence of Kerr nonlinearity. *Optik*. 164772: <https://doi.org/10.1016/j.ijleo.2020.164772>

Mukherjee, T., Majumdar, A. and Gangopadhyay, S. (2022), “Effect of Kerr nonlinearity on signal and pump intensities in EDFA comprising single-mode step index fiber: estimation by a simple but accurate mathematical formalism”, *Results Opt*, **8**: 100263.

Mukhopadhyay, S. (2016), “Coupling of a laser diode to single mode circular core graded index fiber via parabolic microlens on the fiber tip and identification of the suitable refractive index profile with consideration for possible misalignments”, *J. Opt.*, **45**: 312.

Mukhopadhyay, S., Gangopadhyay, S. and Sarkar, S.N. (2007), “Coupling of a laser diode to a mono mode elliptic core fiber via a hyperbolic microlens on the fiber tip: efficiency computation with the ABCD matrix”, *Opt Eng*, **46**: 1–5.

Mukhopadhyay, S., Gangopadhyay, S. and Sarkar, S.N. (2010), “Coupling of a laser diode to mono mode elliptic core fiber via upside down tapered microlens on the fiber tip: estimation of coupling efficiency with consideration for misalignments by ABCD matrix formalism”, *Optik*, **121**: 142–50.

Mukhopadhyay, S., Sarkar, S.N. (2011), “Coupling of a laser diode to single mode circular core graded index fiber via hyperbolic microlens on the fiber tip and identification of the suitable refractive index profile with consideration for possible misalignments”, *Opt Eng*, **50**: 1–9.

Namihara Y. (1997a). “Wavelength dependence of correction on effective core and mode field diameter for various single-mode optical fibers”, *Electron Lett.*, **33**: 1483–5.

Namihira Y. (1997b). “Measurement results of effective area ( $A_{eff}$ ) and MFD and their correction factor for non-zero dispersion shifted fibers (NZFs, G.655) and dispersion shifted fibers (DSFs, G.633) by using variable aperture technique”, *ITU Com.*, **15**: 53-E.

Neumann, E. G. (1988), “Single mode fibers fundamentals”, Springer-Verlag, **57**, New York.

Ohashi, M., Kitayama, K., Kobayashi, T. and Ishida, (1984), “ $LP_{11}$  mode loss measurements in the two mode propagation region of optical fibers”, *Opt. Lett.*, **9** : 303 – 5.

Okamoto, K. and Marcatelli, E.A.J. (1994), “Chromatic dispersion characteristics of fibers with optical Kerr-types nonlinearity. *J Lightwave Technol*”; **7**:1988–9.

Olshansky, R. and Keck, D. B. (1976), “Pulse broadening in Graded-index optical fibers”, *App. Opt.*, **15**: 483 – 91.

Olsson, N. A., Hegarty, J., Logen, R. A., Johnson, L. F., Walker, K. L., Cohen, L. G., Kasper, B. L. and Campbell, J. C. (1985), “68.3 km transmission with 1.37 T Bit Km/s capacity using wavelength division multiplexing of ten single frequency lasers at 1.5  $\mu\text{m}$ ”, *Electron. Lett.*; **21**: 105.

Paek U. C. (1983), “Dispersionless single mode fibers with trapezoidal index profiles in the wavelength region near 1.5  $\mu\text{m}$ ”, *Appl. Opt.*, **22**: 2363.



Patra P., Gangopadhyay S., Sarkar S. N. (2000) “A simple method for studying single-mode graded index fibers in the low V region”, J. Opt. Commun., **21**: 225-8.

Patra P., Gangopadhyay S., Sarkar S.N. (2001a) “Confinement and excitation of the fundamental mode in single-mode graded index fibers of low V number: estimation by a simple technique”, J. optical commun., **22**(5): 166-170.

Patra P., Gangopadhyay S., Sarkar S.N. (2001b), “Evaluation of Petermann I and II spot sizes and dispersion parameters of single-mode graded index fibers in the low V region by a simple technique”, J. optical commun., **22**(1): 19-23.

Patra, P., Gangopadhyay, S. and Goswami, K. (2008), “A simple method for prediction of first order modal field and cladding decay parameter in graded index fiber”, Optik, **119**: 209–12.

Patra, P., Gangopadhyay, S., Sarkar, S.N. (2002), “A simple method for studying single-mode graded index fibers in the low V region”, JOpt Commun, **21**:225–8.

Patrick H.J., Williams G.M., Kersey A.D., Pedrazzani J.R., Vengsarkar A.M. (1996), “Hybrid fiber Bragg grating long period fiber grating sensor for strain temperature discrimination”, IEEE Photon Technol Lett, **8**:1223–5.

Pattojoshi, P. and Hosain, S. I. (1998), “Single-parameter variational approximations for linear and nonlinear effects in single – mode fibers: A comparative study”, Microwave and Opt Tech Letters, **18**: 63 -73.

Payne, D. N. and Gambling, W. A. (1975), “Zero material dispersion on optical fibers”, Electron. Lett., **11**: 176.

Pedersen. B. (1994), “Small-signal erbium-doped fiber amplifiers pumped at 980nm: a design study”, Opt. Quantum Electron., **26**: S237.

Presby, H.M. and Edwards, C.A. (1992a), “Near 100% efficient fiber microlenses”, Electron Letter, **28**: 582–4.

Presby, H.M. and Edwards, C.A. (1992b), “Efficient coupling of polarization maintaining fiber to laser diodes”, IEEE Photon Technol Lett, **4**: 897–9.

Rahman, F. A., Takahashi, K. and Teik, C. H. (2002), “A scheme to improve the coupling efficiency and working distance between laser diode and single mode fiber”, Opt. Commun., **208**: 103.

Rakshit R., Majumdar A., Gangopadhyay S. (2022a), “A Simple Method for Accurate Prediction of Splice Loss for First Higher-Order Mode of Step-Index Fiber in Presence of Kerr Nonlinearity - In Proceedings of the 3rd International Conference on Communication, Devices and Computing” (pp. 201-211). Springer, Singapore.

Rakshit R., Majumdar A., Maiti S., Gangopadhyay S. (2022b), “Influence of Kerr nonlinearity on single-mode dispersion-shifted and dispersion-flattened directional couplers: analysis by a simple but accurate method”, Optical and Quantum Electronics, **54**(2): 1-27.

Rakshit, R., Majumdar, A. and Gangopadhyay, S. (2021), “A simple but accurate method for prediction of splice loss in mono-mode dispersion shifted and dispersion flattened fibers in presence of Kerr nonlinearity”, J Opt Commun., <https://doi.org/10.1515/joc-2020-0259>

Ray B.K., Majumdar A., Gangopadhyay S. (2022a), “Analysis of splitting ratio of a symmetric directional coupler fabricated with triangular-index fibers in nonlinear condition-a design perspective” Res. In Optics., **10**: 100341. <https://doi.org/10.1016/j.rio.2022.100341>

Ray, B.K., Majumdar, A. and Gangopadhyay, S. (2021), “Analysis of Kerr type nonlinear single-mode triangular index fiber directional coupler by a simple method”, Opt Eng, **60**: 086110.

Ray, B.K., Majumdar, A. and Gangopadhyay, S. (2022b), “Radial distribution of pump and signal intensities in step index EDFA for LP<sub>11</sub> mode in Kerr nonlinear condition”, J Opt Commun., <https://doi.org/10.1515/joc-2022-0109>

Roy, K., Majumdar, A. and Gangopadhyay, S. (2020), “A Simple but accurate method for estimation of the effect of Kerr nonlinearity on confinement and excitation of the fundamental mode in single mode graded index fiber”, Optik, **216**: 164939.

Roy, K., Majumdar, A. and Gangopadhyay, S. (2022), “An accurate but simple method for estimation of the influence of Kerr nonlinearity on the far field pattern of LP<sub>11</sub> mode in dispersion-shifted and dispersion-flattened fibers”, J Opt Commun. <https://doi.org/10.1515/joc-2022-0050>

- Roy, K., Majumdar, A., Maity, S. and Gangopadhyay, S. (2020), “Laser diode to single-mode graded index fiber coupling cylindrical microlens on the fiber tip: evaluation of coupling efficiency by ABCD matrix formalism”, J Opt Commun. <https://doi.org/10.1515/joc-2020-0234>
- Ryu, S. Y., Choi, H. Y., Chang, K. S., Kim, G. H., Choi, W. J., Ahn, S. G., Kim, Y. C., Yoon, J. H. and Lee, B. H. (2012), “A fiber based single unit dual mode optical imaging system: Swept source optical coherence tomography and fluorescence spectroscopy”, Optics Communications, **285**(9): 2478 – 82.
- Sadhu, A., Karak, A. and Sarkar, S.N. (2013), “A simple and effective method to analyze the propagation characteristics of nonlinear single mode fiber using Chebyshev method”, Microw Opt Technol Lett, **56**:787–90.
- Saitoh, K., Fujisawa, T., Kirihaara, T. and Koshiba, M. (2006), “Approximate empirical relations for nonlinear photonic crystal fibers”. OptExpress; **14**: 6572–82.
- Sambanthan, K. Rahman, F. A. (2005), “Method to improve the coupling efficiency of a hemispherically lensed asymmetric tapered-core fiber”, Opt. Commun., **254**: 112.
- Sammur, R. A., Li, Q.Y. and Pask, C. (1992), “Variational approximations and mode stability in planar nonlinear waveguides”, J. Opt. Soc. Am. B., **9**: 884.
- Sanyal, S., Gangopadhyay, S. and Sarkar, S.N. (2000), “Single mode graded index fiber directional coupler: Analysis by a simple and accurate method”, J. Opt. Commun., **21**: 232.
- Sarkar, S.N., Pal, B.P. and Thyagrajan, K. (1986), “Lens coupling of laser diodes to multimode elliptic core fibers”, J Opt Commun, **7**: 92–6.
- Sarkar, S.N., Thyagrajan, K. and Kumar, A. (1984), “Gaussian approximation of the fundamental mode in single mode elliptic core fibers”, Opt Commun, **49**: 178–83.
- Saruwatari, M. and Nawata, K. (1979), “Semiconductor laser to single mode fiber coupler”, Applied Optics, **18**: 1847.
- Savolinen J.M., Gruner-Nielson L., Kristensen P., Balling P. (2012). Measurement of effective refractive index differences in a fewmode fiber by axial fiber stretching, Opt. Express., **20**: 1864–5.

Senior, J. M. (1994), “Optical fiber communications principles and practice”, Prentice Hall of India Pvt. Ltd., New Delhi.

Sharma, E., K.; Goyal, I., C.; Ghatak, A., K. (1981); “Calculation of Cutoff Frequencies in Optical Fibers for Arbitrary Profiles Using the Matrix Method”, IEEE, Journal of Quant. Electr., **QE – 17**: 2317 – 21.

Shijun, J. (1987), “Simple explicit formula for calculating the LP<sub>11</sub> mode cut-off frequency”, Electron Lett, **23**: 534–5.

Snyder A.W., Chen Y., Poladian L., Mitchel D.J. (1990), “Fundamental mode of highly nonlinear fibres”, Electron Lett., **26**: 643–4.

Spajer, M. and Charquille, B. (1986), “Application of intermodal interference to fiber sensors”, Optics Comm., **60**: 216.

Strecker J., Wilezowski F. (1996), “Relationship between nonlinear effective core area and backscattering capture fraction for singlemode optical fibers”, Electron Lett, **32**: 760–1.

Tang H., Zhang Q. J., Zhao F., Xue H. (2002), “Cylindrical lensed fibers optimized for 980-nm pump laser diode coupling. Proc SPIE-Int Soc Opt Eng. 4905: 157-160.

Tewari, R. B., Pal, P. U. and Das, K., (1992), “Dispersion-shifted dual shape core fibers: optimization based on spot size definitions”, IEEE J. Lightwave., Tech., **10**: 1.

Tewari, R., Hosain, S.I. and Thyagarajan, K. (1983), “Scalar Variational Analysis of single mode fibers with Gaussian and smoothed out profiles”, Opt. Commun., **48**:176.

Thual, M., Chanclo, P. Gautreau, O., Caledec, L., Guignard, C. and Besnard, P. (2003), “Appropriate micro-lens to improve coupling between laser diodes and single mode fibers”, Electron. Lett., **39**: 1504.

Tian, Ma., Markov A., Wang, L. and Skorobogatiy, M. (2015), “Graded index porous optical fiber - dispersion management in terahertz range”, Opt. Exp., **23**: 7856.

Triki H., Azzouzi F., Biswas A., Moshokoa S.P., Belic M. (2017), “Bright optical solitons with Kerr law nonlinearity and fifth order dispersion”, Optik, **128**: 172-177.

Triki H., Biswas A., Moshokoa S.P., Belic M. (2017), “Dipole solitons in optical metamaterials with Kerr law nonlinearity” *Optik*, **128**: 71-76.

Watson, G.N. (1995), “A treatise on the theory of bessel functions”, Cambridge, UK: Cambridge University Press.

Wen, B., Hu, Y., Rui, G., Lv, C., He, J., Gu, B. and Cui, Y. (2014), “Anisotropic nonlinear Kerr media: Z-scan characterization and interaction with hybridly polarized beams”, *Opt Express*, **22**: 30826–32.

Yang, H. M., Chen, C. T., Ro, R. and Liang, T. C. (2010), “Investigation of the efficient coupling between a highly elliptical Gaussian profile output from a laser diode and a single mode fiber using a hyperbolic-shaped microlens”, *Opt. & Laser Tech.*, **42**: 918.

Yariv, A. (1991), *Optical Electronics*, Saunders College Publishing.

Yuan, L. and Qui, A. (1992), “Analysis of a single-mode fiber with taper lens end”, *J Opt Soc Am*, **A9**: 950–2.

Yuan, L.B. and Shou, R.L. (1990), “Formation and power distribution properties of an upside-down tapered lens at the end of an optical fiber”, *Sens Actuator*, **A23**: 1158–61.

Zhang, C., Liu, J., Fan, X.W., Peng, Q.Q., Guo, X.S., Jiang, D.P., Qian, X. and Su, L. (2018), “Compact passive Q-switching of a diode-pumped Tm, Y: CaF<sub>2</sub> laser near 2  $\mu$ m”, *Opt Laser Technol*, **103**: 89–92.

Zhang, F., Wu, Y.J., Liu, J., Pang, S.Y., Ma, F.K., Jiang, D.P., Wu, Q. and Su, L. (2018), “Mode locked Nd<sup>3+</sup> and Gd<sup>3+</sup> co-doped calcium fluoride crystal laser at dual gain lines”, *Opt Laser Technology*, **100**: 294–7.

Zhang, Q. (2003), “Angular alignment tolerances for a 980 nm pump laser diode coupled to a cylindrical lensed fiber”, *Acta Photonica Sin*, **32**: 92–6.

Zhang, Q.J. (2002), “Cylindrical lensed fibers optimized for 980-nm pump laser diode coupling”, *Proc SPIE*, **4905**: 157–60.

Zhu, H.T., Liu, J., Jiang, S.Z., Xu, S.C., Su, L.B., Jiang, D.P., Qian, X. and Xu, J. (2015), “Diode-pumped Yb, Y: CaF<sub>2</sub> laser mode-locked by monolayer graphene. *Opt Laser Technol*, **75**: 83–6.

Zou, X., Zhang, S., Qi, L., Wang, H., Zhang, Z., Zhang, Y. and Liu, Y. (2020), “Flexible ultra-wide frequency microwave down-conversion based on recirculating four-wave mixing in a semiconductor optical amplifier”, *Opt Express*, **28**: 17782–92.

# *LIST OF JOURNAL PUBLICATIONS*

1. Anindita Chattopadhyay, Angshuman Majumdar and Sankar Gangopadhyay, A simple but accurate technique for prediction of confinement and normalized group delay parameters for propagation of first higher order mode in graded index fiber, J. Opt. Commun. 2022; aop, <https://doi.org/10.1515/joc-2022-0274>, (Scopus indexed).
  
2. Anindita Chattopadhyay, Angshuman Majumdar and Sankar Gangopadhyay, Study of coupling optics of cylindrical microlens fabricated on tips of graded index fibers having different profile exponents, J. Opt. Commun. 2023; aop, <https://doi.org/10.1515/joc-2023-0129>, (Scopus indexed).



*REPRINTS OF  
PUBLICATIONS*

Anindita Chattopadhyay, Angshuman Majumdar and Sankar Gangopadhyay\*

# A simple but accurate technique for prediction of confinement and normalized group delay parameters for propagation of first higher order mode in graded index fiber

<https://doi.org/10.1515/joc-2022-0274>

Received October 26, 2022; accepted November 21, 2022;

published online December 12, 2022

**Abstract:** This paper deals with expressions for simple but precise analyses of fractional modal power (FMP) inside the core of optical fibers, the excitation efficiency and the normalized group delay (NGD) for the first higher order ( $LP_{11}$ ) mode in step and parabolic index fibers both with and without Kerr type non linearity. To get the analytical results, we have employed simple power series Chebyshev expansion for the  $LP_{11}$  mode of the above mentioned fibers. At first, the analytical expression for linear case is found out and then by applying the method of iteration the propagation parameters are estimated when there is nonlinearity of the Kerr type. Here, some typical step and parabolic profile fibers have been used for our investigation. Our findings of confinement and group delay parameters perfectly match with the precise numerical findings made by the intricate finite element method (FEM). This implies the precision of our formalism. The study of nonlinear optical transmission systems will benefit from the findings.

**Keywords:** Chebyshev technique; excitation efficiency; fractional modal power; Kerr nonlinearity; normalized group delay.

## 1 Introduction

The rapid expansion of information has put immense strain on the backbone as society moves into the information era. As time goes on, optical fiber technology emerges and advances toward high speed and high carrying capacity in order to relieve the transmission pressure brought on by a huge volume of data and to meet the need for information in present-day society [1–5]. Again, nonlinear effects and dispersion are unavoidable during the transmission process, which makes it challenging to boost the optical fiber's transmission rate. Transmitted optical pulses can successfully generate solitons when the dispersion and nonlinear effects achieve equilibrium. As a result, several theoretical and experimental studies on solitons have been conducted [6–10]. How to manage the equilibrium between dispersion and nonlinear effects in the use of solitons becomes a significant issue in ultrafast optics [11–14]. Nonlinear optics is the study of phenomena that result from changes in a material system's optical properties as a result of interaction with intense light. It is feasible to design multiple wave mixing processes in which energy is transmitted between distinct waves in the system due to the inherent nonlinearity of a medium.

If the electromagnetic field of the incident light is of high intensity, it generates nonlinearity in silica made optical fiber. This causes nonlinear variation of total induced polarization  $P$  with the electric field  $E$ . Further, the centrosymmetric  $SiO_2$  being the material of the fiber, the refractive index of the material does not depend on terms like  $E$ ,  $E^3$ ,  $E^5$  etc. Accordingly, the refractive index comprises terms containing intensity of light and its higher powers. Kerr nonlinearity is concerned with the dependence of the refractive index on the intensity of light ( $E^2$ ) only. Further, it is also known as third order nonlinearity as the concerned scalar wave equation contains cubic term in  $E$ . This change of refractive index causes change in the modal field inside the fiber and consequently the different propagation parameters associated with the fiber undergo change. It is relevant to mention in

\*Corresponding author: Sankar Gangopadhyay, Department of Electronics and Communication Engineering, Brainware University, Barasat, Kolkata 700125, West Bengal, India,

E-mail: sankar.gangopadhyay@yahoo.co.in

Anindita Chattopadhyay, Department of Basic Science and Humanities, Shree Ramkrishna Institute of Science and Technology, Dakshin Gobindapur, Rajpur Sonarpur, Kolkata, West Bengal 700145, India, E-mail: chattopadhyay.anindita@gmail.com

Angshuman Majumdar, Department of Electronics and Communication Engineering, Brainware University, Barasat, Kolkata 700125, West Bengal, India, E-mail: angshumankol2012@gmail.com

this connection that other higher orders of nonlinearity are generated due to dependence on terms like  $E^4$ ,  $E^6$  etc.

Recently, polarized light manipulation utilizing Kerr nonlinearity has been contributed to the literature [15]. Again, it has already been investigated how Kerr nonlinearity affects the propagation-related concerns of graded index (GI) and PCFs [16–19]. Additionally, there is literature that discusses how Kerr nonlinearity affects the  $LP_{11}$  mode cutoff  $V$  number for both dispersion-shifted and dispersion-flattened fibers [20]. However, the approaches in Refs. [16–20] require time-consuming calculations to be performed. Accordingly, the literature demands the development of a realistic yet straightforward methodology for estimating of optical fiber propagation parameters in the nonlinear domain in the context of both communication systems and sensor technology. In this aspect, it is pertinent to note that the Chebyshev technique-based simple series formulation of the fundamental ( $LP_{01}$ ) mode of GI fiber has been reported to be outstanding at projecting its propagation properties in the linear realm [21–24]. Additionally, by using the iterative method, the aforementioned formulations have been used to project the propagation-related concerns and the performance of directional couplers of GI and dispersion-managed fibers in the Kerr category nonlinear area [25–33]. Recent literature reports on the far field pattern of the  $LP_{11}$  mode dispersion-controlled fibers utilizing the same formalism [34]. Moreover, using the same technique, the effect of Kerr nonlinearity on signal and pump intensities in an EDFA built of  $LP_{11}$  mode SI fiber has also been introduced to the literature [35]. Actually, the study of Kerr nonlinearity has come to light as a possible issue of current interest. Technologists and researchers are working to develop fresh concepts in this field. In this regard, the study such as the impact of nonlinearity regarding characteristics such as FMP directed via the fiber core, excitation efficiency, and normalized group delay for  $LP_{11}$  mode GI fibers is significant for the domain of optical engineering. The FEM can be used to estimate how Kerr nonlinearity will affect the above-mentioned parameters [17]. However, this method is stringent and requires time-consuming computation.

We chose to use the Chebyshev formalism to estimate the aforementioned propagation characteristics of Kerr-type nonlinear GI fibers because of the accuracy and simplicity of the formalism. To get the constants in the series expression of the  $LP_{11}$  modal field for GI fiber in this setting, we employ the approach of iteration while taking care of the relevant nonlinearity. Step and parabolic profile fibers are used in our investigation as typical instances of GI fibers, along with one common type of Kerr nonlinearity, with each being taken into account for both

+Ve and –Ve diversity. Moreover, we compare our results to the exact results produced by employing a strict FEM in order to confirm the accuracy of our formalism. In this regard, it is noteworthy to note that, to the best of our knowledge, no easy method based on the Chebyshev formalism for the evaluation of these key parameters of Kerr-type nonlinear fibers have been described to date, making our approach innovative.

## 2 Theory

The RI profile  $n(R)$  for a GI fiber can be presented as

$$\begin{aligned} "n^2(R) &= n_1^2(1 - 2\delta f(R)), R \leq 1" \\ "n^2(R) &= n_2^2, R > 1" \end{aligned} \quad (1)$$

Here, " $\delta = (n_1^2 - n_2^2)/2n_1^2$ ",  $n_1$  and  $n_2$  are the RI of the core and cladding respectively.  $f(R)$  = shape of RI profile and

$$\begin{aligned} "f(R) &= 0, 0 < R \leq 1" \text{ for SI fiber} \\ "f(R) &= R^2, 0 < R \leq 1" \text{ for PI fiber} \end{aligned} \quad (2)$$

In presence of Kerr-type nonlinearity, the RI is written as [20]

$$"n^2(R) = n_L^2(R) + \frac{n_2^2 n_{NL}(R)}{\eta_0} \psi^2(R)" \quad (3)$$

where  $\eta_0 = \sqrt{\frac{\mu_0}{\epsilon_0}}$  with  $\mu_0$  = free space permeability,  $\epsilon_0$  = free space permittivity and  $n_{NL}(R)$  = nonlinear Kerr coefficient. Here,  $\psi(R)$  is the field of  $LP_{11}$  mode that satisfies the equation given below [20]

$$\begin{aligned} \left[ \frac{d^2 \psi(R)}{dR^2} + \frac{1}{R} \frac{d\psi(R)}{dR} + [V^2(1 - f(R)) - W^2] \right] \psi(R) \\ - \frac{\psi(R)}{R^2} + V^2 g(R) \psi^3(R) \\ = 0" \end{aligned} \quad (4)$$

where,

$$"g(R) = \frac{n_2 n_{NL} P}{\pi a^2 (n_1^2 - n_2^2)}" \quad (5)$$

Here,  $P$  is the power. Again, at the interface of core-clad of the fiber the boundary condition is as under

$$\left[ \frac{1}{R} \frac{d\psi}{dR} \right]_{R=1} = - \left[ 1 + \frac{WK_0(W)}{K_1(W)} \right]" \quad (6)$$

Here, " $K_0(W)$  and  $K_1(W)$ " are the modifications of Bessel functions [36–38].



In case of LP<sub>11</sub> mode the field  $\psi(R)$  is expressed as [39]

$$\psi(R) = a_1 R + a_3 R^3 + a_5 R^5, R \leq 1$$

$$= (a_1 R + a_3 R^3 + a_5 R^5) \frac{K_1(WR)}{K_1(R)} \quad R > 1 \quad (7) \quad \text{where,}$$

Using Eqs. (7) and (4) we get,

$$\begin{aligned} & a_1 \{V^2(1-f(R)) - W^2 + V^2 g \psi^2(R)\} + a_3 \{8 \\ & + R^2 [V^2(1-f(R)) - W^2 + V^2 g \psi^2(R)]\} + a_5 \{24R^2 \\ & + R^4 [V^2(1-f(R)) - W^2 + V^2 g \psi^2(R)]\} \\ & = 0 \end{aligned} \quad (8)$$

The Chebyshev points are given as [40, 41]

$$R_m = \cos \left( \frac{2m-1}{2M-1} \pi \right) \quad m = 1, 2, \dots, (M-1) \quad (9)$$

Eqs. (10) and (11) can be obtained if we consider Eq. (6) and take  $M = 3$  in Eq. (7) to get two Chebyshev values  $R_1$  and  $R_2$  [42].

$$\begin{aligned} & a_1 \{V^2(1-f(R_1)) - W^2 + V^2 g \psi^2(R_1)\} + a_3 \{8 \\ & + R_1^2 [V^2(1-f(R_1)) - W^2 + V^2 g \psi^2(R_1)]\} + a_5 \{24R_1^2 \\ & + R_1^4 [V^2(1-f(R_1)) - W^2 + V^2 g \psi^2(R_1)]\} \\ & = 0 \end{aligned} \quad (10)$$

and

$$\begin{aligned} & a_1 \{V^2(1-f(R_2)) - W^2 + V^2 g \psi^2(R_2)\} + a_3 \{8 \\ & + R_2^2 [V^2(1-f(R_2)) - W^2 + V^2 g \psi^2(R_2)]\} + a_5 \{24R_2^2 \\ & + R_2^4 [V^2(1-f(R_2)) - W^2 + V^2 g \psi^2(R_2)]\} \\ & = 0 \end{aligned} \quad (11)$$

It is the relation of  $\frac{K_1(W)}{K_0(W)}$  with  $\frac{1}{W}$  in the range  $0.6 \leq W \leq 2.5$  [23]

$$\frac{K_1(W)}{K_0(W)} = \alpha + \frac{\beta}{W} \quad (12)$$

where  $\alpha = 1.034623$  and  $\beta = 0.3890323$  [23]

Using Eqs. (6), (7) and (12) we get

$$\begin{aligned} & a_1 [2(\alpha W + \beta) + W^2] + a_3 [4(\alpha W + \beta) + W^2] \\ & + a_5 [6(\alpha W + \beta) + W^2] \\ & = 0 \end{aligned} \quad (13)$$

Eqs. (10), (11) and (13) will give non-trivial solution, subjected to below condition has to obey

$$\begin{vmatrix} A_1 & B_1 & C_1 \\ A_2 & B_2 & C_2 \\ A_3 & B_3 & C_3 \end{vmatrix} = 0 \quad (14)$$

$$A_1 = V^2(1-f(R_1)) - W^2 + V^2 g \psi^2(R_1)$$

$$A_2 = V^2(1-f(R_1)) - W^2 + V^2 g \psi^2(R_1)$$

$$A_3 = 2(\alpha W + \beta) + W^2$$

$$B_1 = 8 + R_1^2 [V^2(1-f(R_1)) - W^2 + V^2 g \psi^2(R_1)]$$

$$B_2 = 8 + R_2^2 [V^2(1-f(R_2)) - W^2 + V^2 g \psi^2(R_2)]$$

$$B_3 = 4(\alpha W + \beta) + W^2$$

$$C_1 = 24R_1^2 + R_1^4 [V^2(1-f(R_1)) - W^2 + V^2 g \psi^2(R_1)]$$

$$C_2 = 24R_2^2 + R_2^4 [V^2(1-f(R_2)) - W^2 + V^2 g \psi^2(R_2)]$$

$$C_3 = 6(\alpha W + \beta) + W^2 \quad (15)$$

Solution of Eq. (14) is essential to extract the  $W$  value for a certain  $V$  quantity in linear space where  $g$  value equal to zero. Then, by substituting this  $W$  value for that individual  $V$  value any two of Eqs. (10), (11) and (13), one may determine the values of normalized coefficients of Eq. (7) in relation to  $a_1$  in the linear domain. Now, we will first select a certain  $g$  value for a specific fiber with the stated  $V$  number and then employ the iteration process in order to acquire converging values of  $W$  in the nonlinear zone. For a single  $g$  value corresponding to a specific fiber with the given  $V$  number, one may calculate the values of normalized coefficients in respect of  $a_1$  using this convergent value of  $W$  in any two of Eqs. (10), (11) and (13). For each and every value of  $g$ , this method of evaluation is used for various fibers.

The fractional power  $f_{CO}$  of the LP<sub>11</sub> mode is as follows [43]

$$f_{CO} = \frac{\int_0^1 |\psi(R)|^2 R dR}{\int_0^\infty |\psi(R)|^2 R dR} \quad (16)$$

Using  $\psi(R)$  from Eqs. (7) and (16), we are able to obtain

$$f_{CO} = \frac{S_2}{S_2 - S_1(1 - (K_0(W)K_2(W)/K_1^2(W)))} \quad (17)$$

here,  $S_1 = \frac{(a_1 + a_3 + a_5)^2}{2}$  and  $S_2 = \frac{a_1^2}{4} + \frac{a_1 a_3}{3} + \frac{a_3^2 + 2a_1 a_5}{8} + \frac{a_3 a_5}{5} + \frac{a_5^2}{12}$

Think about a light source that is consistent, expressed as [21]

$$E_s = 1, 0 < r < a_s \quad (18a)$$

$$E_s = 0, a_s < r < \infty \quad (18b)$$

The excitation efficiency ( $\eta$ ) associated with LP<sub>11</sub> mode of the fiber along with an intense light source having intensity  $E_s$  identified as [21]

$$\eta = \frac{\left| \int_0^\infty E_s \psi^* r dr \right|^2}{\int_0^\infty |E_s|^2 r dr \int_0^\infty |\psi|^2 r dr} \quad (19)$$

Utilizing  $\psi(R)$  from Eq. (7),  $E_s$  from Eqs. (18a) and (18b), we have [43]

$$\eta = \frac{\left( \frac{2}{R_s^2} \right) \left[ S_3 + S_4 \left( \left( \frac{R_s^2 K_1(WR_s)}{K_1(W)} - 1 \right) \right)^2 \right]}{S_2 - \left( \frac{S_4^2}{2} \right) \left( 1 - \left( \frac{K_0(W)K_2(W)}{K_1^2(W)} \right) \right)} \quad (20)$$

where,  $S_3 = \frac{a_1}{3} + \frac{a_2}{5} + \frac{a_3}{7}$  and  $S_4 = a_1 + a_3 + a_5$

Now the value of normalized Petemann II ( $W_d$ ) spot sizes is evaluated to determine normalized group delay as follows

$$b_1 = b + \frac{4}{V^2 W_d^2} \quad (21)$$

where  $b = \frac{W^2}{V^2}$  and

$$W_d^2 = \frac{2 \left[ S_2 - S_1 \left( 1 - \frac{K_0(W)K_2(W)}{K_1^2(W)} \right) \right]}{S_5 - S_4^2 \left[ - \left( \frac{W^6}{6} \right) \left( \frac{10K_0^2(W) - 4K_2^2(W) - K_3^2(W)}{10K_1^2(W)} - \frac{1}{2} \right) - \left( \frac{K_0^2(W)}{2K_1^2(W)} \right) - 1 - \left( \frac{W^3}{3} \right) \left( \frac{K_0(W) - K_2(W)}{K_1(W)} \right) \right]}$$

here,  $S_5 = \frac{a_1^2}{2} + \frac{3}{2}a_3^2 + \frac{5}{2}a_5^2 + \frac{3}{2}a_1a_3 + \frac{5}{3}a_1a_5 + \frac{15}{4}a_3a_5$

### 3 Results and discussions

For several typical  $V$  numbers, specifically 2.6, 2.8, 3.0, 3.2 and 3.4, the FMP of the LP<sub>11</sub> mode steered via the core of the SI fiber is assessed using the prescribed formulation in both the occurrence and absence of nonlinearity. We continue the analysis for two typical positive and negative nonlinearity parameters [20] when nonlinearity is there. Table 1a displays the outcomes that were obtained. We have shown  $f_{co}$  versus  $V$  plot in Figure 1a depending on the outcomes shown in Table 1a.

We also employ some standard  $V$  numbers for dual-mode PI fiber, such 3.7, 3.9, 4.1, 4.3 and 4.5. In this context, Table 1b displays our data for both the removal and inclusion of the nonlinearities. The results from

**Table 1a:** LP<sub>11</sub> mode fractional power  $f_{co}$  for SI fiber.

$V$	Values of $f_{co}$ for +ve nonlinearity	Values of $f_{co}$ without nonlinearity	Values of $f_{co}$ for -ve nonlinearity
2.6	0.477889096	0.44961939	0.4222013758
2.8	0.59097979	0.57387879	0.5553249715
3.0	0.668779884	0.6561005	0.6426416216
3.2	0.725988028	0.716006005	0.7055417962
3.4	0.760071487	0.76164498	0.7531325033

Table 1b were used to generate the  $f_{co}$  versus  $V$  graph in Figure 1b.

Obtained values for excitation efficiency ( $\eta$ ) of dual-mode SI fiber for  $R_s = 2.0$  and  $5.0$ , respectively, in both the existence and absence of nonlinearity are shown in Tables 2a and 2b. The results shown in Tables 2a and 2b are graphically presented in Figures 2a and 2b.

Results for the  $\eta$  of LP<sub>11</sub> mode PI fiber for  $R_s = 1.5$  and  $3.0$  are presented in Tables 2c and 2d in both the presence and absence of nonlinearity, while the related graphical response is shown in Figures 2c and 2d.

Tables 3a and 3b presents the obtained values of normalized group delay ( $b_1$ ) for the LP<sub>11</sub> mode in absence of nonlinearity and in presence of positive and negative nonlinearities for SI and PI fibers of different  $V$  numbers. Figures 3a and 3b exhibit a graphical representation of the findings shown in Tables 3a and 3b.

All of the figures show that there is almost no difference between our outcomes and the simulated exact results. This illustrates how accurate our straightforward formalism is. In the case of the selected LP<sub>11</sub> mode SI and PI fibers, the curves depict the Kerr effect over various  $V$  regions. The current analysis can be used to reduce modal noise in a variety of sensors and gadgets that use nonlinear LP<sub>11</sub> mode GI optical fibers. Therefore, the outcomes will be useful from the standpoint of selecting an effective fiber in the communication and sensing fields.

### 4 Conclusions

In order to predict the fractional power, excitation efficiency and normalized group delay parameters for the propagation of the LP<sub>11</sub> mode in GI fiber in the absence and the involvement of Kerr nonlinearity, we have proposed a clear and simple but accurate methodology based on iteration. Two types of GI fibers, step and parabolic have

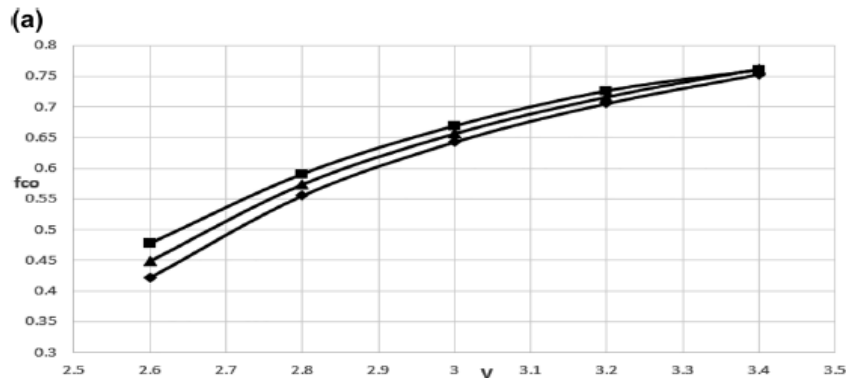


Figure 1a: Variation of fractional power  $f_{co}$  for different  $V$  values in absence and in the involvement of positive and negative nonlinearities for SI fiber. (Here,  $\blacktriangle$  for  $n_{NL}P = 0$ ,  $\blacksquare$  for  $n_{NL}P = +ve$  nonlinearity, and  $\blacklozenge$  for  $n_{NL}P = -ve$  nonlinearity. Solid lines—are the simulated exact results).

Table 1b:  $LP_{11}$  mode fractional power  $f_{co}$  for PI fiber.

$V$	Values of $f_{co}$ for +ve nonlinearity	Values of $f_{co}$ without nonlinearity	Values of $f_{co}$ for -ve nonlinearity
3.7	0.565607088	0.521512793	0.466637995
3.9	0.66343525	0.635746006	0.60335142
4.1	0.731776563	0.712353639	0.6902515
4.3	0.782212484	0.76775564	0.75159888
4.5	0.82070013	0.809488537	0.797157685

Table 2b:  $LP_{11}$  mode excitation efficiency  $\eta$  for SI fiber for  $R_S = 5$ .

$V$	Values of $\eta$ for +ve nonlinearity	Values of $\eta$ without nonlinearity	Values of $\eta$ for -ve nonlinearity
2.6	0.055224076	0.03347864	0.013439998
2.8	0.144545561	0.133676601	0.120673722
3.0	0.180343374	0.176434494	0.171624908
3.2	0.192982441	0.191829652	0.190284028
3.4	0.196605068	0.196620453	0.196476845

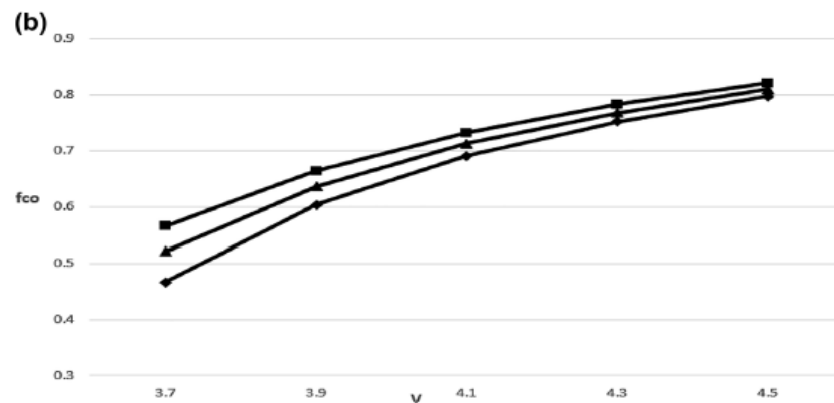


Figure 1b: Variation of fractional power  $f_{co}$  for different  $V$  values in absence and in the involvement of positive and negative nonlinearities for PI fiber. (Here,  $\blacktriangle$  for  $n_{NL}P = 0$ ,  $\blacksquare$  for  $n_{NL}P = +ve$  nonlinearity and  $\blacklozenge$  for  $n_{NL}P = -ve$  nonlinearity. Solid lines—are the simulated exact results).

Table 2a:  $LP_{11}$  mode excitation efficiency  $\eta$  for SI fiber for  $R_S = 2$ .

$V$	Values of $\eta$ for +ve nonlinearity	Values of $\eta$ without nonlinearity	Values of $\eta$ for -ve nonlinearity
2.6	0.027869029	0.012193293	0.002574913
2.8	0.187417482	0.153540148	0.120896641
3.0	0.388250429	0.352688569	0.316247077
3.2	0.571614297	0.541042625	0.508831917
3.4	0.718989562	0.695212547	0.669923583

been the subject of our work. In this perspective, our analysis makes use of some sample  $V$  numbers for each type of fiber. We continue to look into two common nonlinearity parameters,  $n_{NL}P = \pm 1.5 \times 10^{-14} \text{ m}^2$ . Interestingly, the data obtained using our straightforward method perfectly match those obtained using the time-consuming FEM. This reveals how accurate our uncomplicated formalism is. The desired outcomes encourage careful fiber selection in the fields of sensing and communication engineering.

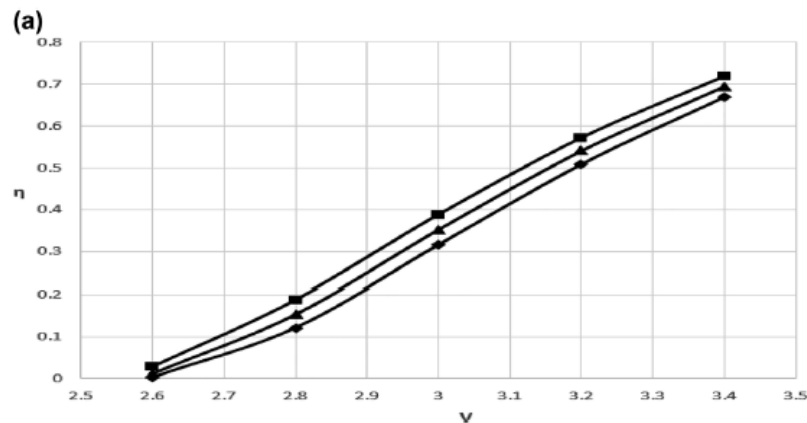


Figure 2a: Variation of  $\eta$  for different  $V$  values and for  $R_s = 2$  in absence and in the involvement of positive and negative nonlinearities in case of SI fiber. (Here,  $\blacktriangle$  for  $n_{NL}P = 0$ ,  $\blacksquare$  for  $n_{NL}P = +ve$  nonlinearity and  $\blacklozenge$  for  $n_{NL}P = -ve$  nonlinearity. Solid lines—are the simulated exact results).

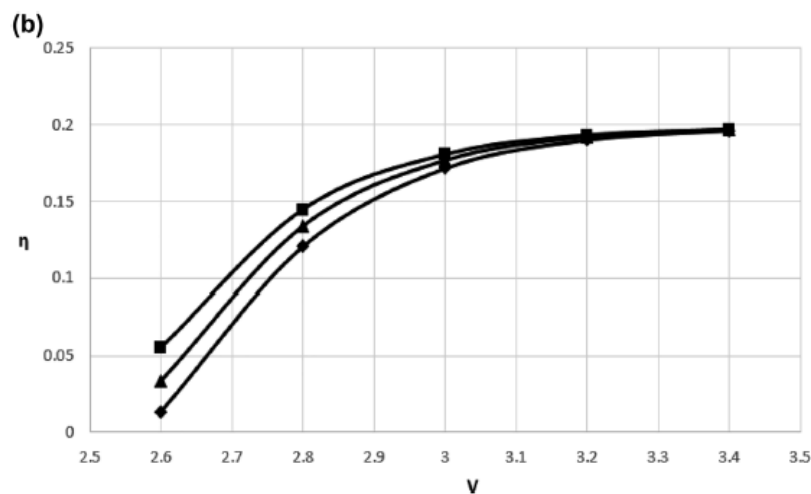


Figure 2b: Variation of  $\eta$  for different  $V$  values and for  $R_s = 5$  in absence and in the involvement of positive and negative nonlinearities in case of SI fiber. (Here,  $\blacktriangle$  for  $n_{NL}P = 0$ ,  $\blacksquare$  for  $n_{NL}P = +ve$  nonlinearity and  $\blacklozenge$  for  $n_{NL}P = -ve$  nonlinearity. Solid lines—are the simulated exact results).

Table 2c:  $LP_{11}$  mode  $\eta$  for PI fiber for  $R_s = 1.5$ .

$V$	Values of $\eta$ for +ve nonlinearity	Values of $\eta$ without nonlinearity	Values of $\eta$ for -ve nonlinearity
3.7	0.119114004	0.07923979	0.044411175
3.9	0.255082506	0.207395177	0.160411528
4.1	0.39912551	0.351618859	0.302454499
4.3	0.534631602	0.491158553	0.445326882
4.5	0.65384785	0.616081522	0.57563983

Table 2d:  $LP_{11}$  mode  $\eta$  for PI fiber for  $R_s = 3$ .

$V$	Values of $\eta$ for +ve nonlinearity	Values of $\eta$ without nonlinearity	Values of $\eta$ for -ve nonlinearity
3.7	0.052202397	0.015058212	0.000145865
3.9	0.187708385	0.142326698	0.094024725
4.1	0.295697583	0.264112416	0.226868202
4.3	0.362491593	0.343906398	0.321051694
4.5	0.397968641	0.388474178	0.376132746

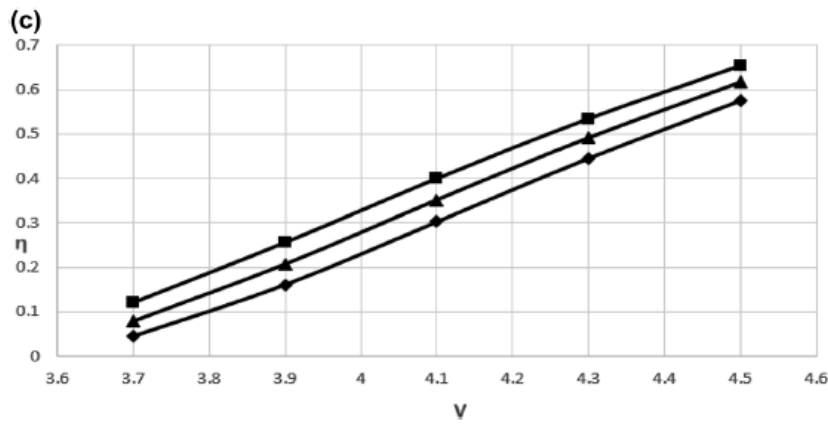


Figure 2c: Variation of  $\eta$  for different  $V$  values and for  $R_S = 1.5$  in absence and in the involvement of positive and negative nonlinearities in case of PI fiber. (Here, ▲ for  $n_{NLP} = 0$ , ■ for  $n_{NLP} = +ve$  nonlinearity and ◆ for  $n_{NLP} = -ve$  nonlinearity. Solid lines—are the simulated exact results).

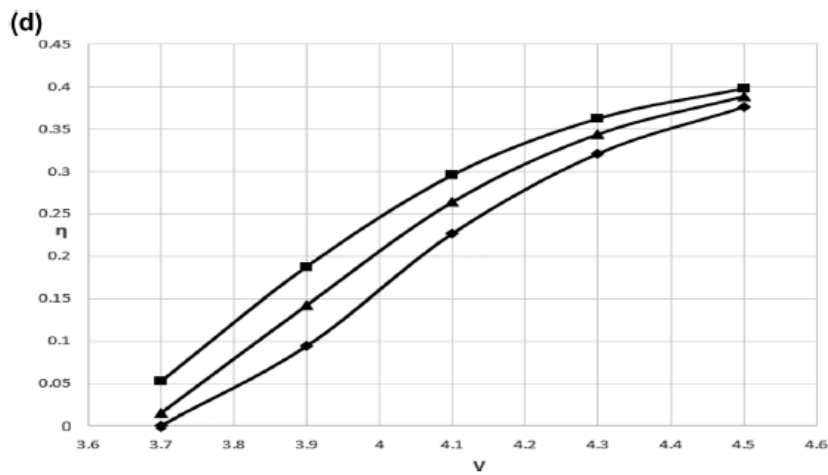


Figure 2d: Variation of  $\eta$  for different  $V$  values and for  $R_S = 3$  in absence and in the involvement of positive and negative nonlinearities in case of PI fiber. (Here, ▲ for  $n_{NLP} = 0$ , ■ for  $n_{NLP} = +ve$  nonlinearity and ◆ for  $n_{NLP} = -ve$  nonlinearity. Solid lines—are the simulated exact results).

Table 3a:  $LP_{11}$  mode normalized group delay parameter ( $b_1$ ) for SI fiber.

$V$	Values of $b_1$ for +ve nonlinearity	Values of $b_1$ without nonlinearity	Values of $b_1$ for -ve nonlinearity
2.6	0.2665696554	0.261227167	0.090815047
2.8	0.726923589	0.455608744	0.3890241693
3.0	4.7563457	2.803363663	1.887725928
3.2	3.0147425264	2.6570162179	1.522944475

Table 3b:  $LP_{11}$  mode normalized group delay parameter  $b_1$  for PI fiber.

$V$	Values of $b_1$ for +ve nonlinearity	Values of $b_1$ without nonlinearity	Values of $b_1$ for -ve nonlinearity
3.7	0.1627375817	0.1098405228	0.0517396928
3.9	0.2736966587	0.187880704	0.1209294298
4.1	0.5910951828	0.432049784	0.3249002357
4.3	0.9149238242	0.7262457731	0.5675927609



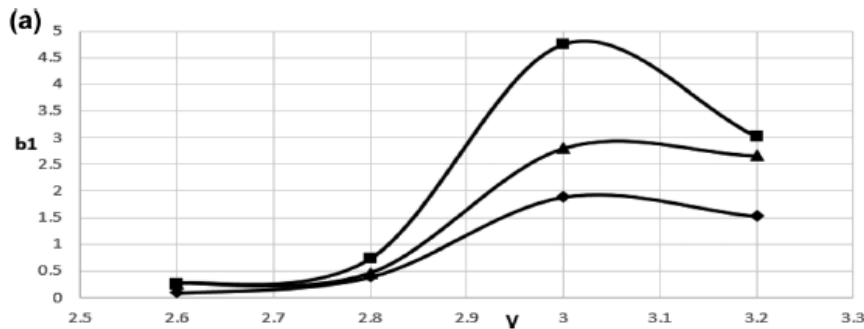


**Figure 3a:** Variation of  $b_1$  for different  $V$  values in absence and in the involvement of positive and negative nonlinearities in case of SI fiber. (Here,  $\blacktriangle$  for  $n_{NL}P = 0$ ,  $\blacksquare$  for  $n_{NL}P = +ve$  nonlinearity and  $\blacklozenge$  for  $n_{NL}P = -ve$  nonlinearity. Solid lines—are the simulated exact results).

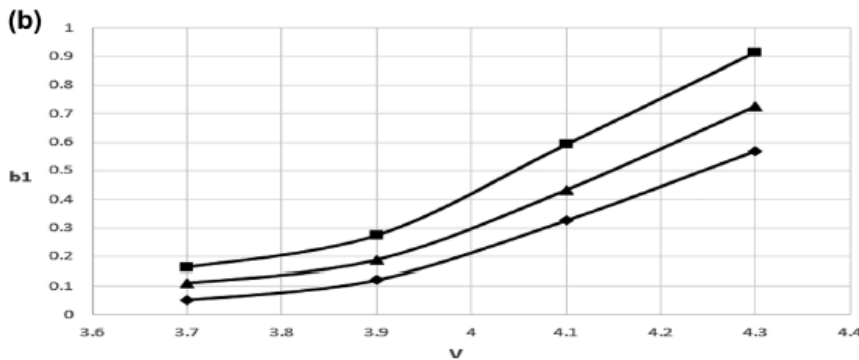


**Figure 3b:** Variation of normalized group delay parameter  $b_1$  for different  $V$  values in absence and in the involvement of positive and negative nonlinearities in case of PI fiber. (Here,  $\blacktriangle$  for  $n_{NL}P = 0$ ,  $\blacksquare$  for  $n_{NL}P = +ve$  nonlinearity and  $\blacklozenge$  for  $n_{NL}P = -ve$  nonlinearity. Solid lines—are the simulated exact results).

**Acknowledgment:** The authors are grateful to the honorable reviewers for their constructive suggestions.

**Author contributions:** All the authors have accepted responsibility for the entire content of this submitted manuscript and approved submission.

**Research funding:** None declared.

**Conflict of interest statement:** The authors declare no conflicts of interest regarding this article.

## References

1. Agrawal GP. Nonlinear fiber optics, 4th ed. San Diego: Academic Press; 2007.
2. Lei MZ, Zheng ZN, Qian JW, Xie MT, Bai YP, Gao XL, et al. Broadband chromatic-dispersion-induced power-fading compensation for radio-over-fiber links based on Hilbert transform. *Opt Lett* 2019;44:155–8.
3. Zou X, Zhang S, Qi L, Wang H, Zhang Z, Zhang Y, et al. Flexible ultra-wide frequency microwave down-conversion based on re-circulating four-wave mixing in a semiconductor optical amplifier. *Opt Express* 2020;28:17782–92.
4. Gao XL, Zhao MY, Xie MT, Lei MZ, Song XY, Bi K, et al. 2D optically controlled radio frequency orbital angular momentum beam steering system based on a dual-parallel Mach–Zehnder modulator. *Opt Lett* 2019;44:255–8.
5. Li X, Zhang L, Tang Y, Gao T, Zhang YJ, Huang SG. On-demand routing, modulation level and spectrum allocation (OD-RMSA) for multicast service aggregation in elastic optical networks. *Opt Express* 2018;26:24506–30.
6. Biswas A, Kara AH, Ullah MZ, Zhou Q, Triki H, Belic M. Conservation laws for cubic–quartic optical solitons in Kerr and power law media. *Optik* 2017;145:650–4.
7. Aouadi S, Bouzida A, Daoui AK, Triki H, Zhou Q, Liu S. W-shaped, bright and dark solitons of Biswas–Arshed equation. *Optik* 2019; 182:227–32.
8. Guo M, Zhang Y, Wang M, Chen YD, Yang HW. A new ZK-ILW equation for algebraic gravity solitary waves in finite depth stratified atmosphere and the research of squall lines formation mechanism. *Comput Math Appl* 2018;75:3589–603.
9. Lu C, Fu C, Yang HW. Time-fractional generalized Boussinesq equation for Rossby solitary waves with dissipation effect in

- stratified fluid and conservation laws as well as exact solutions. *Appl Math Comput* 2018;327:104–16.
10. Biswas A, Zhou Q, Ullah MZ, Triki H, Moshokoa SP, Belic M. Optical soliton perturbation with anti-cubic nonlinearity by semi-inverse variational principle. *Optik* 2017;143:131–4.
  11. Liu WJ, Liu ML, Liu B, Quhe RG, Lei M, Fang SB, et al. Nonlinear optical properties of  $\text{MoS}_2\text{-WS}_2$  heterostructure in fiber lasers. *Opt Express* 2019;27:6689–99.
  12. Zhu HT, Liu J, Jiang SZ, Xu SC, Su LB, Jiang DP, et al. Diode-pumped  $\text{Yb,Y:CaF}_2$  laser mode-locked by monolayer graphene. *Opt Laser Technol* 2015;75:83–6.
  13. Zhang C, Liu J, Fan XW, Peng QQ, Guo XS, Jiang DP, et al. Compact passive Q-switching of a diode-pumped  $\text{Tm,Y:CaF}_2$  laser near 2  $\mu\text{m}$ . *Opt Laser Technol* 2018;103:89–92.
  14. Zhang F, Wu YJ, Liu J, Pang SY, Ma FK, Jiang DP, et al. Mode locked  $\text{Nd}^{3+}$  and  $\text{Gd}^{3+}$  co-doped calcium fluoride crystal laser at dual gain lines. *Opt Laser Technol* 2018;100:294–7.
  15. Wen B, Hu Y, Rui G, Lv C, He J, Gu B, et al. Anisotropic nonlinear Kerr media: Z-scan characterization and interaction with hybridly polarized beams. *Opt Express* 2014;22:30826–32.
  16. Saitoh K, Fujisawa T, Kirihaara T, Koshiha M. Approximate empirical relations for nonlinear photonic crystal fibers. *Opt Express* 2006;14:6572–82.
  17. Hayata K, Koshiha M, Suzuki M. Finite-element solution of arbitrarily nonlinear, graded-index slab waveguides. *Electron Lett* 1987;23:429–31.
  18. Okamoto K, Marcyali EAJ. Chromatic dispersion characteristics of fibers with optical Kerr-types nonlinearity. *J Lightwave Technol* 1994;7:1988–9.
  19. Khijwania SK, Nair VM, Sarkar SN. Propagation characteristics of single-mode graded-index elliptical core linear and nonlinear fiber using super-Gaussian approximation. *Appl Opt* 2009;48:G156–62.
  20. Mondal SK, Sarkar SN. Effect of optical Kerr effect nonlinearity on  $\text{LP}_{11}$  mode cutoff frequency of single-mode dispersion shifted and dispersion flattened fibers. *Opt Commun* 1996;127:25–30.
  21. Gangopadhyay S, Sarkar SN. Confinement and excitation of the fundamental mode in single-mode graded index fibers: computation by a simple technique. *Int J Optoelectron* 1997;11:285–9.
  22. Patra P, Gangopadhyay S, Sarkar SN. Confinement and excitation of the fundamental mode in single-mode graded index fibers of low V number: estimation by a simple technique. *J Opt Commun* 2001;22:166–70.
  23. Gangopadhyay S, Sengupta M, Mondal SK, Das G, Sarkar SN. Novel method for studying single-mode fibers involving Chebyshev technique. *J Opt Commun* 1997;18:75–8.
  24. Patra P, Gangopadhyay S, Sarkar SN. A simple method for studying single-mode graded index fibers in the low V region. *J Opt Commun* 2000;21:225–8.
  25. Sadhu A, Karak A, Sarkar SN. A simple and effective method to analyze the propagation characteristics of nonlinear single mode fiber using Chebyshev method. *Microw Opt Technol Lett* 2013;56:787–90.
  26. Roy K, Majumdar A, Gangopadhyay S. Simple but accurate method for estimation of the effect of Kerr nonlinearity on confinement and excitation of the fundamental mode in single mode graded index fiber. *Optik* 2020;216:164939.
  27. Rakshit R, Majumdar A, Gangopadhyay S. A simple but accurate method for prediction of splice loss in mono-mode dispersion shifted and dispersion flattened fibers in presence of Kerr nonlinearity. *J Opt Commun* 2021. <https://doi.org/10.1515/joc-2020-0259>.
  28. Mukherjee T, Majumdar A, Gangopadhyay S. Effect of Kerr nonlinearity on signal and pump intensities in EDFA comprising single-mode step index fiber: estimation by a simple but accurate mathematical formalism. *Results Opt* 2022;8:100263.
  29. Aich J, Maiti AK, Majumdar A, Gangopadhyay S. A novel and simple formalism for study of effect of Kerr nonlinearity on Petermann I and II spot sizes of single-mode-graded index fiber. *J Opt Commun* 2019. <https://doi.org/10.1515/joc-2019-0167>.
  30. Aich J, Majumdar A, Gangopadhyay S. Analysis of optical Kerr effect on effective core area and index of refraction in single-mode dispersion shifted and dispersion flattened fibers. *J Opt Commun* 2021. <https://doi.org/10.1515/joc-2021-0211>.
  31. Rakshit R, Majumdar A, Maiti A, Gangopadhyay S. Influence of Kerr nonlinearity on single-mode dispersion-shifted and dispersion-flattened directional couplers: analysis by a simple but accurate method. *Opt Quant Electron* 2022;54:118.
  32. Ray BK, Majumdar A, Gangopadhyay S. Analysis of Kerr type nonlinear single-mode triangular index fiber directional coupler by a simple method. *Opt Eng* 2021;60:086110.
  33. Mukherjee T, Maiti S, Majumdar A, Gangopadhyay S. A simple but accurate formalism for study of single-mode graded index fiber directional coupler in presence of Kerr nonlinearity. *Optik* 2020;213:164772.
  34. Roy K, Majumdar A, Gangopadhyay S. An accurate but simple method for estimation of the influence of Kerr nonlinearity on the far field pattern of  $\text{LP}_{11}$  mode in dispersion-shifted and dispersion-flattened fibers. *J Opt Commun* 2022. <https://doi.org/10.1515/joc-2022-0050>.
  35. Ray BK, Majumdar A, Gangopadhyay S. Radial distribution of pump and signal intensities in step index EDFA for  $\text{LP}_{11}$  mode in Kerr nonlinear condition. *J Opt Commun* 2022. <https://doi.org/10.1515/joc-2022-0109>.
  36. Watson GN. A treatise on the theory of Bessel functions. Cambridge, UK: Cambridge University Press; 1995.
  37. Gradshteyn IS, Ryzhik IM. Table of integrals, series and products. London: Academic Press; 2014.
  38. Abramowitz M, Stegun IA. Handbook of mathematical functions: with formulas, graphs, and mathematical tables. New York, USA: Dover Books on Mathematics; 2012.
  39. Bose A, Gangopadhyay S, Saha SC. A simple technique of prediction of far-field pattern for first order ( $\text{LP}_{11}$ ) mode in graded index fibers. *Optik* 2013;124:189–91.
  40. Chen PYP. Fast method for calculating cut-off frequencies in single-mode fibers with arbitrary index profile. *Electron Lett* 1982;18:1048–9.
  41. Shijun J. Simple explicit formula for calculating the  $\text{LP}_{11}$  mode cut-off frequency. *Electron Lett* 1987;23:534–5.
  42. Patra P, Gangopadhyay S, Goswami K. A simple method for prediction of first order modal field and cladding decay parameter in graded index fiber. *Optik* 2008;119:209–12.
  43. Bose A, Gangopadhyay S, Saha SC. A simple method of prediction of fractional modal power guided inside the core, excitation efficiency of the mode by uniform light source and Petermann I and II spot sizes: All for first higher order mode in graded index fibers. *Optik* 2011;122:215–9.



Anindita Chattopadhyay, Angshuman Majumdar and Sankar Gangopadhyay\*

# Study of coupling optics of cylindrical microlens fabricated on tips of graded index fibers having different profile exponents

<https://doi.org/10.1515/joc-2023-0129>

Received April 17, 2023; accepted July 3, 2023;

published online July 25, 2023

**Abstract:** With the help of ABCD matrix concept, we examine the coupling efficiency of a single mode circular core graded index fiber (GIF) excited by laser diode via cylindrical micro lens on the fiber tip. We investigate the efficiencies for refractive index distribution of some specific profile exponents such as  $g = 4.0, 8.0, 10.0$  and  $20.0$ . The refractive index distribution for GIFs had been studied earlier. The efficiency is calculated along the vertical plane as the efficiency is very poor along the horizontal plane. For two very common wavelengths  $1.3 \mu\text{m}$  and  $1.5 \mu\text{m}$  the efficiencies have been calculated and for  $1.3 \mu\text{m}$  wavelength the refractive index distribution of profile exponent ( $g$ ) having the value  $g = 4$  is found to be most efficient in this context. The results are very much important in the design of optical optimization.

**Keywords:** ABCD matrix formalism; coupling efficiency; cylindrical micro lens; Gaussian approximation; refractive index distribution

## 1 Introduction

An optical fiber having single mode is the most favorite one in case of optical studies as it provides maximum bandwidth. To maximize the efficiency of a single mode GIF, micro lenses are put at the tip of it as it triggers the laser to optical fiber coupling [1–5]. When a hyperbolic micro lens is put on the tip

of a step index fiber, it has been observed that, theoretically, it produces nearly one hundred percent coupling efficiency among various types of micro lenses [1–3, 5–8]. But its fabrication needs sophisticated laser micromachining technique [1]. The refractive index (RI) profiles of some particular step index, parabolic index and triangular index cases have been studied for coupling via cylindrical micro lenses (CMLs) on the end face of the fibers [9]. To find out the maximum coupling efficiency of the source of light and the fiber, suitable refractive index profile, for different profile exponents has been studied [10]. Though hemispherical micro lens is popular due to its simple photographic technique, it is not an efficient coupler due to its limited aperture, spherical aberration and modal mismatch [1, 2]. To optimize the coupling, multiple forms of tapered lenses are put on the tip of optical fibers having different kind of refractive index profile [11–20]. More laser light enters in an optical fiber and increases the coupling efficiency, if a tapered lens of large aperture is used. Due to this advantage, tapered lens is used widely in micro optical studies, light amplification techniques and sensors of large span. CML is a very good coupler and also it is very easy to fabricate, thus it is widely used in the field of coupling optics [21, 22].

ABCD matrix formalism is a very useful and simple theoretical technique in optical coupling system when multiple forms of micro lenses and the tapered lenses are used on the tips of optical fibers [5, 8, 10, 13, 16–20, 23–26]. Thus we apply this formalism to compute the coupling efficiency of the CML on the graded index optical fiber for different refractive index profile exponents ( $g$ ) having values  $g = 4.0, 8.0, 10.0$  and  $20.0$ . The study of the coupling efficiencies of the CMLs on the GIFs are investigated earlier [9]. In this paper the coupling is studied for two laser diodes having different wavelengths of  $1.3 \mu\text{m}$  and  $1.5 \mu\text{m}$  [3]. In this study we have applied the limited aperture technique and the field distribution associated with the source and the fiber are considered to be Gaussian [27–29]. Using the ABCD matrix concept, a simple analytical expression of the coupling efficiency has been found by which one can easily find out the most effective coupler for a particular wavelength of light. The most efficient coupler thus studied should be not only cost effective but also simple to use. Thus, the simple approach developed will benefit the

\*Corresponding author: Sankar Gangopadhyay, Department of Electronics and Communication Engineering, Brainware University, Barasat, Kolkata 700125, West Bengal, India, E-mail: sankar.gangopadhyay@yahoo.co.in

Anindita Chattopadhyay, Department of Basic Science and Humanities, Shree Ramkrishna Institute of Science and Technology, Dakshin Gobindapur, Rajpur Sonarpur, Kolkata, West Bengal 700145, India, E-mail: chattopadhyay.anindita@gmail.com

Angshuman Majumdar, Department of Electronics and Communication Engineering, Brainware University, Barasat, Kolkata 700125, West Bengal, India, E-mail: angshumankol2012@gmail.com

**Table 1.1:** Values of coupling efficiencies for the refractive index of profile exponent  $g = 4$ ,  $V$  value 1.924, excited by wavelength  $1.5 \mu\text{m}$  with  $w_f = 5.008 \mu\text{m}$ ,  $w_{1x} = 0.843 \mu\text{m}$  and  $w_{1y} = 0.857 \mu\text{m}$ .

$u$	$R_L = 1$	$R_L = 6$	$R_L = 6.5$	$R_L = 7$	$R_L = 7.5$	$R_L = 11$	$R_L = 16$	$R_L = 21$
1	0.375	8.464	9.034	9.563	9.962	11.127	11.025	10.883
6	0.059	25.889	24.562	24.244	23.072	18.821	15.471	14.003
8	0.029	44.030	39.761	37.929	34.436	23.765	17.813	15.488
10	0.017	62.992	59.951	57.313	51.031	30.207	20.516	17.101
11	0.013	63.048	66.209	65.673	59.893	34.017	21.999	17.948
12	0.011	55.199	65.363	68.979	66.613	38.155	23.559	18.816
13	0.009	44.167	57.918	65.536	68.764	42.481	25.181	19.697
16	0.005	20.068	29.596	37.747	48.964	53.614	30.159	22.335
21	0.003	7.115	10.340	13.326	18.341	47.856	36.053	25.918
31	0.001	2.032	2.816	3.521	4.676	15.539	26.645	24.709

**Table 1.2:** Values of coupling efficiencies for the refractive index profile exponent  $g = 4$ ,  $V$  value 2.405, excited by  $1.5 \mu\text{m}$  with  $w_f = 3.831 \mu\text{m}$ ,  $w_{1x} = 0.843 \mu\text{m}$  and  $w_{1y} = 0.857 \mu\text{m}$ .

$u$	$R_L = 1$	$R_L = 5.5$	$R_L = 6$	$R_L = 6.5$	$R_L = 7$	$R_L = 11$	$R_L = 16$	$R_L = 21$
1	1.046	16.395	17.262	17.767	18.206	18.516	18.058	17.818
6	0.170	46.807	44.793	41.908	40.532	29.120	24.030	21.912
8	0.084	65.237	62.341	57.363	54.630	34.418	26.501	23.405
9	0.063	69.386	68.477	64.027	61.162	37.087	27.669	24.071
10	0.049	67.133	69.917	67.856	65.728	39.618	28.752	24.663
11	0.039	59.597	66.058	67.621	67.126	41.865	29.717	25.170
12	0.032	49.844	58.444	63.403	64.938	43.668	30.531	25.577
16	0.016	21.196	27.500	34.45	39.067	44.177	31.764	26.044
21	0.009	8.888	11.628	15.026	17.615	32.689	28.485	24.017
31	0.004	2.875	3.696	4.732	5.593	13.493	16.740	16.171

**Table 1.3:** Values of coupling efficiencies for the refractive index profile exponent  $g = 4$ ,  $V$  value 3.000, excited by  $1.5 \mu\text{m}$  with  $w_f = 3.284 \mu\text{m}$ ,  $w_{1x} = 0.843 \mu\text{m}$  and  $w_{1y} = 0.857 \mu\text{m}$ .

$u$	$R_L = 1$	$R_L = 5.5$	$R_L = 6$	$R_L = 6.5$	$R_L = 7$	$R_L = 11$	$R_L = 16$	$R_L = 21$
1	2.175	24.504	24.909	25.014	25.103	24.244	23.640	23.361
6	0.364	59.702	56.116	52.050	49.743	35.491	29.778	27.384
7	0.249	67.401	63.218	58.258	55.364	37.633	30.719	27.880
8	0.180	72.000	68.319	63.216	60.038	39.516	31.483	28.231
9	0.316	71.911	70.041	65.904	62.953	41.023	32.040	28.426
10	0.106	67.168	67.851	65.663	63.499	42.045	32.367	28.459
11	0.084	59.402	62.423	62.556	61.551	42.502	32.447	28.329
16	0.036	24.377	28.784	33.035	35.385	36.630	29.404	25.544
21	0.019	11.201	13.516	16.117	17.811	25.322	23.175	20.806
31	0.008	3.878	4.672	5.619	6.268	11.219	12.612	12.332

evaluated for the source wavelength  $1.5 \mu\text{m}$ . The same has been done for the source wavelength  $1.3 \mu\text{m}$  as well. Tables 5.1–5.3, 6.1–6.3, 7.1–7.3, and 8.1–8.3 represent those

corresponding to wavelength  $1.3 \mu\text{m}$ . Figures 1.1a, 1.2a, 1.2b, 1.3a, and 1.3b present the variations of coupling efficiency versus  $R_L$  for the fixed value of  $u$  for which the efficiency is

**Table 2.1:** Values of coupling efficiencies for the refractive index profile exponent  $g = 8$ ,  $V$  value 1.924, excited by  $1.5 \mu\text{m}$  with  $w_f = 4.714 \mu\text{m}$ ,  $w_{1x} = 0.843 \mu\text{m}$  and  $w_{1y} = 0.857 \mu\text{m}$ .

$u$	$R_L = 1$	$R_L = 6$	$R_L = 6.5$	$R_L = 7$	$R_L = 7.5$	$R_L = 11$	$R_L = 16$	$R_L = 21$
1	0.473	10.055	10.658	11.204	11.592	12.549	12.344	12.187
6	0.075	29.856	28.254	27.761	26.311	20.968	17.173	15.566
10	0.021	65.910	63.208	60.699	54.517	32.678	22.382	18.758
11	0.017	65.041	68.040	67.629	62.278	36.350	23.845	19.590
12	0.014	57.174	66.308	69.552	67.464	40.176	25.344	20.429
13	0.011	46.469	58.922	65.581	68.303	43.970	26.856	21.257
14	0.009	36.414	49.096	57.477	64.472	47.466	28.351	22.060
16	0.007	22.180	31.566	39.160	49.005	52.264	31.129	23.560
21	0.004	8.155	11.589	14.648	19.587	44.323	32.736	26.020
31	0.001	2.374	3.244	4.005	5.229	15.425	24.067	22.610

**Table 2.2:** Values of coupling efficiencies for the refractive index profile exponent  $g = 8$ ,  $V$  value 2.164, excited by  $1.5 \mu\text{m}$  with  $w_f = 4.136 \mu\text{m}$ ,  $w_{1x} = 0.843 \mu\text{m}$  and  $w_{1y} = 0.857 \mu\text{m}$ .

$u$	$R_L = 1$	$R_L = 5.5$	$R_L = 6$	$R_L = 6.5$	$R_L = 7$	$R_L = 11$	$R_L = 16$	$R_L = 21$
1	0.773	13.437	14.254	14.862	15.372	16.078	15.707	15.511
6	0.124	40.912	39.134	36.826	35.810	25.959	21.315	19.399
8	0.061	61.162	57.983	53.197	50.671	31.408	23.879	20.990
9	0.046	67.337	66.069	61.474	58.593	34.370	25.179	21.760
10	0.036	66.451	69.509	67.413	65.148	37.385	26.462	22.496
11	0.028	59.020	66.671	68.973	68.571	40.322	27.700	23.187
12	0.023	48.698	58.917	65.531	67.712	43.011	28.859	23.819
16	0.012	19.286	25.984	34.161	39.969	47.558	32.032	25.510
21	0.006	7.745	10.416	13.997	16.883	36.764	30.992	25.146
31	0.002	2.436	3.193	4.204	5.025	14.411	19.170	18.389

**Table 2.3:** Values of coupling efficiencies for the refractive index profile exponent  $g = 8$ ,  $V$  value 2.700, excited by  $1.5 \mu\text{m}$  with  $w_f = 3.526 \mu\text{m}$ ,  $w_{1x} = 0.843 \mu\text{m}$  and  $w_{1y} = 0.857 \mu\text{m}$ .

$u$	$R_L = 1$	$R_L = 5$	$R_L = 5.5$	$R_L = 6$	$R_L = 6.5$	$R_L = 11$	$R_L = 16$	$R_L = 21$
1	1.418	19.060	20.072	20.827	21.263	21.439	20.895	20.644
6	0.234	56.266	52.882	50.328	47.099	32.552	27.075	24.807
7	0.160	65.342	61.697	58.412	54.128	34.993	28.210	25.471
8	0.115	69.807	68.190	65.235	60.541	37.339	29.244	26.041
9	0.087	67.405	70.026	68.974	65.102	39.473	30.144	26.502
10	0.068	59.397	66.428	68.0369	66.653	41.266	30.878	26.842
11	0.054	49.199	58.875	63.636	64.746	42.591	31.418	27.049
16	0.023	16.635	22.729	28.134	33.730	40.132	30.733	26.034
21	0.012	7.292	10.010	12.601	15.676	28.542	25.602	22.404
31	0.005	2.482	3.353	4.185	5.212	12.298	14.379	13.999

maximum. It is done for three different  $V$  values and for the refractive index profile exponent  $g = 4$  when  $1.5 \mu\text{m}$  light source is used, whereas Figures 1.1b, 1.2b and 1.3b

shows the variations of coupling efficiency with the  $u$  values for the maximum value of  $R_L$  obtained from the previous plotting. Similar graphical representation is given



**Table 3.1:** Values of coupling efficiencies for the refractive index profile exponent  $g = 10$ ,  $V$  value 2.700, excited by  $1.5 \mu\text{m}$  with  $w_f = 4.715 \mu\text{m}$ ,  $w_{1x} = 0.843 \mu\text{m}$  and  $w_{1y} = 0.857 \mu\text{m}$ .

$u$	$R_L = 1$	$R_L = 6$	$R_L = 6.5$	$R_L = 7$	$R_L = 7.5$	$R_L = 11$	$R_L = 16$	$R_L = 21$
1	0.472	10.051	10.654	11.200	11.587	12.544	12.339	12.182
6	0.074	29.848	28.246	27.753	26.303	20.961	17.197	15.561
10	0.021	65.915	63.210	60.699	57.513	32.670	22.376	18.752
11	0.017	65.050	68.047	67.635	62.280	36.344	23.838	19.588
12	0.014	57.180	66.319	69.563	67.472	40.171	25.338	20.424
13	0.011	46.470	58.931	65.593	68.315	43.967	26.851	21.251
14	0.009	39.414	49.101	57.486	64.486	47.466	28.346	22.059
16	0.007	22.178	31.566	39.162	49.013	52.271	31.126	23.562
21	0.004	8.153	11.587	14.645	19.586	44.337	34.742	26.021
31	0.001	2.373	3.243	4.004	5.227	15.426	24.076	22.619

**Table 3.2:** Values of coupling efficiencies for the refractive index profile exponent  $g = 10$ ,  $V$  value 2.124, excited by  $1.5 \mu\text{m}$  with  $w_f = 4.230 \mu\text{m}$ ,  $w_{1x} = 0.843 \mu\text{m}$  and  $w_{1y} = 0.857 \mu\text{m}$ .

$u$	$R_L = 1$	$R_L = 5.5$	$R_L = 6$	$R_L = 6.5$	$R_L = 7$	$R_L = 11$	$R_L = 16$	$R_L = 21$
1	0.709	12.631	13.452	14.055	14.579	15.424	15.066	14.878
6	0.114	39.126	37.490	35.282	34.370	25.073	20.548	18.687
8	0.056	59.680	56.536	51.734	49.288	30.521	23.112	20.286
9	0.042	66.396	65.128	60.311	57.527	33.538	24.434	21.286
10	0.032	65.920	69.155	66.914	64.617	36.659	25.755	21.836
11	0.026	58.543	66.640	69.028	68.649	39.765	27.051	22.565
12	0.021	48.088	58.855	65.853	68.230	42.689	28.291	23.247
16	0.011	18.635	25.428	33.858	40.004	48.502	31.983	25.246
21	0.006	7.394	10.037	13.615	16.560	38.031	31.681	25.382
31	0.002	2.309	3.046	4.036	4.853	14.649	19.938	19.066

**Table 3.3:** Values of coupling efficiencies for the refractive index profile exponent  $g = 10$ ,  $V$  value 2.650, excited by  $1.5 \mu\text{m}$  with  $w_f = 3.596 \mu\text{m}$ ,  $w_{1x} = 0.843 \mu\text{m}$  and  $w_{1y} = 0.857 \mu\text{m}$ .

$u$	$R_L = 1$	$R_L = 5.5$	$R_L = 6$	$R_L = 6.5$	$R_L = 7$	$R_L = 11$	$R_L = 16$	$R_L = 21$
1	1.304	19.165	19.943	20.411	20.786	20.714	20.186	19.940
6	0.215	51.517	49.060	45.935	44.308	31.737	26.338	24.109
7	0.0146	60.643	57.398	53.160	50.857	34.234	27.510	24.806
8	0.106	67.669	64.688	59.951	57.174	36.679	28.600	25.420
9	0.079	70.054	69.002	65.033	62.299	38.960	29.576	25.941
10	0.062	66.755	68.859	67.112	65.163	40.945	30.405	26.638
11	0.498	59.193	64.312	65.568	65.045	42.500	31.056	26.638
16	0.021	22.436	28.062	34.010	37.714	41.100	31.029	26.093
21	0.011	9.766	12.401	15.576	17.859	29.486	26.280	22.815
31	0.005	3.243	4.075	5.112	5.884	12.591	14.906	14.492

in Figures 2.1a–2.3b, respectively, for the refractive index profile exponent  $g = 8$ . Graphical representations are shown in Figures 3.1a–3.3b, respectively, for the refractive

index profile exponent  $g = 10$  and also the graphical representations in Figures 4.1a–4.3b, respectively, are shown for the refractive index profile exponent  $g = 20$ . All these

**Table 4.1:** Values of coupling efficiencies for the refractive index profile exponent  $g = 20$ ,  $V$  value 1.924, excited by  $1.5 \mu\text{m}$  with  $w_j = 4.858 \mu\text{m}$ ,  $w_{1x} = 0.843 \mu\text{m}$  and  $w_{1y} = 0.857 \mu\text{m}$ .

$u$	$R_L = 1$	$R_L = 6$	$R_L = 6.5$	$R_L = 7$	$R_L = 7.5$	$R_L = 11$	$R_L = 16$	$R_L = 21$
1	0.409	9.240	9.826	10.358	10.752	11.828	11.670	11.521
6	0.064	27.856	26.390	25.968	24.660	19.888	16.309	14.771
10	0.018	64.568	61.686	59.065	52.818	31.468	21.447	17.924
11	0.014	64.163	67.244	66.726	61.155	35.225	22.925	18.769
12	0.012	56.296	65.949	69.335	67.112	39.224	24.461	19.625
13	0.010	45.410	58.527	65.621	68.593	43.301	26.036	20.484
14	0.008	35.261	48.451	57.354	64.992	47.195	27.623	21.336
16	0.006	21.152	30.640	38.508	49.042	53.020	30.685	22.973
21	0.003	7.635	10.972	13.995	18.987	46.093	35.431	26.009
31	0.001	2.200	3.029	3.760	4.952	15.515	25.324	23.646

**Table 4.2:** Values of coupling efficiencies for the refractive index profile exponent  $g = 20$ ,  $V$  value 2.124, excited by  $1.5 \mu\text{m}$  with  $w_j = 4.642 \mu\text{m}$ ,  $w_{1x} = 0.843 \mu\text{m}$  and  $w_{1y} = 0.857 \mu\text{m}$ .

$u$	$R_L = 1$	$R_L = 6$	$R_L = 6.5$	$R_L = 7$	$R_L = 7.5$	$R_L = 11$	$R_L = 16$	$R_L = 21$
1	0.501	10.491	11.096	11.643	12.026	12.940	12.702	12.542
6	0.079	30.899	29.210	28.665	27.145	21.547	17.628	15.986
10	0.023	66.517	63.873	61.396	55.272	33.307	22.863	19.190
11	0.018	65.411	68.322	67.929	62.709	36.927	24.313	20.018
12	0.014	57.548	66.373	69.502	67.490	40.653	25.788	20.841
13	0.012	46.947	59.014	65.410	68.009	44.292	27.263	21.647
14	0.010	36.957	49.327	57.401	64.073	47.578	28.704	22.427
16	0.007	22.687	31.978	39.390	48.870	51.861	31.325	23.851
21	0.004	8.422	11.892	14.952	19.847	43.450	32.353	25.995
31	0.001	2.465	3.354	4.126	5.363	15.367	23.444	22.090

**Table 4.3:** Values of coupling efficiencies for the refractive index profile exponent  $g = 20$ ,  $V$  value 2.500, excited by  $1.5 \mu\text{m}$  with  $w_j = 3.868 \mu\text{m}$ ,  $w_{1x} = 0.843 \mu\text{m}$  and  $w_{1y} = 0.857 \mu\text{m}$ .

$u$	$R_L = 1$	$R_L = 5.5$	$R_L = 6$	$R_L = 6.5$	$R_L = 7$	$R_L = 11$	$R_L = 16$	$R_L = 21$
1	1.009	15.436	16.826	17.384	17.536	18.180	17.729	17.512
6	0.164	44.447	43.991	41.277	34.390	28.694	23.657	21.586
8	0.080	62.502	61.719	56.895	44.548	34.022	26.146	23.098
9	0.061	66.759	68.102	63.782	49.737	36.736	27.334	23.780
10	0.047	64.746	69.787	67.879	54.307	39.337	28.447	24.396
11	0.038	57.485	66.056	67.858	57.568	41.677	29.452	24.929
12	0.031	48.005	58.438	63.726	58.903	43.596	360.314	25.370
16	0.016	20.238	27.288	34.463	45.672	44.583	31.800	26.003
21	0.008	8.439	11.461	14.917	23.446	33.159	28.779	24.178
31	0.003	2.720	3.626	4.669	7.526	13.607	17.013	16.437

graphs are drawn from the data obtained from the source of light of wavelength  $1.5 \mu\text{m}$ . For the source of light of wavelength  $1.3 \mu\text{m}$ , graphical representations are shown in

Figures 5.1a–5.3b, respectively, for the refractive index of profile exponent  $g = 4$ , in Figures 6.1a–6.3b, respectively, graphical representations are shown for the refractive

**Table 5.1:** Values of coupling efficiencies for the refractive index profile exponent  $g = 4$ ,  $V$  value 1.924, excited by  $1.3 \mu\text{m}$  with  $w_f = 5.008 \mu\text{m}$ ,  $w_{1x} = 1.081 \mu\text{m}$  and  $w_{1y} = 1.161 \mu\text{m}$ .

$u$	$R_L = 1$	$R_L = 6$	$R_L = 9$	$R_L = 9.5$	$R_L = 10$	$R_L = 11$	$R_L = 16$	$R_L = 21$
1	0.201	13.209	17.430	17.722	17.915	18.185	18.204	18.735
6	0.076	33.714	32.123	31.559	30.837	29.731	25.181	27.435
11	0.021	62.545	62.872	59.694	56.228	51.099	35.376	35.466
13	0.015	51.051	77.596	74.011	69.626	62.606	40.427	38.706
14	0.013	42.865	83.080	80.148	75.913	68.451	43.115	40.307
15	0.011	35.260	86.019	84.510	81.096	73.884	45.870	41.876
16	0.009	28.831	85.813	86.357	84.482	78.430	48.646	43.396
17	0.008	23.641	82.504	85.343	85.540	81.595	51.382	44.846
21	0.005	11.673	54.410	61.827	68.584	75.897	60.335	49.514
31	0.002	3.514	15.452	18.306	21.697	27.971	50.522	47.911

**Table 5.2:** Values of coupling efficiencies for the refractive index profile exponent  $g = 4$ ,  $V$  value 2.405, excited by  $1.3 \mu\text{m}$  with  $w_f = 3.831 \mu\text{m}$ ,  $w_{1x} = 1.081 \mu\text{m}$  and  $w_{1y} = 1.161 \mu\text{m}$ .

$u$	$R_L = 1$	$R_L = 6$	$R_L = 6.5$	$R_L = 7$	$R_L = 7.5$	$R_L = 11$	$R_L = 16$	$R_L = 21$
1	0.638	26.250	27.623	28.505	29.130	30.169	29.934	29.763
6	0.284	60.124	60.213	60.133	58.729	50.549	44.078	41.089
11	0.084	80.549	85.701	87.527	86.749	69.545	54.416	47.794
12	0.069	75.843	83.276	86.510	87.400	72.055	55.815	48.597
13	0.058	69.111	78.320	82.889	85.668	73.793	56.915	49.200
14	0.050	61.491	71.720	77.307	81.849	74.657	57.668	49.597
16	0.037	46.808	57.053	63.431	70.254	73.627	58.180	49.757
21	0.021	23.323	29.754	34.352	40.598	59.131	53.622	46.742
31	0.009	8.117	10.415	12.129	14.679	28.075	34.245	33.296

**Table 5.3:** Values of coupling efficiencies for the refractive index profile exponent  $g = 4$ ,  $V$  value 3.000, excited by  $1.3 \mu\text{m}$  with  $w_f = 3.284 \mu\text{m}$ ,  $w_{1x} = 1.081 \mu\text{m}$  and  $w_{1y} = 1.161 \mu\text{m}$ .

$u$	$R_L = 1$	$R_L = 5$	$R_L = 5.5$	$R_L = 6$	$R_L = 6.5$	$R_L = 11$	$R_L = 16$	$R_L = 21$
1	1.137	33.030	36.337	36.415	37.352	38.573	38.248	38.080
6	0.512	72.660	76.621	73.926	72.718	59.883	53.006	49.835
7	0.385	78.562	83.496	80.688	79.273	63.335	54.922	51.087
8	0.296	81.186	87.817	85.533	84.382	66.296	56.462	52.008
9	0.233	79.973	88.797	87.723	87.417	68.659	57.614	52.608
10	0.186	75.338	86.315	86.926	87.974	70.327	58.366	52.900
11	0.152	68.423	80.976	83.362	86.023	71.229	58.713	52.893
16	0.068	33.656	44.255	49.754	56.478	64.603	54.873	49.058
21	0.038	17.066	23.060	26.717	31.650	48.389	45.260	41.95
31	0.016	6.351	8.610	10.049	12.121	23.790	26.570	26.071

index of profile exponent  $g = 8$ , in Figures 7.1a–7.3b, respectively, graphical representations are given for the refractive index profile of exponent  $g = 10$  and finally, in Figures 8.1a–8.3b, respectively, graphical representations

are shown for the refractive index of profile exponent  $g = 20$ .

Tables 9 and 10 show the  $\eta$  for the optimized values of  $R_L$  and  $u$  for the laser wavelengths  $1.5 \mu\text{m}$  and  $1.3 \mu\text{m}$ ,



**Table 6.1:** Values of coupling efficiencies for the refractive index profile exponent  $g = 8$ ,  $V$  value 1.924, excited by  $1.3 \mu\text{m}$  with  $w_f = 4.714 \mu\text{m}$ ,  $w_{1x} = 1.081 \mu\text{m}$  and  $w_{1y} = 1.161 \mu\text{m}$ .

$u$	$R_L = 1$	$R_L = 6$	$R_L = 8$	$R_L = 8.5$	$R_L = 9$	$R_L = 11$	$R_L = 16$	$R_L = 21$
1	0.284	15.775	19.373	19.874	20.250	20.941	20.988	20.863
6	0.125	40.965	41.515	41.408	40.424	37.758	32.693	30.233
11	0.036	68.187	76.549	75.363	71.548	60.940	44.963	38.361
12	0.030	64.847	81.960	81.250	77.602	65.946	47.4849	39.910
13	0.025	58.701	85.084	85.332	82.519	70.699	49.970	41.415
14	0.021	51.282	85.370	86.977	85.708	74.929	52.375	42.861
16	0.016	37.095	77.858	82.377	85.460	80.661	56.736	45.506
21	0.009	16.608	44.229	50.079	58.335	72.904	62.385	49.773
31	0.004	5.293	13.984	16.146	19.754	31.407	46.707	44.505

**Table 6.2:** Values of coupling efficiencies for the refractive index profile exponent  $g = 8$ ,  $V$  value 2.164, excited by  $1.3 \mu\text{m}$  with  $w_f = 2.164 \mu\text{m}$ ,  $w_{1x} = 1.081 \mu\text{m}$  and  $w_{1y} = 1.161 \mu\text{m}$ .

$u$	$R_L = 1$	$R_L = 7$	$R_L = 7.5$	$R_L = 8$	$R_L = 8.5$	$R_L = 11$	$R_L = 16$	$R_L = 21$
1	0.469	24.290	25.009	25.523	25.506	26.482	26.326	26.173
6	0.208	53.606	52.584	51.680	50.334	45.749	39.695	36.884
11	0.061	85.412	84.892	83.181	80.416	67.108	51.251	44.504
12	0.051	85.553	86.958	86.291	83.952	70.697	53.190	45.681
13	0.043	82.642	86.325	87.142	85.582	73.651	54.920	46.715
14	0.036	77.292	83.137	85.633	85.106	75.787	56.397	47.592
16	0.027	62.984	71.516	76.826	78.457	77.086	58.441	48.821
21	0.015	32.774	39.991	46.016	49.503	64.463	57.332	48.526
31	0.006	11.021	13.685	16.153	17.818	29.752	38.575	37.284

**Table 6.3:** Values of coupling efficiencies for the refractive index profile exponent  $g = 8$ ,  $V$  value 2.700, excited by  $1.3 \mu\text{m}$  with  $w_f = 5.008 \mu\text{m}$ ,  $w_{1x} = 1.081 \mu\text{m}$  and  $w_{1y} = 1.161 \mu\text{m}$ .

$u$	$R_L = 1$	$R_L = 6$	$R_L = 6.5$	$R_L = 7$	$R_L = 7.5$	$R_L = 11$	$R_L = 16$	$R_L = 21$
1	0.871	31.632	32.691	33.480	33.938	34.511	34.213	34.058
6	0.391	68.102	67.254	66.831	64.974	55.642	48.874	45.785
10	0.142	85.901	87.470	87.747	85.607	68.975	56.066	50.332
11	0.116	83.199	86.693	87.971	86.877	70.961	57.086	50.846
12	0.096	77.934	83.323	85.736	86.034	72.184	57.752	51.112
13	0.081	71.061	77.960	81.430	83.230	72.151	58.050	51.132
16	0.051	49.174	57.382	62.402	67.412	68.985	56.788	49.806
21	0.029	25.543	31.178	35.098	40.115	53.261	49.171	44.096
31	0.012	9.263	11.457	13.064	15.354	25.852	29.915	29.259

respectively, for the four kind of optical fibers having refractive index distribution profile indices 4, 8, 10 and 20, respectively, and for different  $V$  values. From the analysis it is clear that wavelength  $1.3 \mu\text{m}$  is more efficient coupler than the wavelength  $1.5 \mu\text{m}$ .

Analyzing Tables 9 and 10, it is observed that the maximum coupling efficiency is obtained for the refractive index profile exponent  $g = 4$ , excited by the wavelength  $1.3 \mu\text{m}$  for different  $V$  values used. The micro or macro optical designers will be beneficial from the detail data given in

**Table 7.1:** Values of coupling efficiencies for the refractive index profile exponent  $g = 10$ ,  $V$  value 1.924, excited by  $1.3 \mu\text{m}$  with  $w_f = 4.715 \mu\text{m}$ ,  $w_{1x} = 1.081 \mu\text{m}$  and  $w_{1y} = 1.161 \mu\text{m}$ .

$u$	$R_L = 1$	$R_L = 6$	$R_L = 8$	$R_L = 8.5$	$R_L = 9$	$R_L = 11$	$R_L = 16$	$R_L = 21$
1	0.284	15.770	19.366	19.867	20.242	20.933	20.980	20.855
6	0.125	40.954	41.503	41.396	40.412	37.746	32.682	30.223
11	0.036	68.184	76.543	75.356	71.540	60.930	44.952	38.351
12	0.030	64.845	81.958	81.248	77.598	65.938	47.475	39.901
13	0.025	58.699	85.086	85.333	82.519	70.694	49.961	41.406
14	0.021	51.278	85.375	86.982	85.712	74.927	52.368	42.853
15	0.018	43.838	82.799	85.930	86.741	78.343	54.644	44.224
16	0.016	37.090	77.865	82.386	85.470	80.667	56.732	45.500
21	0.009	16.604	44.228	50.081	58.340	72.919	62.393	49.774
31	0.004	5.291	13.981	16.144	19.752	31.409	46.721	44.517

**Table 7.2:** Values of coupling efficiencies for the refractive index profile exponent  $g = 10$ ,  $V$  value 2.124, excited by  $1.3 \mu\text{m}$  with  $w_f = 4.230 \mu\text{m}$ ,  $w_{1x} = 1.081 \mu\text{m}$  and  $w_{1y} = 1.161 \mu\text{m}$ .

$u$	$R_L = 1$	$R_L = 7$	$R_L = 7.5$	$R_L = 8$	$R_L = 8.5$	$R_L = 11$	$R_L = 16$	$R_L = 21$
1	0.429	23.109	23.855	24.404	24.793	25.461	25.337	25.189
6	0.190	51.626	50.731	49.945	49.431	44.346	38.444	35.689
11	0.068	80.833	79.163	77.041	75.385	61.963	48.028	42.108
12	0.056	84.421	84.005	82.372	80.847	66.211	50.235	43.482
13	0.046	84.897	86.478	85.912	84.868	70.085	52.305	44.747
14	0.039	82.203	86.175	87.162	86.950	73.380	54.194	45.885
16	0.033	76.936	83.189	85.952	86.821	75.890	55.859	46.883
21	0.014	31.139	39.605	45.956	50.464	65.988	58.332	48.910
31	0.006	10.657	13.333	15.851	17.836	30.155	39.910	38.495

**Table 7.3:** Values of coupling efficiencies for the refractive index profile exponent  $g = 10$ ,  $V$  value 2.650, excited by  $1.3 \mu\text{m}$  with  $w_f = 3.596 \mu\text{m}$ ,  $w_{1x} = 1.081 \mu\text{m}$  and  $w_{1y} = 1.161 \mu\text{m}$ .

$u$	$R_L = 1$	$R_L = 6$	$R_L = 6.5$	$R_L = 7$	$R_L = 7.5$	$R_L = 11$	$R_L = 16$	$R_L = 21$
1	0.799	30.370	31.431	32.267	32.783	33.443	33.152	33.002
6	0.358	66.395	65.599	65.301	63.576	47.726	47.726	44.666
9	0.162	84.567	84.623	84.339	81.727	54.434	53.830	48.667
10	0.0130	85.375	87.023	87.444	85.381	68.459	55.329	49.542
11	0.106	82.918	86.580	88.044	87.055	70.731	56.517	50.183
12	0.088	77.771	83.429	86.089	86.556	72.265	57.368	50.588
16	0.047	48.840	57.409	62.785	68.233	70.138	57.197	49.887
21	0.026	25.127	30.906	35.019	40.350	54.637	50.235	44.779
31	0.011	9.022	11.227	12.874	15.243	26.401	30.894	30.185

**Table 8.1:** Values of coupling efficiencies for the refractive index profile exponent  $g = 20$ ,  $V$  value 1.924, excited by  $1.3 \mu\text{m}$  with  $w_f = 4.858 \mu\text{m}$ ,  $w_{1x} = 1.081 \mu\text{m}$  and  $w_{1y} = 1.161 \mu\text{m}$ .

$u$	$R_L = 1$	$R_L = 6$	$R_L = 9$	$R_L = 9.5$	$R_L = 10$	$R_L = 11$	$R_L = 16$	$R_L = 21$
1	0.253	14.534	19.010	19.307	19.480	19.792	19.878	19.779
6	0.111	38.313	38.332	37.805	37.046	35.987	31.159	28.817
11	0.032	65.667	69.586	66.948	63.825	59.224	43.385	36.917
12	0.027	62.516	76.019	73.216	69.750	64.463	45.979	38.510
13	0.022	56.504	81.427	78.816	75.274	69.550	48.576	40.078
14	0.019	49.202	85.154	83.197	79.965	74.210	51.133	41.609
16	0.014	35.303	85.759	86.395	85.112	80.977	55.927	44.492
21	0.008	15.572	58.366	64.279	69.265	74.618	63.178	49.710
31	0.003	4.911	19.218	22.232	25.608	31.517	48.637	46.200

**Table 8.2:** Values of coupling efficiencies for the refractive index profile exponent  $g = 20$ ,  $V$  value 2.004, excited by  $1.3 \mu\text{m}$  with  $w_f = 4.642 \mu\text{m}$ ,  $w_{1x} = 1.081 \mu\text{m}$  and  $w_{1y} = 1.161 \mu\text{m}$ .

$u$	$R_L = 1$	$R_L = 7$	$R_L = 8$	$R_L = 8.5$	$R_L = 9$	$R_L = 11$	$R_L = 16$	$R_L = 21$
1	0.301	18.616	20.042	20.534	20.897	21.560	21.565	21.436
6	0.133	43.547	42.691	42.538	41.493	38.702	33.478	30.975
11	0.039	79.002	77.529	76.303	72.468	61.822	45.739	39.099
12	0.032	80.775	82.700	81.953	78.310	66.699	48.214	40.621
13	0.027	78.975	85.568	85.763	82.962	71.271	50.633	42.087
14	0.023	74.087	85.641	87.155	85.870	75.274	52.950	43.483
15	0.020	67.198	82.933	85.916	86.645	78.427	55.115	44.792
16	0.017	59.490	77.960	82.281	85.192	80.477	57.071	45.993
21	0.009	28.950	44.600	50.280	58.226	72.036	61.897	49.754
31	0.004	9.079	14.277	16.428	19.997	31.330	45.707	43.639

**Table 8.3:** Values of coupling efficiencies for the refractive index profile exponent  $g = 20$ ,  $V$  value 2.500, excited by  $1.3 \mu\text{m}$  with  $w_f = 3.868 \mu\text{m}$ ,  $w_{1x} = 1.081 \mu\text{m}$  and  $w_{1y} = 1.161 \mu\text{m}$ .

$u$	$R_L = 1$	$R_L = 6$	$R_L = 7$	$R_L = 7.5$	$R_L = 8$	$R_L = 11$	$R_L = 16$	$R_L = 21$
1	0.603	25.866	27.959	28.606	29.056	29.691	29.428	29.291
6	0.269	59.642	59.334	57.994	56.841	49.952	43.472	40.549
10	0.097	82.298	85.371	83.477	81.210	66.039	52.260	46.359
11	0.079	80.749	87.364	86.639	84.895	69.300	53.987	47.398
12	0.065	76.074	86.489	87.468	86.687	71.952	55.461	48.254
13	0.055	69.312	82.954	85.868	86.373	73.846	56.645	48.918
14	0.047	61.629	77.398	82.122	84.025	74.868	57.510	49.380
16	0.035	46.816	63.459	70.506	74.722	74.113	58.199	49.681
21	0.019	23.212	34.204	40.594	45.692	59.812	54.048	47.000
31	0.008	8.041	12.003	14.578	16.884	28.311	34.731	33.781

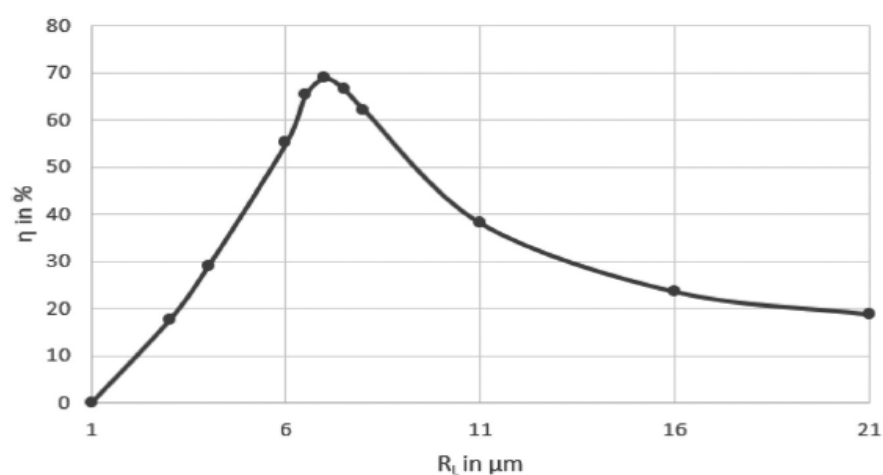


**Figure 1.1a:**  $\eta$  versus radius of the fiber ( $r$ ) for RI profile exponent  $g = 4$  having  $V$  value 1.924 ( $w_f = 5.008 \mu\text{m}$ ) and excitation wavelength  $1.5 \mu\text{m}$ .

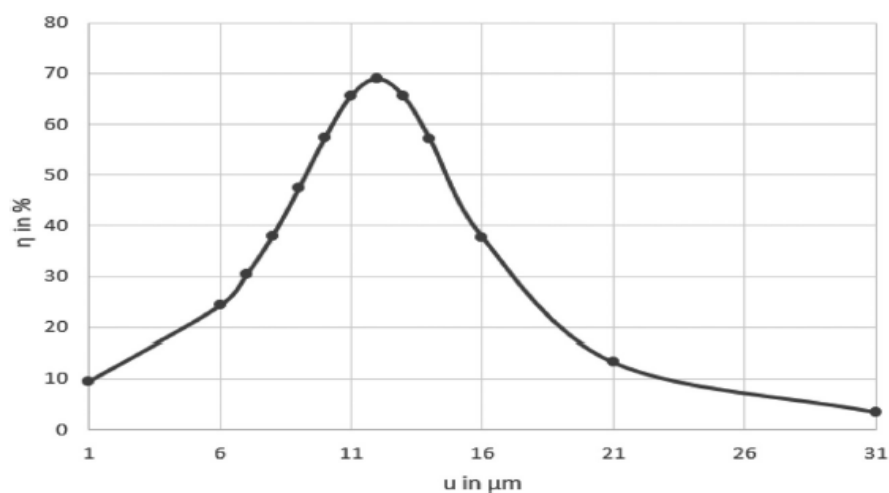


**Figure 1.1b:**  $\eta$  versus  $u$  of the fiber for RI profile exponent  $g = 4$  having  $V$  value 1.924 ( $w_f = 5.008 \mu\text{m}$ ) and excitation wavelength  $1.5 \mu\text{m}$ .

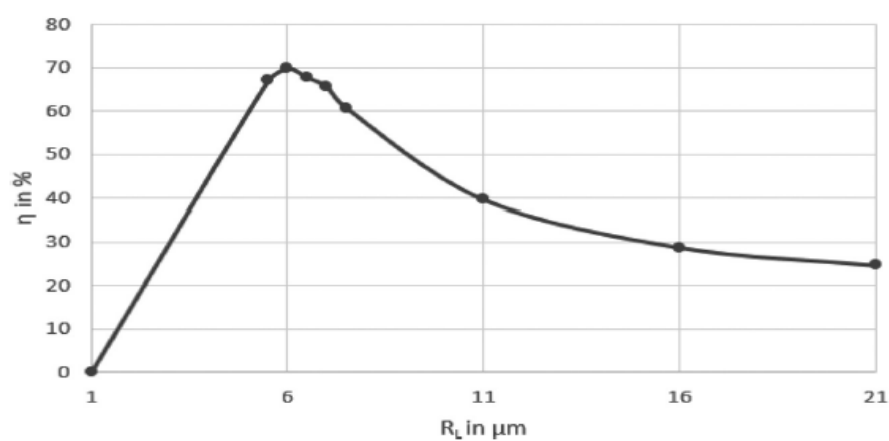


**Figure 1.2a:**  $\eta$  versus radius of the fiber ( $r$ ) for RI profile exponent  $g = 4$  having  $V$  value 2.405 ( $w_f = 3.831 \mu\text{m}$ ) and excitation wavelength  $1.5 \mu\text{m}$ .

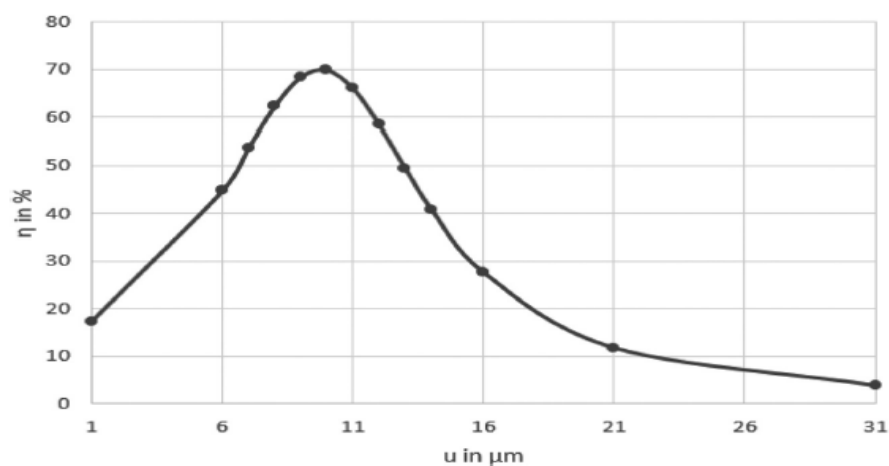


**Figure 1.2b:**  $\eta$  versus  $u$  of the fiber for RI profile exponent  $g = 4$  having  $V$  value 2.405 ( $w_f = 3.831 \mu\text{m}$ ) and excitation wavelength  $1.5 \mu\text{m}$ .

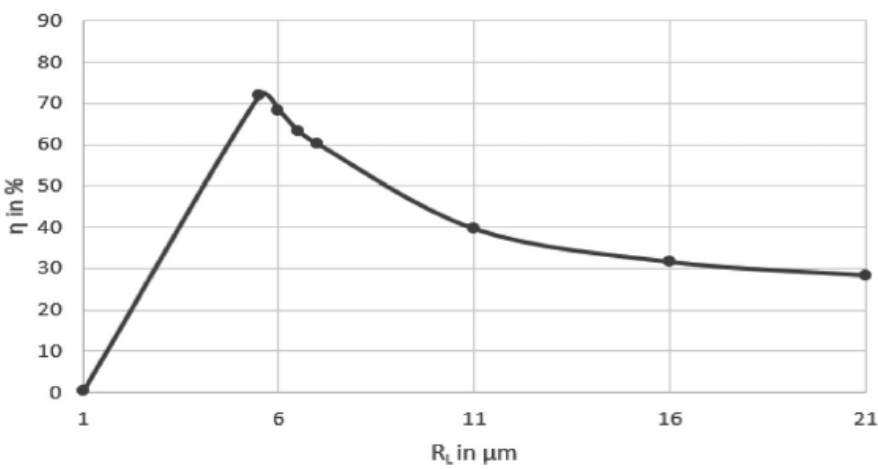


**Figure 1.3a:**  $\eta$  versus radius of the fiber ( $\eta$ ) for RI profile exponent  $g = 4$  having  $V$  value 3.000 ( $w_f = 3.284 \mu\text{m}$ ) and excitation wavelength  $1.5 \mu\text{m}$ .

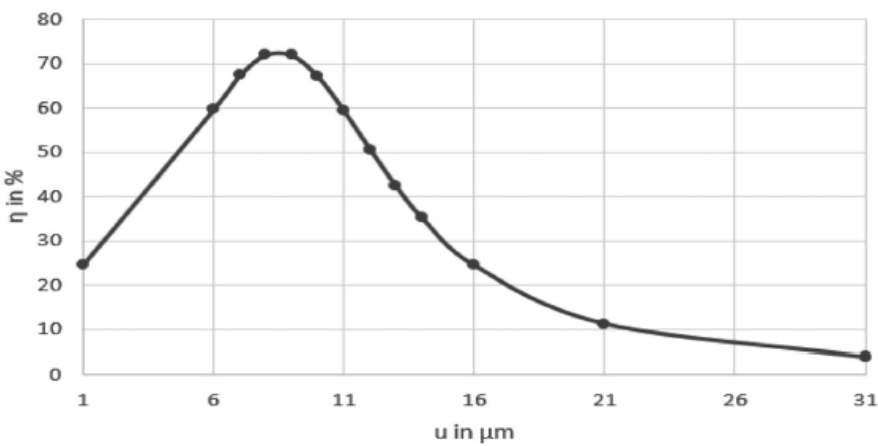


**Figure 1.3b:**  $\eta$  versus  $u$  of the fiber for RI profile exponent  $g = 4$  having  $V$  value 3.000 ( $w_f = 3.284 \mu\text{m}$ ) and excitation wavelength  $1.5 \mu\text{m}$ .

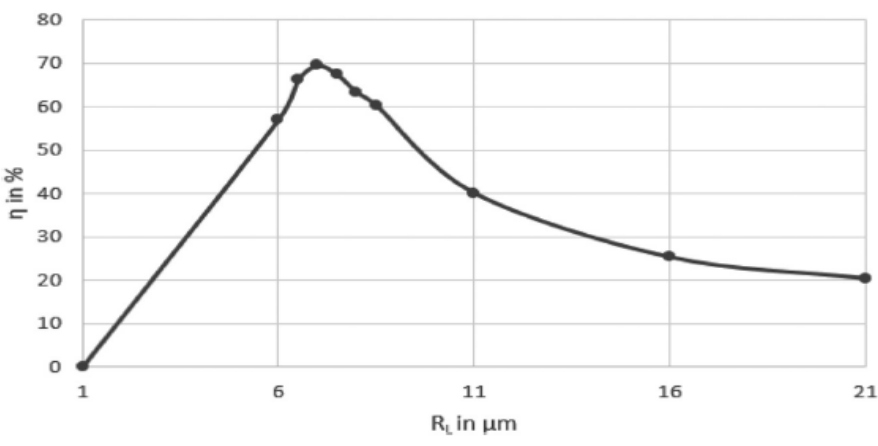


**Figure 2.1a:**  $\eta$  versus radius of the fiber ( $\eta$ ) for RI profile exponent  $g = 8$  having  $V$  value 1.924 ( $w_f = 4.714 \mu\text{m}$ ) and excitation wavelength  $1.5 \mu\text{m}$ .

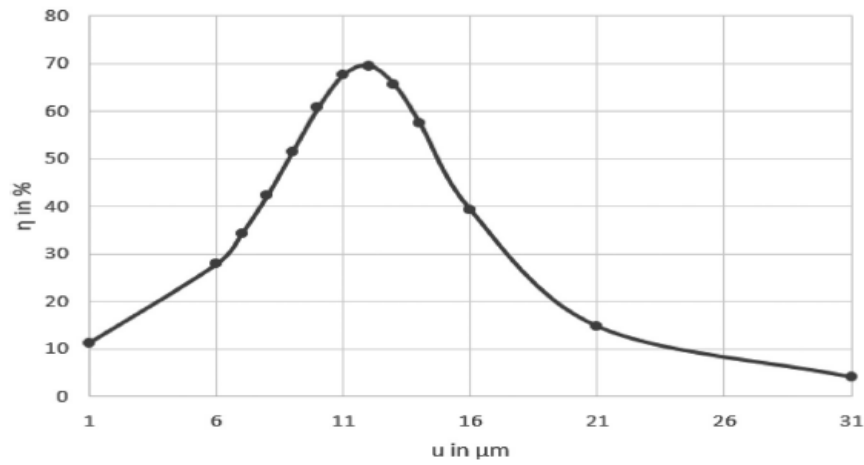


**Figure 2.1b:**  $\eta$  versus  $u$  of the fiber for RI profile exponent  $g = 8$  having  $V$  value 1.924 ( $w_f = 4.714 \mu\text{m}$ ) and excitation wavelength  $1.5 \mu\text{m}$ .

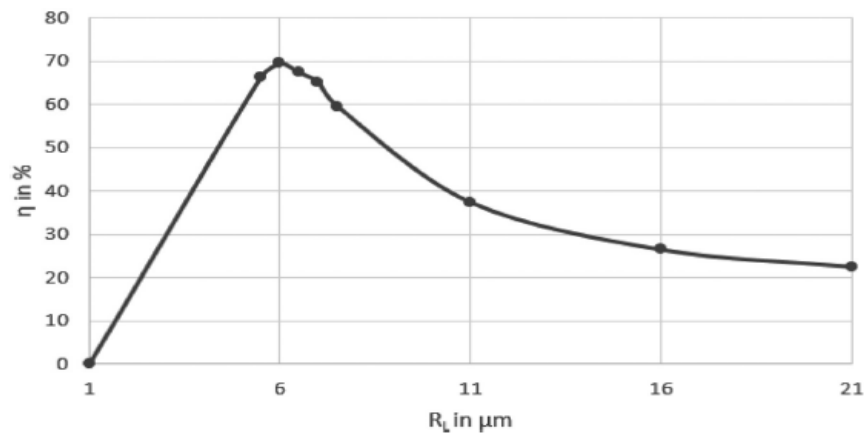


**Figure 2.2a:**  $\eta$  versus radius of the fiber ( $r$ ) for RI profile exponent  $g = 8$  having  $V$  value 2.164 ( $w_f = 4.136 \mu\text{m}$ ) and excitation wavelength  $1.5 \mu\text{m}$ .

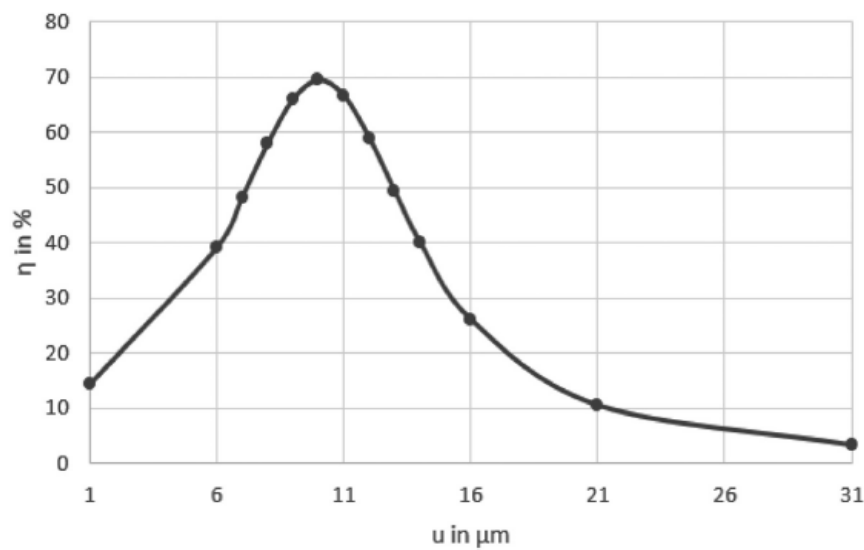


**Figure 2.2b:**  $\eta$  versus  $u$  of the fiber for refractive index profile exponent  $g = 8$  having  $V$  value 2.164 ( $w_f = 4.136 \mu\text{m}$ ) and excitation wavelength  $1.5 \mu\text{m}$ .

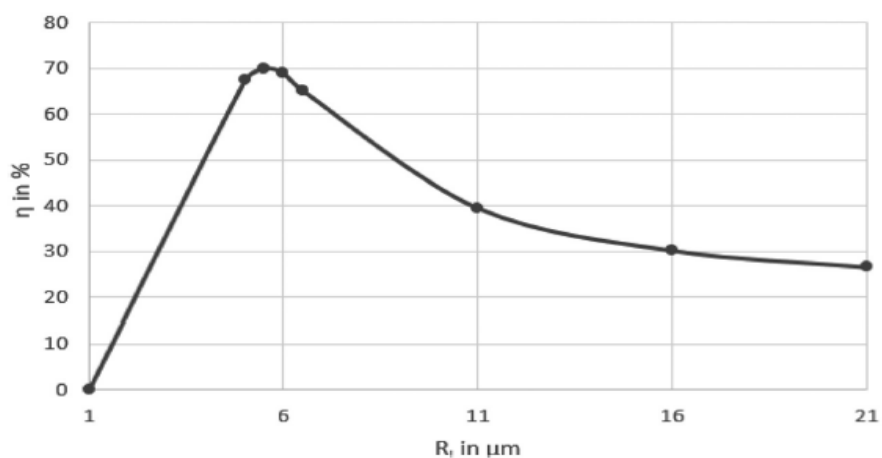


**Figure 2.3a:**  $\eta$  versus radius of the fiber ( $r$ ) for RI profile exponent  $g = 8$  having  $V$  value 2.700 ( $w_f = 3.526 \mu\text{m}$ ) and excitation wavelength  $1.5 \mu\text{m}$ .

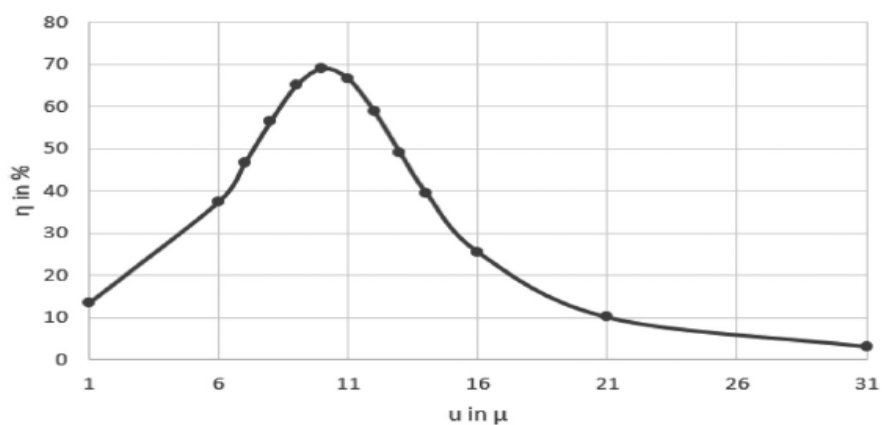


**Figure 2.3b:**  $\eta$  versus  $u$  of the fiber for RI profile exponent  $g = 8$  having  $V$  value 2.700 ( $w_f = 3.526 \mu\text{m}$ ) and excitation wavelength  $1.5 \mu\text{m}$ .

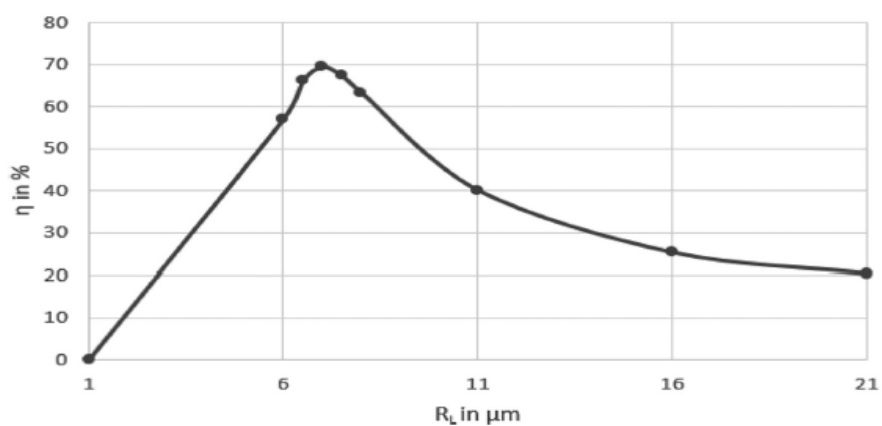


**Figure 3.1a:**  $\eta$  versus radius of the fiber ( $r$ ) for RI profile exponent  $g = 10$  having  $V$  value 1.924 ( $w_f = 4.715 \mu\text{m}$ ) and excitation wavelength  $1.5 \mu\text{m}$ .

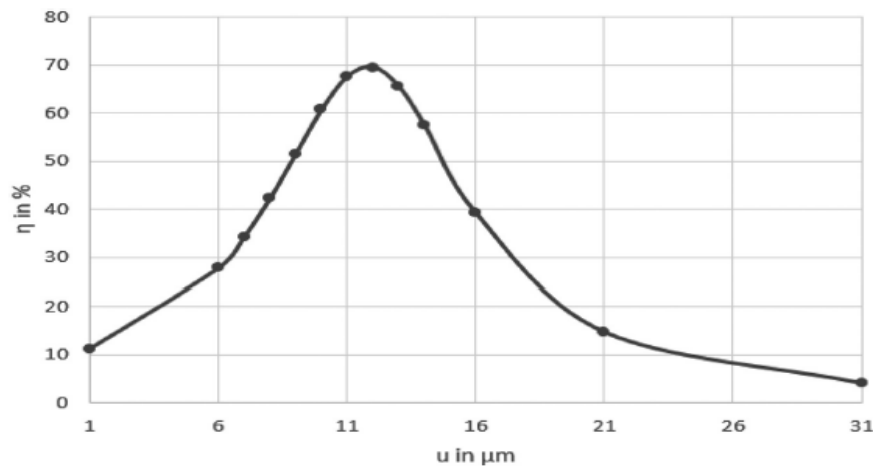


**Figure 3.1b:**  $\eta$  versus  $u$  of the fiber for RI profile exponent  $g = 10$  having  $V$  value 1.924 ( $w_f = 4.715 \mu\text{m}$ ) and excitation wavelength  $1.5 \mu\text{m}$ .

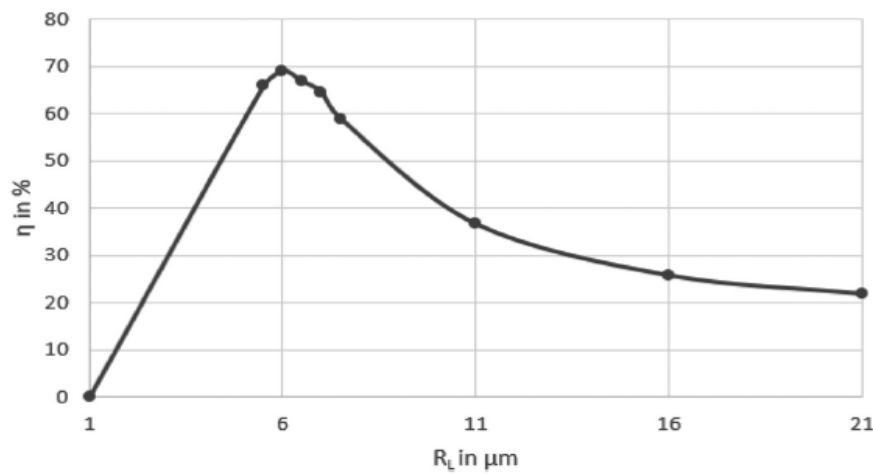


**Figure 3.2a:**  $\eta$  versus radius of the fiber ( $r$ ) for RI profile exponent  $g = 10$  having  $V$  value 2.124 ( $w_f = 4.230 \mu\text{m}$ ) and excitation wavelength  $1.5 \mu\text{m}$ .

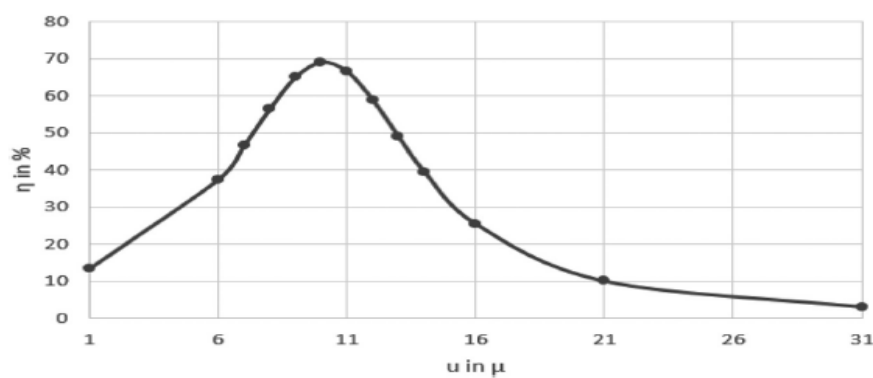


**Figure 3.2b:**  $\eta$  versus  $u$  of the fiber for RI profile exponent  $g = 10$  having  $V$  value 2.124 ( $w_f = 4.230 \mu\text{m}$ ) and excitation wavelength  $1.5 \mu\text{m}$ .



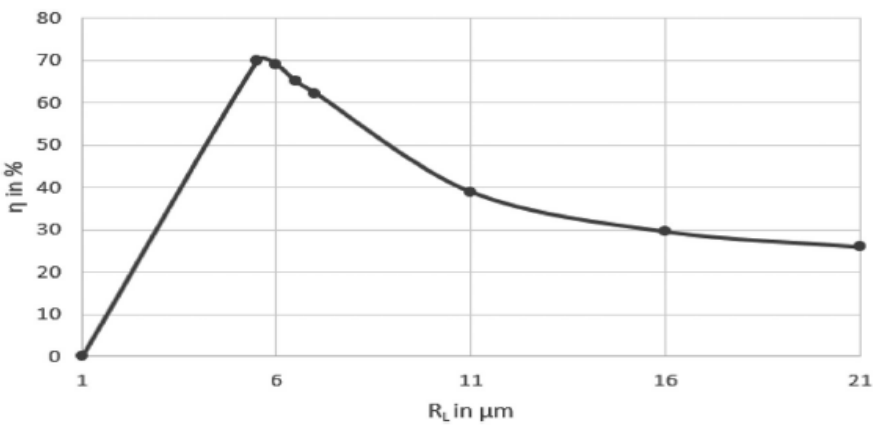


Figure 3.3a:  $\eta$  versus radius of the fiber ( $r$ ) for RI profile exponent  $g = 10$  having  $V$  value 2.650 ( $w_f = 3.596 \mu\text{m}$ ) and excitation wavelength  $1.5 \mu\text{m}$ .

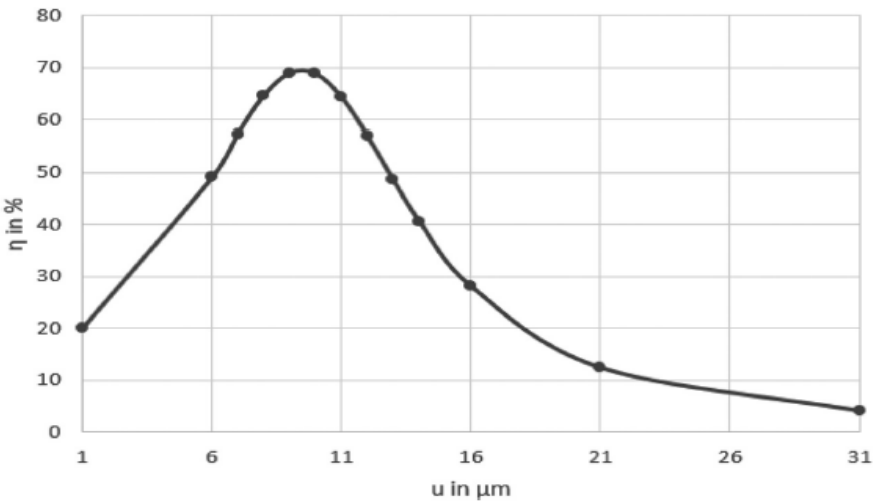


Figure 3.3b:  $\eta$  versus  $u$  of the fiber for RI profile exponent  $g = 10$  having  $V$  value 2.650 ( $w_f = 3.596 \mu\text{m}$ ) and excitation wavelength  $1.5 \mu\text{m}$ .

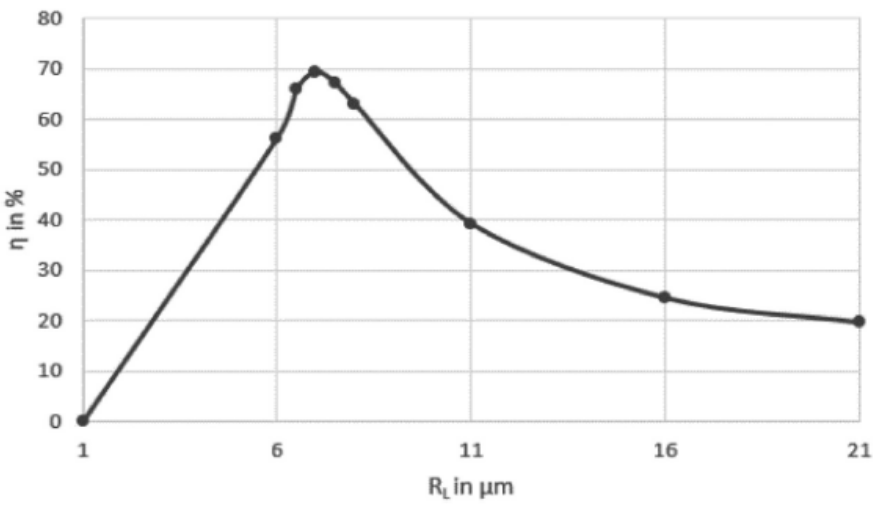
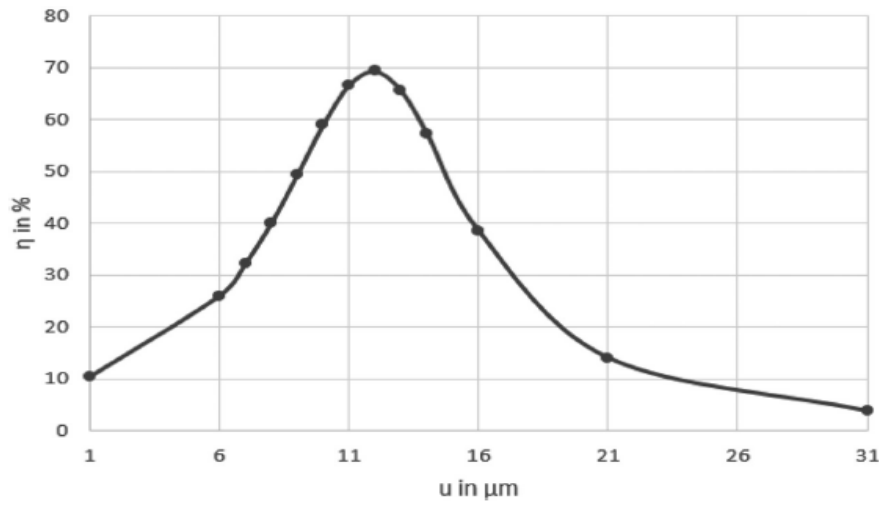
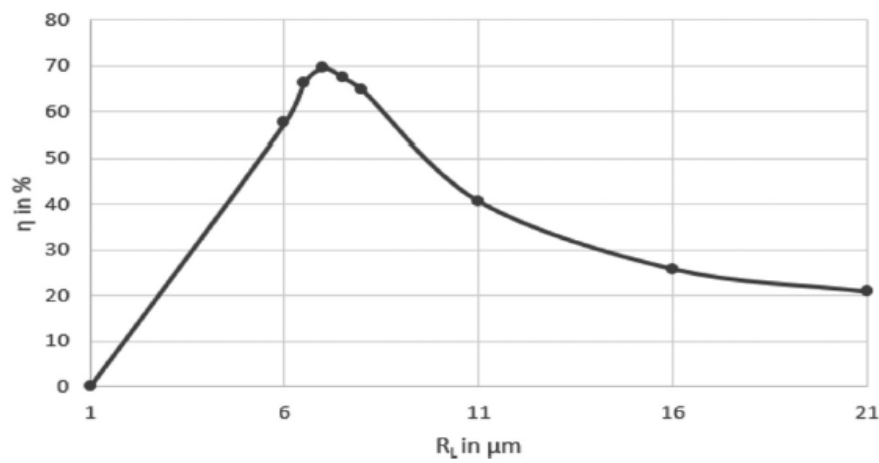


Figure 4.1a:  $\eta$  versus radius of the fiber ( $r$ ) for RI profile exponent  $g = 10$  having  $V$  value 1.924 ( $w_f = 4.858 \mu\text{m}$ ) and excitation wavelength  $1.5 \mu\text{m}$ .



**Figure 4.1b:**  $\eta$  versus  $u$  of the fiber for RI profile exponent  $g = 10$  having  $V$  value 1.924 ( $w_f = 4.858 \mu\text{m}$ ) and excitation wavelength  $1.5 \mu\text{m}$ .



**Figure 4.2a:**  $\eta$  versus radius of the fiber ( $r$ ) for RI profile exponent  $g = 10$  having  $V$  value 2.004 ( $w_f = 4.642 \mu\text{m}$ ) and excitation wavelength  $1.5 \mu\text{m}$ .

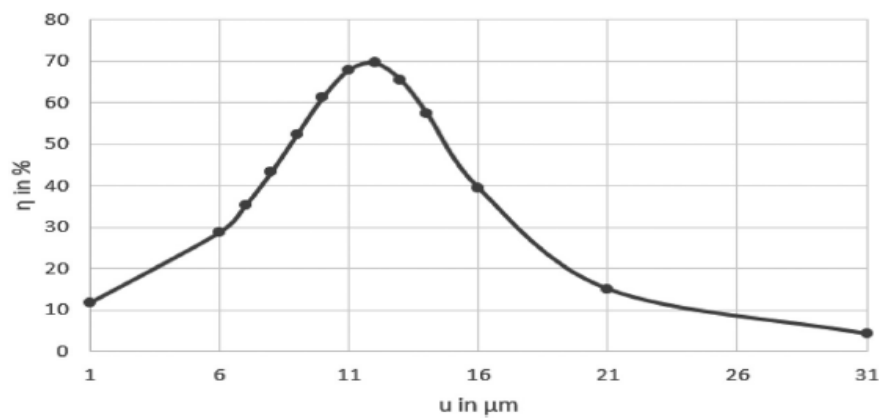


**Figure 4.2b:**  $\eta$  versus  $u$  of the fiber for RI profile exponent  $g = 10$  having  $V$  value 2.004 ( $w_f = 4.642 \mu\text{m}$ ) and excitation wavelength  $1.5 \mu\text{m}$ .

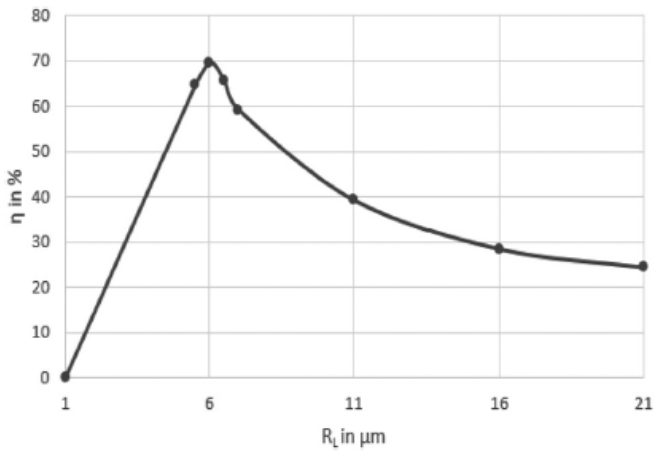


Figure 4.3a:  $\eta$  versus radius of the fiber ( $r$ ) for RI profile exponent  $g = 20$  having  $V$  value 2.500 ( $w_f = 3.868 \mu\text{m}$ ) and excitation wavelength  $1.5 \mu\text{m}$ .

the tables. Also as stated earlier, as the coupling efficiency along the horizontal plane of the source is quiet low, the study of the concerned coupling optics is restricted along the vertical plane only.

4 Conclusions

By ABCD matrix formalism, in this paper we had studied the coupling efficiencies of the laser to graded index fiber excitation via cylindrical micro lens for different profile exponents and for two different laser light sources. The wavelength  $1.3 \mu\text{m}$  is found to provide more efficient

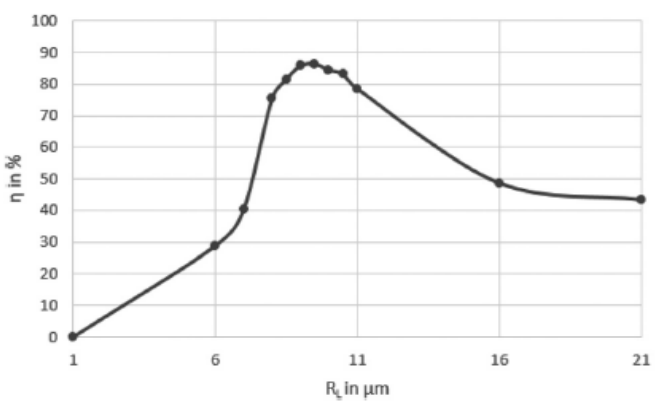


Figure 5.1a:  $\eta$  versus radius of the fiber ( $r$ ) for RI profile exponent  $g = 4$  having  $V$  value 1.924 ( $w_f = 5.008 \mu\text{m}$ ) and excitation wavelength  $1.3 \mu\text{m}$ .

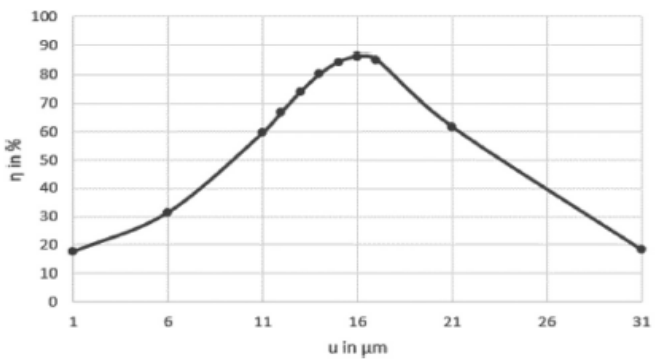


Figure 5.1b:  $\eta$  versus  $u$  of the fiber for RI profile exponent  $g = 4$  having  $V$  value 1.924 ( $w_f = 5.008 \mu\text{m}$ ) and excitation wavelength  $1.3 \mu\text{m}$ .

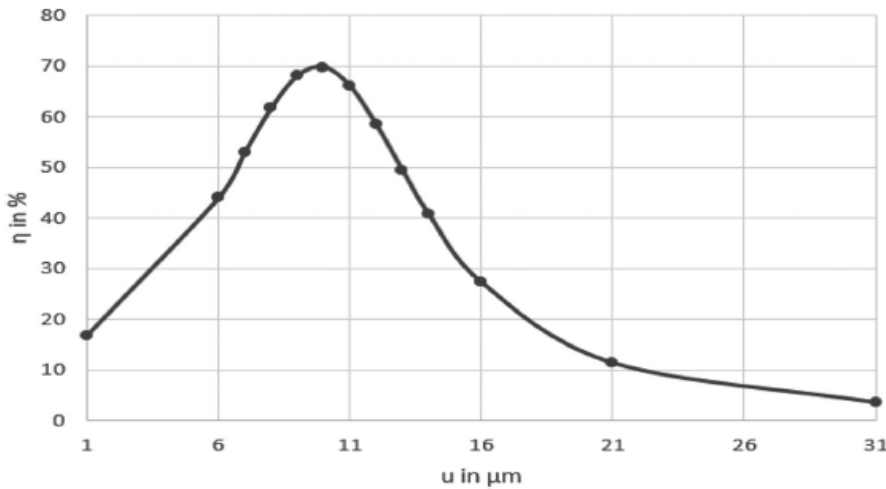
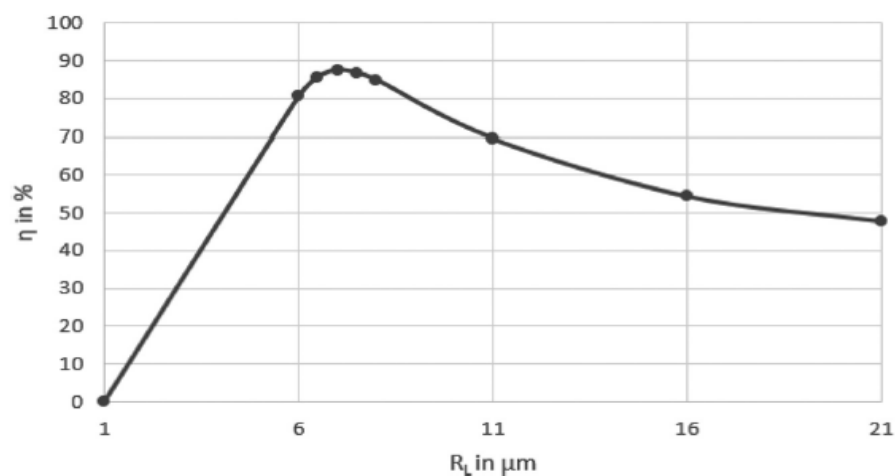
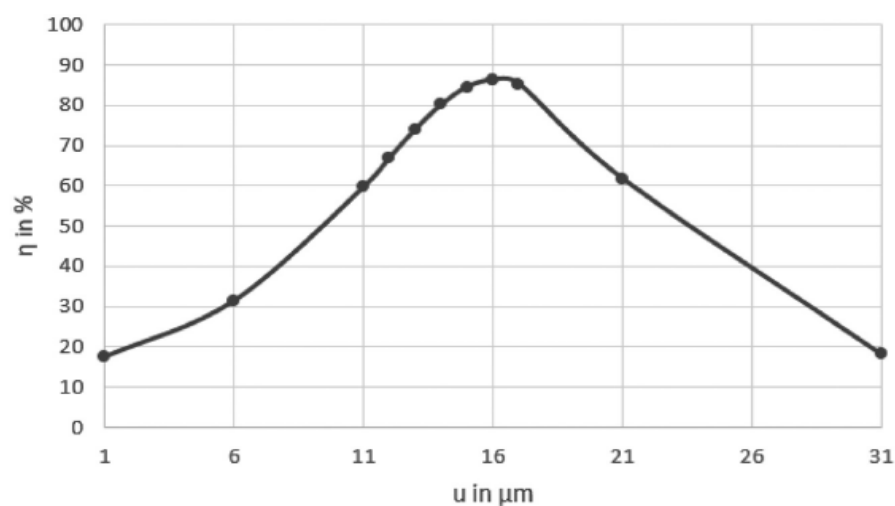


Figure 4.3b:  $\eta$  versus  $u$  of the fiber for RI profile exponent  $g = 20$  having  $V$  value 2.500 ( $w_f = 3.868 \mu\text{m}$ ) and excitation wavelength  $1.5 \mu\text{m}$ .



**Figure 5.2a:**  $\eta$  versus radius of the fiber ( $r$ ) for RI profile exponent  $g = 4$  having  $V$  value 2.405 ( $w_f = 3.831 \mu\text{m}$ ) and excitation wavelength  $1.3 \mu\text{m}$ .



**Figure 5.2b:**  $\eta$  versus  $u$  of the fiber for refractive index profile exponent  $g = 4$  having  $V$  value 2.405 ( $w_f = 3.831 \mu\text{m}$ ) and excitation wavelength  $1.3 \mu\text{m}$ .

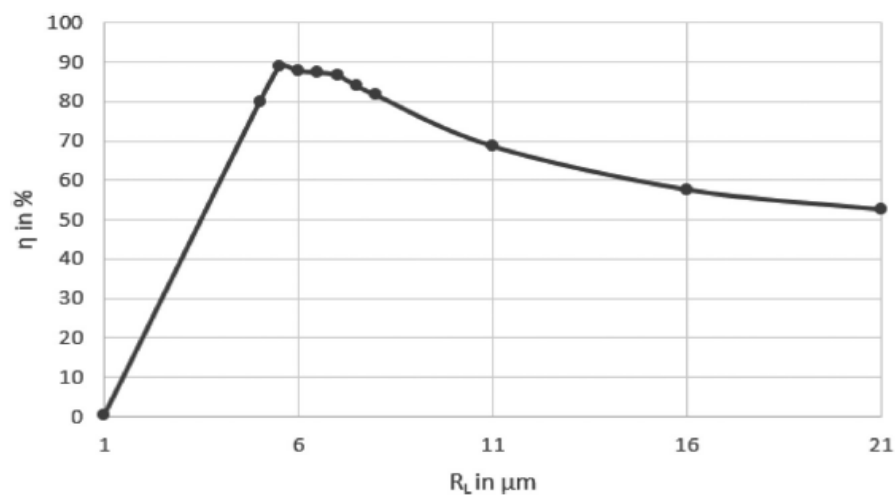


**Figure 5.3a:**  $\eta$  versus radius of the fiber ( $r$ ) for RI profile exponent  $g = 4$  having  $V$  value 3.000 ( $w_f = 3.284 \mu\text{m}$ ) and excitation wavelength  $1.3 \mu\text{m}$ .

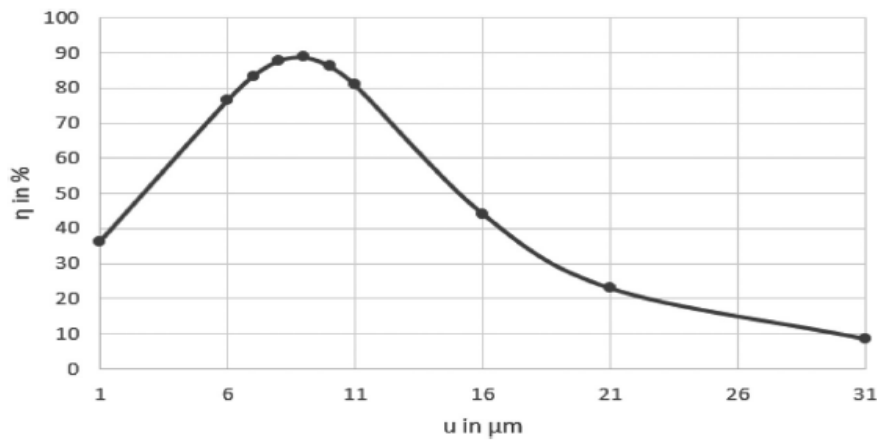


Figure 5.3b:  $\eta$  versus  $u$  of the fiber for RI profile exponent  $g = 4$  having  $V$  value 3.000 ( $w_f = 3.284 \mu\text{m}$ ) and excitation wavelength  $1.3 \mu\text{m}$ .

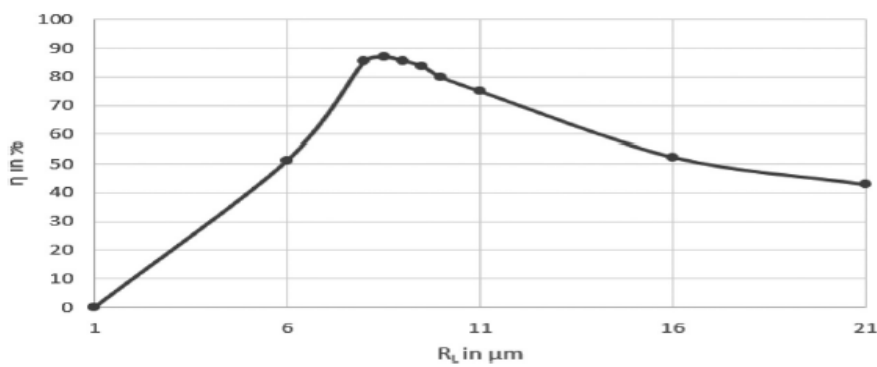


Figure 6.1a:  $\eta$  versus radius of the fiber ( $r$ ) for RI profile exponent  $g = 8$  having  $V$  value 1.924 ( $w_f = 4.714 \mu\text{m}$ ) and excitation wavelength  $1.3 \mu\text{m}$ .

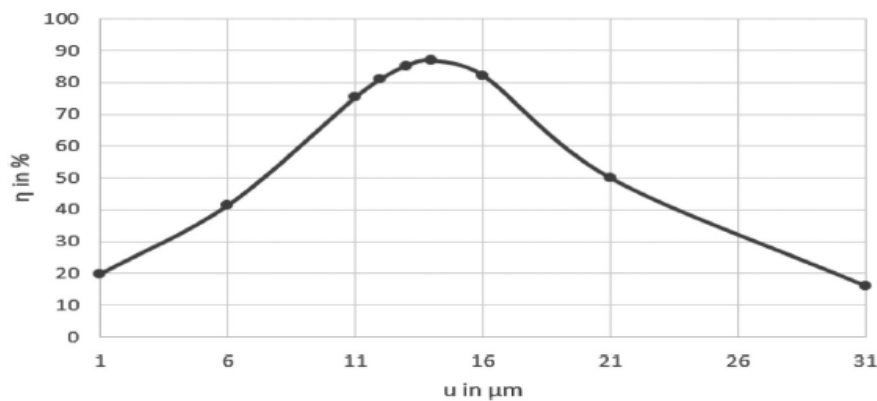


Figure 6.1b:  $\eta$  versus  $u$  of the fiber for RI profile exponent  $g = 8$  having  $V$  value 1.924 ( $w_f = 4.714 \mu\text{m}$ ) and excitation wavelength  $1.3 \mu\text{m}$ .

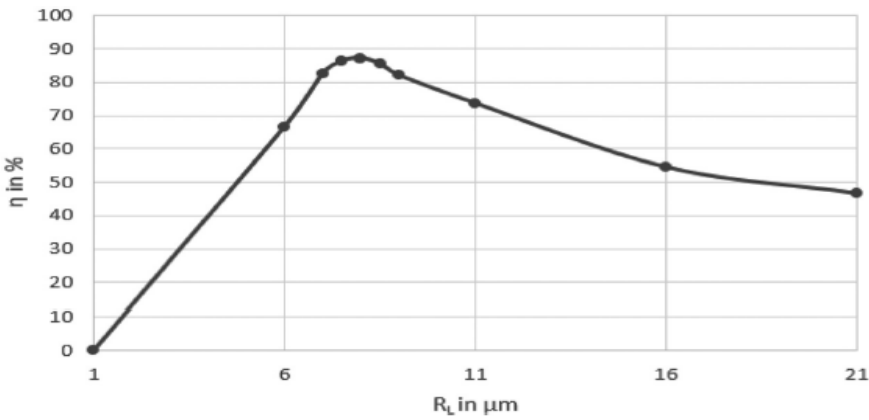


Figure 6.2a:  $\eta$  versus radius of the fiber ( $r$ ) for RI profile exponent  $g = 8$  having  $V$  value 2.164 ( $w_f = 4.136 \mu\text{m}$ ) and excitation wavelength  $1.3 \mu\text{m}$ .

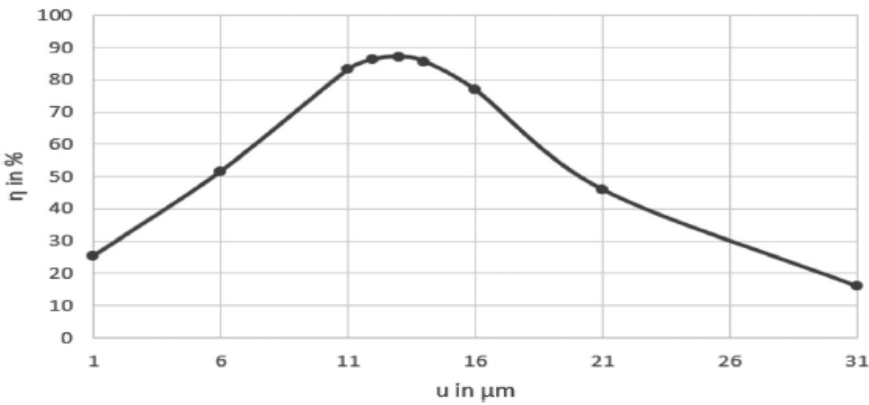


Figure 6.2b:  $\eta$  versus  $u$  of the fiber for RI profile exponent  $g = 8$  having  $V$  value 2.164 ( $w_f = 4.136 \mu\text{m}$ ) and excitation wavelength  $1.3 \mu\text{m}$ .

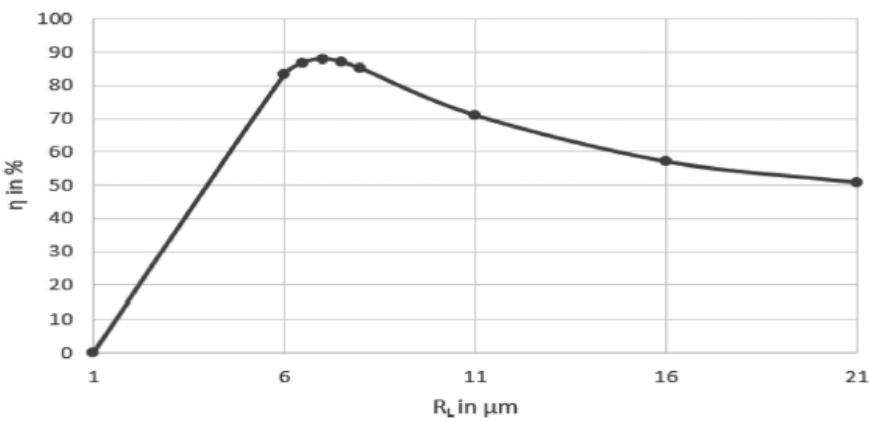


Figure 6.3a:  $\eta$  versus radius of the fiber ( $r$ ) for RI profile exponent  $g = 8$  having  $V$  value 2.700 ( $w_f = 3.526 \mu\text{m}$ ) and excitation wavelength  $1.3 \mu\text{m}$ .

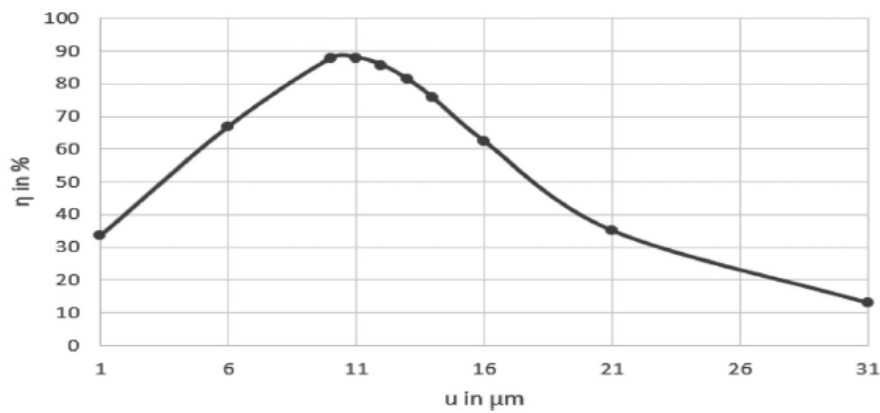


Figure 6.3b:  $\eta$  versus  $u$  of the fiber for RI profile exponent  $g = 8$  having  $V$  value 2.7000 ( $w_f = 3.526 \mu\text{m}$ ) and excitation wavelength  $1.3 \mu\text{m}$ .

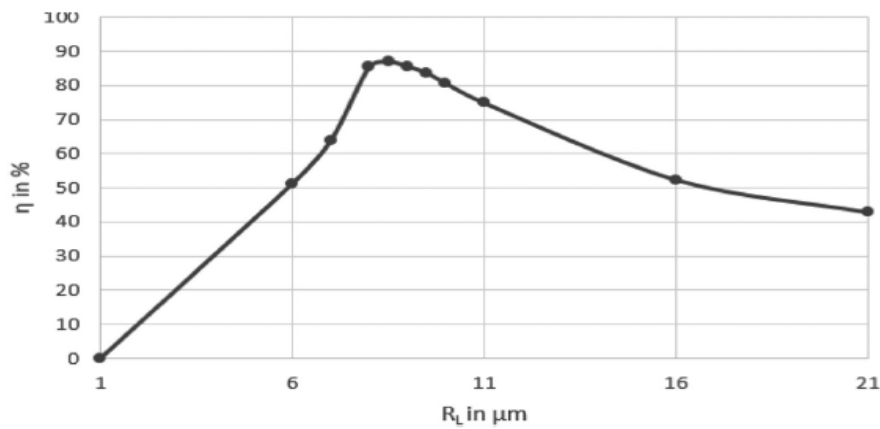


Figure 7.1a:  $\eta$  versus radius of the fiber ( $r$ ) for RI profile exponent  $g = 10$  having  $V$  value 1.924 ( $w_f = 4.715 \mu\text{m}$ ) and excitation wavelength  $1.3 \mu\text{m}$ .

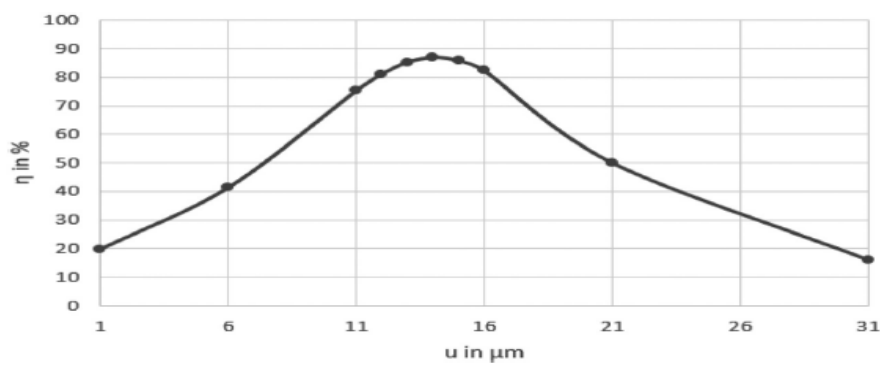


Figure 7.1b:  $\eta$  versus  $u$  of the fiber for RI profile exponent  $g = 10$  having  $V$  value 1.924 ( $w_f = 4.715 \mu\text{m}$ ) and excitation wavelength  $1.3 \mu\text{m}$ .

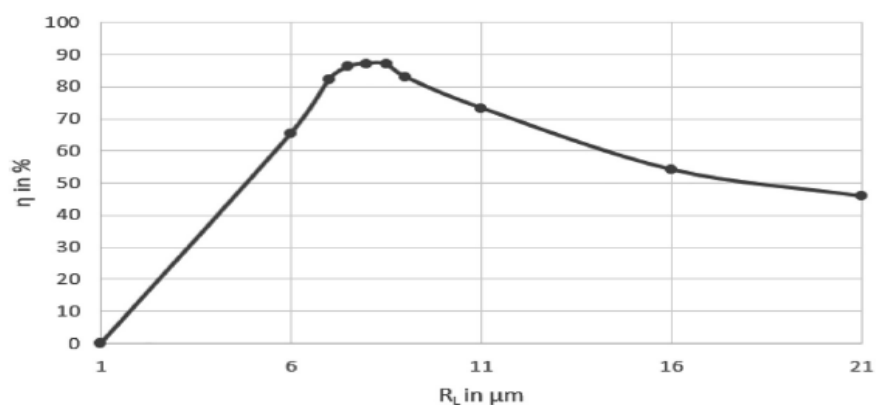


Figure 7.2a:  $\eta$  versus radius of the fiber ( $r$ ) for RI profile exponent  $g = 10$  having  $V$  value 2.124 ( $w_f = 4.230 \mu\text{m}$ ) and excitation wavelength  $1.3 \mu\text{m}$ .

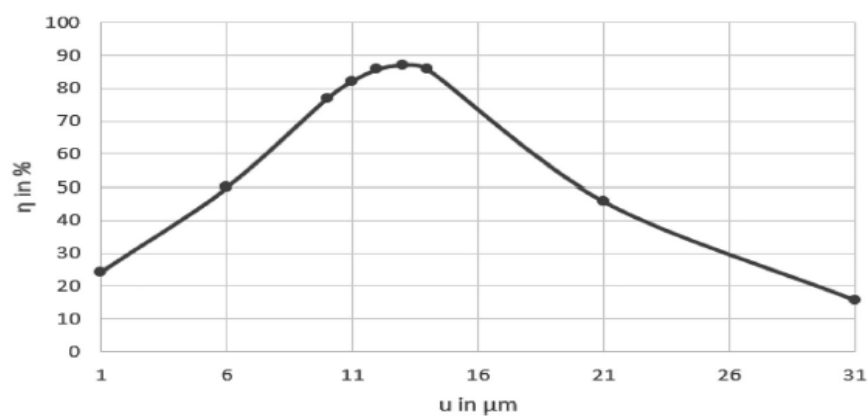


Figure 7.2b:  $\eta$  versus  $u$  of the fiber for RI profile exponent  $g = 10$  having  $V$  value 2.124 ( $w_f = 4.230 \mu\text{m}$ ) and excitation wavelength  $1.3 \mu\text{m}$ .

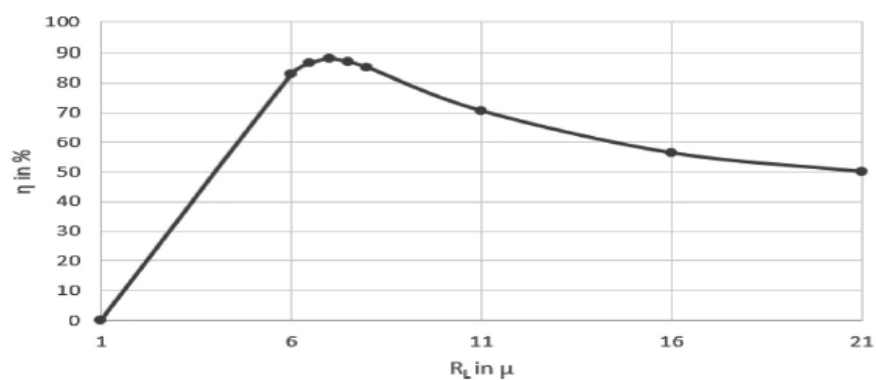
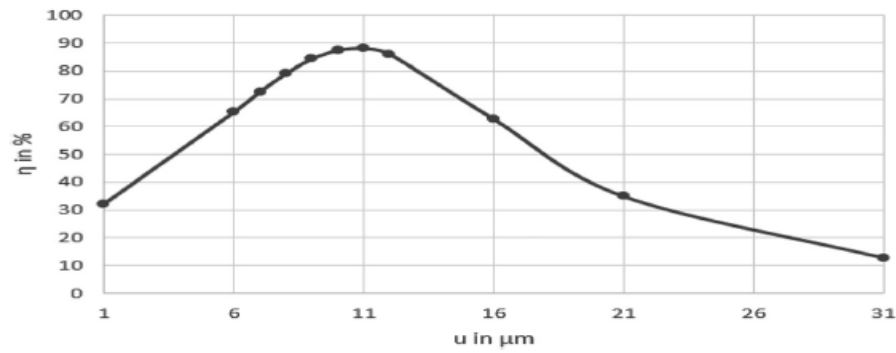
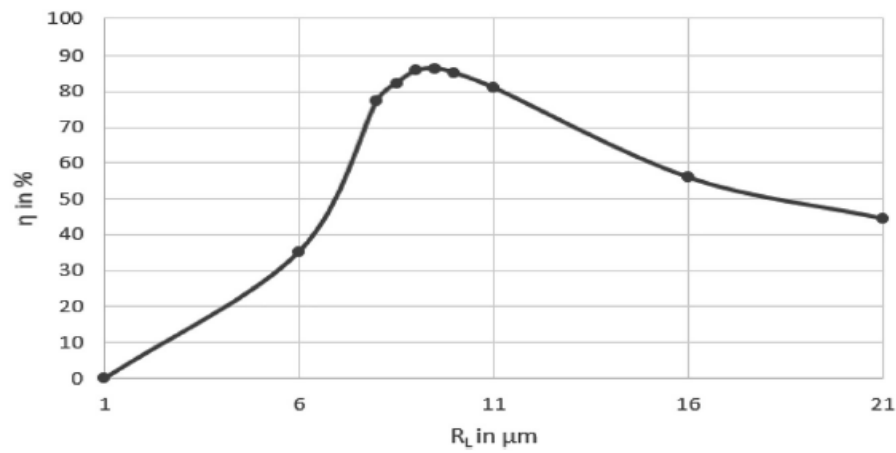


Figure 7.3a:  $\eta$  versus radius of the fiber ( $r$ ) for RI profile exponent  $g = 10$  having  $V$  value 2.650 ( $w_f = 3.596 \mu\text{m}$ ) and excitation wavelength  $1.3 \mu\text{m}$ .





**Figure 7.3b:**  $\eta$  versus  $u$  of the fiber for RI profile exponent  $g = 20$  having  $V$  value 2.650 ( $w_f = 3.596 \mu\text{m}$ ) and excitation wavelength  $1.3 \mu\text{m}$ .



**Figure 8.1a:**  $\eta$  versus radius of the fiber ( $r$ ) for RI profile exponent  $g = 20$  having  $V$  value 1.924 ( $w_f = 4.858 \mu\text{m}$ ) and excitation wavelength  $1.3 \mu\text{m}$ .

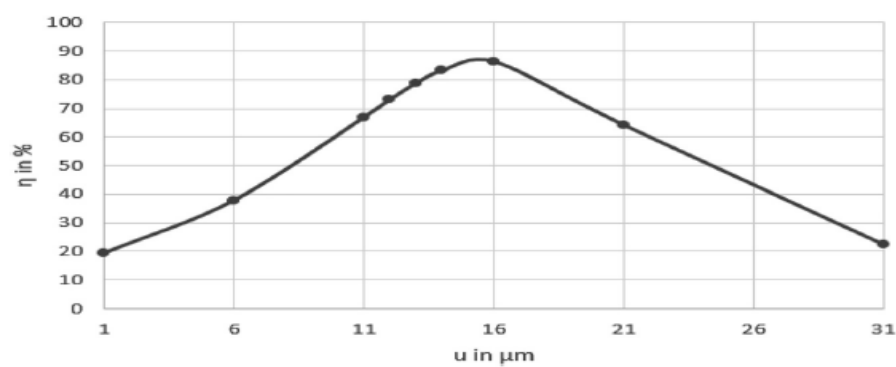


**Figure 8.1b:**  $\eta$  versus  $u$  of the fiber for RI profile exponent  $g = 20$  having  $V$  value 1.924 ( $w_f = 4.858 \mu\text{m}$ ) and excitation wavelength  $1.3 \mu\text{m}$ .

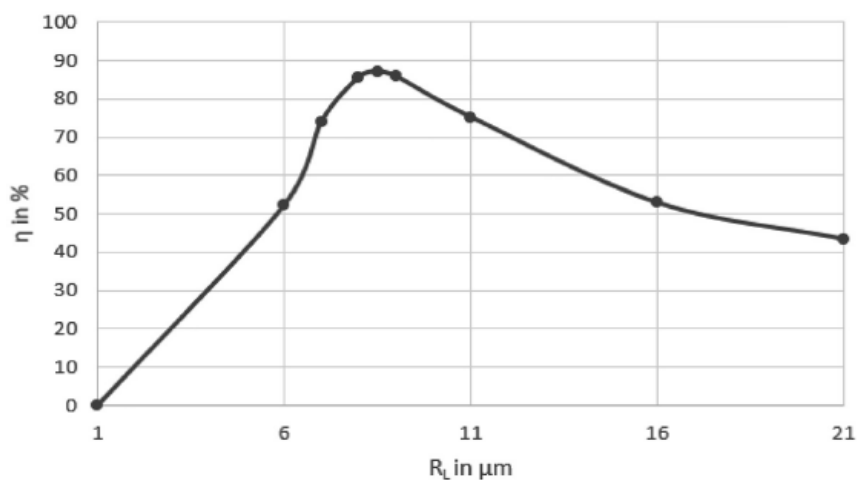


**Figure 8.2a:**  $\eta$  versus radius of the fiber ( $r$ ) for RI profile exponent  $g = 20$  having  $V$  value 2.004 ( $w_f = 4.645 \mu\text{m}$ ) and excitation wavelength  $1.3 \mu\text{m}$ .

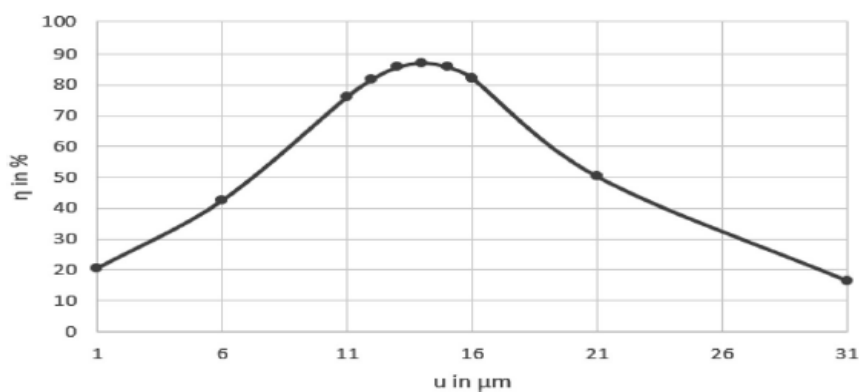


**Figure 8.2b:**  $\eta$  versus  $u$  of the fiber for RI profile exponent  $g = 20$  having  $V$  value 2.004 ( $w_f = 4.645 \mu\text{m}$ ) and excitation wavelength  $1.3 \mu\text{m}$ .

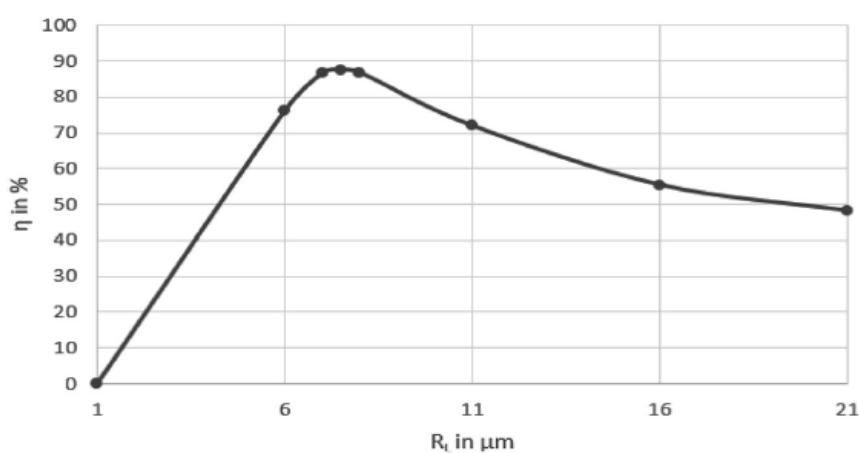


**Figure 8.3a:**  $\eta$  versus radius of the fiber ( $r$ ) for RI profile exponent  $g = 20$  having  $V$  value 2.500 ( $w_f = 3.868 \mu\text{m}$ ) and excitation wavelength  $1.3 \mu\text{m}$ .

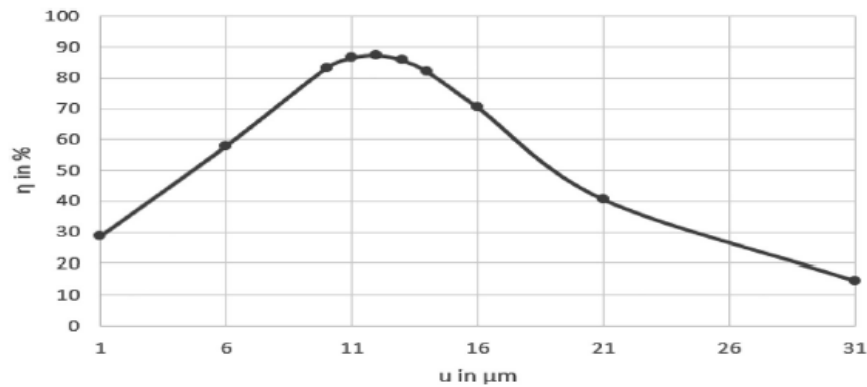


**Figure 8.3b:**  $\eta$  versus  $u$  of the fiber for RI profile exponent  $g = 20$  having  $V$  value 2.500 ( $w_f = 3.868 \mu\text{m}$ ) and excitation wavelength  $1.3 \mu\text{m}$ .

**Table 9:** Values of  $\eta$  for the refractive index profile exponents  $g = 4, 8, 10$  and 20, excitation wavelength  $1.5 \mu\text{m}$ ,  $w_{1x} = 0.843 \mu\text{m}$  and  $w_{1y} = 0.857 \mu\text{m}$ .

Profile index	$V$	$w_f$ in $\mu\text{m}$	$R_L$ in $\mu\text{m}$	$u$ in $\mu\text{m}$	$\eta_{\max}$ in %
4	1.924	5.008	7.0	12.0	68.979
	2.405	3.831	6.0	10.0	69.917
	3.000	3.284	5.5	8.0	72.000
8	1.924	4.714	7.0	12.0	69.552
	2.164	4.136	6.0	10.0	69.509
	2.700	3.526	5.5	9.0	70.026
10	1.924	4.715	7.0	12.0	69.563
	2.124	4.230	6.0	10.0	69.155
	2.650	3.596	5.5	9.0	70.054
20	1.924	4.858	7.0	12.0	69.335
	2.004	4.642	7.0	12.0	69.502
	2.500	3.868	6.0	10.0	69.787

**Table 10:** Values of  $\eta$  for the refractive index profile exponents  $g = 4, 8, 10$  and 20, excitation wavelength  $1.3 \mu\text{m}$ ,  $w_{1x} = 1.081 \mu\text{m}$ , and  $w_{1y} = 1.161 \mu\text{m}$ .

Profile index	$V$	$w_f$ in $\mu\text{m}$	$R_L$ in $\mu\text{m}$	$u$ in $\mu\text{m}$	$\eta_{\max}$ in %
4	1.924	5.008	9.5	16.0	86.357
	2.405	3.831	7.0	11.0	87.529
	3.000	3.284	5.5	9.0	88.797
8	1.924	4.714	8.5	14.0	86.977
	2.164	4.136	8.0	13.0	87.142
	2.700	3.526	7.0	11.0	87.971
10	1.924	4.715	8.5	14.0	86.982
	2.124	4.230	8.0	14.0	87.162
	2.650	3.596	7.0	11.0	88.045
20	1.924	4.858	9.5	16.0	86.395
	2.004	4.642	8.5	14.0	87.155
	2.500	3.868	7.5	12.0	87.468

coupling while the graded index fiber of profile exponent 4 is more effective in the context of coupling. The results reported in the paper will help the optical designers and packagers to choose the suitable coupler.

**Author contributions:** All the authors have accepted responsibility for the entire content of this submitted manuscript and approved submission.

**Research funding:** None declared.

**Conflict of interest statement:** The authors declare no conflicts of interest regarding this article.

## References

1. Edwards CA, Presby HM, Dragone C. Ideal microlenses for laser to fiber coupling. *IEEE J Lightwave Technol* 1993;11:252–7.
2. Presby HM, Edwards CA. Near 100% efficient fiber microlenses. *Electron Lett* 1992;28:582–4.
3. John J, Maclean TSM, Ghafouri-Shiraz H, Niblett J. Matching of single-mode fiber to laser diode by microlenses at 1.5–1.3  $\mu\text{m}$  wavelength. *IEEE Proc J Optoelectron* 1994;141:178–84.
4. Presby HM, Edwards CA. Efficient coupling of polarization maintaining fiber to laser diodes. *IEEE Photon Technol Lett* 1992;4:897–9.
5. Gangopadhyay S, Sarkar SN. Laser diode to single-mode fibre excited via hyperbolic lens on the fibre tip: formulation of ABCD matrix and efficiency computation. *J Opt Commun* 1996;132:55–60.
6. Edwards CA, Presby HM. Coupling-sensitivity comparison of hemispheric and hyperbolic microlens. *Appl Opt* 1993;32:1573–7.
7. Kurokawa K, Becker EE. Laser fiber coupling with a hyperbolic lens. *IEEE Trans Microw Theor Tech* 1975;23:309–11.
8. Gangopadhyay S, Sarkar SN. ABCD matrix for reflection and refraction of Gaussian light beams at surfaces of hyperboloid of revolution and efficiency computation for laser diode to singlemode fiber coupling by way of a hyperbolic lens on the fiber tip. *Appl Opt* 1997;36:8582–6.

9. Roy K, Majumdar A, Maity S, Gangopadhyay S. Laser diode to single-mode graded index fiber coupling via cylindrical microlens on the fiber tip: evaluation of coupling efficiency by ABCD matrix formalism. *J Opt Commun* 2020. <https://doi.org/10.1515/joc-2020-0234>.
10. Bose A, Gangopadhyay S, Saha SC. Laser diode to single mode circular core graded index fiber excitation via hemispherical microlens on the fiber tip: identification of suitable refractive index profile for maximum efficiency with consideration for allowable aperture. *J Opt Commun* 2012;33:15–9.
11. Mondal SK, Gangopadhyay S, Sarkar SN. Analysis of an upsidedown taper lens end from a single-mode step-index fiber. *Appl Opt* 1998;37:1006–9.
12. Yuan L, Qui A. Analysis of a single-mode fiber with taper lens end. *J Opt Soc Am* 1992;A9:950–2.
13. Mondal SK, Sarkar SN. Coupling of a laser diode to single-mode fiber with an upside-down tapered lens end. *Appl Opt* 1999;38:6272–7.
14. Yuan LB, Shou RL. Formation and power distribution properties of an upside-down tapered lens at the end of an optical fiber. *Sens Actuator* 1990;A23:1158–61.
15. Lie Y. Theoretical analysis of tapered fiber microlens parameter and its new fabricating technique. *IEEE Int Con on Comp App and Sys Mod* 2010;13:448–51.
16. Mukhopadhyay S, Gangopadhyay S, Sarkar SN. Coupling of a laser diode to mono mode elliptic core fiber via upside down tapered microlens on the fiber tip: estimation of coupling efficiency with consideration for misalignments by ABCD matrix formalism. *Optik* 2010;121:142–50.
17. Majumdar A, Mandal CK, Gangopadhyay S. Laser diode to single-mode circular core parabolic index fiber coupling via upside down tapered hyperbolic micro lens on the tip of the fiber: prediction of coupling optics by ABCD matrix formalism. *J Opt Commun* 2017;40:171–80.
18. Maiti S, Maiti AK, Gangopadhyay S. Laser diode to single-mode triangular-index fiber excitation via upside down hemispherical microlens on the fiber tip: prescription of ABCD matrix of transmission and estimation of coupling efficiency. *Optik* 2017;144:481–9.
19. Mandal H, Maiti S, Chiu TL, Gangopadhyay S. Mismatch considerations in laser diode to single-mode circular core triangular index fiber excitation via upside down tapered hemispherical microlens on the fiber tip. *Optik* 2018;168:533–40.
20. Maiti S, Biswas SK, Gangopadhyay S. Study of coupling optics involving graded index fiber excitation via upside down tapered parabolic microlens on the fiber tip. *Optik* 2019;199:1–8.
21. Zhang QJ. Cylindrical lensed fibers optimized for 980-nm pump laser diode coupling. *Proc SPIE* 2002;4905:157–60.
22. Zhang Q. Angular alignment tolerances for a 980 nm pump laser diode coupled to a cylindrical lensed fiber. *Acta Photonica Sin* 2003;32:92–6.
23. Mukhopadhyay S, Sarkar SN. Coupling of a laser diode to single mode circular core graded index fiber via hyperbolic microlens on the fiber tip and identification of the suitable refractive index profile with consideration for possible misalignments. *Opt Eng* 2011;50:1–9.
24. Gangopadhyay S, Sarkar SN. Misalignment considerations in laser diode to single-mode fibre excitation via hyperbolic lens on the fibre tip. *Opt Commun* 1998;146:104–8.
25. Gangopadhyay S, Sarkar SN. Laser diode to single-mode fiber excitation via hemispherical lens on the fiber tip: efficiency computation by ABCD matrix with consideration for allowable aperture. *J Opt Commun* 1998;19:42–4.
26. Mukhopadhyay S, Gangopadhyay S, Sarkar SN. Coupling of a laser diode to a mono mode elliptic core fiber via a hyperbolic microlens on the fiber tip: efficiency computation with the ABCD matrix. *Opt Eng* 2007;46:1–5.
27. Sarkar SN, Thyagrajan K, Kumar A. Gaussian approximation of the fundamental mode in single mode elliptic core fibers. *Opt Commun* 1984;49:178–83.
28. Marcuse D. Gaussian approximation of the fundamental modes of graded index fibers. *J Opt Soc Am* 1978;68:103–9.
29. Sarkar SN, Pal BP, Thyagrajan K. Lens coupling of laser diodes to monomode elliptic core fibers. *J Opt Commun* 1986;7:92–6.